Publishing House ASV

begell house, inc. publishers

Scientific coordination is carried out by the Russian Academy of Architecture and Construction Sciences (RAACS)

Volume 17 • Issue 4 • 2021

ISSN 2588-0195 (Online)
ISSN 2587-9618 (Print) Continues ISSN 1524-5845

International Journal for

Computational Civil and Structural Engineering

Международный журнал по расчету гражданских и строительных конструкций

http://raasn.ru/public.php
http://ijccse.iasv.ru/index.php/IJCCSE

DOI: 10.22337/2587-9618
GICID: 71.0000.1500.2830

EXECUTIVE EDITOR

Vladimir I. Travush,
Full Member of RAACS, Professor, Dr.Sc.,
Vice-President of the Russian Academy
of Architecture and Construction Sciences;
Urban Planning Institute
of Residential and Public Buildings;
24, Ulitsa Bolshaya Dmitrovka, 107031, Moscow, Russia

EDITOR-IN-CHIEF

Vladimir N. Sidorov,
Corresponding Member of RAACS, Professor, Dr.Sc.,
National Research Moscow State University of Civil
Engineering; Russian University of Transport (RUT –
MIIT); Russian University of Friendship of Peoples;
Moscow Institute of Architecture (State Academy);
Perm National Research Polytechnic University;
9b9, Obrazcova Street, Moscow, 127994, Russia

EDITORIAL DIRECTOR

Valery I. Telichenko,
Full Member of RAACS, Professor, Dr.Sc.,
The First Vice-President of the Russian Academy
of Architecture and Construction Sciences;
Honorary President of National Research
Moscow State University of Civil Engineering;
24, Ulitsa Bolshaya Dmitrovka, 107031, Moscow, Russia

MANAGING EDITOR

Nadezhda S. Nikitina,
Professor, Ph.D.,
Director of ASV Publishing House;
National Research Moscow State University
of Civil Engineering;
26, Yaroslavskoe Shosse, 129337, Moscow, Russia

ASSOCIATE EDITORS

Pavel A. Akimov,
Full Member of RAACS, Professor, Dr.Sc.,
Acting Rector of National Research
Moscow State University of Civil Engineering;
Vice-President of the Russian Academy
of Architecture and Construction Sciences;
Tomsk State University of Architecture and Building;
Russian University of Friendship of Peoples;
26, Yaroslavskoe Shosse, 129337, Moscow, Russia

Alexander M. Belostotsky,
Corresponding Member of RAACS, Professor, Dr.Sc.,
Research & Development Center “STADYO”;
National Research Moscow State University of Civil
Engineering; Russian University of Transport (RUT –
MIIT); Russian University of Friendship of Peoples;
Perm National Research Polytechnic University;
Tomsk State University of Architecture and Building;
Irkutsk National Research Technical University;
8th Floor, 18, ul. Tretya Yamskogo Polya,
125040, Moscow, Russia

Mikhail Belyi, Professor, Dr.Sc.,
Dassault Systèmes Simulia;
1301 Atwood Ave Suite 101W
02919 Johnston, RI, United States

Vitaly Bulgakov, Professor, Dr.Sc.,
Micro Focus;
Newbury, United Kingdom

Nikolai P. Osmolovskii, Professor, Dr.Sc.,
Systems Research Institute, Polish Academy of Sciences;
Kazimierz Pulaski University
of Technology and Humanities in Radom;
29, ul. Malczewskiego, 26-600, Radom, Poland

Gregory P. Panasenko, Professor, Dr.Sc.,
Equipe d’Analise Numerique; NMR CNRS 5585
University Gean Mehnet;
23 rue. P.Michelon 42023, St.Etienne, France

Leonid A. Rozin, Professor, Dr.Sc.,
Peter the Great Saint-Petersburg
Polytechnic University;
29, Ul. Politechnicheskaya,
195251 Saint-Petersburg, Russia

Scientific coordination is carried out by the Russian Academy of Architecture and Construction Sciences (RAACS)

PUBLISHER

ASV Publishing House
(ООО «Издательство АСВ»)
19/1,12, Yaroslavskoe Shosse, 120338, Moscow, Russia
Tel. +7(925)084-74-24; E-mail: iasv@iasv.ru; Интернет-сайт: http://iasv.ru/

ADVISORY EDITORIAL BOARD

Robert M. Aloyan,
Corresponding Member
of RAACS, Professor, Dr.Sc.,
Russian Academy of Architecture
and Construction Sciences;
24, Ul. Bolshaya Dmitrovka,
107031, Moscow, Russia

Vladimir I. Andreev,
Full Member of RAACS,
Professor, Dr.Sc.,
National Research Moscow State
University of Civil Engineering;
Yaroslavskoe Shosse 26,
Moscow, 129337, Russia

Mojtaba Aslami, Ph.D,
Fasa University; Daneshjou blvd,
Fasa, Fars Province, Iran

Klaus-Jurgen Bathe, Professor
Massachusetts Institute
of Technology;
Cambridge, MA 02139, USA

Alexander T. Bekker,
Corresponding Member
of RAACS, Professor, Dr.Sc.,
Far Eastern Federal University;
Russian Academy of Architecture
and Construction Sciences;
8, Sukhanova Street, Vladivostok,
690950, Russia

Tomas Bock, Professor, Dr.-Ing.,
Technical University of Munich,
Arcisstrasse 21, D-80333
Munich, Germany

Jan Buynak, Professor, Ph.D.,
University of Žilina;
1, Univerzitná, Žilina, 010 26,
Slovakia

Evgeniy M. Chernishov,
Full Member of RAACS,
Professor, Dr.Sc.,
Voronezh State Technical University;
14, Moscow Avenue,
Voronezh, 394026, Russia

Vladimir T. Erofeev,
Full Member of RAACS,
Professor, Dr.Sc.,
Ogarev Mordovia State University;
68, Bolshevistskaya Str., Saransk
430005, Republic of Mordovia,
Russia

Victor S. Fedorov,
Full Member of RAACS,
Professor, Dr.Sc.,
Russian University of Transport
(RUT – MIIT);
9b9 Obrazcova Street, Moscow,
127994, Russia

Sergey V. Fedosov,
Full Member of RAACS,
Professor, Dr.Sc.,
Russian Academy of Architecture
and Construction Sciences;
24, Ul. Bolshaya Dmitrovka, 107031,
Moscow, Russia

Sergiy Yu. Fialko,
Professor, Dr.Sc.,
Cracow University of Technology;
24, Warszawska Street, Kraków,
31-155, Poland

Vladimir G. Gagarin,
Corresponding Member
of RAACS, Professor, Dr.Sc.,
Research Institute of Building
Physics of Russian Academy
of Architecture and Construction
Sciences;
21, Lokomotivny Proezd,
Moscow, 127238, Russia

Alexander S. Gorodetsky,
Foreign Member of RAACS,
Professor, Dr.Sc.,
LIRA SAPR Ltd.;
7a Kiyanovsky Side Street
(Pereulok), Kiev, 04053, Ukraine

Vyatcheslav A. Ilyichev,
Full Member of RAACS,
Professor, Dr.Sc.,
Russian Academy of Architecture
and Construction Sciences;
Podzemproekt Ltd.;
24, Ulitsa Bolshaya Dmitrovka,
Moscow, 107031, Russia

Marek Iwański,
Professor, Dr.Sc.,
Kielce University of Technology;
7, al. Tysiąclecia Państwa Polskiego
Kielce, 25 – 314, Poland

Sergey Yu. Kalashnikov,
Advisor of RAACS,
Professor, Dr.Sc.,
Volgograd State Technical
University; 28, Lenin avenue,
Volgograd, 400005, Russia

Semen S. Kaprielov,
Corresponding Member
of RAACS, Professor, Dr.Sc.,
Research Center of Construction;
6, 2nd Institutskaya St., Moscow,
109428, Russia

Nikolay I. Karpenko,
Full Member of RAACS,
Professor, Dr.Sc.,
Research Institute of Building
Physics of Russian Academy
of Architecture and Construction
Sciences; Russian Academy of
Architecture and Construction
Sciences; 21, Lokomotivny Proezd,
Moscow, 127238, Russia

Vladimir V. Karpov,
Professor, Dr.Sc.,
Saint Petersburg State University
of Architecture and Civil
Engineering;
4, 2-nd Krasnoarmeiskaya Steet,
Saint Petersburg, 190005, Russia

Galina G. Kashevarova,
Corresponding Member
of RAACS, Professor, Dr.Sc.,
Perm National Research
Polytechnic University;
29 Komsomolsky pros., Perm,
Perm Krai, 614990, Russia

John T. Katsikadelis,
Professor, Dr.Eng, PhD, Dr.h.c.,
National Technical University of
Athens; Zografou Campus
9, Iroon Polytechniou str
15780 Zografou, Greece

Vitaly I. Kolchunov,
Full Member of RAACS,
Professor, Dr.Sc.,
Southwest State University;
Russian Academy of Architecture
and Construction Sciences;
94, 50 let Oktyabrya, Kursk,
305040, Russia

Markus König, Professor
Ruhr-Universität Bochum;
150, Universitätsstraße, Bochum,
44801, Germany

Sergey B. Kositsin,
Advisor of RAACS,
Professor, Dr.Sc.,
Russian University of Transport
(RUT – MIIT); 9b9 Obrazcova
Street, Moscow, 127994, Russia

Sergey B. Krylov,
Corresponding Member
of RAACS, Professor, Dr.Sc.,
Research Center of Construction;
6, 2nd Institutskaya St., Moscow,
109428, Russia

Sergey V. Kuznetsov,
Professor, Dr.Sc.,
Ishlinsky Institute for Problems
in Mechanics of the Russian
Academy of Sciences;
101-1, Prosp. Vernadskogo,
Moscow, 119526, Russia

Vladimir V. Lalin,
Professor, Dr.Sc.,
Peter the Great Saint-Petersburg
Polytechnic University;
29, Ul. Politechnicheskaya,
Saint-Petersburg, 195251, Russia

Leonid S. Lyakhovich,
Full Member of RAACS,
Professor, Dr.Sc.,
Tomsk State University
of Architecture and Building;
2, Solyanaya Sq., Tomsk,
634003, Russia

Rashid A. Mangushev,
Corresponding Member
of RAACS, Professor, Dr.Sc.,
Saint Petersburg State University
of Architecture and Civil
Engineering;
4, 2-nd Krasnoarmeiskaya Steet,
Saint Petersburg, 190005, Russia

Ilizar T. Mirsayapov,
Advisor of RAACS,
Professor, Dr.Sc., Kazan State
University of Architecture and
Engineering; 1, Zelenaya Street,
Kazan, 420043, Republic
of Tatarstan, Russia

Vladimir L. Mondrus,
Corresponding Member
of RAACS, Professor, Dr.Sc.,
National Research Moscow State
University of Civil Engineering;
Yaroslavskoe Shosse 26,
Moscow, 129337, Russia

Valery I. Morozov,
Corresponding Member
of RAACS, Professor, Dr.Sc.,
Saint Petersburg State University
of Architecture and Civil
Engineering;
4, 2-nd Krasnoarmeiskaya Steet,
Saint Petersburg, 190005, Russia

Anatoly V. Perelmuter,
Foreign Member of RAACS,
Professor, Dr.Sc., SCAD Soft;
Office 1,2, 3a Osvity street,
Kiev, 03037, Ukraine

Alexey N. Petrov,
Advisor of RAACS, Professor,
Dr.Sc., Petrozavodsk State
University; 33, Lenina Prospect,
Petrozavodsk, 185910,
Republic of Karelia, Russia

Vladilen V. Petrov,
Full Member of RAACS,
Professor, Dr.Sc.,
Yuri Gagarin State Technical
University of Saratov;
77 Politechnicheskaya Street,
Saratov, 410054, Russia

Jerzy Z. Piotrowski,
Professor, Dr.Sc.,
Kielce University of Technology;
al. Tysiąclecia Państwa Polskiego 7,
Kielce, 25 – 314, Poland

Chengzhi Qi, Professor, Dr.Sc.,
Beijing University of Civil
Engineering and Architecture;
1, Zhanlanlu, Xicheng District,
Beijing, China

Vladimir P. Selyaev,
Full Member of RAACS,
Professor, Dr.Sc., Ogarev
Mordovia State University;
68, Bolshevistskaya Str., Saransk
430005, Republic of Mordovia,
Russia

Eun Chul Shin,
Professor, Ph.D.,
Incheon National University;
(Songdo-dong)119 Academy-ro,
Yeonsu-gu, Incheon, Korea

D.V. Singh,
Professor, Ph.D,
University of Roorkee;
Roorkee, India, 247667

Wacław Szcześniak,
Foreign Member of RAACS,
Professor, Dr.Sc.,
Lublin University of Technology;
Ul. Nadbystrzycka 40,
20-618 Lublin, Poland

Tadatsugu Tanaka,
Professor, Dr.Sc.,
Tokyo University; 7-3-1 Hongo,
Bunkyo, Tokyo, 113-8654, Japan

Josef Vican,
Professor, Ph.D,
University of Žilina;
1, Univerzitná, Žilina, 010 26,
Slovakia

Zbigniew Wojcicki,
Professor, Dr.Sc.,
Wroclaw University
of Technology;
11 Grunwaldzki Sq., 50-377,
Wrocław, Poland

Artur Zbiciak, Professor, Dr.Sc.,
Warsaw University of Technology;
Pl. Politechniki 1, 00-661 Warsaw,
Poland

Segrey I. Zhavoronok, Ph.D.,
Institute of Applied Mechanics of
Russian Academy of Sciences;
Moscow Aviation Institute
(National Research University);
7, Leningradsky Prt.,
Moscow, 125040, Russia

Askar Zhussupbekov,
Professor, Dr.Sc.,
Eurasian National University;
5, Munaitpassov street, Astana,
010000, Kazakhstan

TECHNICAL EDITOR

Taymuraz B. Kaytukov,
Advisor of RAACS,
Associate Professor, Ph.D.,
Vice-Rector of National Research
Moscow State University
of Civil Engineering;
Yaroslavskoe Shosse 26,
Moscow, 129337, Russia

EDITORIAL TEAM

Vadim K. Akhmetov, Professor, Dr.Sc., National Research Moscow State University of Civil Engineering; 26, Yaroslavskoe Shosse, 129337 Moscow, Russia

Pavel A. Akimov, Full Member of RAACS, Professor, Dr.Sc., Acting Rector of National Research Moscow State University of Civil Engineering; Vice-President of the Russian Academy of Architecture and Construction Sciences; Tomsk State University of Architecture and Building; Russian University of Friendship of Peoples; 26, Yaroslavskoe Shosse, 129337, Moscow, Russia

Alexander M. Belostotsky, Corresponding Member of RAACS, Professor, Dr.Sc., Research & Development Center "STADYO"; National Research Moscow State University of Civil Engineering; Russian University of Transport (RUT – MIIT); Russian University of Friendship of Peoples; Perm National Research Polytechnic University; Tomsk State University of Architecture and Building; Irkutsk National Research Technical University; 8th Floor, 18, ul. Tretya Yamskogo Polya, 125040, Moscow, Russia

Mikhail Belyi, Professor, Dr.Sc., Dassault Systèmes Simulia; 1301 Atwood Ave Suite 101W 02919 Johnston, RI, United States

Vitaly Bulgakov, Professor, Dr.Sc., Micro Focus; Newbury, United Kingdom

Charles El Nouty, Professor, Dr.Sc., LAGA Paris-13 Sorbonne Paris Cite; 99 avenue J.B. Clément, 93430 Villetaneuse, France

Natalya N. Fedorova, Professor, Dr.Sc., Novosibirsk State University of Architecture and Civil Engineering (SIBSTRIN); 113 Leningradskaya Street, Novosibirsk, 630008, Russia

Darya Filatova, Professor, Dr.Sc., Probability, Assessment, Reasoning and Inference Studies Research Group, EPHE Laboratoire CHART (PARIS) 4-14, rue Ferrus, 75014 Paris

Vladimir Ya. Gecha, Professor, Dr.Sc., Research and Production Enterprise All-Russia Scientific-Research Institute of Electromechanics with Plant Named after A.G. Iosiphyan; 30, Volnaya Street, Moscow, 105187, Russia

Taymuraz B. Kaytukov, Advisor of RAACS, Associate Professor, Ph.D, Vice-Rector of National Research Moscow State University of Civil Engineering; 26, Yaroslavskoe Shosse, 129337, Moscow, Russia

Amirlan A. Kusainov, Foreign Member of RAACS, Professor, Dr.Sc., Kazakh Leading Architectural and Civil Engineering Academy; Kazakh-American University, 9, Toraighyrov Str., Almaty, 050043, Republic of Kazakhstan

Marina L. Mozgaleva, Professor, Dr.Sc., National Research Moscow State University of Civil Engineering; 26, Yaroslavskoe Shosse, 129337 Moscow, Russia

Nadezhda S. Nikitina, Professor, Ph.D., Director of ASV Publishing House; National Research Moscow State University of Civil Engineering; 26, Yaroslavskoe Shosse, 129337 Moscow, Russia

Nikolai P. Osmolovskii, Professor, Dr.Sc., Systems Research Institute Polish Academy of Sciences; Kazimierz Pulaski University of Technology and Humanities in Radom; 29, ul. Malczewskiego, 26-600, Radom, Poland

Gregory P. Panasenko, Professor, Dr.Sc., Equipe d'Analise Numerique NMR CNRS 5585 University Gean Mehnet; 23 rue. P.Michelon 42023, St.Etienne, France

Andreas Rauh, Prof. Dr.-Ing. habil. Carl von Ossietzky Universität Oldenburg, Germany School II - Department of Computing Science Group Distributed Control in Interconnected Systems D-26111 Oldenburg, Germany

Leonid A. Rozin, Professor, Dr.Sc., Peter the Great Saint-Petersburg Polytechnic University; 29, Ul. Politechnicheskaya, 195251 Saint-Petersburg, Russia

Zhan Shi, Professor LPSM, Université Paris VI 4 place Jussieu, F-75252 Paris Cedex 05, France

Marina V. Shitikova, National Research Moscow State University of Civil Engineering, Advisor of RAACS, Professor, Dr.Sc., Voronezh State Technical University; 14, Moscow Avenue, Voronezh, 394026, Russia

Igor L. Shubin, Corresponding Member of RAACS, Professor, Dr.Sc., Research Institute of Building Physics of Russian Academy of Architecture and Construction Sciences; 21, Lokomotivny Proezd, Moscow, 127238, Russia

Vladimir N. Sidorov, Corresponding Member of RAACS, Professor, Dr.Sc., National Research Moscow State University of Civil Engineering; Russian University of Transport (RUT – MIIT); Russian University of Friendship of Peoples; Moscow Institute of Architecture (State Academy); Perm National Research Polytechnic University; Kielce University of Technology (Poland); 9b9 Obrazcova Street, Moscow, 127994, Russia

Valery I. Telichenko, Full Member of RAACS, Professor, Dr.Sc., The First Vice-President of the Russian Academy of Architecture and Construction Sciences; National Research Moscow State University of Civil Engineering; 24, Ulitsa Bolshaya Dmitrovka, 107031, Moscow, Russia

Vladimir I. Travush, Full Member of RAACS, Professor, Dr.Sc., Vice-President of the Russian Academy of Architecture and Construction Sciences; Urban Planning Institute of Residential and Public Buildings; 24, Ulitsa Bolshaya Dmitrovka, 107031, Moscow, Russia

INVITED REVIEWERS

Akimbek A. Abdikalikov, Professor, Dr.Sc.,
Kyrgyz State University of Construction, Transport and Architecture n.a. N. Isanov;
34 Maldybayeva Str., Bishkek, 720020, Biskek, Kyrgyzstan

Vladimir N. Alekhin, Advisor of RAACS, Professor, Dr.Sc.,
Ural Federal University named after the first President of Russia B.N. Yeltsin;
19 Mira Street, Ekaterinburg, 620002, Russia

Irina N. Afanasyeva, Ph.D., University of Florida; Gainesville, FL 32611, USA

Ján Čelko, Professor, PhD, Ing., University of Žilina; Univerzitná 1, 010 26, Žilina, Slovakia

Tatyana L. Dmitrieva, Professor, Dr.Sc.,
Irkutsk National Research Technical University; 83, Lermontov street, Irkutsk, 664074, Russia

Petr P. Gaidzhurov, Advisor of RAACS, Professor, Dr.Sc.,
Don State Technical University; 1, Gagarina Square, Rostov-on-Don, 344000, Russia

Jacek Grosel, Associate Professor, Dr inz.
Wroclaw University of Technology; 11 Grunwaldzki Sq., 50-377, Wrocław, Poland

Stanislaw Jemioło, Professor, Dr.Sc.,
Warsaw University of Technology; 1, Pl. Politechniki, 00-661, Warsaw, Poland

Konstantin I. Khenokh, M.Ing., M.Sc.,
General Dynamics C4 Systems; 8201 E McDowell Rd, Scottsdale, AZ 85257, USA

Christian Koch, Dr.-Ing., Ruhr-Universität Bochum;
Lehrstuhl für Informatik im Bauwesen, Gebäude IA, 44780, Bochum, Germany

Gaik A. Manuylov, Professor, Ph.D.,
Moscow State University of Railway Engineering; 9, Obraztsova Street, Moscow, 127994, Russia

Alexander S. Noskov, Professor, Dr.Sc.,
Ural Federal University named after the first President of Russia B.N. Yeltsin;
19 Mira Street, Ekaterinburg, 620002, Russia

Grzegorz Świt, Professor, Dr.hab. Inż.,
Kielce University of Technology; 7, al. Tysiąclecia Państwa Polskiego, Kielce, 25 – 314, Poland

AIMS AND SCOPE

The aim of the Journal is to advance the research and practice in structural engineering through the application of computational methods. The Journal will publish original papers and educational articles of general value to the field that will bridge the gap between high-performance construction materials, large-scale engineering systems and advanced methods of analysis.

The scope of the Journal includes papers on computer methods in the areas of structural engineering, civil engineering materials and problems concerned with multiple physical processes interacting at multiple spatial and temporal scales. The Journal is intended to be of interest and use to researches and practitioners in academic, governmental and industrial communities.

ОБЩАЯ ИНФОРМАЦИЯ О ЖУРНАЛЕ

International Journal for Computational Civil and Structural Engineering

(Международный журнал по расчету гражданских и строительных конструкций)

Международный научный журнал "International Journal for Computational Civil and Structural Engineering (Международный журнал по расчету гражданских и строительных конструкций)" (IJCCSE) является ведущим научным периодическим изданием по направлению «Инженерные и технические науки», издаваемым, начиная с 1999 года (ISSN 2588-0195 (Online); ISSN 2587-9618 (Print) Continues ISSN 1524-5845). В журнале на высоком научно-техническом уровне рассматриваются проблемы численного и компьютерного моделирования в строительстве, актуальные вопросы разработки, исследования, развития, верификации, апробации и приложений численных, численно-аналитических методов, программно-алгоритмического обеспечения и выполнения автоматизированного проектирования, мониторинга и комплексного наукоемкого расчетно-теоретического и экспериментального обоснования напряженно-деформированного (и иного) состояния, прочности, устойчивости, надежности и безопасности ответственных объектов гражданского и промышленного строительства, энергетики, машиностроения, транспорта, биотехнологий и других высокотехнологичных отраслей.

В редакционный совет журнала входят известные российские и зарубежные деятели науки и техники (в том числе академики, члены-корреспонденты, иностранные члены, почетные члены и советники Российской академии архитектуры и строительных наук). Основной критерий отбора статей для публикации в журнале − их высокий научный уровень, соответствие которому определяется в ходе высококвалифицированного рецензирования и объективной экспертизы, поступающих в редакцию материалов.

Журнал входит в Перечень ВАК РФ ведущих рецензируемых научных изданий, в которых должны быть опубликованы основные научные результаты диссертаций на соискание ученой степени кандидата наук, на соискание ученой степени доктора наук по научным специальностям и соответствующим им отраслям науки:

- 01.02.04 – Механика деформируемого твердого тела (технические науки),
- 05.13.18 – Математическое моделирование численные методы и комплексы программ (технические науки),
- 05.23.01 – Строительные конструкции, здания и сооружения (технические науки),
- 05.23.02 – Основания и фундаменты, подземные сооружения (технические науки),
- 05.23.05 – Строительные материалы и изделия (технические науки),
- 05.23.07 – Гидротехническое строительство (технические науки),
- 05.23.17 – Строительная механика (технические науки).

В Российской Федерации журнал индексируется Российским индексом научного цитирования (РИНЦ).

Журнал входит в базу данных Russian Science Citation Index (RSCI), полностью интегрированную с платформой Web of Science. Журнал имеет международный статус и высылается в ведущие библиотеки и научные организации мира.

Издатели журнала – *Издательство Ассоциации строительных высших учебных заведений /АСВ/* (Россия, г. Москва) и до 2017 года *Издательский дом Begell House Inc*. (США, г. Нью-Йорк). Официальными партнерами издания является *Российская академия архитектуры и строительных наук* (РААСН), осуществляющая научное курирование издания, и *Научно-исследовательский центр СтаДиО* (ЗАО НИЦ СтаДиО).

Цели журнала – демонстрировать в публикациях российскому и международному профессиональному сообществу новейшие достижения науки в области вычислительных методов

решения фундаментальных и прикладных технических задач, прежде всего в области строительства.

Задачи журнала:

• предоставление российским и зарубежным ученым и специалистам возможности публиковать результаты своих исследований;

• привлечение внимания к наиболее актуальным, перспективным, прорывным и интересным направлениям развития и приложений численных и численно-аналитических методов решения фундаментальных и прикладных технических задач, совершенствования технологий математического, компьютерного моделирования, разработки и верификации реализующего программно-алгоритмического обеспечения;

• обеспечение обмена мнениями между исследователями из разных регионов и государств.

Тематика журнала. К рассмотрению и публикации в журнале принимаются аналитические материалы, научные статьи, обзоры, рецензии и отзывы на научные публикации по фундаментальным и прикладным вопросам технических наук, прежде всего в области строительства. В журнале также публикуются информационные материалы, освещающие научные мероприятия и передовые достижения Российской академии архитектуры и строительных наук, научно-образовательных и проектно-конструкторских организаций.

Тематика статей, принимаемых к публикации в журнале, соответствует его названию и охватывает направления научных исследований в области разработки, исследования и приложений численных и численно-аналитических методов, программного обеспечения, технологий компьютерного моделирования в решении прикладных задач в области строительства, а также соответствующие профильные специальности, представленные в диссертационных советах профильных образовательных организациях высшего образования.

Редакционная политика. Политика редакционной коллегии журнала базируется на современных юридических требованиях в отношении авторского права, законности, плагиата и клеветы, изложенных в законодательстве Российской Федерации, и этических принципах, поддерживаемых сообществом ведущих издателей научной периодики.

За публикацию статей плата с авторов не взымается. Публикация статей в журнале бесплатная. На платной основе в журнале могут быть опубликованы материалы рекламного характера, имеющие прямое отношение к тематике журнала.

Журнал предоставляет непосредственный открытый доступ к своему контенту, исходя из следующего принципа: свободный открытый доступ к результатам исследований способствует увеличению глобального обмена знаниями.

Индексирование. Публикации в журнале входят в системы расчетов индексов цитирования авторов и журналов. «Индекс цитирования» – числовой показатель, характеризующий значимость данной статьи и вычисляющийся на основе последующих публикаций, ссылающихся на данную работу.

Авторам. Прежде чем направить статью в редакцию журнала, авторам следует ознакомиться со всеми материалами, размещенными в разделах сайта журнала (интернет-сайт Российской академии архитектуры и строительных наук (http://raasn.ru); подраздел «Издания РААСН» или интернет-сайт Издательства АСВ (http://iasv.ru); подраздел «Журнал IJCCSE»): с основной информацией о журнале, его целями и задачами, составом редакционной коллегии и редакционного совета, редакционной политикой, порядком рецензирования направляемых в журнал статей, сведениями о соблюдении редакционной этики, о политике авторского права и лицензирования, о представлении журнала в информационных системах (индексировании), информацией о подписке на журнал, контактными данными и пр. Журнал работает по лицензии Creative Commons типа cc by-nc-sa (Attribution Non-Commercial Share Alike) – Лицензия «С указанием авторства – Некоммерческая – Копилефт».

Рецензирование. Все научные статьи, поступившие в редакцию журнала, проходят обязательное двойное слепое рецензирование (рецензент не знает авторов рукописи, авторы рукописи не знаю рецензентов).

Заимствования и плагиат. Редакционная коллегия журнала при рассмотрении статьи проводит проверку материала с помощью системы «Антиплагиат». В случае обнаружения многочисленных заимствований редакция действует в соответствии с правилами COPE.

Подписка. Журнал зарегистрирован в Федеральном агентстве по средствам массовой информации и охраны культурного наследия Российской Федерации. Индекс в общероссийском каталоге РОСПЕЧАТЬ − 18076.

По вопросам подписки на международный научный журнал “International Journal for Computational Civil and Structural Engineering (Международный журнал по расчету гражданских и строительных конструкций)” обращайтесь в Агентство «Роспечать» (Официальный сайт в сети Интернет: http://www.rosp.ru/) или в издательство Ассоциации строительных вузов (АСВ) в соответствии со следующими контактными данными:

ООО «Издательство АСВ»

Юридический адрес: 129337, Россия, г. Москва, Ярославское ш., д. 26, офис 705;

Фактический адрес: 129337, Россия, г. Москва, Ярославское ш., д. 19, корп. 1, 5 этаж, офис 12 (ТЦ Соле Молл);

Телефоны: +7 (925) 084-74-24, +7 (926) 010-91-33;

Интернет-сайт: www.iasv.ru. Адрес электронной почты: iasv@iasv.ru.

Контактная информация. По всем вопросам работы редакции, рецензирования, согласования правки текстов и публикации статей следует обращаться к главному редактору журнала члену-корреспонденту РААСН *Сидорову Владимиру Николаевичу* (адреса электронной почты: sidorov.vladimir@gmail.com, sidorov@iasv.ru, iasv@iasv.ru, sidorov@raasn.ru) или к техническому редактору журнала советнику РААСН *Кайтукову Таймуразу Батразовичу* (адреса электронной почты: tkaytukov@gmail.com; kaytukov@raasn.ru). Кроме того, по указанным вопросам, а также по вопросам размещения в журнале рекламных материалов можно обращаться к генеральному директору ООО «Издательство АСВ» *Никитиной Надежде Сергеевне* (адреса электронной почты: iasv@iasv.ru, nsnikitina@mail.ru, ijccse@iasv.ru).

Журнал становится технологичнее. Издательство АСВ с сентября 2016 года является членом Международной ассоциации издателей научной литературы (Publishers International Linking Association (PILA)), осуществляющей свою деятельность на платформе CrossRef. Оригинальным статьям, публикуемым в журнале, будут присваиваться уникальные номера (индексы DOI – Digital Object Identifier), что значительно облегчит поиск метаданных и местонахождение полнотекстового произведения. DOI – это система определения научного контента в сети Интернет.

С октября 2016 года стал возможен прием статей на рассмотрение и рецензирование через онлайн систему приема статей Open Journal Systems на сайте журнала (электронная редакция): http://ijccse.iasv.ru/index.php/IJCCSE.

Автор имеет возможность следить за продвижением статьи в редакции журнала в личном кабинете Open Journal Systems и получать соответствующие уведомления по электронной почте.

В феврале 2018 года журнал был зарегистрирован в Directory of open access journals (DOAJ) (это один из самых известных поисковых сервисов в мире, который предоставляет открытый доступ к материалам и индексирует не только заголовки журналов, но и научные статьи), в сентябре 2018 года включен в продукты EBSCO Publishing.

В ноябре 2020 года журнал начал индексироваться в международной базе Scopus.

International Journal for
Computational Civil and Structural Engineering
(Международный журнал по расчету гражданских и строительных конструкций)
Volume 17, Issue 4 ***2021***

Scientific coordination is carried out by the Russian Academy of Architecture and Construction Sciences (RAACS)

CONTENTS

International Journal for
Computational Civil and Structural Engineering
(Международный журнал по расчету гражданских и строительных конструкций)
Volume 17, Issue 4 ***2021***

Scientific coordination is carried out by the Russian Academy of Architecture and Construction Sciences (RAACS)

СОДЕРЖАНИЕ

DOI:10.22337/2587-9618-2021-17-4-14-21

NONLOCAL IN TIME MODEL OF MATERIAL DAMPING IN COMPOSITE STRUCTURAL ELEMENTS DYNAMIC ANALYSIS

Vladimir N. Sidorov [1,2], Elena. S. Badina [1,2,3], Elena P. Detina [2]

[1] Russian University of Transport (MIIT), Moscow, RUSSIA
[2] National Research Moscow State University of Civil Engineering, Moscow, RUSSIA
[3] Institute of Applied Mechanics of Russian Academy of Sciences, Moscow RUSSIA

Abstract: In this paper the problem of numerical simulation of composite bending elements dynamic considering internal (material) damping. For this purpose the nonlocal in time damping model, called damping with memory, is proposed as an alternative to the classic local Kelvin-Voigt model. Damping with memory makes damping forces not only dependent on the instant value of the strain rate, but also on the previous history of the vibration process. Since finite element analysis is the most common method of structural analysis, the nonlocal damping model is integrated into FEA algorithm. The FEA dynamic equilibrium equation is solved using the explicit scheme. The damping matrix was developed using the stationary full energy requirement. One-dimensional nonlocal in time model was implemented in MATLAB software package. The results of three-dimensional numerical simulation of the composite beam vibration obtained in SIMULIA Abaqus were used for model calibration. The obtained results were compared to the results based on classic Kelvin-Voight damping model.

Keywords: material damping, nonlocal damping, numerical simulation, finite element analysis.

НЕЛОКАЛЬНАЯ ВО ВРЕМЕНИ МОДЕЛЬ ДЕМПФИРОВАНИЯ МАТЕРИЛА ПРИ ДИНАМИЧЕСКОМ РАСЧЁТЕ КОМПОЗИТНЫХ ЭЛЕМЕНТОВ СТРОИТЕЛЬНЫХ КОНСТРУКЦИЙ

В.Н. Сидоров [1,2], Е.С. Бадьина [1,2,3], Е.П. Детина [2]

[1] Российский университет транспорта (МИИТ), г. Москва, РОССИЯ
[2] Национальный исследовательский Московский государственный строительный университет, г. Москва, РОССИЯ
[3] Институт прикладной механики Российской академии наук, г. Москва, РОССИЯ

Аннотация: В настоящей работе рассматривается задача численного динамического расчёта изгибаемых элементов конструкций из композитных и нано- материалов с моделированием их демпфирующих свойств, вызываемых внутренним трением в материале. С этой целью нелокальная во времени модель демпфирования материала, называемая демпфированием с памятью, предлагается как альтернатива классической локальной модели Кельвина-Фойгта. При таком подходе силы демпфирования считаются зависящими не только от мгновенного значения скоростей деформаций в рассматриваемый момент времени, но и от значений скоростей деформаций на предыдущих стадиях колебательного процесса. Поскольку метод конечных элементов (МКЭ) является наиболее предпочтительным численным методом анализа механических систем, нелокальная модель демпфирования интегрирована в алгоритм этого метода. Уравнение равновесия конструкции в движении МКЭ решается по явной схеме. Матрица демпфирования получена из условия стационарности полной энергии деформирования движущейся механической системы. Одномерная нелокальная во времени модель была реализована в программном комплексе MATLAB. Для калибровки модели были использованы результаты трехмерного численного моделирования колебаний композитной балки, полученные в SIMULIA Abaqus. Полученные результаты были сопоставлены с результатами, основанными на классической модели демпфирования Кельвина-Фойгта.

Ключевые слова: внутреннее трение, нелокальное демпфирование, численное моделирование, метод конечных элементов.

INTRODUCTION

Simulation of the material damping properties is the complicated problem, which still does not have an unambiguous solution [1]. It becomes especially sophisticated speaking of materials with complicated internal structure, such as composite and nano-materials. In such cases special hypothesis of internal friction are required, flexible and controllable enough to describe damping properties of the orthotropic or anisotropic material, consisting of two or more phases.

At the same time the damping model have to be not overly complex, so it can be used in applied engineering calculations.

Since the finite element analysis is the most common numerical method used in engineering practice, we felt it worthwhile to develop the internal damping model, that can be simply built in the FEA algorithm.

In this paper nonlocal in time damping model is used as such a flexible model [2].

FINITE ELEMENT EQUILIBRIUM EQUATION WITH INTEGRATED NONLOCAL IN TIME DAMPING MODEL

In finite element analysis the dynamic equilibrium equation is presented in matrix form [3]:

$$M \cdot \ddot{\bar{V}}(t) + D \cdot \dot{\bar{V}}(t) + K \cdot \bar{V}(t) = \bar{F}(t). \qquad (1)$$

Here $\bar{\boldsymbol{V}}(\boldsymbol{t})$ – vector of nodes displacements (dot indicates time derivative), $\boldsymbol{K}$ – stiffness matrix of the finite element model, $\boldsymbol{D}$ – damping matrix, $\boldsymbol{M}$ – mass matrix, $\bar{\boldsymbol{F}}(\boldsymbol{t})$ – load vector.

For nonlocal in time damping model we consider that damping of the structure at the current time moment t is assumed to be dependent not only on instant value of strain rate at this moment $\dot{\boldsymbol{\varepsilon}}(t)$, but also on the values of strain rates $\dot{\boldsymbol{\varepsilon}}(\boldsymbol{\tau})$ of the previous time history $\tau = 0 \div t$ [4]. The longer is the gap between the two time points the lower is the influence that one of them has on the other.

To simulate the nonlocal in time properties of material damping («damping with memory») equation (1) is represented as:

$$M \cdot \ddot{\bar{V}}(t) + D \cdot \int_0^t G(t-\tau) \cdot \dot{\bar{V}}(\tau) d\tau + K \cdot \bar{V}(t) = \bar{F}(t). \qquad (2)$$

Here $\boldsymbol{G}(\boldsymbol{t}-\boldsymbol{\tau})$ is the kernel function that describes the decrease of the strain rate influence at the moment $\boldsymbol{\tau}$ on the damping at the current moment $\boldsymbol{t}$, and it satisfies the normalization requirement:

$$\int_0^t G(t-\tau) d\tau = 1. \qquad (3)$$

In this research the kernel function is constructed on the base of Gauss integral:

$$\int_{-\infty}^{\infty} e^{-x^2} dx = \sqrt{\pi}, \qquad (4)$$

that, taking into account the condition (3), can be written as:

$$G(t-\tau) = \frac{2\mu}{\sqrt{\pi}} \cdot e^{-\mu^2 (t-\tau)^2}, \qquad (5)$$

Here $\boldsymbol{\mu}$ is a parameter, that characterize the level of damping nonlocality in time. It is further called “influence distance”.

Assuming that the material damping with memory model depends on values of strain rate, the material damping matrix is obtained according to the requirement of stationary full energy of the vibrating system. The dissipation of energy by a material during deformation of a finite element under the dynamic loads will be represented by a dissipative function:

$$\Phi_D = \frac{1}{2} \chi \dot{\varepsilon}^2, \qquad (6)$$

where $\dot{\boldsymbol{\varepsilon}}$ – strain rate, $\boldsymbol{\chi}$ – coefficient that defines material viscosity. It can be obtained as:

$$\chi = E \cdot t_\kappa. \tag{7}$$

Here $\boldsymbol{E}$ – is Young modulus. Time delay $\boldsymbol{t_\kappa}$ can be determined through the damping coefficient (critical fraction) $\boldsymbol{\xi}$ [5]:

$$t_\kappa = \frac{2\xi}{\omega}. \tag{8}$$

Here ω – is the first natural frequency of the system.

Energy dissipation through the material of the whole system can be presented as summation of energy dissipations through each finite element:

$$\Phi_D = \sum_{i-1}^{N} \Phi_{Di}, \tag{9}$$

where i – finite element number ($i = 1, 2, \ldots, N$), N – number of elements in the whole FE computational model.

Here damping matrix is developed for the frame element in bending and tension. In this case energy dissipation through the element material is:

$$\Phi_{Di} = \frac{1}{2}\int_l \chi \dot{\varepsilon}_a^2 A dz + \frac{1}{2}\int_l \int_A \chi \dot{\varepsilon}_b^2 dA dz\,, \tag{10}$$

where A – element cross-section area, z – longitudinal coordinate, l – element length, $\dot{\varepsilon}_a$ – tension-induced axial strain rate, $\dot{\varepsilon}_b$ - bending-induced axial strain rate:

Tension-induced axial strain, is [6]:

$$\varepsilon_a = \frac{du}{dz}, \tag{11}$$

where u – axial displacement.

Bending-induced axial strain, of ~~for~~ the Euler-Bernoulli beam:

$$\varepsilon_b = \frac{1}{\rho} y = \kappa y \approx \frac{d^2 v}{dz^2} y. \tag{12}$$

Here ρ – radius of curvature of the beam neutral layer, y – distance to the considered beam fiber from its neutral layer, v – transverse displacement, κ – curvature of the v-line in the cross-section with the longitudinal coordinate z.

Then:

$$\Phi_{Di} = \frac{1}{2} A\chi \int_l \left(\frac{d\dot{u}}{dz}\right)^2 dz + \frac{1}{2} I\chi \int_l \left(\frac{d^2 v}{dz^2}\right)^2 dz, \tag{13}$$

where I – element cross-section moment of inertia.

Within the FEA the axial displacements are approximated inside the beam element with linear shape function $[N_u] = [1-\xi \quad \xi]$, and the transverse displacements – with cubic shape function

$$[N_v]^T = \begin{bmatrix} 1 - 3\xi^2 + 2\xi^3 \\ l(\xi - 2\xi^2 + \xi^3) \\ 3\xi^2 - 2\xi^3 \\ l(-\xi^2 + \xi^3) \end{bmatrix}.$$

$\xi = \frac{z}{l}$ – is the reduced local longitudinal coordinate.

Taking this into account we can transform the expression (13) to:

$$\Phi_{Di} \approx \approx \frac{1}{2} A\chi \int_0^1 (A_u[N_u])^T \cdot A_u[N_u] \cdot \dot{u}_i \cdot \dot{u}_i l d\xi + \frac{1}{2} I\chi \int_0^1 (A_v[N_v])^T \cdot A_v[N_v] \cdot \dot{v}_i \cdot \dot{v}_i l d\xi. \tag{14}$$

Here $\dot{u}_i = \begin{pmatrix} \dot{u}_0 \\ \dot{u}_l \end{pmatrix}$ and $\dot{v}_i = \begin{pmatrix} \dot{v}_0 \\ \dot{\varphi}_0 \\ \dot{v}_l \\ \dot{\varphi}_l \end{pmatrix}$ are axial and bending nodal displacements strain rate vectors,

where $\dot{v}_0$ and $\dot{v}_l$ are transverse strain rates, and $\dot{\varphi}_0$ and $\dot{\varphi}_l$ – rotation strain rates.

In (14) $A_u = \frac{d}{l \cdot d\xi}$ and $A_v = \frac{d^2}{l^2 \cdot d\xi^2}$.

Participation (14) in the stationarity requirements of the full energy change:

$$\frac{\partial \Phi_D}{\partial \dot{v}} = 0 \tag{6a}$$

gives us a $D \cdot \dot{\bar{V}}$ member in the equilibrium equation in motion.

System damping matrix D is obtained by topological summation of element damping matrices D_i:

$$D_i = \\ = A\chi \int_0^1 (A_u[N_u])^T \cdot A_u[N_u] l d\xi \\ + I\chi \int_0^1 (A_v[N_v])^T \cdot A_v[N_v] l d\xi. \tag{15}$$

In this way D_i matrix for the plane frame elements is:

$$\mathbf{D}_i = \chi \cdot \begin{bmatrix} \frac{\mathbf{A}}{l} & 0 & 0 & -\frac{\mathbf{A}}{l} & 0 & 0 \\ 0 & \frac{12 \cdot \mathbf{J}}{l^3} & \frac{6 \cdot \mathbf{J}}{l^2} & 0 & -\frac{12 \cdot \mathbf{J}}{l^3} & \frac{6 \cdot \mathbf{J}}{l^2} \\ 0 & -\frac{6 \cdot \mathbf{J}}{l^2} & \frac{4 \cdot \mathbf{J}}{l} & 0 & -\frac{6 \cdot \mathbf{J}}{l^2} & \frac{2 \cdot \mathbf{J}}{l} \\ -\frac{\mathbf{A}}{l} & 0 & 0 & \frac{\mathbf{A}}{l} & 0 & 0 \\ 0 & -\frac{12 \cdot \mathbf{J}}{l^3} & -\frac{6 \cdot \mathbf{J}}{l^2} & 0 & \frac{12 \cdot \mathbf{J}}{l^3} & -\frac{6 \cdot \mathbf{J}}{l^2} \\ 0 & \frac{6 \cdot \mathbf{J}}{l^2} & \frac{2 \cdot \mathbf{J}}{l} & 0 & -\frac{6 \cdot \mathbf{J}}{l^2} & \frac{4 \cdot \mathbf{J}}{l} \end{bmatrix}$$

NUMERICAL EXAMPLE

As a simple example we consider GFRP beam with the fixed ends made of orthotropic thermoset vinyl ester class 1 GFRP under instantly applied distributed load $q = 10\ kN/m$. The beam is 12 m long and has a rectangular cross-section 20x30 cm. The characteristics of the material obtained experimentally in [7,8,9].

To solve the dynamic equilibrium equation, the method of the central differences is used [Бате]. In this case, the first and second order time derivatives of the displacement vector $\bar{V}(t)$ participating in (1) and (2) are approximated by central finite differences. Then the equation (1), obviously, takes the following form:

$$\frac{1}{\Delta t^2} \cdot M \cdot (\bar{V}_{i+1} - 2\bar{V}_i + \bar{V}_{i-1}) + \\ + \frac{1}{2 \cdot \Delta t} \cdot D \cdot (\bar{V}_{i+1} - \bar{V}_{i-1}) + \\ + K \cdot \bar{V}(t) = \bar{F}_i. \tag{16}$$

Here i = 1, 2, 3, … – number of the considered moment in time t, Δt – time increment.

In order to replace the classic damping model in (16) with the damping model with memory, at first we represent the central difference in the second term on the left-hand side of equation (16), which is responsible for damping, as average of the «forward» and «backward» differences:

$$\frac{1}{\Delta t^2} \cdot M \cdot (\bar{V}_{i+1} - 2\bar{V}_i + \bar{V}_{i-1}) + \\ + \frac{1}{2 \cdot \Delta t} \cdot D \cdot (\bar{V}_i - \bar{V}_{i-1}) + \\ + \frac{1}{2 \cdot \Delta t} \cdot D \cdot (\bar{V}_{i+1} - \bar{V}_i) + \\ + K \cdot \bar{V}(t) = \bar{F}_i. \tag{17}$$

The term with the «backward» difference is replaced by nonlocal numerical operator:

$$\frac{1}{2 \cdot \Delta t} \cdot D \cdot (\bar{V}_i - \bar{V}_{i-1}) \rightarrow \\ \rightarrow \frac{D}{2} \sum_{j=1}^{i} \bar{G}(i,j) \left(\bar{V}_j - \bar{V}_{j-1}\right), \tag{18}$$

where i – number of the time step which is corresponding to the considered time moment t,

$t = \Delta t \cdot i$, $\tau = \Delta t \cdot j$, $j = 1, 2, \ldots, i$ – number of the time step when calculating the kernel $\bar{G}(i,j)$.

$\bar{G}(i,j)$ is the discrete analogue of $G(t-\tau)$ kernel, which for the error function (5) is calculated as follows:

$$\bar{G}(i,j) = \frac{2\mu}{\sqrt{\pi}} \cdot e^{-\mu^2\left(t-\left(\tau-\frac{\Delta t}{2}\right)\right)^2}. \tag{19}$$

After the described transformations equation (17) can be written as:

$$\frac{1}{\Delta t^2} \cdot M \cdot (\bar{V}_{i+1} - 2\bar{V}_i + \bar{V}_{i-1}) + \frac{D}{2} \cdot \bar{Z} + \\ + \frac{1}{2 \cdot \Delta t} \cdot D \cdot (\bar{V}_{i+1} - \bar{V}_i) + \\ + K \cdot \bar{V}(t) = \bar{F}_i, \tag{20}$$

Where

$$\bar{Z} = \sum_{j=1}^{i} \frac{2\mu}{\sqrt{\pi}} e^{-\mu^2[t-(\tau-\Delta t/2)]^2} \cdot \\ \cdot \left(V_j - V_{j-1}\right). \tag{21}$$

The influence distance μ determine the nonlocality level in element material. The higher is μ, the closer is the damping model to the classic local one (fig. 1).

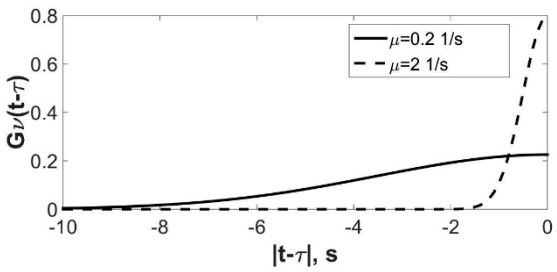

Figure 1. Error kernel functions for different influence distance parameters μ

Transform (20) to the computational scheme for the step-by-step calculating of $\bar{V}_{i+1}$ using the vectors $\bar{V}_i$ and $\bar{V}_{i-1}$, which are calculated on the previous increments i and $i-1$:

$$\bar{V}_{i+1} = Q \cdot \bar{F}_i - Q_1 \cdot \bar{V}_i - \\ Q_2 \cdot \bar{V}_{i-1} - Q_3 \cdot \bar{Z}, \tag{22}$$

where:

$$Q = \left(\frac{1}{\Delta t^2} M + \frac{1}{2 \cdot \Delta t} D\right)^{-1}, \\ Q_1 = Q \cdot \left(-\frac{2}{\Delta t^2} M - \frac{1}{2 \cdot \Delta t} D + K\right), \\ Q_2 = \frac{1}{\Delta t^2} Q \cdot M, \\ Q_3 = \frac{1}{2} Q \cdot D. \tag{23}$$

For the first two steps of the simulated vibration process $i = 1,2$ we assume $\bar{V}_1 = 0$ and $\dot{\bar{V}}_1 = \frac{\bar{V}_2 - \bar{V}_1}{\Delta t} = 0$ as the initial conditions.

The main problem of all nonlocal models [10, 11, 12] is obtaining the value of the influence distance, which characterizes the nonlocal damping properties of the material. The solution of this problem with regard to damping model nonlocal in space was proposed in [13]. In that paper μ was determined using the least squares method based on the numerical simulation data. Likewise, here the calibration of the nonlocal in time damping model was implemented based on the results of the numerical simulation of three-dimensional finite element beam vibration in SIMULIA Abaqus CAE. The beam computational model was constructed in SIMULIA Abaqus taking into account the orthotropic properties of the material. The determined optimum value of μ for the beam, that was considered in privious section, is $\mu = 0.1\ 1/s$. The displacements of middle section of the beam in time are shown in fig. 2. The solid line shows the displacements of the beam which is obtained using a calibrated nonlocal model, and the dashed curve - using a 3D model built in SIMULIA Abaqus.

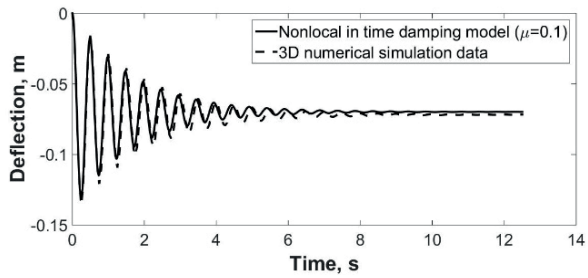

Figure 2. Deflection of the beam obtained with calibrated nonlocal in time damping model in comparison to 3D numerical simulation data

It is obvious, that calibrated nonlocal model allows to obtain much more accurate results, than the Kelvin-Voight classic model (fig. 3).

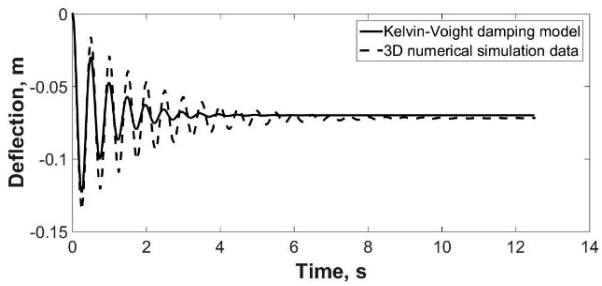

Figure 3. Deflection of the beam obtained with classic local in time damping model in comparison to 3D numerical simulation data

CONCLUSION

Nonlocal in time damping model presented in this paper makes it possible to quite effectively use one-dimensional models of beam elements in the dynamic analysis of structures which are made of modern composite materials.

The damping matrix, obtained from the stationarity requirements of the energy change, allows to consider internal friction which is the dominant type of damping for the polymer composites.

The damping with memory model can be seamlessly integrated to the FEA algorithm, which makes it applicable to the real-life engineering problems.

ACKNOWLEDGEMENT

This research has been supported by the Russian Science Foundation (Project No 21-19-00634).

REFERENCES

1. **Sorokin E.S.** On the theory of internal friction during vibrations of elastic systems. 1960, Gosstroyizdat, Moscow, (in Russian).
2. **Sidorov V.N., Badina E.S.** Computer Simulation of Structural Vibration Damping With Allowance for Nonlocal Properties, 2020 // International Journal for Computational Civil and Structural Engineering, Volume 16, Issue 4, pp. 84-90.
3. **Bathe K.J., Wilson E.L.** Numerical methods in finite element analysis. 1976, Prentice Hall, New York.
4. **Banks H.T., Inman D.J.** On damping Mechanisms in Beams Journal of Applied Mechanics. 1991, 58(3), pp. 716–723.
5. **Alexandrov A.V., Potapov V. D., Zylyov V.B.** Structural mechanics. In 2 books. Book 2. Dynamic and stability of the elastic systems. 2008, Highschool, Moscow (in Russian).
6. **Sidorov V.N.** Mechanics of materials. “Architechture-S”. 2013, Moscow – 395 pp (in Russian).
7. **Landherr J.C.** Dynamic analysis of a FRP deployable box beam. Master of Applied Science Thesis. Kingston: Queen's University, 2008.
8. **Lim R.A.** Structural monitoring of a 10m fibre reinforced polymer bridge subjected to severe damage (Kingston: Queen's University), 2016.
9. **Xie A.** Development of an FRP Deployable Bridge, Master of Applied Science Thesis, Department of Civil Engineering, Royal Military College of Canada, 2007.
10. **Lei Y., Friswell M.I., Adhikari S**. A Galerkin Method for Distributed Systems with Non-local Damping Int. Journal of Solids and Structures 43, p. 3381–3400, 2006.

11. **Eringen A.C., Edelen D.G.B.**, 1972, Nonlocal elasticity. Int J Eng Sci; 10(3): 233–48.
12. **Polizzotto C.** Nonlocal elasticity and related variational principles. Int J Solids Struct; 2001, 38 (42–43): 7359-80. DOI: 10.1016/S0020-7683(01)00039-7.
13. **E.S. Shepitko, V.N. Sidorov.** Defining of nonlocal damping model parameters based on composite beam dynamic behaviour numerical simulation results, 2019 // IOP Conf. Series: Materials Science and Engineering 675 012056.

СПИСОК ЛИТЕРАТУРЫ

1. **Сорокин Е.С.** К теории внутреннего трения при колебаниях упругих систем – Москва: Госстройиздат, 1960, 131 с.
2. **Sidorov V.N., Badina E.S.** Computer Simulation of Structural Vibration Damping With Allowance for Nonlocal Properties // International Journal for Computational Civil and Structural Engineering, Volume 16, Issue 4, 2020 – с. 84-90.
3. **Bathe K.J., Wilson E.L.** Numerical methods in finite element analysis. Prentice Hall, New York, 1976.
4. **Banks H.T., Inman D.J.** On damping Mechanisms in Beams Journal of Applied Mechanics 58(3), 1991, pp. 716–723.
5. **Александров А.В., Потапов В.Д., Зылёв В.Б.**, Строительная механика. В 2-х книгах. Книга 2. Динамика и устойчивость упругих систем. Издательство: Высшая школа, 2008.
6. **Сидоров В.Н.** Сопротивление материалов. Издательство «Архитектура-С», 2013**,** – 395 стр.
7. **Landherr J.C.** Dynamic analysis of a FRP deployable box beam. Master of Applied Science Thesis. Kingston: Queen's University, 2008
8. **Lim R.A.** Structural monitoring of a 10m fibre reinforced polymer bridge subjected to severe damage (Kingston: Queen's University), 2016.
9. **Xie A.** Development of an FRP Deployable Bridge, Master of Applied Science Thesis, Department of Civil Engineering, Royal Military College of Canada, 2007
10. **Lei Y., Friswell M.I., Adhikari S.** A Galerkin Method for Distributed Systems with Non-local Damping Int.Journal of Solids and Structures 43, 2006, pp. 3381–3400.
11. **Eringen A.C., Edelen D.G.B.** Nonlocal elasticity. Int J Eng Sci;10(3):233–48. 1972.
12. **Polizzotto C.** Nonlocal elasticity and related variational principles. Int J Solids Struct; 2001, 38(42–43):7359-80. DOI: 10.1016/S0020-7683(01)00039-7
13. **E.S. Shepitko, V.N. Sidorov.** Defining of nonlocal damping model parameters based on composite beam dynamic behaviour numerical simulation results. 2019 // IOP Conf. Series: Materials Science and Engineering 675 012056

Vladimir N. Sidorov, Corresponding Member of Russian Academy of Architecture and Construction Science, Professor, Dr.Sc, Rectorate Counselor, Head of the Department of Computer Science and Applied Mathematics, National Research University Moscow State University of Civil Engineering, Professor of «Building Structures, Buildings and Facilities» Department, Institute of Railway Track, Construction and Structures, Russian University of Transport (MIIT), Professor of Department «Engineering Structures and Numerical Mechanics», Perm National Research Polytechnic University; 127994, Russia, Moscow, Obraztsova st., 9, b. 9, phone: +74956814381, e-mail: sidorov.vladimir@gmail.com.

Elena S. Badina, Ph.D, Associate Professor of «Computer Aided Design» Department, Institute of Railway Track, Construction and Structures, Russian University of Transport (MIIT), Senior Researcher at the Scientific and Educational Center for Computer Modeling of Unique Buildings, Structures and Complexes of the Moscow State

University of Civil Engineering, Senior Researcher at the Department of Mechanics of Structured and Heterogeneous Environment of the Institute of Applied Mechanics of the Russian Academy of Sciences; 127994, Russia, Moscow, Obraztsova st., 9, b. 9, phone: +74956092116, e-mail: shepitko-es@mail.ru.

Elena P. Detina, Research Engineer, Department of Analytical Fundamental Scientific Research on the Dynamics of Building Structures, Scientific and Educational Center for Computer Modeling of Unique Buildings, Structures and Complexes (REC KM), Lecturer at the Department of Applied Mathematics and Informatics, Moscow State University of Civil Engineering (NRU MGSU); 129337, Russia, Moscow, Yaroslavskoe shosse, 26, phone +74957819988, e-mail: detinaep@mgsu.ru

Сидоров Владимир Николаевич, член-корреспондент РААСН, профессор, доктор технических наук, советник при ректорате, заведующий кафедрой информатики и прикладной математики Национального исследовательского Московского государственного строительного университета, профессор кафедры «Строительные конструкции, здания и сооружения» Института пути, строительства и сооружений Российского университета транспорта (МИИТа); 127994, Россия, г. Москва, ул. Образцова, д.9, стр. 9, телефон: +74956814381, e-mail: sidorov.vladimir@gmail.com.

Бадьина Елена Сергеевна, кандидат технических наук, доцент кафедры «Системы автоматизированного проектирования» Института пути, строительства и сооружений Российского университета транспорта (МИИТа), старший научный сотрудник Научно-образовательного центра компьютерного моделирования уникальных зданий, сооружений и комплексов Московского государственного строительного университета, старший научный сотрудник Отдела механики структурированной и гетерогенной среды Института прикладной механики Российской академии наук, 127994, Россия, г. Москва, ул. Образцова, д.9, стр. 9, телефон: +74956092116, e-mail: shepitko-es@mail.ru.

Детина Елена Петровна, инженер-исследователь отдела аналитических фундаментальных научных исследований по динамике строительных конструкций Научно-образовательного центра компьютерного моделирования уникальных зданий, сооружений и комплексов (НОЦ КМ), преподаватель кафедры Прикладной математики и информатики Московского государственного строительного университета (НИУ МГСУ); 129337, Россия, г. Москва, Ярославское шоссе, д. 26, телефон +74957819988, e-mail: detinaep@mgsu.ru

DOI:10.22337/2587-9618-2021-17-4-22-39

CRITICAL REVIEW OF PHYSICAL MODELLING OF SNOW ACCUMULATION ON ROOFS WITH ARBITRARY GEOMETRY

Alexander M. Belostotsky [1,2,3]***, Oleg S. Goryachevsky*** [1,2]***, Nikita A. Britikov*** [2,3]

[1] Scientific Research Center StaDyO, Moscow, RUSSIA
[2] National Research Moscow State University of Civil Engineering, Moscow, RUSSIA
[3] Russian University of Transport (RUT-MIIT), Moscow, RUSSIA

Abstract. A review of the most significant domestic and, due to numerical superiority, foreign works on physical modelling of snow transport and snow accumulation processes, in particular, for the purpose of determining snow loads on roofs with arbitrary geometry, is presented. The existing practice of development of recommendations on assignment of snow loads in Russian laboratories is considered and critically evaluated. Comparison of do-mestic works with scientific articles in the advanced world scientific journals and foreign regulatory documents leads to unfavorable conclusions. Recommendations on assigning snow loads, issued by Russian laboratories on the basis of extremely outdated and poorly substantiated methodology, bear a serious risk for evaluating mechan-ical safety of modern structures, for which such recommendations are developed. Recommendations are offered to remedy this current dangerous practice. The article also gives some suggestions on forming a basis for field observations of snow loads on existing roofs.

Keywords: physical modeling, wind tunnel, water flume, snow accumulation, structure roofs.

МЕТОДЫ ФИЗИЧЕСКОГО МОДЕЛИРОВАНИЯ СНЕГОНАКОПЛЕНИЯ НА ПОКРЫТИЯХ СООРУЖЕНИЙ ПРОИЗВОЛЬНОЙ ФОРМЫ КРИТИЧЕСКИЙ ОБЗОР

А.М. Белостоцкий [1,2,3]***, О.С. Горячевский*** [1,2]***, Н.А. Бритиков*** [2,3]

[1] Научно-исследовательский центр СтаДиО, г. Москва, РОССИЯ
[2] Национальный исследовательский Московский государственный строительный университет, г. Москва, РОССИЯ
[3] Российский университет транспорта (МИИТ), г. Москва, РОССИЯ

Аннотация: Представлен обзор наиболее значимых отечественных и, по вынужденному преимуществу, иностранных работ по физическому моделированию процессов снегопереноса и снегонакопления, в частности, для целей определения снеговых нагрузок на покрытия сооружений произвольной формы. Рассматривается и критический оценивается существующая практика разработки рекомендаций по назначению снеговых нагрузок в российских лабораториях. Сравнение отечественных работ с научными статьями в передовых мировых научных изданиях и иностранными нормативными документами приводит к неутешительным выводам. Рекомендации по назначению снеговых нагрузок, выдаваемые российскими лабораториями на основе крайне устаревшей и плохо обоснованной методики, несут серьезный риск для оценки механической безопасности современных сооружений, для которых такие рекомендации разрабатываются. Предложены рекомендации для исправления этой сложившейся опасной практики. В статье также даются некоторые предложения по формированию базы натурных наблюдений снеговых нагрузок на существующих покрытиях.

Ключевые слова: физическое моделирование, аэродинамическая труба, экспериментальный водосток, снегонакопление, покрытия сооружений.

INTRODUCTION

At present, the most widespread approach in Russia and abroad to determining snow loads on roofs with arbitrary geometry is physical simulation of snow accumulation in a wind tunnel (hereinafter, WT) or a water flume. Despite the long history of the issue, among the domestic publications there are no full-fledged review studies sufficiently covering the historical and modern practices. Such an information vacuum in the Russian scientific field creates prerequisites for oversimplification and distortion of the methods of relevant experiments developed, tested and time-proven in advanced scientific laboratories of the world. Unfortunately, domestic laboratories actively use these prerequisites of general ignorance, which carries significant risks for the adequate assessment of the mechanical safety of unique and critical structures, for which the corresponding research is conducted. The authors hope that this article will direct the development of domestic techniques for physical modelling of snow accumulation towards the implementation of best scientific practices.

Apparently, one of the first scientists to conduct large-scale physical experiments to simulate snow drift and compare them with field data was Finney [1] in 1934. His experiments to simulate snow transport near road barriers were carried out at an intuitive level. Similarity issues, cohesion of the snow-like material, wind profile and other important modelling subtleties were not addressed in the study.

The greatest contribution to the development of physical modelling of snow accumulation and snow drift, including on roofs of buildings and structures, was made by foreign scientists: Anno [2-4], Irwin [5-7], Iversen [8-9], Kind [10-11], Odar [12-13] and Izyumov [14-15]. This list of authors and their works is far from complete.

There are only a few Russian papers on the subject matter of this article. Some of them focus on field measurements and the creation of snow zoning maps [51-55]. Another part of works is devoted directly to snow loads on roofs [57-59]. It should be noted that only a few papers [52, 55] are of a high scientific level and the other ones are either reports or blatant compilations (the paper [56] is simply a translation of the corresponding chapter of the ASCE standard [19], even without referencing the original source).

MAIN APPROACHES TO PHYSICAL MODELLING OF SNOW ACCUMULATION

One of the most extensive studies of determin-ing the snow loads, including a synthesis of previous accumulated experience, many new experiments and scientific conclusions, was carried out as part of the Eurocode development [17, 18]. The study elaborates in detail the improvement of snow zoning maps of European territories, assignment of load combination coefficients (including snow load), and distribution of snow loads on the roofs of buildings and structures. As far as the snow load distribution is concerned, much attention is given to description of the field measurements performed, large-scale experiments at the climatic WT (CSTB, France) and details of processing the results. A thorough description of the conditions and the results of many experiments in graphical (photos, graphs, diagrams, etc.) and tabular form make this study a kind of reference book, which can be used as a basis for one's own research.

The study [17, 18] clearly and unambiguously shows that it is very difficult to carry out field observations of snow loads on the roofs of buildings. A sufficiently large sample of data is necessary for the correct statistical processing of the results and the determination of dependencies. Snow loads are influenced not only by the geometry of the building (controllable parameter), but also by climatic factors (uncontrollable parameters) and landscape (partially controllable parameters), so multi-year studies in different climatic zones and landscapes are necessary. Unfortunately, a study [17, 18] of snow load distributions on the roofs of buildings located near weather stations in several European countries was conducted only for one season. Many of the field data proved to

be unrepresentative due to low snowfall winters in the respective areas, unfortunate location selection and other reasons. The data obtained did not allow to conduct a full regression analysis to determine the dependence of the shape coefficient on climatic factors and the geometry of the building. Nevertheless, dependencies of shape coefficient on roof pitch, wind speed and ambient temperature were obtained with satisfactory reliability.

Due to the aforementioned shortcomings, field experiments do not allow the distribution of snow loads on different roof shapes to be fully normalized. The main data for the normalization of the shape coefficient μ [19] was obtained through experiments in the CSTB climatic WT.

The CSTB climatic WT experiments were performed with fairly large scale models (1:10) and real snow generated by a snow cannon (Fig. 1). Different temperature and humidity regimes and two characteristic wind regimes were considered

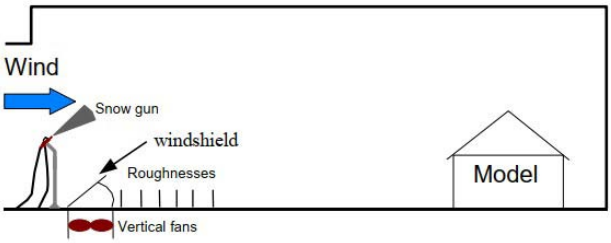

a)

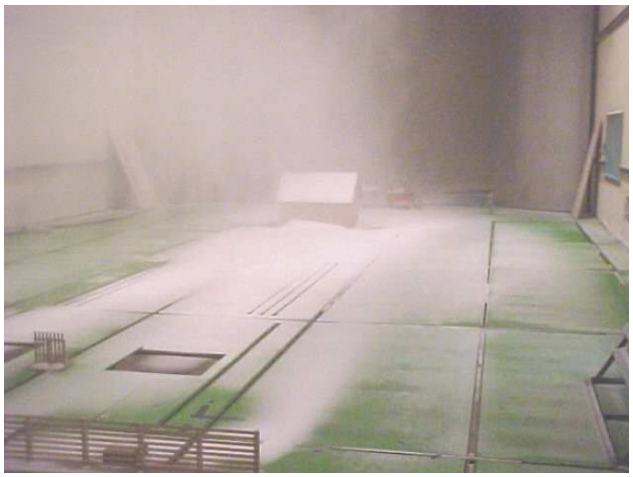

b)

Figure 1. a) Diagram of an experimental setup for simulating snow loads; b) photograph of the experiment process [18]

a) gable roof with lantern and extended edges

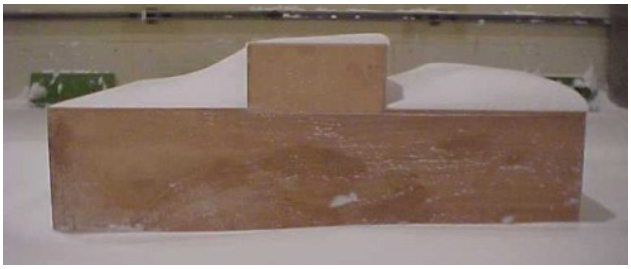

b) multi-level roof

c) multi-span gable roof

d) cylindrical roof

Figure 2. The results of physical modeling of snow loads in the climatic WT CSTB [18]

(windless weather and snow storm were simulated). This approach made it possible to obtain physical pictures of snow distribution (Fig. 2), which distinguishes these experiments from domestic works on experimental determination of the shape coefficient on complex roofs carried out as part of scientific and technical support for construction. The small scale (usually 1:300), the use of snow-like material, and modelling only the entrainment of material without modelling snowfall, result in snow load distribution patterns that obviously have nothing to do with reality (Fig. 3).

One of the important conclusions of the study [18] is the experimental confirmation that the snow density on the building roof is quite strongly dependent on the location (windward or leeward), that is, wind pressure tamps the snow. It is not possible to take this factor into account adequately with snow substitutes.

Large-scale experiments to simulate snow transport and snow deposition fall into two major categories [20]:

1. Particle methods. Experiments are conducted in WTs or special water flumes. The essence of the

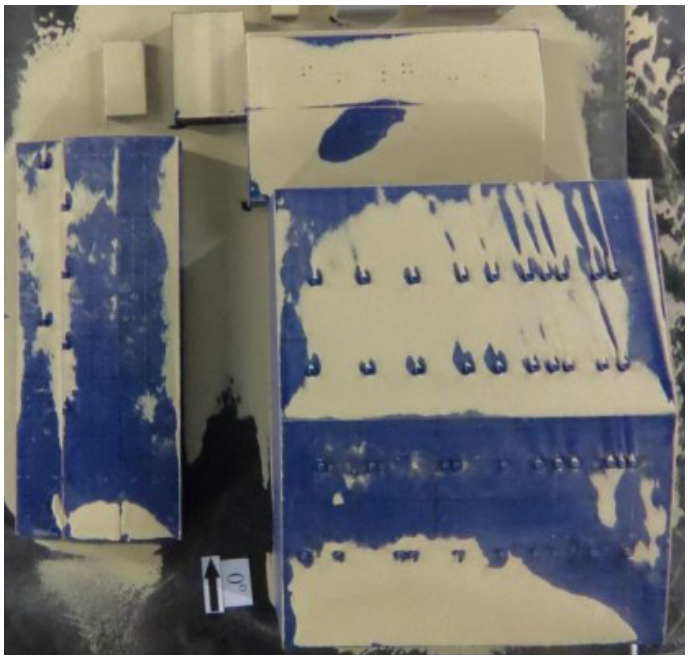

a) UNIKON

b) National Research Moscow State University of Civil Engineering

c) Research Institute of Mechanics, Moscow State University

Figure 3. Results of modeling snow loads in WTs

methods is to simulate snow storms by introducing snow particles or snow substitutes into the flow [44].

2. Methods that measure the nature of wind speeds around a scale model, and snow deposition and snow transport are calculated numerically using field snow data and other climatic information from the nearest weather stations. Snow particles in this approach may or may not be modeled.

Snow accumulation modelling in a water flume is a fairly common approach in foreign practice (e.g. used by the Canadian RWDI). The essence of the method is that a model of a structure is placed under water in a specially designed flume (Fig. 4a). Then water with sand [6, 21, 22] or crushed walnut shells [23] is passed through the flume. Despite the unphysicality of the obtained distributions (Fig. 4b), the experiments in the flume are conducted to determine the locations of potential snow bags. Thus, the results obtained are not used as calculation schemes of snow loads, but are of an auxiliary nature. Note that recommendations for assigning snow loads to the Otkritie Arena roof were developed by RDWI using the described method [35].

Due to the small number of climatic WTs, in most cases researchers have resorted to using snow-like materials in conventional WTs. In the absence of the technical feasibility of introducing snow substitutes into the flow, an even more simplified approach is used, where the material is only poured on the model, and a snowless hurricane condition is actually investigated. Obviously, winter storms without significant snowfall are very rare and do not lead to the largest snow loads. Therefore, the use of such a maximally simplified approach can only be justified by the technical unfitness of WT, rather than by the substantiated features of the scientific approach.

PARTICLE METHODS AND SNOW SUBSTITUTES

Many kinds of snow substitutes can be used with particle methods: sodium tetroborate [24, 25], rice bran [15], sawdust (Fig. 3) [27, 28, 58, 59], clay [4], foam balls [29, 34] (Fig. 5), quartz sand (Fig. 6) [30], baking soda [31], glass beads [10].

Due to a great variety of such materials, studies have been repeatedly carried out to compare them. For example, in [26] wood ash, styrofoam and silica sand are compared under otherwise equal conditions in WT. The comparison indicates that the quartz sand matches the field data better. However, the studies were only carried out on a simple two-level roof geometry

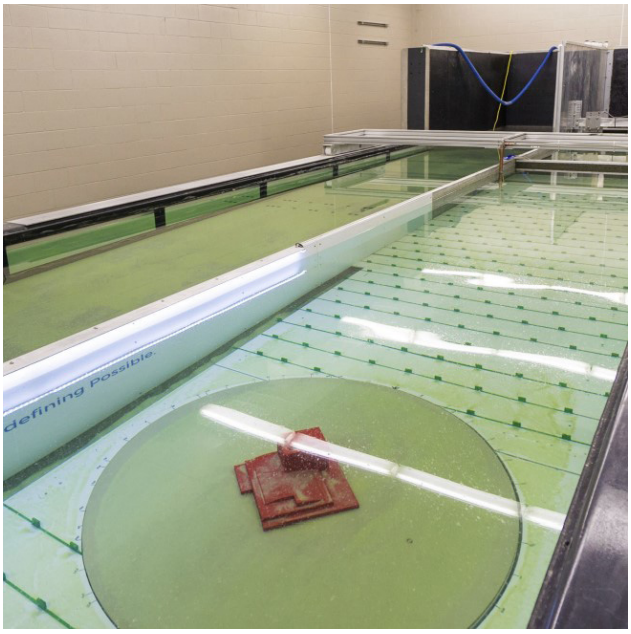

a) before draining the water

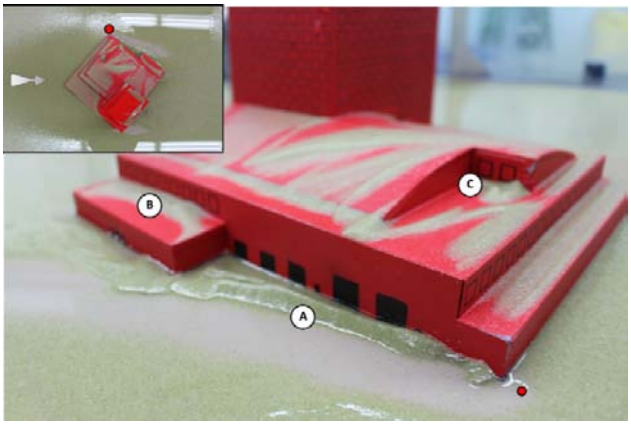

b) after draining the water

Figure 4. Results of an experiment in a water flume [22]

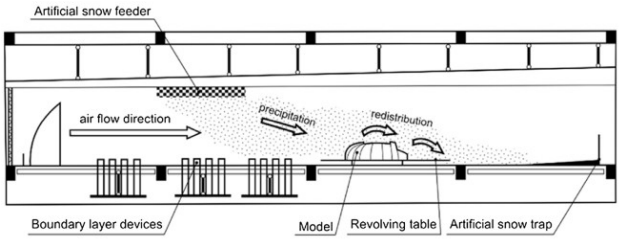

a) the experimental setup

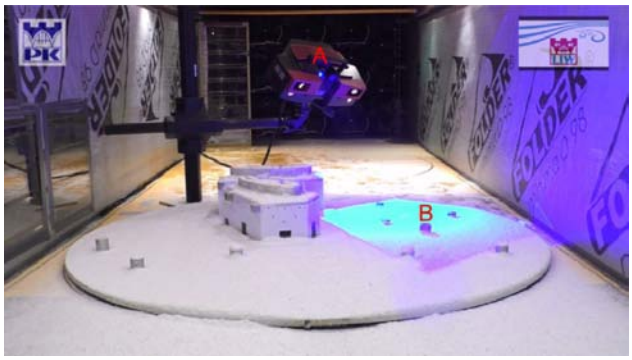

b) the process of 3D scanning of the experimental results

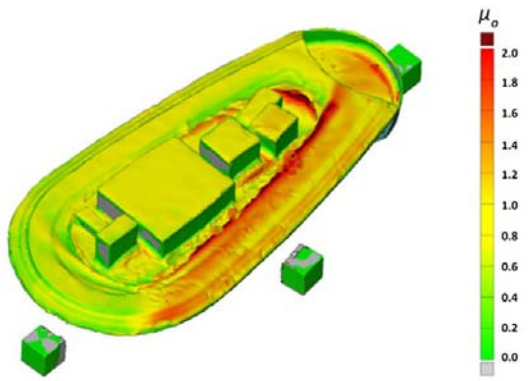

c) shape coefficient μ (snow hurricane simulation)

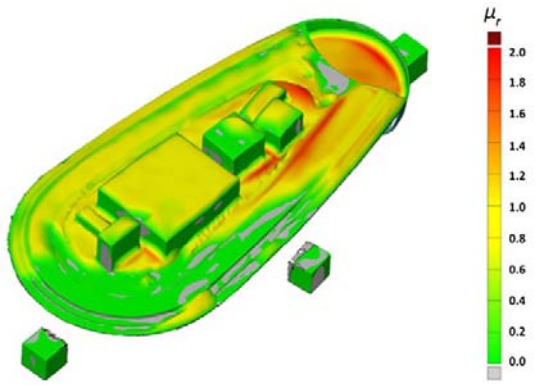

d) shape factor μ

Figure 5. Physical modeling using foam as a snow simulator [34]

and the measurements are provided only for the lower level, whereas practice shows that it is on the upper levels that full drift of snow-like material is observed, which is not consistent with the physical considerations and the field data.

According to the ASCE standards [20], the results obtained by the particle methods in assigning snow loads are of an exclusively qualitative nature and should be used in conjunction with regulatory schemes for simple structures, field and climatic data of the construction site. Unfortunately, recommendations on assignment of snow loads, developed by domestic organizations on the basis of blowing in WT, completely lack a comprehensive approach. In fact, schemes of snow loads are given only on the basis of digitization of obtained snow distribution patterns (Fig. 7).

One of the disadvantages of the particle method is the inability to account for snow accumulation over a long period of time (weeks and months) from different wind directions and wind speeds, temperature and humidity conditions. In order to take these factors into account, the ASCE standards [20] recommend using the

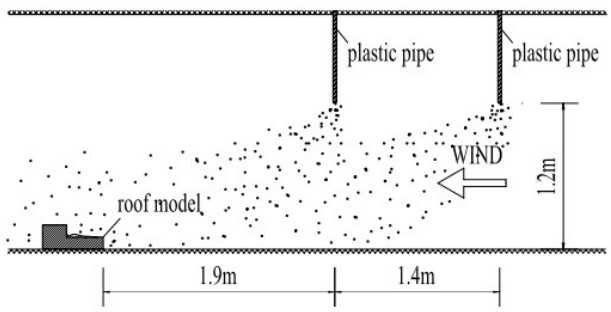

a) the experimental setup

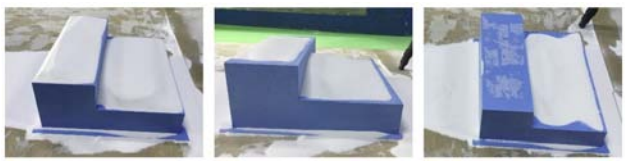

b) results at different wind speeds (from left to right, the wind velocity increases)

Figure 6. Physical modeling using silica sand as a snow-like material [30]

second category of methods [33], which is numerical modelling based on the results of blowing in WT. At that, it is proposed to first use blowing data without snow substitutes (time step method A), determine the most dangerous angles (taking into account data from the nearest weather stations) and then conduct experiments with substitutes for the corresponding angles (time step method B). In both time step methods, all experimental data obtained together with meteorological data are used only as input parameters for numerical modelling of snow loads during the whole winter period.

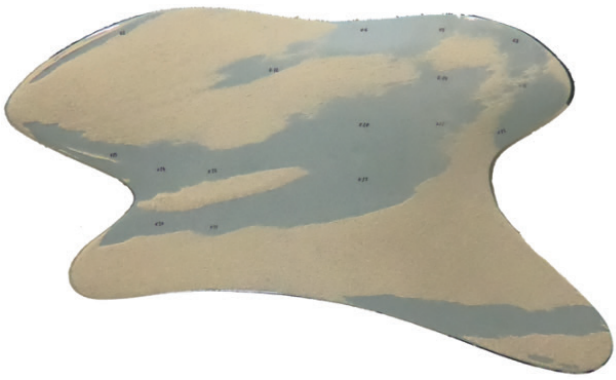

a) distribution of the snow simulator after blowing

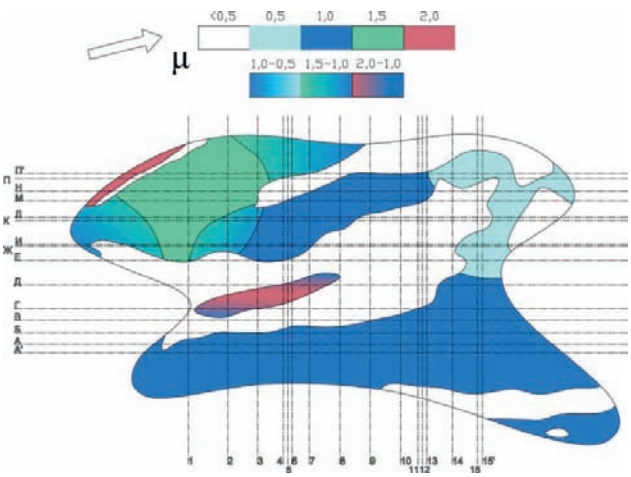

b) recommendations for the appointment of the shape factor μ

Fig. 7 An example of the interpretation of the results of physical modeling "Krylov State Scientific Center"

SIMILARITY CONDITIONS

It is not possible to achieve complete simulations of snow transport and snow accumulation through scaled-down experiments in WTs or water flumes. Nevertheless, the ASCE standards [20], based on a number of scientific papers [7, 12, 32, 36], put forward several requirements for similarity parameters. Firstly, the following expressions must coincide in the scaled model and the full model:

$$\frac{w_t}{U}, \quad \frac{U^2}{Lg\beta}, \tag{1}$$

where w_t is limiting velocity of falling particles, U is average velocity at a characteristic point, L is characteristic building size, g is acceleration due to gravity, $\beta = (\gamma - 1)(\gamma + \gamma_a)$ is ratio of particle density to air or liquid density, γ_a is additional contribution to γ, due to the coupled mass effect. For air, $\gamma_a \approx 0$, $\beta \approx 1$ (air density is low), for water used in flumes, $\gamma_a \approx 0.5$, and for sand, $\beta \approx 0.5$.

The first parameter means that the ratio of particle velocity to flow velocity is the same as in full scale. The second parameter is the densimetric Froude number, the equality of this parameter in real and model ensures that the ratio of aerodynamic force to gravitational force is correct. Satisfying these two parameters can be enough for problems where the interaction of snow particles with surfaces and with each other is not important (for example, the initial deposition of falling snow under the action of the wind or tracking of particles falling from a higher surface to a lower one).

Other parameters must also be observed to correctly account for particle interactions, though. For example, to simulate saltation, the interaction of snow particles with the snow surface must be properly accounted for. An important

parameter then is the ratio of the average flow velocity U to the threshold velocity of the onset of transport U_{th}:

$$\frac{U}{U_{th}} \tag{2}$$

An additional requirement is imposed on the mass flux dependence for the model. The model flux must have a dependence similar to the full-scale flux. The flux can be expressed in the following dimensionless form:

$$\frac{q}{\rho_p h_s U_{th}} = cf\left(\frac{U}{U_{th}}\right), \tag{3}$$

where ρ_p is particle density, h_s is the height at which U is defined in (3), c is dimensionless constant (can be different in model and full scale), $h_s = 0.5-1m$ usually (should be much smaller than the size of the building). The function f must be identical for the model and full scale.

It is shown in [32] that if the ratio (2) is neither too large nor too small, satisfying it has little effect on the experimental result. However, a note is made that this may not be the case for all model geometries. If we discard condition (2), then condition (3) is also not necessary.

Expression (3) can be used to determine the dimensionless time [36]:

$$\bar{t} = \frac{cU_{th}h_s}{L^2}t, \tag{4}$$

where t is dimensionless time, which has the same value in scale and full-scale models. The model time and full-scale time can be found from the following expression:

$$\frac{t_p}{t_m} = \frac{\left(cU_{th}h_s\right)_m}{\left(cU_{th}h_s\right)_p} = \left(\frac{L_p}{L_m}\right)^2, \tag{5}$$

where the indices p and m denote the full-scale model (prototype) and scaled-down model, respectively. Thus, the time of the experiment depends on the square of the characteristic size of the model $L_m{}^2$.

It is shown in [12] that the following conditions must be satisfied:

$$\frac{u_{*th}^3}{2gv} \geq 30, \tag{6}$$

$$\gamma \geq 600, \tag{7}$$

where u_{*th} is threshold surface shear stress rate for saltating snow, v is kinematic viscosity. Inequality (6) imposes a requirement for minimum Reynolds numbers and inequality (7) imposes a requirement for minimum density ratio. For water flumes, inequality (7) is not fulfilled.

Condition (1) is easily satisfied in WTs, but then it proves impossible to satisfy conditions (2), (6) and (7), which have an impact on saltation. To meet (1), the flow velocity is too low to initiate saltation. Usually, for WTs the requirements for densimetric Froude number are relaxed and instead relations (2), (6) and (7) are satisfied. Failing to satisfy the densimetric Froude number results in exaggerated length and height of the trajectories of the saltating particles.

In water flumes it is possible to satisfy conditions (1), (2) and (6), but due to high water density it is not possible to satisfy condition (7). This also affects physicality of modelling, for dunes and ripples can form on smooth surfaces.

Due to the problems with satisfying the similarity conditions, in the ASCE standards [20] it is recommended to place a reference model (e.g. a two-level roof) next to the model under study, for which the normative distributions of snow load are known. The quality of the experiments performed is then assessed by the degree of consistency with the reference model. The reference model is also used to determine the abso-

lute value of the shape coefficient μ on the investigated roof.

PHYSICAL MODELLING AS A MEANS FOR DEVELOPING ADEQUATE MATHEMATICAL MODELS

The development of methods of numerical modelling of snow transport and snow accumulation is impossible without previous extensive experimental work. Field and large-scale experiments in climatic WTs are necessary to identify dependencies, determine empirical parameters and verify the developed mathematical models and the algorithms implementing them.

Most of the current numerical approaches to modeling snow transport and snow deposition are based on the development of the so-called CFD methods. To verify the CFD-based methods being developed, it is necessary to experimentally investigate not only the motion of snow masses in the air flow, but also the effect of particles in saltation and suspension on the air flow. Experimental studies of air-snow flow over surfaces form the basis of existing mathematical approaches to modelling of saltation and suspension [37]. The most significant works in this area are listed below.

The most applied empirical dependencies for snow transport velocity were obtained as early as in the last quarter of the 20th century in the works of American [38] and Canadian scientists [39]. However, the universality of the results obtained in these works has never been proven.

Takeuchi [40] carried out field measurements using a snow trap to study the longitudinal distribution of the total snow transport rate, including saltation and suspension. Tabler [41] determined the dependence of seasonal snow transport on the movement of the precipitation zone in the design of fences. Both studies report that the overall snow transport rate reaches an equilibrium state only over areas of a few hundred meters.

In CFD modelling, surface roughness parameters affecting the wind profile and turbulence characteristics near models are important. In mathematical modelling of snow transport this issue is equally important. Significant studies of snow roughness have been conducted on the basis of data from Antarctica obtained by the SANAE IV expedition [42] and participants of the ALW program [43].

MEASUREMENT TECHNIQUES

This section addresses the measurements used in field observations and large-scale experiments to investigate snow transport and snow accumulation. An overview of measurement methods is not the purpose of this work, so the information given is far from complete. However, knowledge of current technical measurement capabilities gives a better understanding of what can and should be done for snow load research, which is especially relevant in our country. The review does not cover the measurement methods traditionally used in wind load and flow studies.

The known problems of field experiments are high financial cost, long periods of times and substantial labour costs. However, even without specially designed field experiments, simple field measurements of snow cover in winter on roofs of buildings and structures can be of great benefit. The creation of a special database containing snow distributions on different roofs, indicating the year, geographical location and available climatic and meteorological data will be invaluable for developing physical and mathematical modelling, improving the regulatory framework and will be a visual reference for practicing calculation engineers to form an intuitive understanding of snow mechanics. Special atlases [45-47] serve as analogues of such databases in aerodynamics, alt-

hough they are largely outdated now. Increasingly popular machine learning methods require large data sets for their implementation to train neural networks. Such a database could provide suitable material for training.

With the use of drones, modern cameras and special software (all of which are now available at a ridiculously low prices by the standards of modern science), collecting a database of snow distribution on roofs of any shape is not an insurmountable task. Existing photo-processing methods provide three-dimensional pictures of snow distribution with an accuracy that exceeds the practical needs of construction [48]. This digital approach does not require measuring levels or other sensors to be installed on the roofs of buildings [18, 54], which usually presents considerable organizational and technical difficulties.

The results of experiments in WTs or water flumes can be handled in a similar way [49], although a more accurate and technologically advanced method would be to use a dedicated 3D scanner [34]. Previously, achieving snow distribution contours was done in a very simple way, which is by tracing the level on a cardboard submerged in snow or snow-like material [18]. Such a method allows to easily obtain snow distribution in the selected sections, but its main disadvantage is that the snow cap deteriorates with each measurement made.

Snow particle counters [50] for measuring point snow fluxes or high-speed cameras with subsequent software processing for measuring snow fluxes in the area are widely used in the world practice to investigate the processes of saltation and suspension.

RECOMMENDATIONS FOR UPGRADING DOMESTIC WTS AND IMPROVING PHYSICAL MODELLING TECHNIQUES

The above materials clearly show the underdevelopment of the technical equipment of domestic WTs and the low level of the methodology used in developing recommendations for assigning snow loads to roofs with arbitrary geometry. These problems create risks when estimating mechanical safety of modern structures, including long-span structures, for which snow loads make the main contribution.

The following minimum recommendations can be given to remedy this situation:

1. It is necessary to modernize WTs in accordance with international experience:

1.1 Equip WTs with a snow substitute feeding system to simulate snow storms, rather than the rare snowless hurricanes that hardly ever occur in winter. Such systems come in a variety of forms depending on the WT characteristics, but in all cases, verification of the system with simple normative examples is required.

1.2. Equip WTs with the necessary measuring equipment to digitize the resulting snow substitute distribution patterns.

2. On the basis of international experience and in accordance with foreign regulatory documents, develop and verify a methodology for simulating snow loads on roofs with arbitrary geometry:

2.1. Different wind directions and velocities, snow accumulation over a long period of time (weeks and months) under different temperature and humidity regimes must be taken into account. The results of simulations of single snowstorms in the WT should be the input data for such a methodology, not its output.

2.2. The reference snow layer thickness should be determined either by blowing into an empty (without a model) WT or by comparison with a reference model placed next to the test one.

3. Develop regulatory documents [62] establishing requirements for testing in WTs in terms of snow load simulation: similarity conditions, preferred snow substitutes, characteristics of snow substitute feeding systems, measurement methods, etc.

CONCLUSIONS

1. A review of the development and current state of the methods of physical modeling of snow transport and snow accumulation has been conducted according to scientific publications and regulatory documents. A critical analysis of Russian publications and contractual works on the subject of the article is carried out.

2. The review has shown that the experimental works carried out in Russia for the purpose of determining the shape coefficient μ are methodologically at a dismally low level, even in comparison with foreign works of half a century ago:

2.1. Russian WTs do not actually simulate individual snow storms or snowfalls, but rather simulate the removal of a uniform layer of snow from roof during strong winds. This primitive approach has not been used in any foreign laboratory recognized by the world scientific and regulatory community for a long time.

2.2. The reason for the widespread choice of wood flour as a snow-like material is unclear, especially since a number of studies show that silica sand matches the field data best.

2.3. The choice of the reference value of snow cover thickness necessary to calculate the shape coefficient μ is arbitrary and is not based on anything. The reference snow thickness can be determined by the thickness of the snow substitute cover away from the model (or by blowing without the model) when simulating snowfall, or by comparison with a reference standard model of a simple shape, which is located next to the model under study. Neither of these approaches is used in Russian laboratories.

2.4. Recommendations for assigning the shape coefficient μ are "manufactured" from the results of elementary digitization of pictures of the remaining snow cover. Note that these pictures clearly contradict the physical meaning. This approach also directly contradicts foreign standards, where it is clearly stated that the resulting patterns are used as additional data for subsequent analysis and modelling.

2.5. Modelling in WTs or water flumes can reproduce the conditions of a snow storm or just snowfall. Thoughtless use of the results of these experiments for developing recommendations leads to the fact that snow distributions formed throughout the entire cold season by many snowfalls, different wind directions, thermal and moisture regimes are not taken into account at all.

2.6. The current practice in Russian laboratories casts serious doubt on the legitimacy of the recommendations being developed and poses significant risks to the mechanical safety of unique large-span buildings and structures.

3. The Russian Building Code SP 20.13330.2016 [61] prescribes that for buildings and structures with overall dimensions in plan exceeding 100 m, as well as in cases not stipulated in Annex B, model tests in WTs to determine the shape coefficient μ must be carried out. For some reason, it is not allowed to conduct tests in water flumes, which is an absolutely equal and recognized approach (both in regulatory documents and scientific publications) all over the developed world on a par with WTs.

4. Simultaneous satisfaction of all similarity conditions for modelling of snow transport and snow accumulation processes is impossible neither in WTs, nor in water flumes. Therefore, even the model tests carried out at the highest level never fully reproduce the real full-scale effects of creep, saltation and suspension. This situation, coupled with the continuous improvement of mathematical models, numerical methods, computer technologies and related software, makes the development and future implementation of numerical modelling in real construction practice and regulatory documents inevitable.

5. The best results of physical modelling of shape coefficient μ are obtained in large-scale tests in climatic WTs. Normative distributions

are easily guessed in these results for simple roof shapes. Climatic tests are rather complicated and costly (also in terms of time) for their direct application in the industrial sector, but they can be a powerful tool for the development of SP 20 in terms of introducing snow load schemes for more complex roof shapes.

6. Improvement of the regulatory framework, development of methods of both physical and mathematical modelling, is extremely difficult without full-scale experiments or measurements as well as large-scale tests in climatic WTs. Taking into account the lack of climatic WTs in Russia and the difficulties in organizing full-scale experiments, it is proposed to make full-scale measurements by means of drone photography and subsequent processing of the results. Such a low-cost method will make it possible to create a base containing snow distribution on different roofs with indication of year, geographical location and available climatic and meteorological data, which will give an impetus for development of physical and mathematical modeling, improvement of normative base and will be a visual reference for practicing engineers.

7. Recommendations on modernization of domestic WTs, improvement of methodologies and standard-setting to correct the current dangerous practice of domestic laboratories developing scientifically unfounded recommendations on assigning snow loads to roofs with arbitrary geometry are proposed.

ACKNOWLEDGMENTS

This work was financially supported by the Ministry of Science and Higher Education of the Russian Federation (Project: Theoretical and experimental design of new composite materials to ensure safety during the operation of buildings and structures under conditions of technogenic and biogenic threats #FSWG-2020-0007)

REFERENCES

1. **Finney, E. A**. (1934). Snow control on the high-ways. Michigan Engineering Experiment Station Bulletin, 57, 1-62.
2. **Anno, Y.** (1984). Requirements for modeling of a snowdrift. Cold regions science and technology, 8(3), 241-252.
3. **Anno, Y.** (1985). Froude number paradoxes in the modeling of a snowdrift. Cold Regions Science and Technology, 10(2), 191-192.
4. **Anno, Y.** (1985). Modelling a snowdrift by means of activated clay particles. Annals of Glaciology, 6, 48-52.
5. **Irwin, P. A., & Williams, C. J.** (1981). Prevention of excess snow accumulation due to roof mounted solar collectors. Rept. for Ministry of Municipal Affairs and Housing of Ontario.
6. **Irwin, P. A.** (1983). Application of snow simulation model tests to pianning and design. In Proc. Eastern Snow Conference, Vol. 28, 40th annual Meeting (Vol. 28, pp. 118-130).
7. **Irwin, P. A., Hochstenbach, F. M., Gam-ble, S. L., & Davies, R. W.** (2000). Wind and snow considerations for wide span enclosures. In Widespan Roof Structures (pp. 62-72). Thomas Telford Publishing.
8. **Irwin, P.A.** (2020). Lifetime experiences in wind engineering. Journal of Wind Engineering and Industrial Aerodynamics, 205, 104272.
9. **Iversen, J. D.** (1979). Drifting snow similitude. Journal of the hydraulics division, 105(6), 737-753.
10. **Iversen, J. D**. (1980). Drifting-snow similitude–transportrate and roughness modeling. Journal of glaciology, 26(94), 393-403.
11. **Kind, R. J., & Murray, S. B.** (1982). Saltation flow measurements relating to modeling of snowdrifting. Journal of Wind Engineering and Industrial Aerodynamics, 10(1), 89-102.
12. **Kind, R. J.** (1986). Snowdrifting: a review of modelling methods. Cold Regions Science and Technology, 12(3), 217-228.

13. **Odar, F.** (1962). Scale factors for simulation of drifting snow. Journal of the Engineering Mechanics Division, 88(2), 1-16.
14. **Odar, F.** (1965). Simulation of drifting snow. U.S. Cold Regions Research and Engineering Laboratory. Research Report 174
15. **Isyumov, N., & Mikitiuk, M.** (1990). Wind tunnel model tests of snow drifting on a two-level flat roof. Journal of Wind Engineering and Industrial Aerodynamics, 36, 893-904.
16. **Isyumov, N., & Mikitiuk, M.** (1992). Wind tunnel modeling of snow accumulations on large-area roofs. In Proc., 2nd Int. Conf. On Snow Engineering (pp. 181-193).
17. **Sanpaolesi, L., Currie, D., Sims, P., Sacré, C., Stiefel, U., Lozza, S., ... & Formichi, P.** (1998). Scientific support activity in the field of structural stability of civil engineering works: Snow loads. Final report phase I. Report, Commission of the European Communities. DGII-I-D3, 2.Sanpaolesi L. et al. Scientific support activity in the field of structural stability of civil engineering works: Snow loads //Final Report Phase II. Brussels: Commission of the European Communities. DGIII-D3. – 1998.
18. **Standard B.** Eurocode 1: Actions on structures. – 2010.
19. ASCE. Wind Tunnel testing for buildings and other structures. – American Society of Civil Engineers, 2012.
20. **C.J. Williams** (1986). Field Observations of Wind Deflection Fins to Control Snow Accumulations on Roofs // Proc. 1st Int. Conf. on Snow Eng. (pp. 307-314).
21. **Brooks, A., Dale, J., Gamble, S., & Kriksic, F.** (2015). Rapid Assessment of Snow Drifting Conditions Using Physical Model Simulations. In Cold Regions Engineering 2015 (pp. 310-321).
22. **O'Rourke, M., DeGaetano, A., & Tokarczyk, J. D.** (2004). Snow drifting transport rates from water flume simulation. Journal of wind engineering and industrial aerodynamics, 92(14-15), 1245-1264.
23. **Gerdel, R. W., & Strom, G. H.** (1961). Wind tunnel studies with scale model simulated snow. International Association of Scientific Hydrology.
24. **Younger, A**. (2017). Simulate and test different tent arrangements in windy and snowy conditions.
25. **Zhou, X., Hu, J., & Gu, M.** (2014). Wind tunnel test of snow loads on a stepped flat roof using different granular materials. Natural Hazards, 74(3), 1629-1648.
26. **Naaim, M., Naaim-Bouvet, F., & Mar-tinez, H.** (1998). Numerical simulation of drift-ing snow: erosion and deposition models. An-nals of glaciology, 26, 191-196.
27. **Zhou, X., Qiang, S., Peng, Y., & Gu, M.** (2016). Wind tunnel test on responses of a lightweight roof structure under joint action of wind and snow loads. Cold Regions Science and Technology, 132, 19-32.
28. **Kumar, G., Gairola, A., & Vaid, A.** (2020). Flow and deposition measurement of foam beads in a closed recirculating wind tunnel for snowdrift modelling. Flow Measurement and Instrumentation, 72, 101687.
29. **Wang, J., Liu, H., Chen, Z., & Ma, K.** (2020). Wind tunnel test of wind-induced snowdrift on stepped flat roofs during snowfall. Natural Hazards, 104(1), 731-752.
30. **Smedley, D. J., Kwok, K. C. S., & Kim, D. H.** (1993). Snowdrifting simulation around Davis station workshop, Antarctica. Journal of Wind Engineering and Industrial Aerodynamics, 50, 153-162.
31. **Peterka, J. A., & Petersen, R. L.** (1990). On the relaxation of saltation length as a modeling criteria for particulate transport by wind. Journal of Wind Engineering and Industrial Aerodynamics, 36, 867-876.
32. **Peterka, J. A., & Esterday, W. S.** (2004). Roof design snow loads by wind tunnel test and analysis. In Structures 2004: Building on the Past, Securing the Future (pp. 1-9).
33. **Flaga, A., Bosak, G., Pistol, A., & Flaga, Ł.** (2019). Wind tunnel model tests of snow precipitation and redistribution on rooftops, terraces and in the vicinity of high-rise buildings. Archives of Civil and Mechanical Engineering, 19(4), 1295-1303.

34. **Ayres, P., & Webster, T.** (2014). Otkritie Arena: Design of the new Spartak Moscow Stadium. Stahlbau, 83(6), 400-405.
35. **Iversen, J. D.** (1982). Small-scale Modeling of Snow-drift Phenomena, Wind Tunnel Modeling for Civil Engineerin~ ADolications. Cambridge University Press, Cambridge, England, 522-545.
36. **Okaze, T., Mochida, A., Tominaga, Y., Nemoto, M., Sato, T., Sasaki, Y., & Ichinohe, K.** (2012). Wind tunnel investigation of drifting snow development in a boundary layer. Journal of wind engineering and industrial aerodynamics, 104, 532-539.
37. **Iversen, J. D., Greeley, R., White, B. R., & Pollack, J. B.** (1975). Eolian erosion of the Martian surface, part 1: Erosion rate similitude. Icarus, 26(3), 321-331.
38. **Pomeroy, J. W., & Gray, D. M.** (1990). Saltation of snow. Water resources research, 26(7), 1583-1594.
39. **Takeuchi, M.** (1980). Vertical profile and horizontal increase of drift-snow transport. Journal of Glaciology, 26(94), 481-492.
40. **Tabler, R. D.** (2003). Controlling blowing and drifting snow with snow fences and road design (No. NCHRP Project 20-7 (147)).
41. **Beyers, J. H. M., & Harms, T. M.** (2003). Outdoors modelling of snowdrift at SANAE IV Research Station, Antarctica. Journal of Wind Engineering and Industrial Aerodynamics, 91(4), 551-569.
42. **Bintanja, R.** (2001). Modification of the wind speed profile caused by snowdrift: results from observations. Quarterly Journal of the Royal Meteorological Society, 127(577), 2417-2434.
43. **Brooks, A., Gamble, S., Dale, J., & Bond, J.** (2016). Comparison of Physical Snow Accumulation Simulation Techniques. In Proceedings of the International Conference on Snow Engineering (ICSE 2016), Nantes, France.
44. **Ван-Дайк, М.** (1986). Альбом течений жидкости и газа [An Album of Fluid Motion]. М.: Мир.
45. **Ушаков, Б.А.** (2013). Атлас аэродинамических характеристик профилей крыльев, испытанных в трубе Т-1 [Atlas of aerodynamic characteristics of wing profiles tested in a tube T-1]. Рипол Классик.
46. **Березин М.А., Катюшин В.В**. Атлас аэродинамических характеристик строительных конструкций [Atlas of aerodynamic characteristics of building structures]. – 2003.
47. **Chiba T., Thiis T**. (2016). Accuracy of snow depth measurements on roofs measured with photogrammetry. In Proceedings of the International Conference on Snow Engineering (ICSE 2016), Nantes, France.
48. **Yan, K., & Cheng, T.** (2008, August). Close Shot Photogrammetry for Measuring Wind-Drifted Snow Distribution on Stepped Flat Roofs. In 2008 ISECS International Colloquium on Computing, Communication, Control, and Management (Vol. 1, pp. 332-335). IEEE.
49. **Sato, T., Kimura, T., Ishimaru, T., & Maruyama, T.** (1993). Field test of a new snow-particle counter (SPC) system. Annals of Glaciology, 18, 149-154.
50. **Nazarov YU. P., Lebedeva I. V., Popov N. A.** Regional'noye normirovaniye snegovykh nagruzok v Rossii [Regional rationing of snow loads in Russia] //Stroitel'naya mekhanika i raschet sooruzheniy. – 2006. – No 3. – P. 71-77.
51. **Ledovskoy I. V.** Problemy teorii snegovykh nagruzok na sooruzheniya [Problems of the theory of snow loads on structures] //Avtoreferat. P. – 2009.
52. **Vinnik N. S., Matyukh S.A., Morozova, V.A.** Raspredeleniye snegovoy nagruzki na pokrytiyakh zdaniy i sooruzheniy i faktory, na neye vliyayushchiye [Distribution of snow load on the coatings of buildings and structures and factors affecting it]. – 2015.
53. **Lobkina V. A., Kononov I. A., Potapov A. A.** Sistema distantsionnogo monitoringa snegovoy nagruzki na krovle zdaniy [System for remote monitoring of snow load on the roof of buildings] //Lyod i Sneg. – 2016. – Vol. 56. – No. 2. – P. 246-252.

54. **Adzhiyev A. KH. i dr.** Issledovaniya raschetnykh znacheniy vesa snegovogo pokrova i znacheniy vysotnogo koeffitsiyenta v gornykh i maloizuchennykh rayonakh dlya opredeleniya nagruzok na zdaniya i sooruzheniya [Studies of the calculated values of the weight of the snow cover and the values of the altitude coefficient in mountainous and poorly studied areas to determine the loads on buildings and structures] //Prirodnyye i tekhnogennyye riski. Bezopasnost' sooruzheniy. – 2021. – No. 1. – P. 47-50.
55. **Matveyenko, Ye. V.** Obobshchennyy analiz metodov modelirovaniya snegovoy nagruzki [Generalized analysis of methods for modeling snow load] / Ye. V. Matveyenko // Vestnik Brestskogo gosudarstvennogo tekhnicheskogo universiteta. Stroitel'stvo i arkhitektura. – 2018. – No 1(109). – P. 77-81.
56. **Popov N. A. i dr.** Vozdeystviye vetrovykh i snegovykh nagruzok na bol'sheproletnyye pokrytiya [Impact of wind and snow loads on large-span pavements] //Promyshlennoye i grazhdanskoye stroitel'stvo. – 2016. – No 12. – P. 71-76
57. **Poddaeva O.** Experimental modeling of snow action on unique construction facilities // Architecture and Engineering. – 2021. – Vol. 6. – No. 2. – P. 45-51.
58. **Poddaeva O., Churin P.** Experimental study of the distribution of snow deposits on the surface of structures with complex three-dimensional shape of the roof //Proceedings of the International Conference on Snow Engineering (ICSE 2016), Nantes, France. – 2016.
59. **Tominaga, Y., Okaze, T., Mochida, A., Sasaki, Y., Nemoto, M., & Sato, T.** (2013). PIV measurements of saltating snow particle velocity in a boundary layer developed in a wind tunnel. Journal of visualization, 16(2), 95-98.
60. **Belostotsky, A.M., Britikov, N.A., Goryachevsky, O.S.** (2021). Comparison of determination of snow loads for roofs in building codes of various countries. International Journal for Computational Civil and Structural Engineering, 17(3), 39-47.

СПИСОК ЛИТЕРАТУРЫ

1. **Finney E. A.** Snow control on the high-ways //Michigan Enginnering Experiment Station Bulletin. – 1934. – T. 57. – C. 1-62.
2. **Anno Y.** Requirements for modeling of a snowdrift //Cold regions science and technology. – 1984. – T. 8. – №. 3. – C. 241-252.
3. **Anno Y.**Froude number paradoxes in the modeling of a snowdrift //Cold Regions Science and Technology. – 1985. – T. 10. – №. 2. – C. 191-192.
4. **Anno Y.** Modelling a snowdrift by means of activated clay particles //Annals of Glaciology. – 1985. – T. 6. – C. 48-52.
5. **Irwin P. A., Williams C. J.** Prevention of excess snow accumulation due to roof mounted solar collectors //Rept. for Ministry of Municipal Affairs and Housing of Ontario. – 1981.
6. **Irwin P. A.** Application of snow simulation model tests to planning and design //Proc. Eastern Snow Conference, Vol. 28, 40th annual Meeting. – 1983. – T. 28. – C. 118-130.
7. **Irwin P. A., Hochstenbach F. M., Gamble S. L.** Wind and snow considerations for wide span enclosures//Widespan Roof Structures. – 2000. – C. 62.
8. **Irwin P. A.** Lifetime experiences in wind engineering //Journal of Wind Engineering and Industrial Aerodynamics. – 2020. – T. 205. – C. 104272.
9. **Iversen J. D.** Drifting snow similitude //Journal of the hydraulics division. – 1979. – T. 105. – №. 6. – C. 737-753.
10. **Iversen J. D.** Drifting-snow similitude–transport-rate and roughness modeling //Journal of glaciology. – 1980. – T. 26. – №. 94. – C. 393-403.
11. **Kind R. J., Murray S. B.** Saltation flow measurements relating to modeling of snowdrifting //Journal of Wind Engineering and Industrial Aerodynamics. – 1982. – T. 10. – №. 1. – C. 89-102.
12. **Kind R. J.** Snowdrifting: a review of modelling methods // Cold Regions Science and Technology. – 1986. – T. 12. – №. 3. – C. 217-228.

13. **Odar F.** Scale factors for simulation of drifting snow //Journal of the Engineering Mechanics Division. – 1962. – Т. 88. – №. 2. – С. 1-16.
14. **Odar F.** Simulation of Drifting Snow, Cold Regions Research and Engineering Laboratory, Hanover. – NH, Research Report 174, 1965.
15. **Isyumov N., Mikitiuk M.** Wind tunnel model tests of snow drifting on a two-level flat roof //Journal of Wind Engineering and Industrial Aerodynamics. – 1990. – Т. 36. – С. 893-904.
16. **Isyumov N., Mikitiuk M.** Wind tunnel modeling of snow accumulations on large-area roofs //Proc., 2nd Int. Conf. On Snow Engineering. – 1992. – С. 181-193.
17. **Sanpaolesi L. et al.** Scientific support activity in the field of structural stability of civil engineering works: Snow loads //Final Report Phase I. Brussels: Commission of the European Communities. DGIII-D3. – 1998.
18. **Sanpaolesi L. et al.** Scientific support activity in the field of structural stability of civil engineering works: Snow loads //Final Report Phase II. Brussels: Commission of the European Communities. DGIII-D3. – 1998.
19. **Standard B.** Eurocode 1: Actions on structures. – 2010.
20. ASCE. Wind tunnel testing for buildings and other structures. – American Society of Civil Engineers, 2012.
21. **C.J. Williams.** Field Observations of Wind Deflection Fins to Control Snow Accumulations on Roofs // Proc. 1st Int. Conf. on Snow Eng. – 1986. – С. 307-314.
22. **Brooks A. et al.** Rapid Assessment of Snow Drifting Conditions Using Physical Model Simulations //Cold Regions Engineering 2015. – 2015. – С. 310-321.
23. **M. O'Rourke, A. DeGaetano, J.D. Tokarczyk**. Snow Drifting Transport Rates from Water Flume Simulation. Journal of Wind Engineering and Industrial Aerodynamics. 92, (2004) 1245-1264. Gerdel
24. **R. W., Strom G. H.** Wind tunnel studies with scale model simulated snow. – Interna-tional Association of Scientific Hydrology, 1961.
25. **Younger A.** Simulate and test different tent arrangements in windy and snowy conditions. – 2017.
26. **Zhou X., Hu J., Gu M.** Wind tunnel test of snow loads on a stepped flat roof using different granular materials //Natural hazards. – 2014. – Т. 74. – №. 3. – С. 1629-1648
27. **Naaim M., Naaim-Bouvet F., Martinez H.** Numerical simulation of drifting snow: erosion and deposition models //Annals of glaciology. – 1998. – Т. 26. – С. 191-196.
28. **Zhou X. et al**. Wind tunnel test on responses of a lightweight roof structure under joint action of wind and snow loads //Cold Regions Science and Technology. – 2016. – Т. 132. – С. 19-32.
29. **Kumar G., Gairola A., Vaid A.** Flow and deposition measurement of foam beads in a closed recirculating Wind tunnel for snowdrift modelling //Flow Measurement and Instrumentation. – 2020. – Т. 72. – С. 101687.
30. **Wang J. et al.** Wind tunnel test of wind-induced snowdrift on stepped flat roofs during snowfall //Natural Hazards. – 2020. – Т. 104. – №. 1. – С. 731-752.
31. **Smedley D. J., Kwok K. C. S., Kim D. H.** Snowdrifting simulation around Davis station workshop, Antarctica //Journal of Wind Engineering and Industrial Aerodynamics. – 1993. – Т. 50. – С. 153-162.
32. **Peterka J. A., Petersen R. L.** On the relaxation of saltation length as a modeling criteria for particulate transport by wind //Journal of Wind Engineering and Industrial Aerodynamics. – 1990. – Т. 36. – С. 867-876.
33. **Peterka J. A., Esterday W. S.** Roof design snow loads by Wind tunnel test and analysis //Structures 2004: Building on the Past, Securing the Future. – 2004. – С. 1-9.
34. **Flaga A. et al.** Wind tunnel model tests of snow precipitation and redistribution on rooftops, terraces and in the vicinity of high-rise buildings //Archives of Civil and Mechanical Engineering. – 2019. – Т. 19. – С. 1295-1303.
35. **Ayres P., Webster T.** Otkritie Arena: Design of the new Spartak Moscow Stadium //Stahlbau. – 2014. – Т. 83. – №. 6. – С. 400-405.

36. **Iversen J. D.** Small-scale Modeling of Snowdrift Phenomena, Wind Tunnel Modeling for Civil Engineerin~ ADolications //Cambridge University Press, Cambridge, England. – 1982. – С. 522-545.
37. **Okaze T. et al.** Wind tunnel investigation of drifting snow development in a boundary layer //Journal of wind engineering and industrial aerodynamics. – 2012. – Т. 104. – С. 532-539.
38. **Iversen J. D. et al.** Eolian erosion of the Martian surface, part 1: Erosion rate similitude // Icarus. – 1975. – Т. 26. – №. 3. – С. 321-331.
39. **Pomeroy J. W., Gray D. M.** Saltation of snow //Water resources research. – 1990. – Т. 26. – №. 7. – С. 1583-1594.
40. **Takeuchi M**. Vertical profile and horizontal increase of drift-snow transport //Journal of Glaciology. – 1980. – Т. 26. – №. 94. – С. 481-492.
41. **Tabler R. D.** Controlling blowing and drifting snow with snow fences and road design. – 2003. – №. NCHRP Project 20-7 (147).
42. **Beyers J. H. M., Harms T. M.** Outdoors modelling of snowdrift at SANAE IV Research Station, Antarctica //Journal of Wind Engineering and Industrial Aerodynamics. – 2003. – Т. 91. – №. 4. – С. 551-569.
43. **Bintanja R.** Modification of the wind speed profile caused by snowdrift: results from observations //Quarterly Journal of the Royal Meteorological Society. – 2001. – Т. 127. – №. 577. – С. 2417-2434.
44. **Brooks A. et al.** Comparison of Physical Snow Accumulation Simulation Techniques //Proceedings of the International Conference on Snow Engineering (ICSE 2016), Nantes, France. – 2016.
45. **Ван-Дайк М.** Альбом течений жидкости и газа. – М.: Мир, 1986. – 184 с.
46. **Ушаков Б.А.** Атлас аэродинамических характеристик профилей крыльев, испытанных в трубе Т-1. – Рипол Классик, 2013.
47. **Березин М. А., Катюшин В.В.** Атлас аэродинамических характеристик строительных конструкций. – 2003.
48. **Chiba T., Thiis T.** Accuracy of snow depth measurements on roofs measured with photogrammetry //Proceedings of the International Conference on Snow Engineering (ICSE 2016), Nantes, France. – 2016.
49. **Yan K., Cheng T.** Close Shot Photogrammetry for Measuring Wind-Drifted Snow Distribution on Stepped Flat Roofs //2008 ISECS International Colloquium on Computing, Communication, Control, and Management. – IEEE, 2008. – Т. 1. – С. 332-335.
50. **Sato T. et al.** Field test of a new snow-particle counter (SPC) system //Annals of Glaciology. – 1993. – Т. 18. – С. 149-154.
51. **Назаров Ю. П., Лебедева И. В., Попов Н. А.** Региональное нормирование снеговых нагрузок в России //Строительная механика и расчет сооружений. – 2006. – №. 3. – С. 71-77.
52. **Ледовской И. В.** Проблемы теории снеговых нагрузок на сооружения // Автореферат. С. – 2009.
53. **Винник Н. С., Матюх С.А., Морозова, В.А**. Распределение снеговой нагрузки на покрытиях зданий и сооружений и факторы, на нее влияющие. – 2015.
54. **Лобкина В. А., Кононов И. А., Потапов А. А.** Система дистанционного мониторинга снеговой нагрузки на кровле зданий //Лёд и Снег. – 2016. – Т. 56. – №. 2. – С. 246-252.
55. **Аджиев А. Х. и др.** Исследования расчетных значений веса снегового покрова и значений высотного коэффициента в горных и малоизученных районах для определения нагрузок на здания и сооружения //Природные и техногенные риски. Безопасность сооружений. – 2021. – №. 1. – С. 47-50.
56. **Матвеенко, Е. В.** Обобщенный анализ методов моделирования снеговой нагрузки / Е. В. Матвеенко // Вестник Брестского государственного технического университета. Строительство и архитектура. – 2018. – № 1(109). – С. 77-81.
57. **Попов Н. А. и др.** Воздействие ветровых и снеговых нагрузок на большепролетные

покрытия //Промышленное и гражданское строительство. – 2016. – №. 12. – С. 71-76.
58. **Poddaeva O.** Experimental modeling of snow action on unique construction facilities //Architecture and Engineering. – 2021. – Т. 6. – №. 2. – С. 45-51.
59. **Poddaeva O., Churin P.** Experimental study of the distribution of snow deposits on the surface of structures with complex three-dimensional shape of the roof //Proceedings of the International Conference on Snow Engineering (ICSE 2016), Nantes, France. – 2016.
60. **Tominaga Y. et al.** PIV measurements of saltating snow particle velocity in a boundary layer developed in a wind tunnel //Journal of visualization. – 2013. – Т. 16. – №. 2. – С. 95-98.
61. **Белостоцкий А.М., Бритиков Н.А., Горячевский О.С.** Сравнение нормативных документов различных стран в части назначения снеговых нагрузок // International Journal for Computational Civil and Structural Engineering. – 2021. – Т. 17. – №. 3. – С. 39-47.

Belostotsky Alexander Mikhailovich, RAACS academician, professor, D.Sc. in Engineering; General Director of Scientific Research Center StaDyO; Professor of the Department of Informatics and Applied Mathematics of the National Research Center, scientific director of the A.B. Zolotov NICCM of the National Research Moscow State University of Civil Engineering; Professor of the Department of Building Structures, Buildings and Structures of the Russian University of Transport (MIIT); 125040, Russia, Moscow, 3rd Yamsky Pole, 18, office 810; Tel. +7 (499) 706-88-10. E-mail: amb@stadyo.ru

Goryachevsky Oleg Sergeevich, Lead Computing Engineer at Scientific Research Center StaDyO; Deputy Director of the A.B. Zolotov NICCM of the National Research Moscow State University of Civil Engineering; 129337, Russia, Moscow, Yaroslavskoe shosse, 26. E-mail: osgoryachevskij@mail.ru

Britikov Nikita Aleksandrovich, engineer of the A.B. Zolotov NICCM of the National Research Moscow State University of Civil Engineering; postgraduate student of the Russian University of Transport (MIIT); 129337, Russia, Moscow, Yaroslavskoe shosse, 26. E-mail: n.a.britikov@gmail.com

Белостоцкий Александр Михайлович, академик РААСН, профессор, доктор технических наук; генеральный директор ЗАО Научно-исследовательский центр СтаДиО; профессор кафедрыИнформатики и прикладной математики Национального исследовательского, научный руководитель НОЦ КМ им. А.Б. Золотова Московского государственного строительного университета; профессор кафедры «Строительные конструкции, здания и сооружения» Российского университета транспорта (МИИТ); 125040, Россия, Москва, ул. 3-я Ямского Поля, д.18, офис 810; тел. +7 (499) 706-88-10. E-mail: amb@stadyo.ru

Горячевский Олег Сергеевич, ведущий инженер-расчетчик ЗАО Научно-исследовательский центр СтаДиО; заместитель директора НОЦ КМ им. А.Б. Золотова Национального исследовательского Московского государственного строительного университета; 129337, Россия, г. Москва, Ярославское шоссе, д. 26. E-mail: osgoryachevskij@mail.ru

Бритиков Никита Александрович, инженер НОЦ КМ им. А.Б. Золотова Национального исследовательского Московского государственного строительного университета; аспирант Российского университета транспорта (МИИТ); 129337, Россия, г. Москва, Ярославское шоссе, д. 26. E-mail: n.a.britikov@gmail.com

DOI:10.22337/2587-9618-2021-17-4-40-59

CRITICAL REVIEW OF MODERN NUMERICAL MODELLING OF SNOW ACCUMULATION ON ROOFS WITH ARBITRARY GEOMETRY

A.M. Belostotsky [1,2,3]***, N.A. Britikov*** [2,3]***, O.S. Goryachevsky*** [1,2]

[1] Scientific Research Center StaDyO, Moscow, RUSSIA
[2] National Research Moscow State University of Civil Engineering, Moscow, RUSSIA
[3] Russian University of Transport (RUT - MIIT), Moscow, RUSSIA

Abstract: The calculation of snow loads on roofs of buildings and structures with arbitrary geometry is a complex problem, solving which requires simulating snow accumulation with acceptable engineering accuracy. Experiments in wind tunnels, although widely used in recent years, do not allow to reproduce the real full-scale effects of all snow transport subprocesses, since it is impossible to satisfy all the similarity conditions. This situation, coupled with the continuous improvement of mathematical models, numerical methods, computer technologies and related software, makes the development and future implementation of numerical modelling in real construction practice and regulatory documents inevitable. This paper reviews currently existing mathematical models and numerical methods used to calculate the forms of snow deposits. And, although the lack of significant progress in the field of modelling snow accumulation still remains one of the major problems in CFD, use of existing models, supported by field observations and experimental data, allows to reproduce reasonably accurate snow distributions. The importance of the “symbiosis” between classical experimental methods and modern numerical models is specifically emphasized in the paper, as well as the fact that only the joint use of approaches can comprehensively describe modelling of snow accumulation and snow transport and provide better solutions to a wider range of problems.

Keywords: neural networks, numerical modelling, snow accumulation, snow transport, structure roofs, numerical methods.

СОВРЕМЕННЫЕ МЕТОДЫ МАТЕМАТИЧЕСКОГО (ЧИСЛЕННОГО) МОДЕЛИРОВАНИЯ СНЕГОНАКОПЛЕНИЯ НА ПОКРЫТИЯ СООРУЖЕНИЙ ПРОИЗВОЛЬНОЙ ФОРМЫ. КРИТИЧЕСКИЙ ОБЗОР

Белостоцкий А.М. [1,2,3]***, Бритиков Н.А.*** [2,3]***, Горячевский О.С.*** [1,2]

[1] Научно-исследовательский центр СтаДиО, г. Москва, РОССИЯ
[2] Национальный исследовательский Московский государственный строительный университет, г. Москва, РОССИЯ
[3] Российский университет транспорта (МИИТ), г. Москва, РОССИЯ

Аннотация: Расчёт снеговых нагрузок на покрытия зданий и сооружений произвольной формы является комплексной задачей, для решения которой необходимо с приемлемой инженерной точностью моделировать снегонакопление. Эксперименты в аэродинамических трубах, хотя и применяются последние годы повсеместно, не позволяют воспроизвести реальные полномасштабные эффекты всех процессов снегопереноса, поскольку выполнение всех условий подобия для них невозможно. Такая ситуация, вкупе с постоянным развитием математических моделей, численных методов и соответствующего программного обеспечения, вычислительной техники делает безальтернативным развитие и будущее внедрение технологий математического моделирования в реальную строительную практику и нормативные документы. В данной работе рассмотрены существующие на сегодняшний день математические модели и численные методы, применяемые для расчёта форм снегоотложений. И хотя отсутствие значительного прогресса в области моделирования снегонакопления по-прежнему остаётся одной из проблем вычислительной аэродинамики, использование уже существующих моделей, подкреплённое натурными наблюдениями и экспериментальными данными, способно воспроизводить достаточно

точные картины распределений снега. В работе отдельно подчёркнута важность «симбиоза» между классическими экспериментальными методами и современными численными моделями и того, что только совместное использование подходов способно всесторонне раскрыть проблему моделирования снегоотложений и снегопереноса и дать наилучшее её решение для широкого спектра задач.

Ключевые слова: нейронные сети, математическое моделирование, снегонакопление, снегоперенос, покрытия сооружений, численные методы.

INTRODUCTION

Snow accumulation (the formation of snow deposits under the influence of air flow) is a complex phenomenon due to the high nonlinearity of its constituent subprocesses, which occur at different scales and are strongly interconnected [2, 3, 21]. One of those, snow transport, is the subject of many years of theoretical, experimental and numerical research [19, 27] because of its involvement in the redistribution of snow masses. The fact that the formation of fairly uniform snowdrifts occurs as a result of the gradual deposition of snowflakes with sizes from tens of microns to tens of millimeters [9] makes a serious computational problem, especially considering that in most industries, where it matters, it must be considered on areas of tens and hundreds of square meters [22].

The known disadvantages of experimental methods for predicting the shape of snow deposits (the use of substitutes, such as sand [23], sawdust [11] and others, loss of accuracy due to scaling, etc.) and the natural randomness of weather conditions that affect field observations force researchers to use numerical methods, which makes it possible to effectively model the properties of real materials at required scales and control all the calculation parameters.

One of the fields that certainly require a computational approach is the construction of unique buildings and structures. Due to the dependence of the snow accumulation process on the geometry of the structure, surrounding buildings, landscape, and climatic conditions, it is necessary to investigate snow loads for each unique roof design. Regulatory documents describe the shape of snow deposits only for basic, typical roofs. Also note that foreign building codes (ISO 4355-2016 [46], Eurocode [5], ASCE standards [24], JSCE [25]), in contrast to the Russian Building Code [26], allow the use of numerical modelling of snowdrifts both together with the results of experimental modelling and to verify the results of experiments, as well as instead of experiments where it is impossible to conduct studies in wind tunnels. E.g., in a separate ASCE standard [42] there is a subsection dedicated specifically to the study of methods for modelling snow transport, their classification and discussion of the limits of their applicability [52].

In connection with the growing tendency to reduce the costs of construction, which puts significant restrictions on the design, the use of numerical modelling could also upgrade the building codes. For example, some researchers believe [19] that the use of the Weibull and Gumbel distributions, which is currently the accepted way to estimate the amount of precipitation, leads to overestimation of the snow loads. Predicting the movement of snow masses in the mountains, formation of avalanches, as well as other natural phenomena associated with snow that threaten human lives, also remains an important and generally unsolved problem [13, 14].

Over the past decades, a standardized, verified and effective numerical methodology for modelling snow accumulation and snow transport, which could be integrated in the building codes, has not been created, despite the increased demand from industries [19]. Obviously, this is due to the imperfection of existing models and methods and lack of qualitative achievements in their development. Since about 2014, there has been an increase in the number of works on the numerical modelling of snow accumulation and

snow transport from China [23, 36, 37, 44, 45], supported by government grants and aimed at upgrading building codes, which will probably lead to verified methodologies emerging soon.

Few Russian scientific works on the topic [47, 48, 49, 50, 51], on the contrary, are mostly derivative in nature, despite the problem of calculating snow loads on the roofs of buildings and structures with arbitrary geometry in our country being way more relevant due to the features of the climate. E.g., one of the more well-known articles [47] contains only a brief overview of some (far from all) works on modelling snow accumulation, does not provide any new results, does not raise important issues of the development and improvement of techniques, as well as their introduction into construction practice, while another example [51] is actually a literal translation of the ASCE standard [42]. The lack of critical reviews that clearly highlight the gap between the regulations and industry demands further aggravates the situation and delays the necessary resolution of the issue.

The problem of numerical modelling of snow accumulation has existed for at least 40 years [19]. Over the time, a number of studies have been carried out and numerical methods and approaches have been developed that, to one degree or another, bring scientists closer to achieving more and more physically realistic forms of snow deposits. Validation of numerical methods was carried out mainly on model cases for which there were data from field observations or experiments in wind tunnels, e.g. for the flow around a cube [12, 20, 32, 33] or a solid fence [11, 20]. Some scientists have tried to apply the models to real-life problems, such as the accumulation of snow on the roofs of buildings [22, 34, 35, 36, 37, 44] or around buildings or landscape formations [16, 17, 38, 39, 40, 41, 45]. In each case, it was necessary to calibrate the models for the specific conditions of the given problem and to individually select the parameters, although even then minimizing the divergences with observations was not sufficient to speak of an “accurate” reproduction of “real” snow deposits [19]. One of the reasons for this is that to adequately model snow transport for arbitrary wind velocities, structural geometries and climatic parameters, it is necessary to take into account all three subprocesses, but in practice it is difficult to do because of scales at which they occur. Of greatest interest is the modelling of suspension and saltation, since it is they that make the greatest contribution to the actual transport of snow (especially saltation, due to the large scatter of particle sizes and lengths up to 5 m of which they are capable to move).

THE PHENOMENON OF SNOW TRANSPORT

One of the fundamental works on the mechanics of aeolian transport (that is, movement of solid particles, or sediments, under the influence of wind), which formed the basis of the vast majority of theoretical developments on this issue, are the works of R.A. Bagnold [2, 3]. He laid the foundation for a scientific approach to describing the transport of sand by wind, the formation of sand dunes and barchans. The experiments, results of which are presented in the book, were carried out in a wind tunnel built by the scientist himself. When considering the problem of modelling snow deposits, the information from this book is also relevant, since snow, like sand, participates in aeolian transport. However, sand grains do not have the property of cohesion, unlike snowflakes, due to which the snow transport can be divided into three subprocesses, namely creep, saltation and suspension (Fig. 1) [3, 19].

1) Creep is a phenomenon in which coarse sediments (500 μm in diameter) are rolling over the surface due to their cohesion with it being stronger than the wind force.

2) Saltation is a jumping movement of medium-sized particles (70-500 μm) at a speed 2-3 times lower than the flow speed. Particles up to 100 μm in diameter are subject to modified saltation, which occurs under the action of turbulent vortices above the surface. The mass of material

that the flow is able to transport in the saltation layer is determined by the formula (1).
3) The suspended layer is formed from fine sediments and is divided into short-term suspension (20-70 μm, particles return to the saltation layer) and long-term suspension (<20 μm, the material is completely carried away by the flow).

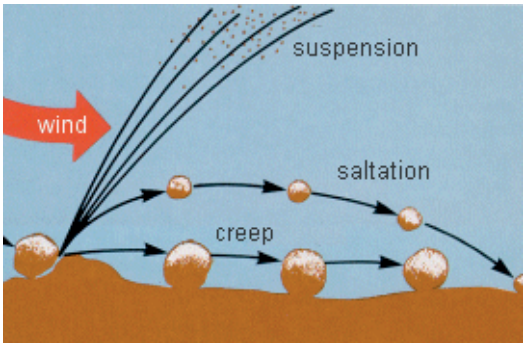

Figure 1. Mechanics of the aeolian transport. Source: NASA (publicly available)

Note that the sediments participating in all three subprocesses, colliding with each other, can either stick together, or break up, or crush other particles, correspondingly changing the characteristics of both transport, while the macro-objects that they form (for example, snowdrifts) affect the entire flow. Complexity, a large number of degrees of freedom of such a system, the natural randomness of the process are all just some of the factors that force researchers to resort to statistical and approximate calculation methods.
Another important result obtained by Bagnold is a formula describing the mass of material that the wind is able to transport in the saltation layer. It is written as:

$$q = C\frac{\rho}{g}\sqrt{\frac{d}{D}}u_*^3, \qquad (1)$$

where q is mass of material transported along a unit length; C is dimensionless constant of the order of one, ρ is air density; g is acceleration due to gravity; d is reference grain size; D is uniform grain size used by Bagnold in his experiments (250 μm); u_* is friction velocity, which is written as:

$$u_* = \sqrt{\frac{\tau_w}{\rho_a}}, \qquad (2)$$

where τ_w is local shear stress on the wall, ρ_a is air density. This value is especially important when simulating snow transport and snow accumulation, its calculation underlies all numerical models of these processes.
The study of snow transport processes was continued by Mellor [9], Izyumov and Davenport [28, 29], Kobayashi [30], Iversen [6, 7], Anderson and Huff [1], Gamble [31]. In particular, the latter were engaged in finding out the average path length of particles in the saltation layer: Bagnold gave a value of 9 m [2], then Anderson and Huff reduced it to a range of 4-8 m, and Gamble expanded it to 5-10 m.

NUMERICAL MODELLING OF SUSPENSION

Suspension is usually modeled using Eulerian approach [19], although there is at least one work where the Lagrangian approach was used [16]. Most likely, this is due to the greater homogeneity of the flow due to the small particle sizes, which allows formulating models in a more applicable way without large losses in accuracy.
Firstly, let us consider the application of the *snow density transport equation*, exampled by the work of Okaze et al. [12]. Using two equations in this paper made it possible to differentiate the inputs from falling and drifting flows of snow into the snowdrift forming around a cube.
To describe the distribution of snow density Φ, defined as the mass of snow particles per unit volume, the following differential equation is used:

$$\frac{\partial\langle\Phi\rangle}{\partial t} + \frac{\partial\langle\Phi\rangle\langle u_i\rangle}{\partial x_i} + \frac{\partial\langle\Phi\rangle\langle wf\rangle}{\partial x_3} = \frac{\partial}{\partial x_i}\left[\frac{\nu_t}{\sigma_s}\left(\frac{\partial\langle\Phi\rangle}{\partial x_i}\right)\right], \qquad (3)$$

where wf is snowfall rate, ν_t is turbulent viscosity, σ_s is turbulent Schmidt number. In this case, the snow accumulation process is divided into addition of the falling snow and transport of the already accumulated snow over the surface (angle brackets mean averaging over spatial dimensions and time):

$$\langle \Phi \rangle = \langle \Phi_{sky} \rangle + \langle \Phi_{surf} \rangle \tag{4}$$

Snow deposition per unit of time and unit of area is expressed as $\langle \Phi \rangle_p \langle wf \rangle$, where the subscript "$p$" means calculation within the control volume. The deposition fluxes (kg/s) for the first and second modes, respectively, are calculated as:

$$D_{sky} = -\langle \Phi_{sky} \rangle_p \langle wf_{sky} \rangle \Delta x \Delta y \tag{5}$$

$$D_{surf} = -\langle \Phi_{surf} \rangle_p \langle wf_{surf} \rangle \Delta x \Delta y, \tag{6}$$

where $\Delta x \Delta y$ is horizontal platform of the control volume. The erosion flux (kg/s) of snow on the surface for $u^* > u_t^*$, caused by shear stress is described by the expression:

$$E_{surf} = -\frac{\pi \zeta}{6} \rho \langle u^* \rangle \left(1 - \frac{\langle u_t^* \rangle^2}{\langle u^* \rangle^2}\right) \Delta x \Delta y \tag{7}$$

where ζ is a dimensionless coefficient that roughly equals 10^{-3}.

The net deposition rate on the bottom surface of the control volume as a result of all processes is given by:

$$M_{total} = D_{sky} + D_{surf} + E_{surf}, \tag{8}$$

and the variation of snow depth per unit of time takes the form:

$$\Delta z_s = \frac{M_{total}}{\rho_s \Delta x \Delta y}, \tag{9}$$

where ρ_s is accumulated snow density.

Also, on the surface where snow deposit is forming, a boundary condition is set, which states that the change in snow density is determined by erosion:

$$\frac{\nu_t}{\sigma_s} \left(\frac{\partial \langle \Phi_{surf} \rangle}{\partial x_3} \right) \Bigg|_{surf} = \frac{E_{surf}}{\Delta x \Delta y} \tag{10}$$

The contribution to snow deposition by transport fluxes on the surface is described by the expression:

$$R_{surf} = \frac{D_{surf} + E_{surf}}{D_{sky} + D_{surf} + E_{surf}} \tag{11}$$

The following are illustrations of the results obtained using this method (Fig. 2). The resulting forms of snowdrifts are in agreement with those obtained in the experiment or during field observation.

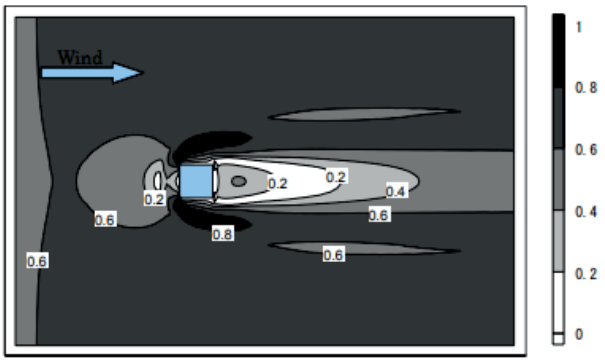

a) Scalar normalized velocity at z = 0.025H

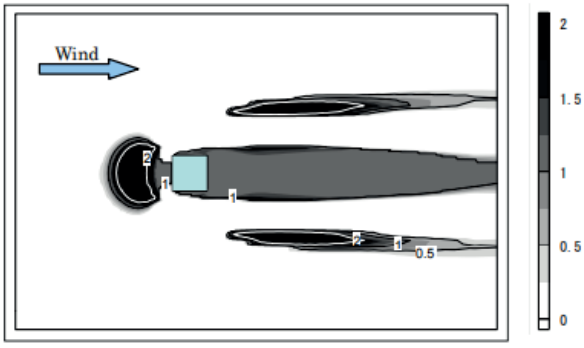

b) Horizontal distribution of normalized snow depth

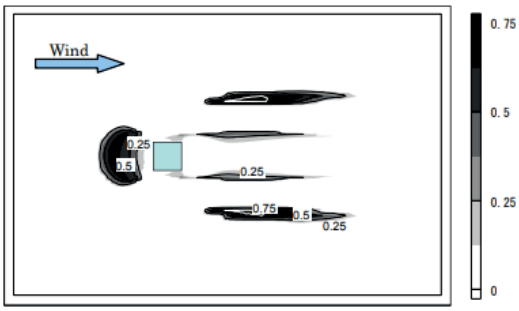

c) Contribution of snow particles from surface to snowdrift, R_{surf}

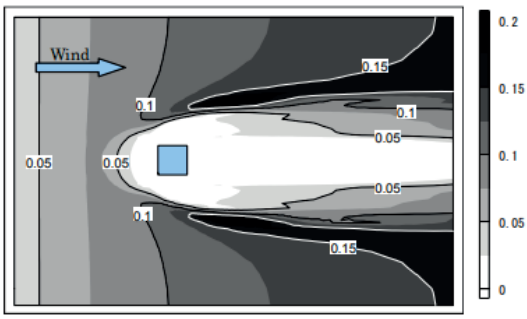

d) Horizontal distribution of density Φ_{surf} of snow particles coming from the surface at z = 0.025H

Figure 2. Results obtained by Okaze et al. using the equation of snow density transport to model the suspended layer

Secondly, let us consider the application of the snow volume fraction transport equation, exampled by the work of Sundsbø [17]. Snow volume fraction f in a control volume can be obtained from the expression for the density of the two-phase flow ρ_m:

$$\rho_m = f\rho_{snow} + (1-f)\rho_{air} \tag{12}$$

To describe the suspension, the convection-diffusion equation is used:

$$\frac{\partial f}{\partial t} + \frac{\partial}{\partial x}(fu) + \frac{\partial}{\partial z}(fw) = \frac{\partial}{\partial x}\left(c_t \nu_t \frac{\partial f}{\partial x}\right) + \frac{\partial}{\partial z}\left(c_t \nu_t \frac{\partial f}{\partial z}\right) - \frac{\partial}{\partial z}(f w_{\text{sus}}), \tag{13}$$

where u and w are wind speeds in directions x and z, respectively, ν_t is turbulent viscosity, c_t is diffusion constant, and w_{sus} is drift velocity between air and snow in suspension, which is assumed to be inversely proportional to turbulence in an air flow:

$$w_{\text{sus}} = 0.3\frac{\mu}{\mu + \mu_t} \tag{14}$$

Here μ and μ_t are laminar and turbulent dynamic viscosities, respectively. It is implied that laminar flow conditions give the highest snow settling rate, which can be considered as the limiting volumetric velocity for suspended snow particles (in the work under discussion, its value is taken as 0.3 m / s).

The formulation of the equation for snow transport in the saltation area is also given by:

$$\frac{\partial f}{\partial t} + \frac{\partial}{\partial x}(fu) + \frac{\partial}{\partial z}(fw) = -\frac{\partial}{\partial z}(f w_{\text{sal}}), \tag{15}$$

where, similarly to the equation (14), w_{sal} is drift velocity between air and snow in the saltation layer. Two expressions are proposed to describe its two "modes", which are settling of snow and accumulation of snow. The expressions for both modes are given by:

$$w_{\text{sal}} = w_{\text{set}} = c_f(1-f)f\frac{\nabla p}{\rho_m} \tag{16}$$

$$w_{\text{sal}} = w_{\text{acc}} = 0.5\,(u_*^3 - u_{*t}^3)/u_{*t}^3 \tag{17}$$

where ∇p is pressure gradient, c_f is reciprocal drag coefficient between air and snow, in this work taken as 0.06 s/m on based on simulation tests. Both expressions apply for $u^* > u_t^*$.

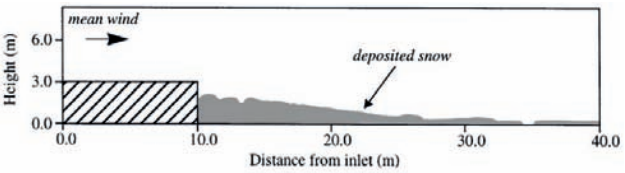

a) Snow accumulation on the side of a building without the use of a deflector.

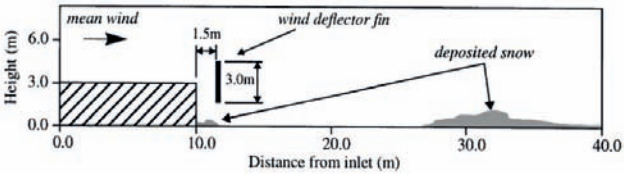

b) Snow accumulation at the side of a building using a deflector

Figure 3. Results obtained by Sundsbø using the snow volume fraction trasport equation to simulate the suspended layer

The described model was used to study the snow accumulation on the side of a building and the use of a reflector to minimize snow formation in this area. Its application made it possible to visualize the difference in the obtained snow distributions.

Finally, let us consider the application of the particles concentration transport equation used in the works of Moore et al. [10] and Naaim et al. [11]. In the latter work the snow transport was both the saltation and the suspension were modeled. The differential equation for the first process is given by:

$$\frac{\partial \bar{C}}{\partial t} + \frac{\partial \bar{C}\left(u_i - U_{F_i}\right)}{\partial x_i} = \frac{\partial}{\partial x_i}\left(\frac{\nu_t}{\sigma_s}\frac{\partial \bar{C}}{\partial x_i}\right) + \vec{e}_i \iint_S \varphi_s \vec{n} \mathrm{d}S \tag{18}$$

where $\bar{C}$ is average concentration of particles in a control volume, U_{F_i} is snowfall speed in the i-th direction, φ_s is mass flux between the suspension and saltation layers. The equation for the second process looks similar:

$$\frac{\partial \bar{C}_s}{\partial t} + \frac{\partial \bar{C}_s u_i}{\partial x_i} = \vec{e}_i \iint_S \left(\varphi_g + \varphi_s\right)\vec{n} \mathrm{d}S \tag{19}$$

Here φ_g is mass flux between the air flow and the surface, which will be discussed below.

NUMERICAL MODELLING OF SALTATION

Among the methods for modelling snow in the saltation layer, the most frequently used are the mass transport models formulated by Iversen et al., Pomeroy and Gray, and the erosion-deposition model formulated by Naaim et al. Let us consider them sequentially.

In the papers of Iversen et al. [6, 7], one of the first numerical models for three-dimensional calculation of snow transport was suggested, with saltation and suspension both taken into account. Later it was implemented by Uematsu et al. [20]. In the proposed methodology, the calculations are carried out in three stages. First, the air flow field is calculated using the RANS turbulence model, then the obtained data is used to calculate the density of the snow flow, and, finally, the snow transport rate is calculated by counting the snow particles that were not transported by saltation. Creep is not taken into account in this model.

The mass transported by saltation is modeled by the classical formula given by Pomeroy and Gray [13]:

$$q = C\frac{\rho}{g}\frac{w_f}{u_{*t}}u_*^2(u_{*t} - u_*) \tag{20}$$

where all quantities correspond to those in the formula (1), and w_f is average snowfall rate.

Saltation was modeled by the diffusion equation:

$$\frac{\partial \Phi}{\partial t} + \nabla(\Phi u_s) = \left(K_s \frac{\partial \Phi}{\partial x}\right) + \left(K_s \frac{\partial \Phi}{\partial y}\right) + \frac{\partial}{\partial x}\left(K_s \frac{\partial \Phi}{\partial z}\right) - \frac{\partial\left(w_f \Phi\right)}{\partial z} \tag{21}$$

where Φ is snow transport density, u_s is particle transport rate, K_s is vortex diffusion coefficient of snow transport density.
The snow deposition rate is calculated using the formula:

$$d = \left|w_f\right| \Phi_h \tag{22}$$

where Φ_h is density of snow transport in the saltation layer of thickness h.
The expression for the ablation rate has the form:

$$e = \frac{q\left|w_f\right|}{u_h h} \tag{23}$$

where u_h is particle transport rate in the saltation layer.
Finally, the snow transport rate, defined as the mass of snow accumulating on a unit area per unit of time, is written as follows:

$$s = -(d + e) \tag{24}$$

Formulas (20) - (24) were used in four calculations of snow transport: near a snow fence, around a cube (Fig. 4), near a wind catcher, and around a hill. The results obtained were consistent with experiments and field observations. With this model, though, only the snow transport rate can be calculated, but not the change in snow depth. The authors point out that this problem should be considered in more detail
The work of Liston et al. [8] was aimed at improving the model used by Uematsu et al. The case was considered in which the wind speed is low enough to neglect the transport of particles from the saltation layer to the turbulent flow layer described by one part of the model, while the second part describes the process of transporting their mass into the layer of accumulating snow. The flow is resolved through the time-averaged 2D Navier-Stokes equations using the k-ε turbulence model in conjunction with the saltation model to compute snow accumulation over time near the snow fence.
The two-dimensional equation of mass accumulation in a turbulent layer has the form:

$$\frac{\partial \bar{C}}{\partial t} + \bar{u}\frac{\partial \bar{C}}{\partial x} + \left(v - \left|w_f\right|\right)\frac{\partial \bar{C}}{\partial y} = \frac{\partial}{\partial x}\left(\frac{v_t}{\sigma_s}\frac{\partial \bar{C}}{\partial x}\right) + \frac{\partial}{\partial y}\left(\frac{v_t}{\sigma_s}\frac{\partial \bar{C}}{\partial y}\right) \tag{25}$$

where v_t is turbulent viscosity coefficient, $\bar{C}$ is particle concentration in density units, σ_s is turbulent Schmidt number. The concentration at the bottom of the suspended layer is equal to the average concentration in the saltation layer.
The change in the height of the snow cover h is written as follows:

$$\frac{\partial h(x,t)}{\partial t} + \frac{1}{\gamma} + \partial\left(\frac{Q_t(x,t) + Q_s(x,t)}{\partial x}\right) = 0 \tag{26}$$

where γ is bulk density of snow, Q_t is mass transport flux in a suspended bed, Q_s is mass transport flux in the saltation layer.

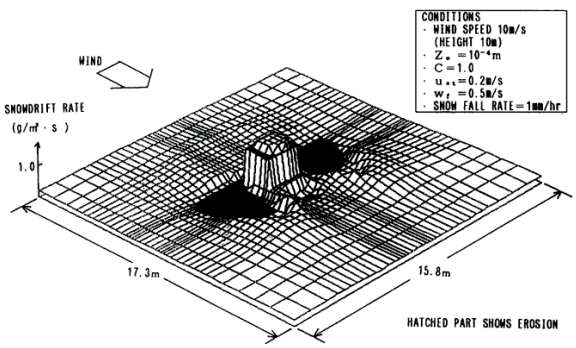

Figure 4. Results obtained by Uematsu et al. for snow accumulation around a hut using the mass transport model of Iversen et al. to model the saltation layer

Snow deposition is calculated on the assumption that accumulation occurs when the shear velocity of the flow falls below threshold friction velocity. The control volumes are filled gradually, and the mesh is rebuilt as they are accumulating. Since it is assumed that Q_s responds instantly to changes in friction velocity, the inertia of erosion and deposition is not taken into account. The model makes it possible to calculate the equilibrium snow deposition, but does not make it possible to estimate the time required for the formation of a snow layer of a given thickness [11].

Let us move on to the mass transport equation formulated by Pomeroy and Gray. In their works [13, 14], the details of snow transport (accumulation and redistribution), snow melting, interaction of melt water with frozen layers and their influence on the descent of snow masses in dangerous regions were investigated. The authors developed physical models to describe these processes and applied them to the description of snow formation in the Canadian province of Saskatchewan. The obtained equation of mass transport indicates an almost linear acceleration of this process with an increase in the friction velocity, which is in agreement with field observations. As with similar models, the equation is sensitive to the cohesion of the snow layer, which is determined by the boundary friction velocity. The authors also showed that generally the direction of the annual snow transport in saltation layer does not always coincide with the direction of the wind.

The flow of a mass of snow having an average weight W_p and saltating at an average speed u_p, is written as follows:

$$Q_{salt} = \frac{u_p W_p}{g} \tag{27}$$

The authors propose the following expression for W_p:

$$W_p = e(\tau - \tau_n - \tau_t) \tag{28}$$

where τ is atmospheric shear stress, τ_n and τ_t are shear stress on non-destructible and destructible surfaces, respectively. The coefficient e is dimensionless and means the “efficiency” of saltation. It is inversely proportional to the kinetic friction arising in the process of collision and separation of particles against the surface.

Formula for u_p is given by:

$$u_p = c u_{*t} \tag{29}$$

where c is a constant parameter and u_{*t} is threshold friction velocity that separates the processes of erosion and deposition.

Substituting (28) and (29) into (27), we obtain a general expression for the saltation layer:

$$Q_{salt} = \frac{ce\rho}{g} u_{*t}(u_*^2 - u_{*n}^2 - u_{*t}^2) \tag{30}$$

Determining the values of the coefficients from the experimental data, the authors give the final form of the expression:

$$Q_{salt} = \frac{0.68\rho}{u_* g} u_{*t}(u_*^2 - u_{*n}^2 - u_{*t}^2) \tag{31}$$

It is shown that, in contrast to the result obtained by Bagnold for sand, the snow flux is a quadratic function of the friction velocity, not a cubic one. The authors point out that this is a consequence of the presence of an average horizontal speed, which does not affect the wind speed in general, and efficiency, which grows reciprocally to the wind speed. It is also noted that saltation models for sand are poorly applicable to snow transport just because of the materials they describe. Grains of sand are separate, non-sticking particles, while snowflakes are crystals that can break up or stick together.

Finally, let us consider the latest and most commonly used way to describe the saltation layer, the erosion-deposition model. It is based on the work of Anderson and Huff [1], who proposed a model of aeolian transport of sand deposits for the case when particles of

the size of sand grains are subject to saltation. It consists of four parts that describe a) aerodynamic entrainment; b) trajectories of grains of sand; c) interaction of particles with the surface; d) influence on the impulse from the wind. Each submodel is responsible for a specific part of the process and is supported by experimental data to refine the values of some constants. Together the parts make it possible to calculate aeolian saltation from the moment of sediment capture by aerodynamic entrainment until the transition to a stationary state. The authors show the important role of long, high-energy trajectories: despite the predominance of short trajectories with low energies in the saltation zone, it is the collisions of sediments with the surface that determine the response of the entire system to changes in wind velocity due to knocking new particles out of the surface. A form of the "splash" function is proposed to take such jumps into account, which can last as long as a few seconds. An accurate calculation of fluctuations in wind velocity allows establishing its relationship with the stationary mass flow in the form of a power function of the shear velocity. This model, in contrast to the previous one, takes into account inertia, but the "splash" function is not suitable for snow in the form given by the authors and requires modification [11]. Using these results, Naaim et al. [11] formulated a model that has been used by researchers from different countries almost unchanged for about quarter of a century. Pointing out the shortcomings in the models developed by Iversen et al. and Liston et al., as well as the limitations that do not allow direct use of the Anderson and Huff model, the team of authors proposed their own version of the erosion-deposition model, in which they tried to level out the failures of their colleagues. Omitting the details of the derivation of the flow equations, described in detail in the article, let us turn our attention to the modelling of snow transport.

For the mass exchange flux between air and snow layer, the following expression is proposed, similar to (24):

$$q_g = q_+ - q_- \tag{32}$$

The erosion flow is written as:

$$q_- = A\rho_a(u_*^2 - u_{*t}^2) \tag{33}$$

where A is coefficient that depends on the degree of cohesion in the surface layer and ρ_a is air density.
The deposition flow is given by:

$$q_+ = \bar{C}w_f\left(1 - \frac{u_*^2}{u_{*t}^2}\right) \tag{34}$$

where all quantities correspond to those in the previous formulae.
At each step of the simulation, expression (2) is recalculated for the flow in each cell of the boundary layer and then compared with the value u_t. The snow deposition process is governed by the following conditions:

$u_* < u_t$	**Deposition:** $q_g = q_+$
$u_* = u_t$	**Unchanged:** $q_g = 0$
$u_* > u_t$	**Erosion:** $q_g = -q_-$

The change in the height of the snow layer is described by an expression similar to (26):

$$\frac{\partial h}{\partial t} = \frac{q_g}{\gamma} \tag{35}$$

This model was applied to the problem of a flow around a solid snow fence (see Fig. 5). In their work, the authors note that the expression for the erosion flux must be revised and improved despite the quality of results obtained using the model, which are in agree-

ment with the experiment. This will require new field observations or development of a "splash" function for snow with different properties. They also neglected the movement of particles due to creep and took into account only those particles that were carried by aerodynamic forces.

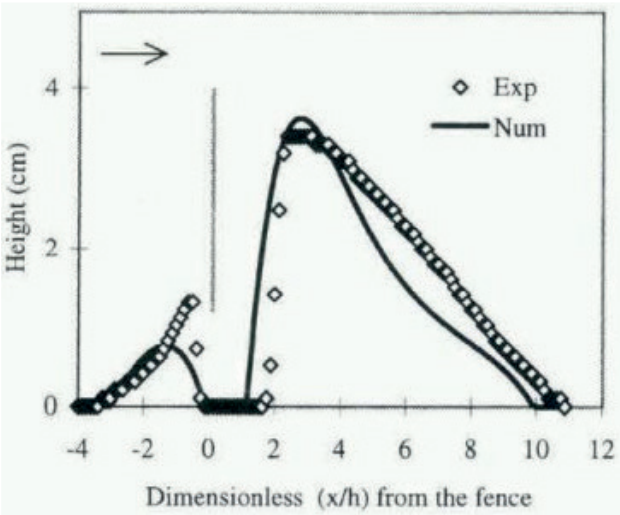

a) $u_* = 0.23$ *m/s*, $u_{*t} = 0.21$ *m/s*

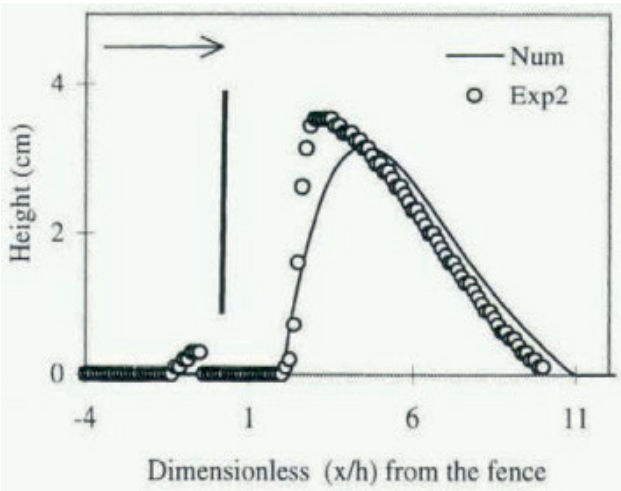

b) $u_* = 0.25$ *m/s*, $u_{*t} = 0.21$ *m/s*

Figure 5. Comparison of the results of modelling a snowdrift behind a solid fence with experimental data [43]

ALTERNATIVE METHODS

Among the most modern CFD methods is the use of neural networks that do not directly solve the Navier-Stokes equations, but simulate their solution, learning from a dataset of flow behaviors. Such an approach allows obtaining sufficiently plausible results, spending orders of magnitude less computing power and physical time, since with classical CFD each problem needs to be computed from the scratch, but a neural network is only required to be trained once.

Sanchez-Gonzalez et al. [15] developed a framework, which they call "graph network-based simulators" (GNS). Physical systems are represented by sets of interacting particles, the dynamics of which are described by graphs. Fig. 6 shows how the algorithm works. The simulator s_θ transforms the initial state X^{t_0} into the state $\tilde{X}^{t_K}$ by iteratively applying the trained dynamic model d_θ (a) according to the "encoder-processor-decoder" scheme (b): first, the input state X is expressed by a graph G^0 (c), then M signal transmissions between its nodes are performed, generating graphs $G^1 \dots G^M$ (d), and finally dynamic information $Y(e)$ is extracted from the graph G^M.

This framework allows simulating many materials, from viscous substances (a) to water (b) and sand (c), as well as their interaction with solid obstacles (d). The model can also be trained on several materials at once (e). A pre-trained model can also handle some cases that it wasn't trained on, like high turbulence flows (f), objects of unknown shape (g), and much more complex design cases compared to the samples (h). In Fig. 9, the top row shows the initial states, the middle row shows the model predictions, and the bottom row shows the results of CFD calculations.

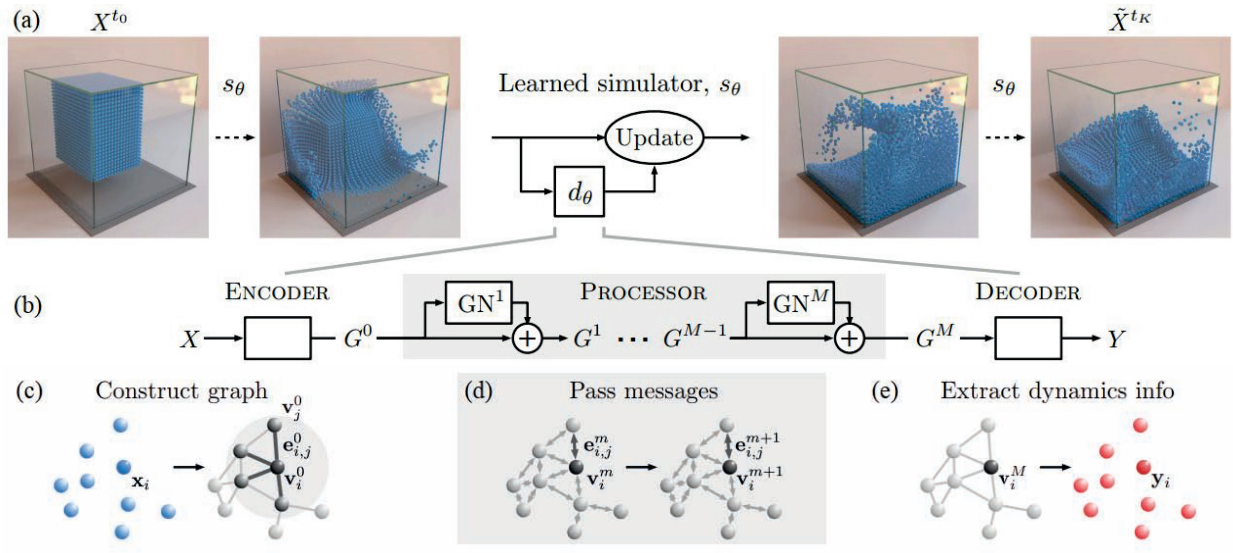

Figure 6. Scheme of the GNS framework

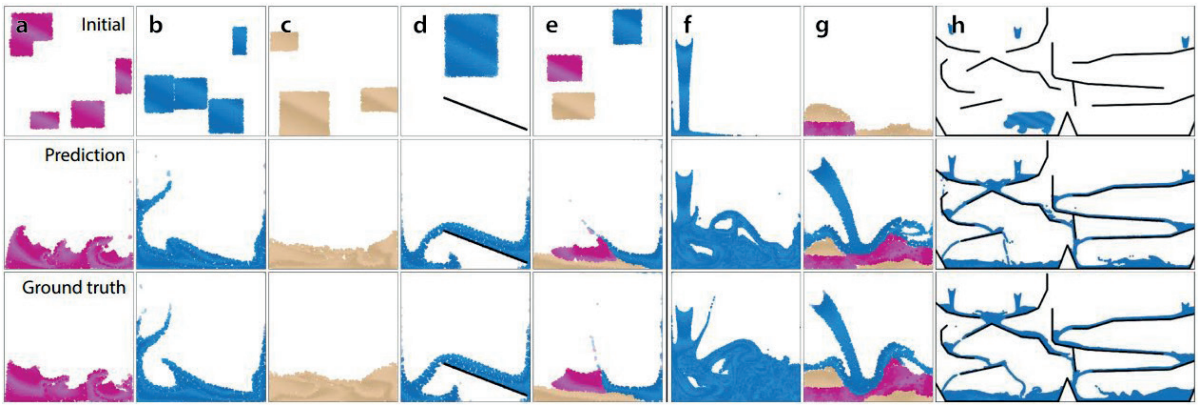

Figure 7. Examples of flow behaviors obtained using the GNS framework for various substances: pink indicates a viscous substance, blue indicates a liquid one, and beige indicates sand

Another promising "fast" alternative method is replacing the Navier-Stokes equations with a system of lattice Boltzmann equations (LBM). In this case, the fluid flow is perceived as a collection of particles on a spatial grid. The LBM algorithm is characterized by a simpler implementation, higher efficiency in parallelization, and it is better suited for more complex boundary conditions. The team [18] has developed a model of snow transport, which does not yet take into account the influence of snow on the air, but already gives quite plausible distributions of snow.

The numerical lattice Boltzmann equation is a prognostic equation for the distribution function of particles in the *i*-th direction, f_i, which is given by:

$$f_i(\boldsymbol{r} + \boldsymbol{c}_i + \Delta t, t + \Delta t) = f_i(\boldsymbol{r}, t) + \Omega_i \Delta t, \quad (36)$$

where $\boldsymbol{r}$ is particle direction vector, $\boldsymbol{c}_i$ is particle velocity vector, Δt is time step, Ω_i is interparticle interaction, which is described using the Bhatnagar-Gross-Krook approximation, replacing it with the relaxation of the equilibrium state of the distribution function:

$$\Omega_i = -\frac{1}{\tau}\left(f_i - \hat{f}_i\right), \tag{37}$$

where τ is relaxation time as a function of kinematic viscosity ν:

$$\tau = \frac{1}{2} + \frac{3\nu}{c^2 \Delta t} \tag{38}$$

and $\hat{f}_i$ is equilibrium distribution function of particles in the i-th direction.
The equation of motion of snow particles is given by:

$$\frac{d\boldsymbol{u_p}}{dt} = -\frac{3}{4}\left(\frac{\rho_a}{\rho_p d}\right) C_d V_R \left(\boldsymbol{u_p} - \boldsymbol{u}\right) - g\boldsymbol{k}, \tag{39}$$

where $\boldsymbol{u_p}$ is particle velocity vector, $\boldsymbol{u}$ is wind speed vector, $V_R = \left|\boldsymbol{u_p} - \boldsymbol{u}\right|$, g is acceleration due to gravity, ρ_a and ρ_p are air density (1.34 kg/m^3) and particle density (910 kg/m^3), respectively, d is particle diameter (100 μm), and C_d is drag coefficient of a particle, equal to

$$C_d = \frac{24\nu_0}{V_R d} + \frac{6}{1 + V_R d/\nu_0} + 0.4, \tag{40}$$

where ν_0 is viscosity, equal to 10^{-5} m^{2}s^{-1}.
The results obtained by the authors are shown in Fig. 8-9.

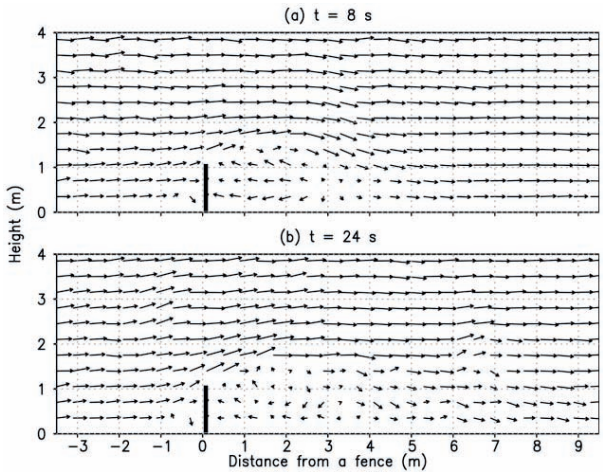

a)

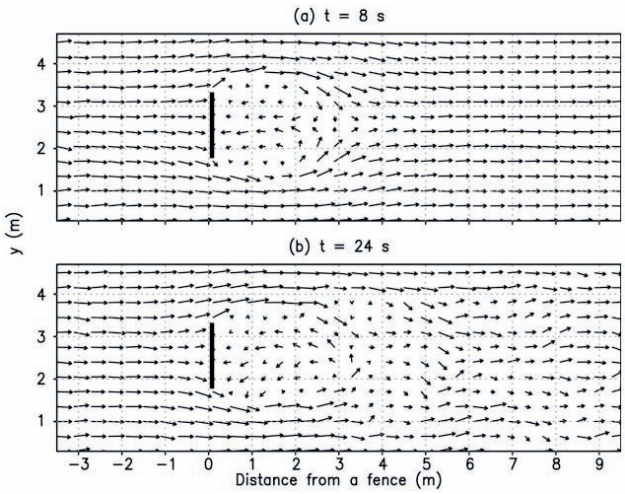

b)

Figure 8. Solution of lattice Boltzmann equations (LBM). Vector field of wind velocity in vertical (a) and horizontal (b, z = 0.5 m) cross-sections for three-dimensional flow around a solid fence.

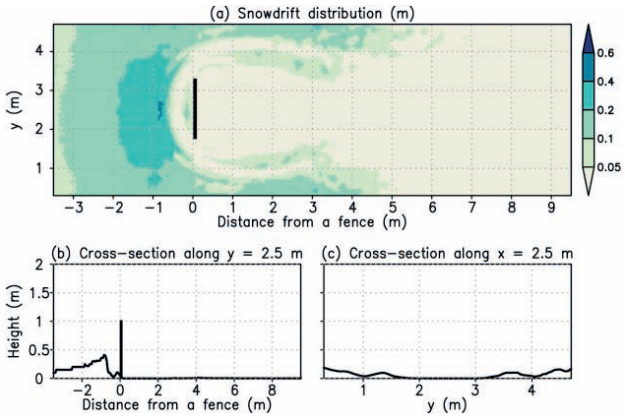

Figure 9. Solution lattice Boltzmann equations (LBM). Contours of the obtained snow layer (a), vertical cross-sections along the x-axis (b) and y-axis (c) for a three-dimensional flow around a solid fence

CONCLUSIONS

This paper provides an overview of various methods of numerical modelling of snow accumulation, primarily based on foreign

scientific publications and regulatory documents. The methods themselves, as well as the limits of their applicability, the experimental data they were calibrated on and/or verified with, are reviewed in detail. Both "classical" methods and modern "alternative" ones are reviewed. Due to the fact that Russian regulatory documents still do not allow the use of numerical modelling of snow accumulation (despite almost half a century of work in this field by scientists from all over the world), it was impossible to carry out a comparative analysis of foreign methods with Russian ones, since original, non-compilatory scientific works in the field do not yet exist.

It is shown that, taking into account: a) the experience of the worldwide scientific and engineering communities and a variety of approaches to numerical modelling of snow accumulation on roofs of buildings and structures; b) the complexity of the subject, which itself dictates this variety; it is impossible to cover the entire range of sample cases and situations using only a limited set of simple schemes from SP and experimental methods. Further rejection of the methods of numerical and physical modelling, which are recognized and applied by the world community, casts serious doubt on the legitimacy of the recommendations being developed and carries significant risks for the mechanical safety of unique buildings and structures with arbitrary geometry. The inclusion of numerical modelling is necessary to form a modern and flexible regulatory framework, which could be used by engineers to solve much more complex design problems than it is possible now. This requires:

1) Modern research, both foreign and domestic, with the latter taking into account specific features of current construction practices and focused on requests from the industry. Also, possibly additional theoretical and practical developments, new or refined methods for modelling snow accumulation.

2) Development, verification and approbation of numerical methods, carried out using appropriate experimental equipment and in the field, that would allow using all the necessary data (climatic, meteorological, etc.) in numerical models for maximum efficiency.

Only a complex and comprehensive approach to the implementation of technologies for numerical modelling of snow accumulations in modern construction practice will provide the required level of technical support for unique buildings and structures with arbitrary geometry and guarantee the safety of their construction.

ACKNOWLEDGMENTS

This work was financially supported by the Ministry of Science and Higher Education of the Russian Federation (Project: Theoretical and experimental design of new composite materials to ensure safety during the operation of buildings and structures under conditions of technogenic and biogenic threats #FSWG-2020-0007)

REFERENCES

1. **Anderson, R. S., & Haff, P. K.** (1991). Wind modification and bed response during saltation of sand in air. In Aeolian Grain Transport 1 (pp. 21-51). Springer, Vienna.
2. **Bagnold, R. A.** (1937). The transport of sand by wind. The Geographical Journal, 89(5), 409-438.
3. **Bagnold, R.A.,** (1941). The Physics of Blown Sand and Desert Dunes. Methuen & Co.: William Morrow, New York.
4. **Beyers, J. H. M., Sundsbø, P. A., & Harms, T. M.** (2004). Numerical simulation of three-dimensional, transient snow drifting around a cube. Journal of Wind Engineering and Industrial Aerodynamics, 92(9), 725-747.
5. Eurocode 1: Actions on structures – Part 1-3: General actions – Snow loads.

6. **Iversen, J. D**. (1979). Drifting snow similitude. Journal of the hydraulics division, 105(6), 737-753.
7. **Iversen, J. D.** (1980). Drifting-snow similitude—transport-rate and roughness modeling. Journal of glaciology, 26(94), 393-403.
8. **Liston, G. E., Brown, R. L., & Dent, J. D.** (1993). A two-dimensional computational model of turbulent atmospheric surface flows with drifting snow. Annals of Glaciology, 18, 281-286.
9. **Mellor, M.** (1977). Engineering properties of snow. Journal of Glaciology, 19(81), 15-66.
10. **Moore, I., Mobbs, S. D., Ingham, D. B., & King, J. C.** (1994). A numerical model of blowing snow around an Antarctic building. Annals of Glaciology, 20, 341-346.
11. **Naaim, M., Naaim-Bouvet, F., & Martinez, H.** (1998). Numerical simulation of drifting snow: erosion and deposition models. Annals of glaciology, 26, 191-196.
12. **Okaze, T., Mochida, A., Tominaga, Y., Ito, Y., & Yoshino, H.** (2010). CFD prediction of snowdrift around a cube using two transport equations for drifting snow density. In The Fifth International Symposium on Computational Wind Engineering (CWE2010).
13. **Gray, D. M., Pomeroy, J. W., & Granger, R. J.** (1989). Modelling snow transport, snowmelt and meltwater infiltration in open, northern regions. Northern Lakes and Rivers, 22, 8-22.
14. **Pomeroy, J. W., & Gray, D. M.** (1990). Saltation of snow. Water resources research, 26(7), 1583-1594.
15. **Sanchez-Gonzalez, A., Godwin, J., Pfaff, T., Ying, R., Leskovec, J., & Battaglia, P.** (2020, November). Learning to simulate complex physics with graph networks. In International Conference on Machine Learning (pp. 8459-8468). PMLR.
16. **Serine, A., Shimura, M., Maruoka, A., & Hirano, H.** (1999). The numerical simulation of snowdrift around a building. International Journal of Computational Fluid Dynamics, 12(3-4), 249-255.
17. **Sundsbø, P. A.** (1998). Numerical simulations of wind deflection fins to control snow accumulation in building steps. Journal of Wind Engineering and Industrial Aerodynamics, 74, 543-552.
18. **Tanji, S., Inatsu, M., & Okaze, T.** (2021). Development of a snowdrift model with the lattice Boltzmann method. Progress in Earth and Planetary Science, 8(1), 1-16.
19. **Tominaga, Y.** (2018). Computational fluid dynamics simulation of snowdrift around buildings: Past achievements and future perspectives. Cold Regions Science and Technology, 150, 2-14.
20. **Uematsu, T., Nakata, T., Takeuchi, K., Arisawa, Y., & Kaneda, Y.** (1991). Three-dimensional numerical simulation of snowdrift. Cold regions science and technology, 20(1), 65-73.
21. **Kind, R. J.** (1990). Mechanics of aeolian transport of snow and sand. Journal of Wind Engineering and Industrial Aerodynamics, 36, 855-866.
22. **Thiis, T. K., & Ramberg, J. F.** (2008). Measurements and numerical simulations of development of snow drifts of curved roofs. Proceedings of the Snow Engineering VI, Whistler, BC, Canada, 21-27.
23. **Wang, J., Liu, H., Chen, Z., & Ma, K.** (2020). Wind tunnel test of wind-induced snowdrift on stepped flat roofs during snowfall. Natural Hazards, 104(1), 731-752.
24. ASCE 7-16 Minimum Design Loads and Associated Criteria for Buildings and Other Structures.
25. JSCE - Standard Specifications for Steel and Composite Structures
26. Building Code of RF 20.13330.2016 Load and actions.
27. **Tominaga, Y., Okaze, T., & Mochida, A.** (2011). CFD modeling of snowdrift around a building: An overview of models and evaluation of a new approach. Building and Environment, 46(4), 899-910.

28. **Isyumov, N.,** 1971. An Approach to the Prediction of Snow Loads, PhD. Thesis, University of Western Ontario, London, Canada.
29. **Isyumov, N., & Davenport, A. G.** (1974). A probabilistic approach to the prediction of snow loads. Canadian Journal of Civil Engineering, 1(1), 28-49.
30. **Kobayashi, D.** (1972). Studies of snow transport in low-level drifting snow. Contributions from the Institute of Low Temperature Science, 24, 1-58.
31. **Gamble, S. L., Kochanski, W. W., & Irwin, P. A.** (1992). Finite area element snow loading prediction-applications and advancements. Journal of wind engineering and industrial aerodynamics, 42(1-3), 1537-1548.
32. **Beyers, J. H. M., Sundsbø, P. A., & Harms, T. M.** (2004). Numerical simulation of three-dimensional, transient snow drifting around a cube. Journal of Wind Engineering and Industrial Aerodynamics, 92(9), 725-747.
33. **Tominaga, Y., Mochida, A., Yoshino, H., Shida, T., & Okaze, T.** (2006, July). CFD prediction of snowdrift around a cubic building model. In The fourth international symposium on computational wind engineering (CWE2006), Yokohama, Japan (pp. 941-944).
34. **Thiis, T. K., & O'Rourke, M.** (2015). Model for snow loading on gable roofs. Journal of Structural Engineering, 141(12), 04015051.
35. **Tominaga, Y., Okaze, T., Mochida, A.**, 2016. CFD simulation of drift snow loads for an isolated gable-roof building. In: Proceedings of the 8th International Conference on Snow Engineering, Nantes, France, pp. 208–214 (June 14–17)
36. **Kang, L. Y., Zhou, X. Y., & Gu, M.** (2016). A new method for predicting snowdrift on flat roofs. In Proceedings of the 8th International Conference on Snow Engineering, Nantes, France, pp. 137–141 (June 14–17).
37. **Zhou, X., Kang, L., Gu, M., Qiu, L., & Hu, J.** (2016). Numerical simulation and wind tunnel test for redistribution of snow on a flat roof. Journal of Wind Engineering and Industrial Aerodynamics, 153, 92-105.
38. **Thiis, T. K.** (2000). A comparison of numerical simulations and full-scale measurements of snowdrifts around buildings. Wind & structures, 3(2), 73-81.
39. **Thiis, T. K.** (2003). Large scale studies of development of snowdrifts around buildings. Journal of Wind Engineering and Industrial Aerodynamics, 91(6), 829-839.
40. **Beyers, M., & Waechter, B.** (2008). Modeling transient snowdrift development around complex three-dimensional structures. Journal of Wind Engineering and Industrial Aerodynamics, 96(10-11), 1603-1615.
41. **Okaze, T., Kato, S., Tominaga, Y., Mochida, A.,** 2016. CFD prediction of snowdrift in a building array. In: Proceedings of the 8th International Conference on Snow Engineering, Nantes, France, pp. 26–29 (June 14–17).
42. ASCE/SEI 49-12 Wind Tunnel Testing for Buildings and Other Structures
43. **Takeuchi, M.** (1980). Vertical profile and horizontal increase of drift-snow transport. Journal of Glaciology, 26(94), 481-492.
44. **Qiang, S., Zhou, X., Gu, M., & Kang, L**. (2021). A novel snow transport model for analytically investigating effects of wind exposure on flat roof snow load due to saltation. Journal of Wind Engineering and Industrial Aerodynamics, 210, 104505.
45. **Ma, W., Li, F., Sun, Y., Li, J., & Zhou, X.** (2021). Field measurement and numerical simulation of snow deposition on an embankment in snowdrift. Wind and Structures, 32(5), 453-469.
46. ISO 4355-2016 – Bases for design of structures — Determination of snow loads on roofs, IDT.
47. **Hitryh, D. P**. (2013). Opyt modelirovaniya processov snegoperenosa i snegootlozheniya [Experience in modeling the processes

of snow transfer and snow deposition]. ANSYS Advantage, 27Y32.

48. **Belostocky A. M. i dr.** O snegovyh nagruzkah na zdaniya i sooruzheniya [About snow loads on buildings and structures] // Vopro-sy prikladnoj matematiki i vychislitel'-noj mekhaniki. – 2017. – P. 212-215.
49. **Belostocky A.M., Akimov P.A., Afanas'eva I.N.** Vychislitel'naya aerodinamika v zadachah stroitel'stva [Computational aerodynamics in construction problems]. M., Izdatel'stvo ASV, 2017, 720 p.
50. **Stoyanov, V.V., ZHgalli, SH.** CHislennoe modelirovanie snegovyh nagruzok na pokrytiyah unikal'nyh i sovremennyh arhitekturnyh form [Numerical modeling of snow loads on coverings of unique and modern architectural forms]. – 2019. – T. 30 (69) No 1 (2).
51. **Matveenko, E.V.** (2018). Obobshchennyj analiz metodov modelirovaniya snegovoj nagruzki [Generalized analysis of snow load modeling methods]. // Vestnik Brestskogo gosudarstvennogo tekhnicheskogo universiteta. – P. 77-80.
52. **Belostotsky, A.M., Britikov, N.A., Goryachevsky, O.S.** (2021). Comparison of determination of snow loads for roofs in building codes of various countries. International Journal for Computational Civil and Structural Engineering, 17(3), 39-47.

СПИСОК ЛИТЕРАТУРЫ

1. **Anderson R. S., Haff P. K**. Wind modification and bed response during saltation of sand in air //Aeolian Grain Transport 1. – Springer, Vienna, 1991. – C. 21-51.
2. **Bagnold R. A.** The transport of sand by wind //The Geographical Journal. – 1937. – T. 89. – №. 5. – C. 409-438.
3. **Bagnold, R.A.,** 1941. The Physics of Blown Sand and Desert Dunes. Methuen & Co.: William Morrow, New York.
4. **Beyers J. H. M., Sundsbø P. A., Harms T. M.** Numerical simulation of three-dimensional, transient snow drifting around a cube //Journal of Wind Engineering and Industrial Aerodynamics. – 2004. – T. 92. – №. 9. – C. 725-747.
5. Eurocode 1: Actions on structures – Part 1-3: General actions – Snow loads.
6. **Iversen J. D.** Drifting snow similitude //Journal of the hydraulics division. – 1979. – T. 105. – №. 6. – C. 737-753.
7. **Iversen J. D.** Drifting-snow similitude—transport-rate and roughness modeling //Journal of glaciology. – 1980. – T. 26. – №. 94. – C. 393-403.
8. **Liston G. E., Brown R. L., Dent J. D.** A two-dimensional computational model of turbulent atmospheric surface flows with drifting snow //Annals of Glaciology. – 1993. – T. 18. – C. 281-286.
9. **Mellor M.** Engineering properties of snow //Journal of Glaciology. – 1977. – T. 19. – №. 81. – C. 15-66.
10. **Moore, I., Mobbs, S.D., Ingham, D.B., King, J.C.,** 1994. A numerical model of blowing snow around an Antarctic building. *Ann. Glaciol.* T. 20 (1), C. 341–346.
11. **Naaim M., Naaim-Bouvet F., Martinez H.** Numerical simulation of drifting snow: erosion and deposition models //Annals of glaciology. – 1998. – T. 26. – C. 191-196.
12. **Okaze T. et al.** CFD prediction of snow-drift around a cube using two transport equations for drifting snow density //The Fifth International Symposium on Computational Wind Engineering (CWE2010). – 2010.
13. **Gray D. M., Pomeroy J. W., Granger R. J.** Modelling snow transport, snowmelt and meltwater infiltration in open, northern regions //Northern Lakes and Rivers. – 1989. – T. 22. – C. 8-22.
14. **Pomeroy, J.W., Gray, D.M.,** 1990. Saltation of Snow. *Wat. Res. Research.* T. 26, Ч. 7, C. 1583-1594.
15. **Sanchez-Gonzalez A. et al.** Learning to simulate complex physics with graph net-

works //International Conference on Machine Learning. – PMLR, 2020. – С. 8459-8468.
16. **Serine A. et al**. The numerical simulation of snowdrift around a building //International Journal of Computational Fluid Dynamics. – 1999. – Т. 12. – №. 3-4. – С. 249-255.
17. **Sundsbø P. A**. Numerical simulations of wind deflection fins to control snow accumulation in building steps //Journal of Wind Engineering and Industrial Aerodynamics. – 1998. – Т. 74. – С. 543-552.
18. **Tanji S., Inatsu M., Okaze T.** Development of a snowdrift model with the lattice Boltzmann method //Progress in Earth and Planetary Science. – 2021. – Т. 8. – №. 1. – С. 1-16.
19. **Tominaga Y**. Computational fluid dynamics simulation of snowdrift around buildings: Past achievements and future perspectives //Cold Regions Science and Technology. – 2018. – Т. 150. – С. 2-14.
20. **Uematsu T. et al.** Three-dimensional numerical simulation of snowdrift //Cold regions science and technology. – 1991. – Т. 20. – №. 1. – С. 65-73.
21. **Kind R. J.** Mechanics of aeolian transport of snow and sand //Journal of Wind Engineering and Industrial Aerodynamics. – 1990. – Т. 36. – С. 855-866.
22. **Thiis T. K., Ramberg J. F.** Measurements and numerical simulations of development of snow drifts of curved roofs //Proceedings of the Snow Engineering VI, Whistler, BC, Canada. – 2008. – С. 21-27.
23. **Wang J. et al.** Wind tunnel test of wind-induced snowdrift on stepped flat roofs during snowfall //Natural Hazards. – 2020. – Т. 104. – №. 1. – С. 731-752.
24. ASCE 7-16 Minimum Design Loads and Associated Criteria for Buildings and Other Structures.
25. JSCE - Standard Specifications for Steel and Composite Structures
26. СП 20.13330.2016 Нагрузки и воздействия
27. **Tominaga Y., Okaze T., Mochida A.** CFD modeling of snowdrift around a building: An overview of models and evaluation of a new approach //Building and Environment. – 2011. – Т. 46. – №. 4. – С. 899-910.
28. **Isyumov N.** An approach to the prediction of snow ioads // PhD. Theis, University of Western Ontario, Canada. – 1971.
29. **Isyumov N., Davenport A. G.** A probabilistic approach to the prediction of snow loads //Canadian Journal of Civil Engineering. – 1974. – Т. 1. – №. 1. – С. 28-49.
30. **Kobayashi D.** Studies of snow transport in low-level drifting snow //Contributions from the Institute of Low Temperature Science. – 1972. – Т. 24. – С. 1-58.
31. **Gamble S. L., Kochanski W. W., Irwin P. A.** Finite area element snow loading prediction-applications and advancements //Journal of wind engineering and industrial aerodynamics. – 1992. – Т. 42. – №. 1-3. – С. 1537-1548.
32. **Beyers J. H. M., Sundsbø P. A., Harms T. M.** Numerical simulation of three-dimensional, transient snow drifting around a cube //Journal of Wind Engineering and Industrial Aerodynamics. – 2004. – Т. 92. – №. 9. – С. 725-747.
33. **Tominaga Y. et al.** CFD prediction of snowdrift around a cubic building model //The fourth international symposium on computational wind engineering (CWE2006), Yokohama, Japan. – 2006. – С. 941-944.
34. **Thiis T. K., O'Rourke M.** Model for snow loading on gable roofs //Journal of Structural Engineering. – 2015. – Т. 141. – №. 12. – С. 04015051.
35. **Tominaga Y. et al.** CFD simulation of drift snow loads for an isolated gable-roof building //8th International Conference on Snow Engineering. – Nantes France, 2016. – С. 14-17.
36. **Kang L. Y., Zhou X. Y., Gu M.** A new method for predicting snowdrift on flat roofs //Proceedings of the 8th International

Conference on Snow Engineering, Nantes, France, pp. 137–141 (June 14–17). – 2016.
37. **Zhou X. et al.** Numerical simulation and wind tunnel test for redistribution of snow on a flat roof //Journal of Wind Engineering and Industrial Aerodynamics. – 2016. – Т. 153. – С. 92-105.
38. **Thiis T. K.** A comparison of numerical simulations and full-scale measurements of snowdrifts around buildings //Wind & structures. – 2000. – Т. 3. – №. 2. – С. 73-81.
39. **Thiis T. K.** Large scale studies of development of snowdrifts around buildings //Journal of Wind Engineering and Industrial Aerodynamics. – 2003. – Т. 91. – №. 6. – С. 829-839.
40. **Beyers M., Waechter B.** Modeling transient snowdrift development around complex three-dimensional structures //Journal of Wind Engineering and Industrial Aerodynamics. – 2008. – Т. 96. – №. 10-11. – С. 1603-1615.
41. **Okaze T. et al.** CFD prediction of snowdrift in a building array //Proceedings of the 8th International Conference on Snow Engineering, Nantes, France. – 2016. – С. 14-17.
42. ASCE/SEI 49-12 Wind Tunnel Testing for Buildings and Other Structures
43. **Takeuchi M.** Vertical profile and horizontal increase of drift-snow transport //Journal of Glaciology. – 1980. – Т. 26. – №. 94. – С. 481-492.
44. **Qiang, S., Zhou, X., Gu, M., & Kang, L.**, 2021. A novel snow transport model for analytically investigating effects of wind exposure on flat roof snow load due to saltation. *J. Wind Eng. Ind. Aerodyn.*, Т. 210, 104505.
45. **Ma W. et al.** Field measurement and numerical simulation of snow deposition on an embankment in snowdrift //Wind and Structures. – 2021. – Т. 32. – №. 5. – С. 453-469.
46. ISO 4355-2016 – Bases for design of structures — Determination of snow loads on roofs, IDT.
47. **Хитрых Д. П.** Опыт моделирования процессов снегопереноса и снегоотложения //ANSYS Advantage. – 2013. – С. 27Y32.
48. **Белостоцкий А.М., Акимов П.А., Афанасьева И.Н., Кайтуков Т.Б.** О снеговых нагрузках на здания и сооружения // Вопросы прикладной математики и вычислительной механики. Сборник трудов №20. – 2017. – С. 212-215.
49. **Белостоцкий А.М., Акимов П.А., Афанасьева И.Н.** Вычислительная аэродинамика в задачах строительства. М., Издательство АСВ, 2017, 720 с.
50. **Стоянов, В.В., Жгалли, Ш.** Численное моделирование снеговых нагрузок на покрытиях уникальных и современных архитектурных форм. – 2019. – Том 30 (69) No 1 Частина 2.
51. **Матвеенко Е.В.** Обобщенный анализ методов моделирования снеговой нагрузки. // Вестник Брестского государственного технического университета. 2018. №1 – С. 77-80.
52. **Белостоцкий А.М., Бритиков Н.А., Горячевский О.С.** Сравнение нормативных документов различных стран в части назначения снеговых нагрузок // International Journal for Computational Civil and Structural Engineering. – 2021. – Т. 17. – №. 3. – С. 39-47.

Belostotsky Alexander Mikhailovich, RAACS academician, professor, D.Sc. in Engineering; General Director of Scientific Research Center StaDyO; Professor of the Department of Informatics and Applied Mathematics and Scientific Director of the A.B. Zolotov NICCM of the National Research Moscow State University of Civil Engineering; Professor of the Department of Building Structures, Buildings and Structures of the Russian University of Transport (MIIT); 125040, Russia, Moscow, 3rd Yamsky Pole, 18, office 810; Tel. +7 (499) 706-88-10 E-mail: amb@stadyo.ru

Britikov Nikita Aleksandrovich, engineer of the A.B. Zolotov NICCM of the National Research Moscow State University of Civil Engineering; postgraduate student of the Russian University of Transport (MIIT); 129337, Russia, Moscow, Yaroslavskoe shosse, 26. E-mail: n.a.britikov@gmail.com

Goryachevsky Oleg Sergeevich, Lead Computing Engineer of Research Center StaDyO; Deputy Director of the A.B. Zolotov NICCM of the National Research Moscow State University of Civil Engineering; 129337, Russia, Moscow, Yaroslavskoe shosse, 26. E-mail: osgoryachevskij@mail.ru

Белостоцкий Александр Михайлович, академик РААСН, профессор, доктор технических наук; генеральный директор ЗАО Научно-исследовательский центр СтаДиО; профессор кафедры Информатики и прикладной математики Национального исследовательского, научный руководитель НОЦ КМ им. А.Б. Золотова Московского государственного строительного университета; профессор кафедры «Строительные конструкции, здания и сооружения» Российского университета транспорта (МИИТ); 125040, Россия, Москва, ул. 3-я Ямского Поля, д.18, офис 810; тел. +7 (499) 706-88-10. E-mail: amb@stadyo.ru

Бритиков Никита Александрович, инженер НОЦ КМ им. А.Б. Золотова Национального исследовательского Московского государственного строительного университета; аспирант Российского университета транспорта (МИИТ); 129337, Россия, г. Москва, Ярославское шоссе, д. 26. E-mail: n.a.britikov@gmail.com.

Горячевский Олег Сергеевич, ведущий инженер-расчетчик ЗАО Научно-исследовательский центр СтаДиО; заместитель директора НОЦ КМ им. А.Б. Золотова Национального исследовательского Московского государственного строительного университета; 129337, Россия, г. Москва, Ярославское шоссе, д. 26. E-mail: osgoryachevskij@mail.ru

DOI:10.22337/2587-9618-2021-17-4-60-72

STRESS-DEFORMED STATE OF THE BOUNDATION OF HYDRAULIC STRUCTURES AT CONTROLLED COMPENSATION DISCHARGE

Alexandra S. Bestuzheva, Ivan V. Chubatov

National Research Moscow State University of Civil Engineering, Moscow, RUSSIA

Abstract. Numerical simulation of the process of injection of mortar into the thickness of the sandy base during the work on lifting and leveling the structure by the method of compensatory injection is carried out. An author's program has been developed that implements the finite element method (FEM) in a spatial formulation, taking into account the elastic-plastic nature of soil deformation, in which a special element in the form of a spheroid has been developed to describe the expanding area at the location of the injector, which changes its volume during the injection of mortar. During the verification of the program, the results of mathematical modeling were compared with the data of a physical experiment conducted by PhD Luca Masini from the University of La Sapienza (Rome, Italy). Numerical modeling of the stress-strain state of the base of the structure during repair work is considered by the example of lifting the foundation plate of the Zagorskaya PSPP-2. A number of tasks are being solved related to minimizing the number of injection columns, their location, the pitch of the cuffs, the selection of portions of the injected solution, taking into account the requirements for uniform lifting of the foundation plate in order to avoid additional cracking.

Keywords: compensatory injection, sediment leveling, stress-strain state of soil structures and foundations, numerical modeling, finite element method, “energy” soil model.

НАПРЯЖЕННО-ДЕФОРМИРОВАННОЕ СОСТОЯНИЕ ОСНОВАНИЯ ГИДРОТЕХНИЧЕСКИХ СООРУЖЕНИЙ ПРИ УПРАВЛЯЕМОМ КОМПЕНСАЦИОННОМ НАГНЕТАНИИ

А.С. Бестужева, И.В. Чубатов

Национальный исследовательский Московский государственный строительный университет, г. Москва, РОССИЯ

Аннотация. Проведено численное моделирование процесса нагнетания строительного раствора в толщу песчаного основания в ходе работ по подъему и выравниванию сооружения методом компенсационного нагнетания (КН). Разработана авторская программа, реализующая метод конечных элементов (МКЭ) в пространственной постановке с учетом упругопластического характера деформирования грунта, в которой для описания расширяющейся области в месте расположения инжектора разработан специальный элемент в виде сфероида, изменяющего свой объем в процессе нагнетания строительного раствора. В ходе верификации программы проведено сопоставление результатов математического моделирования с данными физического эксперимента, поставленного PhD Luca Masini из университета La Sapienza (Рим, Италия). Численное моделирование напряженно-деформированного состояния (НДС) основания сооружения при проведении ремонтных работ рассматривается на примере подъёма фундаментной плиты Загорской ГАЭС-2. Решается ряд задач, связанных с минимизацией количества инъекционных колонн, их местоположением, шагом манжет, подбором порций инъектируемого раствора с учетом требований по равномерному подъему фундаментной плиты во избежание дополнительного трещинообразования.

Ключевые слова: компенсационное нагнетание, выравнивание осадок, напряженно-деформированное состояние грунтовых сооружений и оснований, численное моделирование, метод конечных элементов, «энергетическая» модель грунта.

INTRODUCTION

Non-admission of limit values for uneven precipitation in the foundations of hydraulic structures is one of the main safety criteria and a determining condition in the design of structures according to the second group of limit states. Nevertheless, the inevitable uneven distribution of stresses along the soles of structures, complex geological conditions, interaction with the water environment and filtration flow often cause the collapse of retaining walls, tilting foundations, abnormal settlement of the foundations of hydraulic structures. But the problem of excess settlement of buildings has become most acute in recent decades during the construction of underground transport infrastructure in cities. First of all, to solve these problems associated with tunneling, a method was developed for securing the soil mass using compensation injection technology, in which mortars are injected synchronously with mining operations based on the readings of a system of ground and underground sensors in order to prevent the development of sediments and subsidence of foundations. buildings in excess of the limit values.

The development of compensatory injection ideas related to soil strengthening was the work aimed at obtaining the effect of "lifting" the day surface of the soil, as well as the foundations of buildings and structures by injecting additional volumes of building mixtures into the foundations of structures, which contributes to the subsequent rise of the base, and together with him and structures [1,2].

In world practice, there are a large number of examples of the implementation of compensation injection technology to stabilize sediment or level the position of structures. The most famous examples are: alignment of the building of the hydroelectric power station of the Hessigheim hydroelectric complex on the navigable river Neckar near the city of Hessigheim (Germany), compensation for settlement and tilt of the Elizabeth Tower (Big Ben) of the Palace of Westminster (London, UK) [3], alignment of the building in the city of New Orleans (USA) [4], compensation of the settlement of the Bertelsmann AG office building in Berlin (Germany), etc. The largest values of the compensated settlement for controlled injection today are about 170-200 mm. In our country, studies on leveling the position of the foundation part of the Zagorskaya PSHPP-2 building have been carried out since 2013. Within the framework of these studies, a successful experiment was carried out to raise and set the alignment of the position of a concrete slab on the experimental site near the ZAGPP during controlled compensatory injection, the magnitude of the rise of the day surface of the soil was about 46.8 cm. The experiments carried out are related to the need to substantiate the possibility of leveling the position of the ZAGES-2 station unit after the uneven settlement that occurred in 2013, when the maximum draft was 1.17m. The available data on the compensation injection technology allow us to approach this problem from the side of mathematical modeling, the results of which will help find the best solution in the scheme for supplying mortars to the sandy base of the pumped storage power plant.

Unfortunately, at present there are no known software systems with an interface designed to solve such problems. Different researchers approached the issues of mathematical modeling of the process of injecting a solution into the base of a structure from different positions: assigning the finite elements that simulate the injection zone, the coefficient of additional volumetric deformation or the coefficient of thermal expansion [5].

For the numerical simulation of the solution injection process during compensatory injection, the author's program "JulyS" for a computer, written in the FORTRAN language [6], is used. The program solves the problems of the stress-strain state of the soil by the finite element method in a spatial setting. A tetrahedron is used as a finite element. To create the finite element mesh, the open source Gmsh program version 4.7.1 was used. The same program allows you to

visualize the results of numerical calculations, for which the author's interpolation modules have been added to it.

To obtain adequate information about the stress-strain state of the soil medium, two soil models are used: a model of an elastic-ideal-plastic medium with the Mohr-Coulomb strength criterion [7, 10] and a nonlinear "energy" soil model developed by Professor L.N. Rasskazov [8].

In the nonlinear "energy" soil model by LN Rasskazov, the stage-by-stage loading of the computational domain with specified loads is reproduced, and the recalculation of the strength and deformation characteristics of the soil at each stage reflects the effect of material hardening. Due to the lack of experimental data on the magnitude of dilatancy in sandy soils, the model is used in a simplified form, i.e., without taking into account dilatancy, and also without taking into account the development of creeping deformations in time. In this case, the dependence of the stress tensor on deformation according to the "energy" model is written in the form (1):

$$d\sigma_{ij} = \left[\frac{\delta_{ij} E_0 de}{n\left|\sigma_{cp}\right|^{n-1}}\right] + \left[2\left|\sigma_{cp}\right|^{1-n} \cdot \left[f(\nu)\frac{E_0}{n}\exp(B\bar{K} - B) + G_0\bar{K}(1-\exp(B\bar{K} - B)\right]\right] de_{ij} \quad (1)$$

where: $\delta_{ij} = \begin{cases} 1, & for\ i = j \\ 0, & for\ i \neq j \end{cases}$;

E_0 and G_0 are respectively, the initial moduli of volumetric and shear deformation during all-round compression; $f(\nu)$ is a function expressing the relationship between the modulus of volumetric and shear deformation; n is exponent; σ_{cp} is an average soil stresses; B is dimensionless coefficient determined experimentally; $\bar{K}$ is hardening parameter associated with the energy condition of strength [9].

The numerical implementation of the "energy" model in relation to the calculations of earth dams was carried out by LN Rasskazov in the Dampz program. In addition to the elastoplastic nature of the soil deformation, the model took into account the rheological properties of the soil, which appear over time. Currently, the model is successfully used in the calculations of earth dams at the Department of Hydraulics and Hydraulic Engineering of NRU MGSU [12,13]. Also, the "energy" model was used in the calculations of large hydraulic structures in the software packages of the Research Center STADIO [14-50, 15-51, 1616-53].

To implement the "energy model" in the formulation of the finite element method, the dependence of the stress tensor on deformations (1) is written in the form of a matrix of characteristics [17], while the method of initial stresses is used [11]. The solution is made in increments of loads during the iterative process. Testing of the computational program for solving the problem of the stress-strain state of the computational domain in the elastic and elastoplastic formulation was carried out using examples that have an exact analytical solution, when compared with calculations in the Plaxis software package, with calculations using the StatDam program, which implements the "energy" soil model in within the framework of the finite element method in combination with the method of local variations [18].

Numerical modeling of the stress-strain state of the soil medium in the field of the introduction of mortars is based on the experience of scientists from the Cambridge, Delft, Ghent universities, who, in cooperation, carried out work aimed at studying compensatory injection in soft soils, the research results were published in the works of A. Bezuijen, AF van Tol, Gafar K., L. Masini et al. [19,20,21]. L. Masini's work "Experimental study of the technique of compensatory injections in sandy loam and loamy soils" describes the experimental setup and experimental conditions. According to the results of the experiments, it was noted that the solution injected into the sandy soil forms not a spherical volume, but a volume of a more complex shape, schematically shown in Figure 1 [21].

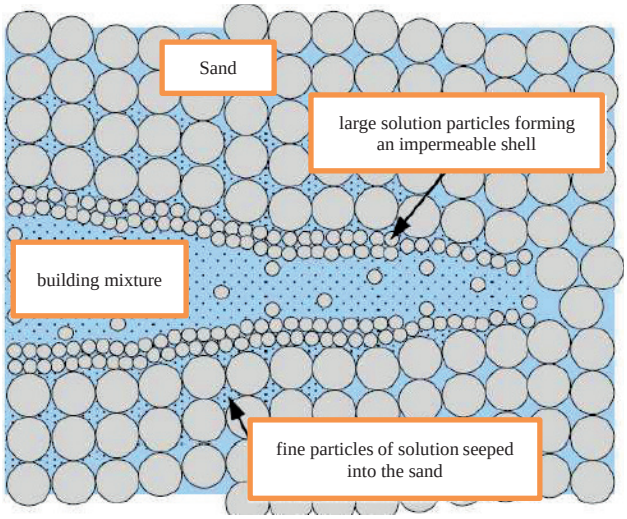

Figure 1. The resulting embedded body. Sectional view

For the numerical simulation of the process of penetration into the soil environment of the mortar, numerical studies were carried out and it was decided to use a spheroid elongated in the horizontal plane with a ratio of the horizontal and vertical semiaxes of 1: 2.5 as a shape for the penetration body. In this case, the equation of the surface of the spheroid takes the form:

$$\left(\frac{10\pi}{3V}\right)^{\frac{1}{3}}\left(\frac{(x-x_0)^2}{2.5}+(y-y_0)^2+\frac{(z-z_0)^2}{2.5}\right)-\left(\frac{3V}{10\pi}\right)^{\frac{2}{3}}=0 \quad (2)$$

where x, y, z are coordinates of a point on the surface of the spheroid; x_0, y_0, z_0 are coordinates of the center of the spheroid; V is discharge volume.

Since the formation of the intrusion body takes place in several stages, when constructing the finite element mesh, it was decided to provide for an "interlayer" of elements, similar to a closed crack, from the edges of which the region will expand, taking the shape of a spheroid. With each additional portion of the injection, the volume of the spheroid increases with the involvement of more and more interlayer nodes in the creation of the embedded volume. In this case, the nodes of the finite element mesh of the "interlayer", which are inside the spheroid, are "pulled" onto the surface of the spheroid along their abscissa (Fig. 2).

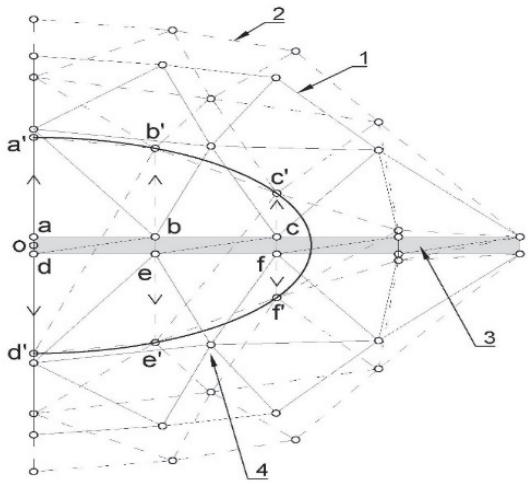

Figure 2. Schematic representation of the process of "pulling" nodes for the elements of the "interlayer" (1 - system mesh before calculation; 2 - system mesh after calculation; 3 - "interlayer" of elements; 4 - boundary of a given spheroid; a, b, c, d , e, f - grid nodes of the system; a ', b', c ', d', e ', f' - given position of grid nodes of the system; o - center of the spheroid)

Before the introduction of the mortar, the elements of the "interlayer" have the properties of the enclosing soil, and after the introduction of the mortar, they are excluded from the calculation. The elements of the interlayer that fall into the zone of influence of the spheroid are also excluded from the calculation. The zone of influence is taken to be equal to the twice-enlarged surface of the spheroid. Thus, the cross-section of the discharge volume looks as shown in Figure 3.

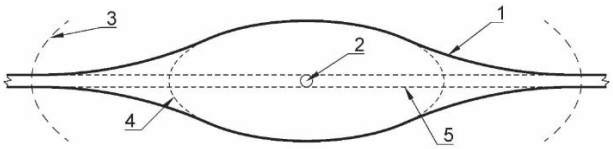

Figure 3. Section of the expansion volume. 1 - resulting surface; 2 - the center of the spheroid; 3 - zone of influence of the spheroid; 4 - a given surface of the spheroid; 5 - the initial position of the interlayer

When using the above assumptions, when calculating the process of injecting tensile stresses around the intrusion body, are not observed. The actual injection volume is calculated as the difference between the pre-injection volume and the post-injection volume.

The verification of the developed numerical model was carried out on the example of a physical experiment described in the works of L. Masini [19]. Figure 4 shows a diagram of the experiment set up. The test chamber has a diameter of 850 mm and a height of 400 mm. At the bottom of the chamber there is a drainage layer of gravel approximately 25 mm thick, covered with a geotextile filter. The drainage system by two pairs of holes on the side surfaces of the chamber is connected to the open cylindrical container with PVC pipes, which determines the conditions for conducting experiments according to the drained scheme. Vertical pressure is applied to the sample through a rubber septum attached circumferentially to a metal cover. The lid has five slots for displacement sensors (LVDTs), each with a through hole to measure vertical displacements directly on the sample surface. The solution is fed into the soil through a horizontal metal tube with external and internal diameters of 15 mm and 12.5 mm, respectively, which is introduced into the chamber at half its length and height so that the solution spreads into the soil in all directions from the open end of the tube located in the center of the camera.

The soil sample was made of medium-sized sand with a particle content of d50 = 0.4mm. The introduced cement slurry with the addition of bentonite had the following characteristics: (W / C) water-cement ratio 1.8, (B / W) bentonite-water ratio 0.08.

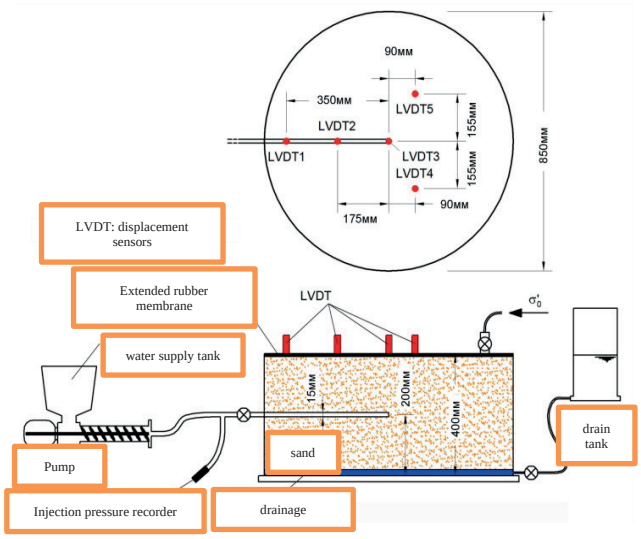

Figure 4. Diagram of the experimental equipment used

Before the injection of the solution into the soil, a pressure of 100 kPa was created on the surface of the sample. In total, 1.11 liters of solution was injected into the ground. As a result of injection, the maximum rise of the sample surface was 4.21 mm, while the volume of the raised surface (useful volume) was about 0.823 L. Thus, the injection efficiency, as the ratio of the useful volume to the volume of the supplied solution, is 74.6%. The results of the experiment are presented graphically in Figure 5.

For numerical simulation of the physical experiment, the finite element mesh of the test chamber was recreated (Fig. 6). The FEM mesh included 1330 elements and 6359 nodes. It was assumed that the embedded volume is modeled in the form of a spheroid conjugated with a contact element in the form of a flat “closed” layer, as shown in Figure 3. Before the introduction of the injection solution, the volume of the layer was equal to zero.

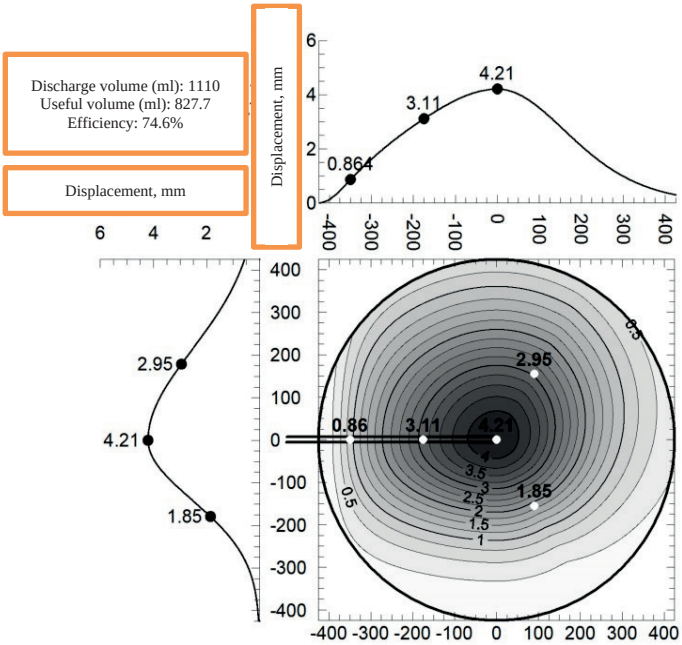

Figure 5. Isolines of the surface displacement at the end of the injection and the profiles of the longitudinal and cross-sectional displacements for the injection point

The calculation consisted of 12 stages. At the first stage, the soil was calculated from its own weight, at the second - the calculation was based on a vertical distributed load equal to 100 kPa. In stages 3–12, the injection of 1.11 liters of solution into the soil in separate portions was simulated. At each stage of injection, the adopted element expands in accordance with the injection volume, and if the nodes of the finite element mesh are inside the spheroid, then they are given such displacements so that they fall on its boundary. The iterative process with one portion of the solution is repeated until a stress-strain state in the computational domain adequate to the specified boundary conditions is obtained. To accelerate the convergence, individual portions of the solution supply are also divided into elementary sub-volumes, the size of which is selected. The accuracy of solving the problem in relative stresses is $1 \cdot 10^{-6}$.

Physical and mechanical characteristics of the soil taken in the calculation: soil deformation modulus E = 30MPa (taken from the manual for the design of the foundations of buildings and structures (to SNiP 2.02.01-83) for medium-sized sand); modulus of elasticity on the unloading branch E_y= 180 MPa; Poisson's ratio ν= 0.3; function value $f(\nu)$ = 1.5; exponent n = 0.8; dimensionless coefficient B = 10; volumetric weight of soil γ = 22kN / m^2.

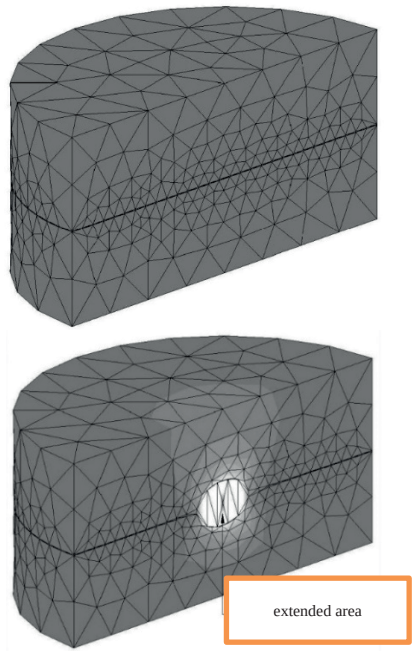

Figure 6. Finite element mesh of half of the test chamber (top - before the start of the experiment, bottom - after injection)

The maximum rise of the sample surface after injection of 1.11 liters of solution was 4.24 mm (in the experiment, 4.21 mm). Isolines of displacements of the sample surface after injection of 1.11 l of solution are shown in Figure 7.

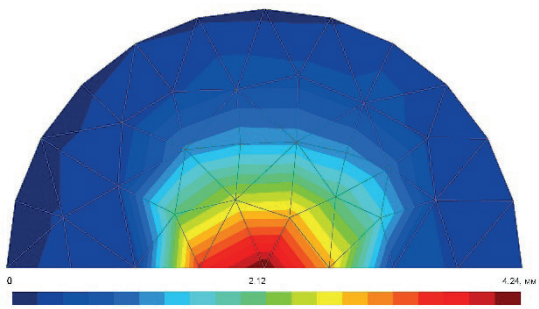

Figure 7. Isolines of displacements of the sample surface after injection of 1.11 l of solution. View from above

The distribution of average stresses in the horizontal section is shown in Figure 9. As can be seen from the solution results, compressive stresses are observed in the entire region. Above and below the expanded area, there is a concentration of large compressive stresses (more than 3000 kN / m^2).

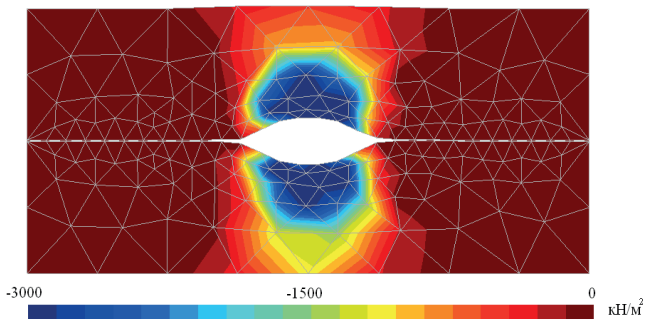

Figure 9. Isolines of average stresses in a horizontal section after injection of 1.11 l of solution

Analyzing the results obtained, it is worth noting that in the experiment, there was probably a loss of part of the volume of the injected solution when water was squeezed into the ground, since the water-cement ratio was large and amounted to W / C = 1.8. Taking this factor into account in the numerical calculation, the volume of expansion of the injection area should be less by the volume of lost "squeezed out" water, which for such mixtures is up to 10% of the injected solution. The obtained results of numerical simulation represent a good accuracy of the description of the physical experiment, the obtained error does not exceed 3%.

A study of grid convergence was carried out for such a formulation of the problem. For the initial finite element mesh, the scheme used in the calculation of the experiment was taken (the level of adaptation of the calculated volume is 3), and 4 meshes were created relative to it, two of which are less often 2 and 1.5 times (the level of adaptation of the calculated volume is 1 and 2, respectively), and the other two are 1.5 and 2 times thicker than the initial one (the level of adaptation of the calculated volume is 4 and 5, respectively).

The value of the maximum rise of the sample was chosen as a control parameter. The characteristics of finite element meshes and the calculation results are shown in Table 1.

Table 1. Results of the study of grid convergence

Adaptation level	Lifting mm	Number of nodes	Number of elements	Counting time, min
1	4.12	352	1455	0.6
2	4.94	623	2818	2.3
3	4.24	1330	6359	6.1
4	4.39	2649	13235	24.9
5	4.34	6012	31276	164.2

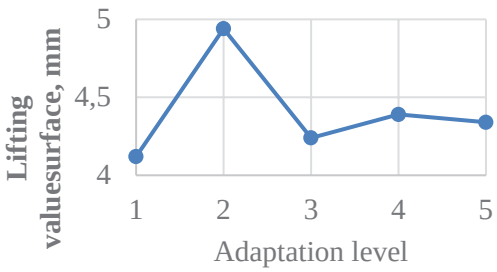

Figure 10. Graph of the dependence of the surface lift value on the level of the calculated volume adaptation

The dependence of the magnitude of the rise of the surface of the sample depending on the level of the calculated adaptation of the grid is shown in the graph (Fig. 10). It should be noted that the automatic mesh generation for each new adaptation level increases the number of finite elements unevenly. The graph shows that thickening the grid by 1.5 times or more of the initially adopted version gives a relatively similar result with an increase in the estimated time by an order of magnitude.

To solve the problem of eliminating the excess settlement of the foundation slab of the Zagorskaya PSHPP-2 using the compensatory injection method, it was necessary to conduct a numerical study of the influence of various technological factors on the amount of surface rise in order to establish a functional relationship between them. As the main factors affecting the amount of lift, one can single out: the volume of injection of the solution into one cuff, the depth of the cuff at the base and the number of cuffs on one vertical.

A study was carried out on the influence of the depth of the collar on the amount of rise of the day surface under the foundation slab. It is assumed that the foundation slab creates a distributed pressure on the base surface of 0.4 MPa [22], and the surface is lifted along the axis of the vertical arrangement of the collars, while up to 10 collars, which are tiers of collar columns, can be located on one axis.

The volume of cement slurry injection into each collar was selected based on the condition of the interstitial bodies closing together, thus, the resulting shape of the intrusion bodies located on the same vertical axis is similar to the structure of a hardened soil pile in a sandy base [23], which in the above studies is called a pillar injection.

To obtain a functional relationship between the magnitude of the rise of the day surface and the volume of the solution injected into the cuff, as well as the depth of the cuffs and their number in one injection column, 10 series of calculations were carried out with different numbers of cuffs on the vertical. In the last calculation, the injection was simulated with ten cuffs located in a single injection column. In this case, the total rise of the surface was 1.17m, while in total, in all 10 cuffs, the injection of 66700l (66.7 m3) of cement slurry was simulated. The useful volume of the raised surface was 37,900 liters or 37.9 m3. For the last calculation, Figure 11 shows the pattern of displacement isofields in the computational domain, and Figure 12 shows the pattern of the isofields of principal stresses.

The generalized results of the calculations performed for all injection columns with different numbers of cuffs are shown in the graph in Figure 13.

The resulting graph of cumulative lift versus the number of cuffs in the column is shown in this upper envelope graph. The upper envelope is the dependence of the lift of the foundation slab on the discharge volume, and the discharge volume determines the layout of the collars in the discharge column.

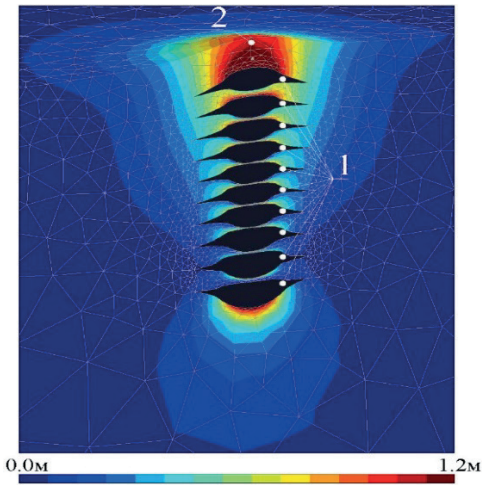

Figure 11. Picture of isofields of displacements in the computational domain when simulating the injection of a solution in ten cuffs

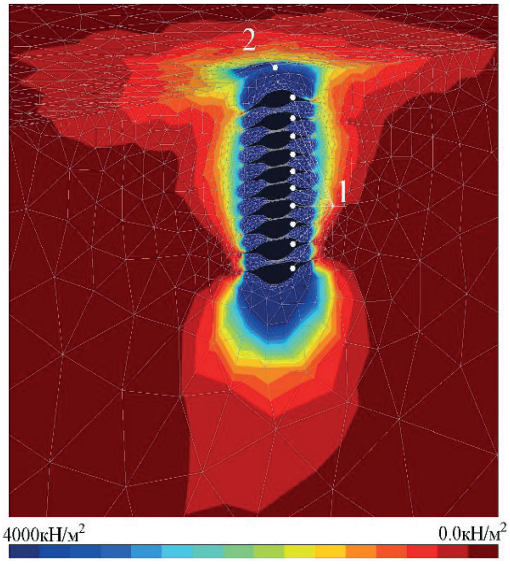

Figure 12. Picture of the isofields of the principal stresses in the computational domain when simulating the injection of a solution into ten cuffs in one injection column

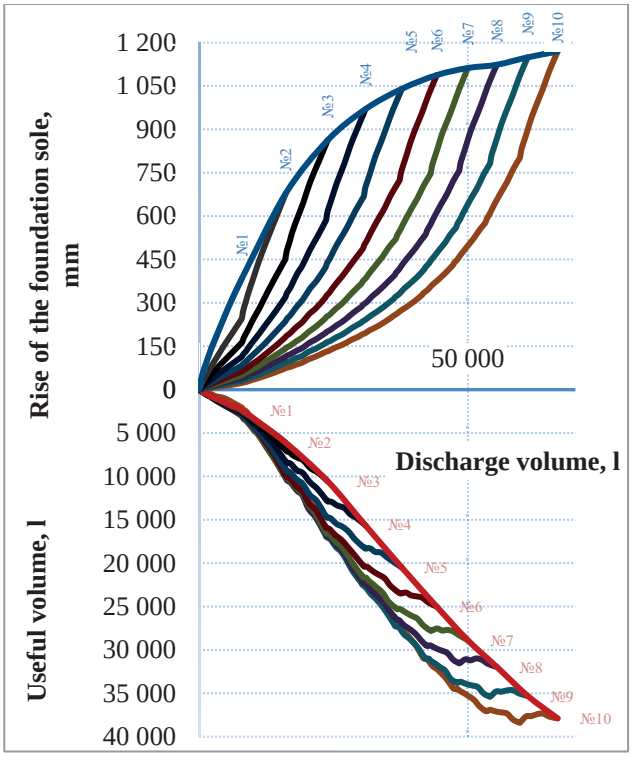

Figure 13. Graphs of the dependence of the rise of the base of the foundation and the useful volume on the volume of injection of the solution (the numbers indicate the dependence curves for individual design cases)

Using the obtained dependencies, it is possible to calculate the total volume that needs to be pumped into the cuffs located on the vertical to lift the base of the foundation by a given value in the range from 0.0 to 1.17m. The volume obtained can be used to calculate the useful volume. According to the calculated total volume, the required number of cuffs in the post can be determined. At the same time, the order of injection is established starting from the lower cuff, discrepancies in the delivery volumes are compensated by the lower cuff.

Based on the data obtained, calculations were made to lift the ZAGES-2 foundation slab. A scheme was developed for feeding the solution into the collar columns using the compensatory injection method, in which the required volume of the injected solution was 9240.8 m3, the arrangement of the collar columns in the plan and along the tiers of the subgrade was developed, the total number of collar injectors was 74 pcs.

CONCLUSIONS

1. Numerical studies to simulate an expanding area in the thickness of soil material led to the development of a computing program JulyS, which allows to recreate the conditions and repeat the result of a physical experiment on the introduction of cement slurry into a sandy base with the goal of obtaining a response in the form of a rise in the day surface. The error of the obtained result is no more than 3%.
2. Within the framework of the finite element method, a special element has been developed that simulates the injection body in the area of injection and volume expansion around the injection pipe (cuff). The shape of the element is taken in the form of a flattened ellipsoid with an axis ratio of 1: 2.5, which grows and expands on the basis of the "interlayer" elements previously built into the grid.
3. The length of each group of elements of the "interlayer" should be selected according to the maximum volume of the total injection in the area of this "interlayer".
4. The effectiveness of the numerical experiment is controlled by the absence of tensile stresses when the nodes are "pulled" to the boundary of the sphere and can be adjusted to the individual task in the course of refining the shape of the spheroid.
5. It has been proven that the most effective way to lift the foundation slab is to create, due to the adopted layout of the collars, injection pillars, in which injection is carried out in the direction from bottom to top.
6. The functional dependences of the height of the foundation slab lift on the depth of the collars in the soil layer, their quantity in the injection column have been obtained, which makes it possible to find the volume of solution injection and the layout of the collar columns for a given lift value.

7. According to the results of numerical modeling of the lifting of the Zagorskaya PSHPP-2 foundation slab by the compensatory injection method, the required volume of the injected solution is 9240.8 m3, while the number of collar columns distributed over the base area is 74 pcs. and the axial distance of the collar holes in the collar columns is 3.5m.
8. In the developed method of modeling the process of compensatory injection using the example of the Zagorskaya PSHPP-2, the injection efficiency is about 38.8%, which correlates with the data of field experiments [1].

REFERENCES

1. **Zertsalov M.G.** Tekhnologiya kompensatsionnogo nagnetaniya dlya zashchity zdaniy i sooruzheniy [Compensatory injection technology for the protection of buildings and structures]/ M.G. Zertsalov, A.N. Simutin, A.V. Aleksandrov // Vestnik MGSU – 2015. – No 6. – P. 32–40.
2. **Bezuijen A.** Compensation Grouting in Sand. Experiments, Field Experiences and Mechanisms [Compensation Grouting in Sand. Experiments, Field Experiences and Mechanisms] / A Bezuijen. – ISBN 978–90–8570–507–9, 2010. – p. 205.
3. Ehab Hamed Flexural time–dependent cracking and post–cracking behaviour of FRP strengthened concrete beams / Ehab Hamed, Mark A. Bradford// International journal of Solid and Structures 49 (2012) 1595–1607.
4. **Knitsch, H.** Visualization of relevant data for compensation grouting / H. Knitsch // Tunnel.- № 3. – 2008. – pp. 38–45.
5. **Simutin A.N.** Metodiki raschota parametrov kompensatsionnogo nagnetaniya dlya upravleniya deformatsiyami osnovaniy zdaniy i sooruzheniy [Methods for calculating the parameters of compensatory injection to control deformations of the foundations of buildings and structures]. Dis. thesis, Moscow, 2015.
6. **Bestuzheva A.S., Chubatov I.V.** Upravleniye napryazhenno-deformirovannym sostoyaniyem osnovaniya sooruzheniya pri adresnom kompensatsionnom nagnetanii rastvora [Management of the stress-strain state of the foundation of a structure during targeted compensation injection of a solution] / In proceedings: II scientific conference «Obespecheniye kachestva, bezopasnosti i ekonomichnosti stroitel'stva. Praktika. Problemy. Perspektivy. Innovatsii» Moscow, 12–13 december 2019
7. **O.C. Zienkiewicz, S. Valliappan, I.P. King**. Elasto-plastic solutions of engineering problems ‘initial stress’, finite element approach / Numerical Methods in Engineering, 1968.
8. Design of earth dams. Study guide/A.L. Gol'din, L.N. Rasskazov – Moscow: Publishing ASV /2001-384 p.
9. Gidrotekhnicheskiye sooruzheniya Uchebnik dlya vuzov [Hydraulic structures Textbook for universities]. 2 parts, under ed. L.N. Rasskazov. – Moscow: Publishing ASV, 2008.-526p
10. **D. V. Griffiths, S. M. Willson** / An explicit form of the plastic matrix for a Mohr–Coulomb material / Communications in Applied Numerical Methods, 1986.
11. **Zenkevich O.** Metod konechnykh elementov v tekhnike (Finite element method in engineering) [Finite element method in engineering] — Moscow: Mir, 1975, 541 p.
12. **A.S. Bestuzheva, D. Gadai**. Search for optimal composition and an investigation of special material for the near-face zone of a dam with reinforced concrete face / Power technology and engineering. 2019. Vol. 52. No 6. p. 660-668.
13. **Sainov M.P.** Avtorskaya vychislitel'naya programma dlya issledovaniy napryazhonno-deformirovannogo sostoyaniya gruntovykh plotin [The author's computational program for researching the

stress-strain state of soil dams] // Vestnik yevraziyskoy nauki. 2020. No 12 (3). P. 14.

14. **Belostotskiy A.M. et al.** Razrabotka kalibrovannykh matematicheskikh modeley napryazhenno-deformirovannogo sostoyaniya gidrotekhnicheskikh sooruzheniy (na primere sklona Zagorskoy GAES) [Development of calibrated mathematical models of the stress-strain state of hydraulic structures (on the example of the slope of the Zagorskaya PSHPP)] // Proceedings of NIIES «Bezopasnost' energeticheskikh sooruzheniy». 2000. P. 10–21.
15. **Belostotskiy A.M. et al.** Chislennoye modelirovaniye prostranstvennogo NDS sistem «sooruzheniye-osnovaniye» s uchetom nelineynykh reologicheskikh svoystv gruntov [Numerical modeling of spatial stress-strain state of the “structure-foundation” systems taking into account the nonlinear rheological properties of soils. scientific works of MGSU "Problems of Applied Mathematics and Computational Mechanics"] // Proceedings MGSU «Voprosy prikladnoy matematiki i vychislitel'noy mekhaniki». 2001. P. 22–33.
16. **Belostotskiy A. M., Belyy M. V., Rasskazov L. N.** Chislennyye issledovaniya NDS sistem «sooruzheniye-osnovaniye» s uchetom nelineynykh reologicheskikh svoystv gruntov [Numerical studies of stress-strain state systems "structure-foundation" taking into account the nonlinear rheological properties of soils] // Proceedings XX international conference «BEM&FEM-2003». 2003. p. 75–82.
17. **Belostotskiy A. M., Akimov P. A**. Aktual'nyye problemy chislennogo modelirovaniya zdaniy, sooruzheniy i kompleksov. Tom 1. K 25-letiyu Nauchno-issledovatel'skogo tsentra StaDiO [Actual problems of numerical modeling of buildings, structures and complexes. Volume 1. To the 25th anniversary of the Research Center StaDiO] / A. M. Belostotskiy, P. A. Akimov, Moscow: ASV, 2016. 1022 p.
18. **Bestuzheva A.S., Chubatov I.V.** Numerical modeling of the controlled lifting of the structure / Materials Science and Engineering, Volume 869, New construction technologies 2020 IOP Conf. Ser.: Mater. Sci. Eng. 869 072018.
19. **Luca Masini.** Studio sperimentale della tecnica delle iniezioni di compensazione in terreni sabbiosi e limosi/ “Sapienza”, Università degli studi di Roma Dipartimento di Ingegneria Strutturale e Geotecnica, 2010.
20. **Gafar K.** Compensation grouting in sand. Ph.D. Thesis, University of Cambridge, Cambridge, UK., 2009.
21. **A.Bezuijen, A.F. van Tol** /Deltares/Delft University of Technology /Compensation grouting: mechanisms determining the shape of the grout body // Compensation grouting
22. **Zertsalov M. G., Simutin A. N., Aleksandrov A. V.** Raschotnoye obosnovaniye upravlyayemogo kompensatsionnogo nagnetaniya pri pod"yome modeli fundamentnoy plity Zagorskoy GAES-2 [Calculation substantiation of controlled compensatory injection when lifting the model of the foundation slab of the Zagorskaya PSHPP-2] // Gidrotekhnicheskoye stroitel'stvo. 2018. (8). P. 2–6.
23. **Ter-Martirosyan Z.G. et al**. Vzaimodeystviye tolstostennogo gruntovogo tsilindra s peschanym yadrom i rostverkom [Interaction of a thick-walled soil cylinder with a sand core and a grillage] // Zhilishchnoye stroitel'stvo. 2014. (9). P. 23–26.

СПИСОК ЛИТЕРАТУРЫ

1. **Зерцалов М.Г.** Технология компенсационного нагнетания для защиты зданий и сооружений / М.Г. Зерцалов, А.Н. Симутин, А.В. Александров // Вестник МГСУ – 2015. – № 6. – С. 32–40.
2. **Bezuijen A.** / Compensation Grouting in Sand. Experiments, Field Experiences and

Mechanisms / A Bezuijen. – ISBN 978–90–8570–507–9, 2010. – p. 205.
3. Ehab Hamed Flexural time–dependent cracking and post–cracking behaviour of FRP strengthened concrete beams / Ehab Hamed, Mark A. Bradford// International journal of Solid and Structures 49 (2012) 1595–1607.
4. **Knitsch, H.** Visualization of relevant data for compensation grouting / H. Knitsch // Tunnel.- № 3. – 2008. – pp. 38–45.
5. **Симутин А.Н.** Методики расчёта параметров компенсационного нагнетания для управления деформациями оснований зданий и сооружений. Диссертация к.т.н., Москва, 2015 г.
6. **Бестужева А.С., Чубатов И.В.** Управление напряженно-деформированным состоянием основания сооружения при адресном компенсационном нагнетании раствора/ Статья в сборнике трудов конференции: Вторая совместная научно-практическая конференция «обеспечение качества, безопасности и экономичности строительства. Практика. Проблемы. Перспективы. Инновации» Москва, 12–13 декабря 2019 года.
7. **O. C. Zienkiewicz, S. Valliappan, I. P. King** / Elasto-plastic solutions of engineering problems ‘initial stress’, finite element approach / Numerical Methods in Engineering, 1968.
8. Проектирование грунтовых плотин. Учебное пособие/А.Л. Гольдин, Л.Н. Рассказов – М.: Изд-во АСВ /2001-384 с.
9. Гидротехнические сооружения Учебник для вузов в 2-х частях под ред. Л.Н.Рассказова. – М.:Изд-во АСВ, 2008.-526с
10. **D. V. Griffiths, S. M. Willson** / An explicit form of the plastic matrix for a Mohr–Coulomb material / Communications in Applied Numerical Methods, 1986.
11. **Зенкевич О.** Метод конечных элементов в технике (Finite element method in engineering) — М.: Мир, 1975, с 541.
12. **A.S.Bestuzheva, D.Gadai** / Search for optimal composition and an investigation of special material for the near-face zone of a dam with reinforced concrete face / Power technology and engineering. 2019. т. 52. № 6. с. 660-668.
13. **Саинов М.П**. Авторская вычислительная программа для исследований напряжённо-деформированного состояния грунтовых плотин // Вестник евразийской науки. 2020. № 12 (3). С. 14.
14. **Белостоцкий А. М.** [и др.]. Разработка калиброванных математических моделей напряженно-деформированного состояния гидротехнических сооружений (на примере склона Загорской ГАЭС) // Сб. научных трудов АО НИИЭС «Безопасность энергетических сооружений». 2000. С. 10–21.
15. **Белостоцкий А. М.** [и др.]. Численное моделирование пространственного НДС систем «сооружение-основание» с учетом нелинейных реологических свойств грунтов // Сб. научных трудов МГСУ «Вопросы прикладной математики и вычислительной механики». 2001. С. 22–33.
16. **Белостоцкий А. М., Белый М. В., Рассказов Л. Н.** Численные исследования НДС систем «сооружение-основание» с учетом нелинейных реологических свойств грунтов // Труды XX международной конференции «BEM&FEM-2003». 2003. С. 75–82.
17. **Белостоцкий А. М., Акимов П. А.** Актуальные проблемы численного моделирования зданий, сооружений и комплексов. Том 1. К 25-летию Научно-исследовательского центра СтаДиО / А. М. Белостоцкий, П. А. Акимов, Москва: АСВ, 2016. 1022 с.
18. **Bestuzheva A.S., Chubatov I.V.** Numerical modeling of the controlled lifting of the structure / Materials Science and Engineering, Volume 869, New construction technologies 2020 IOP Conf. Ser.: Mater. Sci. Eng. 869 072018.

19. **Luca Masini**. Studio sperimentale della tecnica delle iniezioni di compensazione in terreni sabbiosi e limosi/ “Sapienza”, Università degli studi di Roma Dipartimento di Ingegneria Strutturale e Geotecnica, 2010.
20. **Gafar K.** Compensation grouting in sand. Ph.D. Thesis, University of Cambridge, Cambridge, UK., 2009.
21. **A.Bezuijen, A.F. van Tol** /Deltares/Delft University of Technology /Compensation grouting: mechanisms determining the shape of the grout body // Compensation grouting
22. **Зерцалов М.Г., Симутин А.Н., Александров А.В.** Расчётное обоснование управляемого компенсационного нагнетания при подъёме модели фундаментной плиты Загорской ГАЭС-2 // Гидротехническое строительство. 2018. (8). С. 2–6.
23. **Тер-Мартиросян З. Г.** [и др.]. Взаимодействие толстостенного грунтового цилиндра с песчаным ядром и ростверком // Жилищное строительство. 2014. (9). С. 23–26.

Alexandra S. Bestuzheva. Ph.D. in Engineering Science, Associate Professor of the Department of Hydraulics and Hydrotechnical engineering, Moscow State University of Civil Engineering, Yaroslavskoe shosse, 26, Moscow, 129337, Russia, email: alex_bestu@mail.ru

Ivan V. Chubatov. Degree Graduate Student of the Department of Hydraulics and Hydrotechnical engineering, Moscow State University of Civil Engineering, Yaroslavskoe shosse, 26, Moscow, 129337, Russia,email: chubatovz@gmail.com

Бестужева А.С. К.Т.Н., Доц. кафедры Гидравлики и Гидротехнического Строительства, Московского Государственного Строительного Университета, Ярославское шоссе, 26, Москва, 129337, Россия, email: alex_bestu@mail.ru

Чубатов И.В. Аспирант кафедры Гидравлики и Гидротехнического Строительства, Московского Государственного Строительного Университета, Ярославское шоссе, 26, Москва, 129337, Россия,email: chubatovz@gmail.com

DOI:10.22337/2587-9618-2021-17-4-73-82

SYSTEM ANALYSIS OF TECHNOLOGICAL PROCESSES

Alexey D. Zhukov [1,2,3], Ekaterina Yu. Bobrova [2], Ivan I. Popov [4], Demissie Bekele Arega [1]

[1] National Research Moscow State University of Civil Engineering, Moscow, RUSSIA
[2] National Research University "Higher School of Economics", Moscow, RUSSIA
[3] Research Institute of Building Physics, Moscow, RUSSIA
[4] Voronezh State Technical University, Voronezh, RUSSIA

Abstract. The article discusses ways to solve engineering problems in the study of technological processes using methods of system analysis. The essence of this method is to study the technology as a cybernetic system with an assessment of the" reactions" of this system to external influences formed during an active experiment. At the same time, optimization problems are solved analytically. Analytical optimization is based on two main principles. The regression equations obtained as a result of processing experimental data and testing statistical hypotheses are models that adequately describe real processes. Each of these equations is an algebraic function of several variables, to which methods of mathematical analysis are applicable, including the study of extremums of functions in partial derivatives. The next step is to develop a process algorithm and develop computer programs that allow you to select the composition and predict the properties of the product. As an engineering interpretation, it is possible to construct optimized nomograms that allow solving both direct and inverse problems; that is, predicting the result or selecting technological factors. The research methods described in the article are implemented in the study of technologies of cellular concrete, foam concrete, cement-polymer concrete and products made of mineral wool and foam glass. As an example, the article considers the optimization of the selection of the composition of fine-grained concrete reinforced with chopped glass fiber. The implementation of the developed method allowed us to determine the optimal value of the determining parameters, including the consumption of fiber and plasticizer, as well as to form a method for studying the properties of products.

Keywords: concrete, composite material, technology, glass fiber, dispersed reinforcement, analytical optimization.

СИСТЕМНЫЙ АНАЛИЗ ТЕХНОЛОГИЧЕСКИХ ПРОЦЕССОВ

А.Д. Жуков [1,2,3], Е.Ю. Боброва [2], И.И. Попов [4], Д.Б. Арега [1]

[1] Национальный исследовательский Московский государственный строительный университет, Москва, РОССИЯ
[2] Национальный исследовательский университет «Высшая школа экономики», Москва, РОССИЯ
[3] Научно-исследовательский Институт Строительной Физики, Москва, РОССИЯ
[4] Воронежский государственный технический университет, Воронеж, РОССИЯ

Аннотация. В статье рассматриваются способы решения инженерных задач при исследовании технологических процессов с использованием методов системного анализа. Суть этого метода заключается в исследовании технологии как кибернетической системы с оценкой «реакций» этой системы на внешние воздействия, формируемые в процессе активного эксперимента. При этом решение оптимизационных задач осуществляется аналитически. Аналитическая оптимизация базируется на двух основных положениях. Полученные, в результате обработки экспериментальных данных и проверки статистических гипотез уравнения регрессии являются моделями, адекватно описывающими реальные процессы. Каждое из таких уравнений является алгебраической функцией нескольких переменных, к которому применимы методы математического анализа, в том числе исследование экстремумов функций в частных производных. Следующим шагом является разработка алгоритма процесса и разработка компьютерных программ, позволяющих осуществлять подбор состава и прогнозирование свойств продукта. В качестве инженерной интерпретации возможно построение оптимизированных номограмм, позволяющих решать как прямые, так и обратные задачи; то есть прогнозирование результата или выбор технологических факторов. Описанные в статье методы исследования реализованы при изучении технологий ячеистого бетона, пенобетона, цементно-полимербетона и изделий из минеральной ваты и пеностекла. В каче-

стве примера в статье рассматривается оптимизация подбора состава мелкозернистого бетона, армированного рубленым стеклянным волокном. Реализация разработанной методики позволила определить оптимальное значение определяющих параметров, включая расход волокна и пластификатора, а также сформировать методику изучения свойств изделий.

Ключевые слова: бетон, композиционный материал, технология, стеклянное волокно, дисперсное армирование, аналитическая оптимизация.

1. INTRODUCTION

System analysis of technology and process modeling are aimed at solving three types of problems: development of composition selection methods; optimization of the composition or characteristics of the initial components; optimization of parameters that characterize the technology as a whole, or individual technological processes.

The object of research in this case is a technological process and to describe it, a cybernetic system is widely used, called a "black box", which has its own input parameters, control actions and outputs. Methods for studying technological processes by building cybernetic models and optimizing them are constantly being enriched and expanded. Implementation of the system analysis of technology involves addressing two types of technological problems: the development of methods for selecting the composition of the material and optimization of the technology of this material [1, 2].

Certain provisions of the system analysis are implemented in the study of recipes and technologies of building materials for various purposes and various material composition from heat-insulating products to heat-insulating and structural concrete. Modern realities, in which the construction complex is developing, suggest setting new tasks in related areas of research, including utilization of by-products of construction materials production and waste obtained as a result of demolition of construction objects [3-5].

Dispersed reinforcement with natural, synthetic, or mineral fibers can significantly modify the properties of the finished product [6-8]. In domestic and foreign practice, sufficient experience has been gained in the use of various types of fibers in the composition of concretes, building mixes or their analogues: steel fibers, fibers based on alkali-resistant glasses or basalts, polymer, cellulose, nanotubes, steel fibers, etc. [9-11]

The use of these by-products in the manufacture of construction products is a science-intensive method of recycling waste that appears as a result of the demolition of old buildings and structures, as well as waste from the production of building materials [12-14]. It should be noted here that any by-products of the production of mineral binders, Portland cement, concrete, or their derivatives classified as waste contain a certain percentage of clinker minerals. As a result of fine grinding or mechanical or mechanochemical activation, this component ceases to be an inert filler and begins to exhibit astringent properties [15, 16].

Fine grinding of mineral components and the use of fibers with a diameter of 0.1...6 microns allows not only to modify the structure of concrete, with an increase in strength characteristics, and, first of all, Flexural strength, but also changes the nature of chemical and physicochemical processes on the contact surfaces of the mineral matrix and fiber with the formation of ordered Microsystems qualified as nanostructures [17-20]. This suggests the emergence of a new subclass of building composites.

The purpose of the research presented in the article was to develop, using the methodology of system analysis, elements of the methodology for selecting the composition of a dispersed reinforced composite material based on fine-ground concrete scrap waste, mineral binder, alkali-resistant glass fiber and plasticizer.

2. MATERIALS AND METHODS

The system approach is one of the foundations of technological modeling. It consists in dividing

the entire technological process into separate blocks that are adequate for technological processing; studying the functioning of each block separately; establishing the relationship between individual blocks and building a General scheme of the process as a set of blocks and links between them. The basis for the study is modeling, which can be carried out using both statistical methods (discussed above) and deterministic and conceptual (logical) models [21, 22].

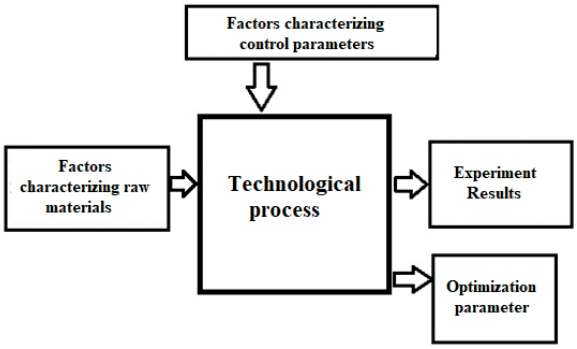

Figure 1. Technology as a cybernetic system

The "black box" (figure 1) can cover the technology as a whole. This technique is widely used when building models based on a "passive" experiment, when conclusions are drawn from observations and collecting statistical information. The "black box" can cover a separate technological conversion, that is, a separate process: selection of the composition, preparation of the mixture, molding, and heat treatment. The technology model, in this case, is obtained from individual bricks-blocks. The connection between individual" blocks "of technology is made through factors that are" outputs "for one block and" inputs" for another. This technique, which is widely used in the analysis of nonlinear technological processes, does not exclude the use of techniques used in the first method.

The cybernetic model, which is based on a flowchart, is a legitimate basis for conducting an experiment, further processing the results, and building its mathematical (statistical) model. A mathematical model of a separate technological process is formed from a set of polynomials describing individual fragments of this process.

If the "black box" covered the technology as a whole, the experiment covers dozens of factors. First, we consider the entire set of factors "involved" in the process of creating the material. Using special techniques, the most significant factors are identified, and then all the problems of technology optimization and simulation solutions are implemented based on the variation of significant factors.

The obtained regression equations are checked for all statistical hypotheses and the models ' adequacy is checked by the Fisher criterion. As a result of statistical checks, only significant factors are left out as a result of comparison with confidence intervals (Δbj), and as a result of checking by the Fisher criterion, a conclusion is made about the adequacy (or inadequacy) of the obtained models.

Evaluation of the influence of each factor on the result is carried out by the value and sign of the coefficient facing the factor (its linear value or quadratic function) or their pair interaction. It should be noted that the experiment is performed in the encoded values of factors (reduced to the interval [-1, +1].

Interpolation of the results consists in calculating the strength and average density of the material depending on the values of the variable factors and is carried out by implementing computer programs. This program includes the following blocks: input data (values of factors in real terms), a block coding factors, calculation block, the output results on the display. Testing of statistical hypotheses, modeling, processing and optimization of results was carried out in accordance with the methods of processing the results of the experiment.

The equations are optimized using an analytical method. Which is based on the following provisions: the obtained regression equations adequately describe the technological process under study; each equation is an algebraic function of several variables (by the number of significant variable factors) and mathematical analysis methods are used to study this function. The experimental conditions are shown in table 1.

Table 1. The intervals of variation of factors

Name of the factor	Symbol X_i	Average value of the factor, Xi	The range of variation, ΔXi	The values of the factor levels	
				-1	+1
Consumption of Portland cement, kg / m^3	X_1	450	50	400	500
The consumption of plasticizer, %	X_2	0.6	0.2	0.4	0.8
Consumption of fine filler, kg / m^3	X_3	650	50	600	700
Consumption of the reinforcing component, %	X_4	1	0.5	0.5	1.5

The costs of cement, fine filler, plasticizer, and reinforcing component are taken as variable factors. The water flow rate is set in accordance with the required level of mobility of the mixture and is a dependent factor. The response function taken the strength of concrete in compression ($У_1$) and its average density ($У_2$).

As the parameter optimization in the third stage of the experiment adopted the coefficient of structural quality concrete (CCQ), equal to the ratio of compressive strength of concrete ($У_1$) to its average density ($У_2$):

$$CCQ = (У_1)/ (У_2)$$

3. RESULTS

Mathematical processing of the experimental results allowed us to obtain regression equations for compressive strength ($У_1$) and average density ($У_2$). The following mathematical models (polynomials):

- for compressive strength

$$У_1= 39.7 +3.9X_1+1.7X_2+1.9X_3 +2.2X_4 + 1.5X_1X_3 +1.2X_1X_4 –1.1X_2^2 –1.2X_4^2$$

- for medium density:

$$У_2 = 1960 + 52X_1 + 24X_2 + 33X_3 + 13X_4 + 11X_1X_3 – 6X_2^2 – 4X_4^2$$

The significance of the coefficient was checked by confidence intervals, respectively, the confidence interval for the density was Δb_1 = 0.8 MPa, and for the average density Δb_2 =3 kg/ m^3. The obtained models are checked for adequacy by the Fisher criterion. The calculated values of the Fischer criteria are equal for the average density model F_1=15.2 and for the compressive strength model F_2=15.7. Table of criteria values, respectively, equal to the 19.2 and 19.3. The calculated value of F-test does not exceed the table, and with the appropriate confidence level (98 %) model can be considered adequate. This fact will be taken into account in the analytical optimization of mathematical models.

Analysis of the coefficients of the equation $У_1 = f_1(X_1, X_2, X_3, X_4)$ shows that the strength increases with increasing expenditure of Portland cement, sand and screening in the intervals taken in the experiment (positive coefficients for X_1, X_2, X_3, X_4). When the polymer costs increase, first there is an increase in strength, and then at high costs – there is a decrease (coefficients at X_2 and X_2^2). This suggests that the function $У_1 = f_1(X_1, X_2, X_3)$ has a local extreme over X_4, and analytical optimization can be applied.

Analysis of the coefficients of the equation $У_2 = f_2(X_1, X_2, X_3, X_4)$ shows that the greatest influence on the increase in concrete density is exerted by an increase in the consumption of Port-

land cement and fine-ground filler (coefficients at X_1 and X_3). Increasing the consumption of the plasticizer and the reinforcing component increases the density: at first, intensive, and at high costs – insignificant.

Analytical optimization is based on the fact that the functions for strength and density $У_1 = f_1(X_1, X_2, X_3, X_4)$ and $У_2 = f_2(X_1, X_2, X_3, X_4)$ are mathematical and mathematical analysis methods can be applied to them, provided that the adequacy condition is not violated. In this case, the following scheme is adopted:

- The equation $У_1 = f_1(X_1, X_2, X_3, X_4)$ is differentiated by X_2 and equated to zero, determining the extreme of the function $У_1$ by X_2;
- the equation $У_1 = f_1(X_1, X_2, X_3, X_4)$ is differentiated by X_4 and equated to zero, determining the extreme of the function $У_1$ by X_4;
- solve the functions $У_1 = f_1(X_1, X_2, X_3, X_4)$ and $У_2 = f_2(X_1, X_2, X_3, X_4)$ with optimized values X_2 and X_4 ($X_2 = opt_2$ and $X_4 = opt_4$), then perform local optimization.

4. DISCUSSIONS

Analysis of the polynomial describing the relationship between compressive strength and variable factors shows that this function (which is essentially a function of several variables) for two of these variables, namely, the flow rate of the plasticizer (X_2) and the flow rate of the reinforcing component (X_4), has local extremes. Therefore, we can use the mathematical apparatus of analytical local optimization.

At the first stage, we perform analytical optimization based on the X4 factor.

$$\partial Y_1 / \partial X_4 = 2.2 - 2.4X_4 = 0 \rightarrow X_4 = \frac{2.2}{2.4} = 0.92$$

We solve the basic equations for $X_4 = 0.92$

-for compressive strength

$$У_1 = 40.7 + 3.9X_1 + 1.7X_2 + 1.9X_3 + 1.5X_1X_3 + 1.1X_1 - 1.1X_2^2$$

- For average density:

$$У_2 = 1969 + 52X_1 + 24X_2 + 33X_3 + 11X_1X_3 - 6X_2^2$$

In natural values, the consumption of chopped glass fiber is determined by decoding: $C_{gv} = 1 + 0.5\times0.92 = 1.46\%$.

Interpolation solutions for the entire range of changes in factors X_1, X_2, and X_3 can be represented graphically (Fig. 2).

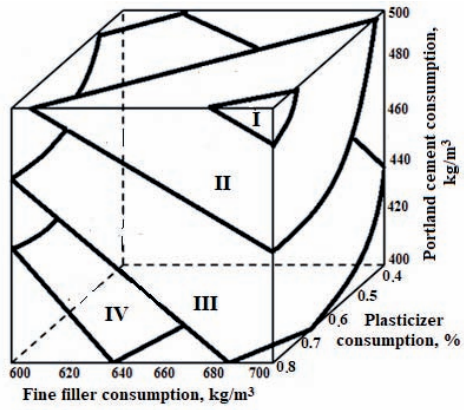

a

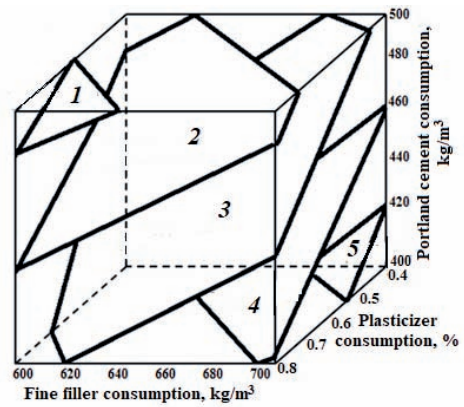

b

Figure 2. Graphical interpretation of the response functions optimized for the consumption of the reinforcing component (consumption is Cgv = 1.46%): a – dependence of the concrete strength on variable factors; b – dependence of the average concrete density on variable factors: I – 40 MPa; II – 35 MPa; III – 30 MPa; IV – 25 MPa; 1 – 2000 kg/m³; 2 – 1950 kg/m³; 3 – 1900 kg/m³; 4 – 1850 kg/m³; 5 – 1800 kg/m³

At the second stage, we perform analytical optimization based on the X_2 factor

$$\partial Y_1 / \partial X_2 = 1.7 - 2.2X_2 = 0 \rightarrow X_2 = \frac{1.7}{2.2} = 0.77$$

We solve the equations already optimized for X_4 at $X_2 = 0.77$

- For compressive strength

$$У_1 = 41.9 + 3.9X_1\ 1.9X_3 + 1.5X_1X_3$$

- For medium density:

$$У_2 = 1984 + 52X_1 + 33X_3 + 11X_1X_3$$

In natural values, the consumption of chopped glass fiber is determined by decoding: $C_{gv} = 0.6 + 0.2 \times 0.77 = 0.75\%$

4) Form an analytical expression for the coefficient of structural quality of concrete (CCQ):

$$CCQ = \frac{У_1}{У_2} = \frac{41.9 + 3.9X_1 + 1.9X_3 + 1.5X_1X_3}{1984 + 52X_1 + 33X_3 + 11X_1X_3}$$

[MPa·м^3/кg]

A graphical interpretation of the resulting equation is shown in Fig. 3

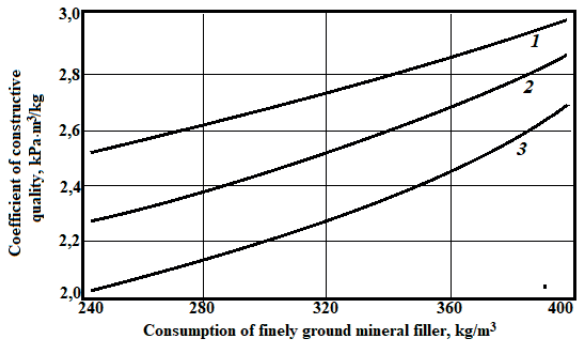

Figure 3. Dependence of the Coefficient of constructive quality on the consumption of fine-ground mineral filler and the consumption of Portland cement, taking into account the optimization of plasticizer consumption and the consumption of reinforcing fiber, kg / m^3: 1 – 500; 2 – 450; 3 – 400

Analyzing the graph of the dependence of the coefficient of structural quality (CCQ) on Portland cement and the consumption of mineral filler obtained by fine grinding of concrete scrap, we can state the following. First, it is an obvious fact that when the optimal values of plasticizer consumption (3.42 ± 0.2 kg/m^3) and the consumption of reinforcing fiber (1.44 ± 0.1%) are obtained analytically, the CCQ increases with the increase in the consumption of Portland cement. Second, it was found that in the intervals of variation of the factor provided for by the experimental conditions (table. 1) there is a tendency for additional CCQ growth with increasing filler costs. This may well be explained by its hydraulic activity, but requires additional research.

Using the methods of system analysis and the approach to technology as a cybernetic system allows you to create a mathematical model of the technology as a whole, or its individual blocks. In particular, to develop methods for selecting the composition and predicting the properties of the product. It is also important to be able to obtain information on the direction and significance of the influence of factors or pair interactions on the result (by the sign and absolute value of the coefficient or pair interaction.

Analysis of regression equations also provides information on the possible appearance of a synergistic or antagonistic joint influence of a group of factors on the result (coefficients for paired or triple interactions). Here it is necessary to emphasize that only the fact of interaction can be registered, since the factors in the equations are represented in encoded form. To estimate the amount of influence, the equations must be converted to the natural values of the factors.

The results of studies of technological processes using system analysis methods are also considered as a basis for further research with the solution of problems of materials science, heat and mass transfer in materials, and the study of phase transformations in the process of technological processing.

5. CONCLUSION

As a result of the research, elements of the methodology for selecting the composition of a dispersed reinforced composite material based on fine-ground concrete scrap waste, mineral binder, alkali-resistant glass fiber and plasticizer were developed. The research was based on the method of system analysis, the essence of which was to study technology as a cybernetic system with an assessment of the" reactions" of this system to external influences formed during an active experiment. At the same time, the solution of optimization problems was carried out within the framework of the General methodology of analytical optimization.

The research methods described in the article were previously implemented in the study of technologies for cellular concrete, foam concrete, cement-polymer concrete, and products made of mineral wool and foam glass. As an example, the article considers the optimization of the selection of the composition of fine-grained concrete reinforced with chopped glass fiber.

ACKNOWLEDGEMENTS

A part of the experimental studies has been carried out using the facilities of the Collective Research Center named after Professor Yu.M. Borisov, Voronezh State Technical University, which is partly supported by the Ministry of Science and Education of the Russian Federation, Contract No 075-15-2021-662.

REFERENCES

1. **Zhukov A.D.** Technological modeling [Electronic resource]: tutorial. - Electron. text data. Moscow: Moscow State University of Civil Engineering, EBS ASV, 2013. 204 pp. Access mode: http://www.iprbookshop.ru/20041. EBS “IPRbooks”, ISBN: 978-5 -7264-0780-7
2. **Zhukov A.D., Smirnova T.V., Gudkov P.K.** Workshop on technological modeling [Electronic resource]: tutorial. - Electron. text data.— Moscow: Moscow State University of Civil Engineering, EBS ASV, 2014. 168 pp. Access mode: http://www.iprbookshop.ru/30351. EBS “IPRbooks”, with a password ISBN: 978-5 - 7264-0903-0.
3. **Gorbunov G.I., Zhukov A.D.** Scientific bases of the formation of the structure and properties of building materials [Electronic resource]: monograph. Electron. text data. Moscow: Moscow State University of Civil Engineering, IP Er Media, EBS ACV, 2016. 555 pp. Access mode: http://www.iprbookshop.ru/49870. EBS “IPRbooks”, ISBN: 978-5-7264-1318-1
4. **Kozlov S., Efimov B., Bobrova E., Zinovieva E., Zhukova E.** Optimization of foamed plastic technology 06010 FORM-2019. E3S Web Conf. Vol. 97, 2019. DOI: https://doi.org/10.1051/e3sconf/20199706010
5. **Telichenko V. I. Oreshkin D. V.** Material science aspects of geoecological and ecological safety in construction // Ecology of urbanized areas .2015. #. 2. P. 31–33.
6. **Li X., Liu J., Qin J., Liu I., Qu Y., Zhang R.** Dissolution behavior of a novel composite fiber made from blast furnace slag // Journal Construction and Building Materials. Vol. 206. 2019, pp. 442-448. DOI: 10.1016/j.conbuildmat.2019.01.136
7. **Zhang S., Caprani C.C., Heidarpour A.** Strang rate studies of pultruded glass fiber reinforced polymer material properties: a literature review // Construction and Building Materials. Vol. 171. 2018, pp. 984-1004. DOI: 10.1016/j.conbuildmat.2018.03.113
8. **Pakravan H.R., Ozbakkaloglu T.** Synthetic fibers for cementations composites: a critical and in-depth review of recent advances // Construction and Building Materials. Vol. 207. 2019, pp. 491-518. DOI: 10.1016/j.conbuildmat.2019.02.078

9. **Falliano D., De Domenico D., Ricciardi G., Gugliandolo E.** Compressive and flexural strength of fiber-reinforced foamed concrete // Construction and Building Materials. Vol. 198. 2019. Pp. 479-493. DOI: 10.1016/j.conbuildmat.2018.11.197
10. **Xu S., Lyu Y., Li Q.** Enhancing the initial cracking fracture toughness of steel polyvinyl alcohol hybrid fibers ultra high togness cementitious composites by incorporating multy-walled carbon nanotube. // Construction and Building Materials. Vol. 195. 2019. Pp: 269-282. DOI: 10.1016/j.conbuildmat.2018.10.133
11. **Shen D., Liu X., Li Q., Sun L., Wang W.** Early-age behavior end cracking resistance of high-strength concrete reinforced with DRAMIX 3D steel fiber // Construction and Building Materials. Vol. 196. 2019. Pp. 307-316. DOI: 10.1016/j.conbuildmat.2018.10.125
12. **Efimov B. , Isachenko S., Kodzoev M.-B., Dosanova G., Bobrova E.** Dispersed reinforcement in concrete technology 01032 //E3S Web Conf.
13. **Parvathhy S.S., Sharma A.K., Anand K.B.** Comparative study on synthesis and proprieties of geopolymer fine aggregate from fly ashes // Construction and Building Materials. Vol. 198. 2019. Pp. 359-367. DOI: 10.1016/j.conbuildmat.2018.11.231
14. **Myrming V., Hackvart F.M., Alekseev K., Avanci M.A., Winter E., Marinho G.P., Iarozinski N. A., Catai R.E.1** Construction materials wastes use to neutralize hazardous municipal water treatment sludge // Construction and Building Materials. Vol. 204. 2019. Pp. 800-808. DOI: 10.1016/j.conbuildmat.2019.01.182
15. **Pyataev E.R., Medvedev A.A., Poserenin A.I., Burtseva M.A., Mednikova E.A. and Mukhametzyanov V.M.** Theoretical principles of creation of cellular concrete with the use of secondary raw materials and dispersed reinforcement // IPICSE. https://doi.org/10.1051/matecconf/201825101012
16. **Sanjay Kumar, P. García-Triñanes, Amândio Teixeira-Pinto, M. Bao.** Development of alkali activated cement from mechanically activated silico-manganese (SiMn) slag. Cement and Concrete Composites, Vol. 40, 2013, P. 7-13. DOI: 10.1016/j.cemconcomp.2013.03.026
17. **Hossein Sasanipour, Farhad Aslani, Javad Taherinezhad.** Effect of silica fume on durability of self-compacting concrete made with waste recycled concrete aggregates // Construction and Building Materials, Volume 227, 2019, Article 116598.
18. **Ivanov L.A.** Establishment of technological startups based on research and development (interview with Polad Malkin, researcher and developer Ph.D., professor, serial technology entrepreneur, CEO of «StartUpLab»). Nanotechnologies in Construction. 2019, Vol. 11, no. 2, pp. 207–216. DOI: 10.15828/2075-8545-2019-11-2-207-216.
19. **Almusaed A., Almassad A. Alasadi A.** Analytical interpretation of energy efficiency concepts in the housing design process from hot climate // Journal of Building Engineering. Vol. 21. 2019, P. 254-266. DOI: 10.1016/j.jobe.2018.10.026.
20. **Artamonova O.V., Slavcheva G.S., Chernyshov E.M.** Effectiveness of Combined Nanoadditives for Cement Systems. Inorganic Materials. 2017. V. 53. P. 1080–1085. DOI: 10.1134/S0020168517100028.
21. **Zhukov A., Shokodko E.** Mathematical Methods for Optimizing the Technologies of Building Materials // VIII International Scientific Siberian Transport Forum. TransSiberia 2019. Advances in Intelligent Systems and Computing, Vol. 1116. P. 413-421. Springer, Cham. 2020. DOI: 10.1007/978-3-030-37919-3_40
22. **I. Bessonov, A. Zhukov, E. Shokodko, A. Chernov.** Optimization of the technology for the production of foam glass aggregate // TPACEE 2019, E3S Web of Conferences, Vol. 164, 14016 (2020). DOI: 10.1051/e3sconf/202016414016

СПИСОК ЛИТЕРАТУРЫ

1. **Жуков А.Д.** Технологичесоке моделирование [электронный ресурс]: учебное пособие. М: Московский государственный строительный университет, ЭБС АСВ, 2013. 204 с.
2. **Жуков А.Д., Смирнова Т.В., Гудков П.К.** Практикум по технологическому моделированию [электронный ресурс]: учебное пособие. М: Московский государственный строительный университет, ЭБС АСВ, 2014. 168 с.
3. **Горбунов Г.И., Жуков А.Д.** Научные основы формирования структуры и свойств строительных материалов [электронный ресурс]: монография. М: Московский государственный строительный университет, Ай Пи Эр Медиа, ЭБС АСВ, 2016. 555 с.
4. **Kozlov S., Efimov B., Bobrova E., Zinovieva E., Zhukova E.** Optimization of foamed plastic technology 06010 FORM-2019. E3S Web Conf. Vol. 97, 2019. DOI: 10.1051/e3sconf/20199706010
5. **Теличенко В.И., Орешкин Д.В.** Материаловедческие аспекты геоэкологической и экологической безопасности в строительстве // Экология урбанизированных территорий, 2015, № 2, С. 31–33.
6. **Li X., Liu J., Qin J., Liu I., Qu Y., Zhang R.** Dissolution behavior of a novel composite fiber made from blast furnace slag // Journal Construction and Building Materials. Vol. 206. 2019, pp. 442-448. DOI: 10.1016/j.conbuildmat.2019.01.136
7. **Zhang S., Caprani C.C., Heidarpour A.** Strang rate studies of pultruded glass fiber reinforced polymer material properties: a literature review // Construction and Building Materials. Vol. 171. 2018, pp. 984-1004. DOI: 10.1016/j.conbuildmat.2018.03.113
8. **Pakravan H.R., Ozbakkaloglu T.** Synthetic fibers for cementations composites: a critical and in-depth review of recent advances // Construction and Building Materials. Vol. 207. 2019, P. 491-518. DOI: 10.1016/j.conbuildmat.2019.02.078
9. **Falliano D., De Domenico D., Ricciardi G., Gugliandolo E.** Compressive and flexural strength of fiber-reinforced foamed concrete // Construction and Building Materials. Vol. 198. 2019. P. 479-493. DOI: 10.1016/j.conbuildmat.2018.11.197
10. **Xu S., Lyu Y., Li Q.** Enhancing the initial cracking fracture toughness of steel polyvinyl alcohol hybrid fibers ultra high togness cementitious composites by incorporating multywalled carbon nanotube. // Construction and Building Materials. Vol. 195. 2019. Pp: 269-282. DOI: 10.1016/j.conbuildmat.2018.10.133
11. **Shen D., Liu X., Li Q., Sun L., Wang W.** Early-age behavior end cracking resistance of high-strength concrete reinforced with DRAMIX 3D steel fiber // Construction and Building Materials. Vol. 196. 2019. Pp. 307-316. DOI: 10.1016/j.conbuildmat.2018.10.125
12. **Efimov B., Isachenko S., Kodzoev M.-B., Dosanova G., Bobrova E.** Dispersed reinforcement in concrete technology 01032 //E3S Web Conf.
13. **Parvathhy S.S., Sharma A.K., Anand K.B.** Comparative study on synthesis and proprieties of geopolymer fine aggregate from fly ashes // Construction and Building Materials. Vol. 198. 2019. P. 359-367. DOI: 10.1016/j.conbuildmat.2018.11.231
14. **Myrming V., Hackvart F.M., Alekseev K., Avanci M.A., Winter E., Marinho G.P., Iarozinski N. A., Catai R.E.1** Construction materials wastes use to neutralize hazardous municipal water treatment sludge // Construction and Building Materials. Vol. 204. 2019. P. 800-808. DOI: 10.1016/j.conbuildmat.2019.01.182
15. **Pyataev E.R., Medvedev A.A., Poserenin A.I., Burtseva M.A., Mednikova E.A. and Mukhametzyanov V.M.** Theoretical principles of creation of cellular concrete with the use of secondary raw materials and dispersed reinforcement // IPICSE. Published online: 14 December 2018. DOI: 10.1051/matecconf/201825101012

16. **Sanjay Kumar, P. García-Triñanes, Amândio Teixeira-Pinto, M. Bao.** Development of alkali activated cement from mechanically activated silico-manganese (SiMn) slag. Cement and Concrete Composites, Vol. 40, 2013, P. 7-13. DOI: 10.1016/j.cemconcomp.2013.03.026
17. **Hossein Sasanipour, Farhad Aslani, Javad Taherinezhad.** Effect of silica fume on durability of self-compacting concrete made with waste recycled concrete aggregates // Construction and Building Materials, Vol. 227, 2019, Article 116598.
18. **Ivanov L.A.** Establishment of technological startups based on research and development (interview with Polad Malkin, researcher and developer Ph.D., professor, serial technology entrepreneur, CEO of «StartUpLab»). Nanotechnologies in Construction. 2019, Vol. 11, no. 2, pp. 207–216. DOI: 10.15828/2075-8545-2019-11-2-207-216.
19. **Almusaed A., Almassad A. Alasadi A.** Analytical interpretation of energy efficiency concepts in the housing design process from hot climate // Journal of Building Engineering. Vol. 21. 2019, P. 254-266. DOI: 10.1016/j.jobe.2018.10.026.
20. **Artamonova O.V., Slavcheva G.S, Chernyshov E.M.** Effectiveness of Combined Nanoadditives for Cement Systems. Inorganic Materials. 2017. V. 53. Pp. 1080–1085. DOI: 10.1134/S0020168517100028.
21. **Zhukov A., Shokodko E.** Mathematical Methods for Optimizing the Technologies of Building Materials // VIII International Scientific Siberian Transport Forum. TransSiberia 2019. Advances in Intelligent Systems and Computing, Vol. 1116. P. 413-421. 2020. Springer, Cham. DOI: https://doi.org/10.1007/978-3-030-37919-3_40
22. **I. Bessonov, A. Zhukov, E. Shokodko, A. Chernov.** Optimization of the technology for the production of foam glass aggregate // TPACEE 2019, E3S Web of Conferences, Vol. 164, 14016 (2020). DOI: https://doi.org/10.1051/e3sconf/202016414016

Alexey D. Zhukov, PhD in Engineering, Assoc. Prof. of the Dept. of Construction Materials, National Research Moscow State University of Civil Engineering (NRU MGSU), Yaroslavl sh. 26, Moscow, 129337, Russia; National Research University "Higher school of Economics", 20 Myasnitskaya str., Moscow, 101000, Russia; Research Institute of Building Physics, Lokomotivny proezd, 21, Moscow, 127238, Russia, e-mail: lj211@yandex.ru.

Ekaterina Yu. Bobrova, PhD in Economics, Advisor to the Director of the Institute of Construction and Housing and Utilities GASIS, National research University "Higher school of Economics", 20 Myasnitskaya str., Moscow, 101000, Russia, e-mail: e.bobrova@hse.ru.

Ivan I. Popov, PhD in Engineering, Researcher, Voronezh State Technical University, 84, 20-Letiya Octyabrya Str., Voronezh, 394006, Russia, e-mail: ipopov@vgasu.vrn.ru.

Demissie Bekele Arega, Master in Construction Engineering, PhD Strudent, National research University "Higher school of Economics", 20 Myasnitskaya str., Moscow, 101000, Russia, e-mail: aregabekalu@gmail.com.

Жуков Алексей Дмитриевич, доцент, кандидат технических наук, доцент кафедры Строительного материаловедения НИУ МГСУ, ведущий научный сотрудник НИИ строительной физики (НИИСФ РААСН), заместитель директора НОЦ комплексной модернизации инфраструктуры ЖКХ института ГАСИС НИУ ВШЭ, член-корреспондент Российской инженерной академии (РИА), г. Москва, Россия, e-mail: lj211@yandex.ru.

Боброва Екатерина Юрьевна, кандидат экономических наук, советник директора Института строительства и жилищно-коммунального хозяйства Государственной академии специалистов инвестиционной сферы Национального исследовательского университета «Высшая школа экономики», г. Москва, Россия, e-mail: e.bobrova@hse.ru.

Попов Иван Иванович, PhD в области технических наук, научный сотрудник, Воронежский государственный технический университет, г. Воронеж, Россия, e-mail: 89042149140@mail.ru

Демисси Бекеле Арега, магистр строительства, аспирант кафедры Строительного материаловедения НИУ МГСУ, г. Москва, Россия. ORCID: https://orcid.org/0000-0003-1689-7003. e-mail: aregabekalu@gmail.com.

DOI:10.22337/2587-9618-2021-17-4-83-90

DERIVATION OF THE EQUATION OF UNSTEADY-STATE MOISTURE BEHAVIOUR IN THE ENCLOSING STRUCTURES OF BUILDINGS USING A DISCRETE-CONTINUOUS APPROACH

Kirill P. Zubarev [1, 2, 3]

[1] National Research Moscow State University of Civil Engineering, Moscow, RUSSIA

[2] Research Institute of Building Physics of Russian Academy of Architecture and Construction Sciences, Moscow, RUSSIA.

[3] Peoples' Friendship University of Russia (RUDN University), Moscow, RUSSIA.

Abstract: Two differential equations of moisture transfer based on the theory of moisture potential have been considered. The first equation includes the record of moisture transfer mechanisms of vapor and liquid phases and their relationship. The second equation is a simplified form of the first equation which makes it possible to apply a discrete-continuous approach. The peculiar properties of the boundary conditions setting of the outside air for temperature and humidity fields have been presented. It is proved that the use of the discrete-continuous method provides high accuracy of calculations and can be used in engineering practice to assess the unsteady humidity regime of enclosing structures.

Keywords: moisture regime, discrete-continuous approach, moisture transfer equation.

ВЫВОД УРАВНЕНИЯ НЕСТАЦИОНАРНОГО ВЛАГОПЕРЕНОСА В ОГРАЖДАЮЩИХ КОНСТРУКЦИЯХ ЗДАНИЙ С ПРИМЕНЕНИЕМ ДИСКРЕТНО-КОНТИНУАЛЬНОГО ПОДХОДА

К.П. Зубарев [1, 2, 3]

[1] Национальный исследовательский Московский государственный строительный университет, г. Москва, РОССИЯ

[2] Научно-исследовательский институт строительной физики Российской академии архитектуры и строительных наук, г. Москва, РОССИЯ

[3] Российский университет дружбы народов, г. Москва, РОССИЯ

Аннотация: Рассмотрено два дифференциальных уравнения влагопереноса, основанных на теории потенциала влажности. Первое уравнение включает учет механизмов влагопереноса парообразной и жидкой фазы и их связь между друг другом. Второе уравнение представляет собой упрощенный вид первого уравнения специально для возможности применения дискретно-континуального подхода. Представлены особенности задания граничных условий наружного воздуха для температурного и влажностного полей. Доказано, что применение дискретно-континуального метода дает высокую точность вычислений и может использоваться в инженерной практике для оценки нестационарного влажностного режима ограждающих конструкций.

Ключевые слова: влажностный режим, дискретно-континуальный подход, уравнение влагопереноса.

1. INTRODUCTION

Heat and moisture transfer in enclosing structures is one of the most complicated and pending issues in construction [1,2]. The main feature of the problem mentioned is that the processes of moisture transfer are non-stationary [3]. The assessment of the moisture state of building materials by stationary methods can lead to serious errors in the design of buildings and structures [4].

Experimental studies of heat and mass transfer problems are constantly being carried out by scientists from all over the world [5,6] in various

branches of technology. As an example, we can mention the problem of drying wood. In construction, new architectural and designer solutions have a great influence on the choice of enclosing structures [7,8].

The humidity regime affects energy saving, thermal protection of buildings, as well as the durability of the enclosing structures [9,10]. The moisture regime assessment is accentuated by the fact that moisture can be in different relationship with the skeleton of the building material and different aggregate states.

The earliest notions about the calculation of building enclosure moisture state were based on the differential equation for the water vapor transfer [11]. Subsequently, it was found that water vapor is not the only moisture transfer potential. In the pores of building materials, some processes, such as capillary fluid flow, moisture transfer under the temperature and air filtration, and the mutual influence of temperature and humidity fields occur. [12]

In after years, the researchers worked with a system of differential equations describing various transfer potentials. However, back in the XX century V.N. Bogoslovsky created the function of the moisture potential that makes it possible to replace several separate transfer potentials with one single moisture potential, which greatly simplified the work with mathematical models of the moisture regime. At present, a large number of moisture or mass transfer potentials have been developed, for instance, the Bogoslovsky potential, the Lykov potential, the L. Pel potential, the H.M. Kunzel, etc [13].

There are diverse regulations governing the assessment of the moisture state of building envelopes all over the world. In Europe it is customary to assess the humidity regime using the WUFI computer program. In the Russian Federation the Set of Rules 50.13330.2012 “Thermal protection of buildings”, which also contains a section called “Protection against water logging of enclosing structures”, is applied. This regulatory document is based on the theory of moisture potential by V.G. Gagarin and V.V. Kozlov [14]. According to the Set of Rules 50.13330.2012 "Thermal protection of buildings", the problem of stationary moisture transfer under the moisture potential *F*, which uniformly takes into account the movement of vaporous and liquid moisture, is considered [15]:

$$\frac{\partial}{\partial x}(\mu \frac{\partial F(w,t)}{\partial x}) = 0. \qquad (1)$$

where F – moisture potential, *Pa*; μ – vapor permeability coefficient, *kg/(m·s·Pa)*; w – material moisture , % by weight (1 *kg/kg* = 100 % by weight), t – temperature, $^{\circ}C$; x – coordinate, *m*.

Nevertheless, creating formulas and methods that allow us to assess the unsteady humidity regime without applying numerical methods remains relevant.

In this regard, the most promising areas of research are discrete-continuous calculation methods, which are used in various construction problems [16,17].

The closest to moisture transfer is the heat transfer problem.

In a discrete-continuous formulation, the heat equation was studied by Zolotov A.B., Akimov P.A., Sidorov V.N., Mozgaleva M.L. and S.M. Matskevich [18-22].

2. THE PROBLEM

Derive the equation of unsteady moisture transfer using the discrete-continuous approach and evaluate its efficiency in comparison with the finite difference method.

3. MATERIALS AND METHODS

In earlier studies, a differential moisture transfer equation was derived based on the moisture potential F [15]:

$$\frac{\partial F(w,t)}{\partial \tau} = \kappa_F(w,t) \cdot E_t(t) \cdot \frac{\partial^2 F(w,t)}{\partial x^2}. \qquad (2)$$

where E_t – saturated water vapor pressure, *Pa*; τ – time, *s*; *x* – coordinate, *m*, κ_F – material heat-humidity characteristic coefficient, $m^2/(s \cdot Pa)$.

However, it is impossible to apply a discrete-continuous method to the equation (2), since the coefficient κ_F depends on the mass moisture content of the material and temperature. This means that in discretization of the space-time domain the coefficient κ_F will have a different value at any point in space, as well as at any time.

To simplify the equation (2), it is proposed to replace the material heat-humidity characteristic coefficient κ_F with the average material heat-humidity characteristic coefficient κ_{F0}.

Thus, the equation (2) will be represented as:

$$\frac{\partial F(w,t)}{\partial \tau} = \kappa_F \cdot E_t(t) \cdot \frac{\partial^2 F(w,t)}{\partial x^2}. \qquad (3)$$

Since moisture transfer processes in the building materials are by four orders of magnitude slower than heat transfer processes, it was proposed that the outdoor air temperature outside the structure will be constant for a month (Figure 1) and the humidity potential outside the building enclosure will have the form of a piecewise linear function (Figure 2).

Inside the structure, both the temperature and the humidity potentials were taken constant throughout the year.

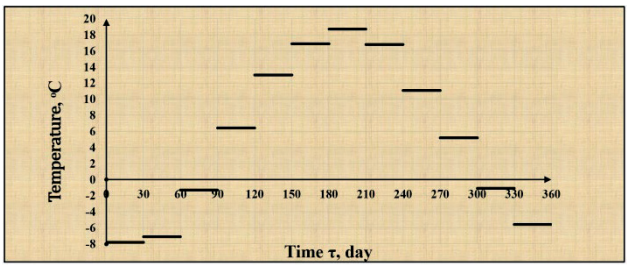

Figure 1. Boundary conditions for the temperature field outside the structure for Moscow (Russian Federation)

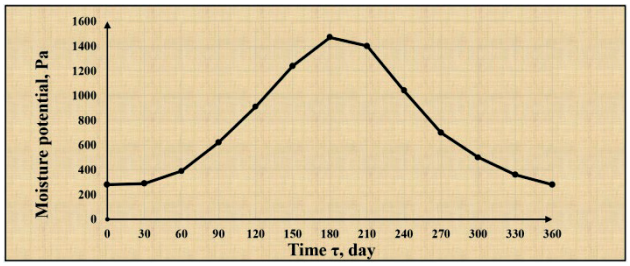

Figure 2. Boundary conditions for the field of moisture potential outside the structure for Moscow (Russian Federation)

Thus, the saturated water vapor pressure in the equation (3) will depend on the coordinate but not on the time during the calculated month.

Setting the boundary conditions of moisture exchange of the third kind for the equation (3) and applying the discrete-continuous approach, we obtain a system of equations in matrix form which represents the Cauchy problem and has an analytical solution in matrices:

$$\begin{cases} \overline{F}'_\tau = E_t \cdot A \cdot \overline{F} + \overline{S} \\ \overline{F}(0) = \overline{\chi}, 0 \le x \le l \end{cases} . \qquad (4)$$

where E_t – a matrix of the saturated water vapour pressure; A – a matrix of coefficients; $\overline{F}$ – a matrix of initial distribution of moisture potential; $\overline{S}$ – a matrix of boundary conditions; $\overline{F}'_\tau$ – a matrix of derivatives to the moisture potential in different sections of the considered area.

The solution of the Cauchy problem (4) can written as the equation:

$$\overline{F} = \int_0^\tau (e^{E_t \cdot A \cdot (\tau - \sigma)} \cdot \overline{S}(\sigma) \cdot d\sigma) + e^{E_t \cdot A \cdot \tau} \cdot \overline{F_0}. \qquad (5)$$

The integral in the equation (5) will depend on the function of the boundary conditions.

To take the integral, we represent the matrix of the boundary conditions as the following an expression:

$$\overline{S} = p \cdot \tau \cdot \overline{L} + \overline{B}. \qquad (6)$$

where p – the coefficient of the external boundary condition for a building enclosing structure, Pa/s^2; $\overline{B}$ – a column vector, the first and last elements of which describe the boundary conditions on the outer and inner surfaces of the enclosing structure, other elements are equal to 0 for a multi-layer enclosing structure; $\overline{L}$ – a column vector, the first element of which is equal to one, other elements are equal to 0 for a building enclosing structure.

Substituting (6) into (5), we can obtain the final expression for the moisture potential using the discrete-continuous approach:

$$\overline{F} = p \cdot \left(\left(E_t \cdot A\right)^{-2} \cdot e^{E_t \cdot A \cdot \tau} - \tau \cdot \left(E_t \cdot A\right)^{-1} - \left(E_t \cdot A\right)^{-2} \right) \cdot . \\ \cdot \overline{L} + \left(E_t \cdot A\right)^{-1} \left(e^{E_t \cdot A \cdot \tau} - E\right) \cdot \overline{B} + e^{E_t \cdot A \cdot \tau} \cdot \overline{F}_0. \qquad (7)$$

As the equation (7) is a numerical-analytical formula and it does not require numerical calculations, it can be used in engineering calculation methods.

4. RESULTS AND DISCUSSION

Replacing the coefficient $\kappa_F(w,t)$ in the equation (2) with the coefficient κ_F in the equation (3) leads to the simplification of the mathematical model of heat-moisture transfer. To prove the effectiveness of the proposed new discrete-continuous formula (7), the results of the non-stationary moisture regime calculations using the finite difference method according to an explicit difference scheme by the equation (2) and by the analytical expression (7) were compared.

A comparison of moisture distribution in the enclosing structure of aerated concrete in Moscow (the Russian Federation) made by the thickness of the enclosing structure (Figure 3) and by the time throughout the year is demonstrated (Figure 4).

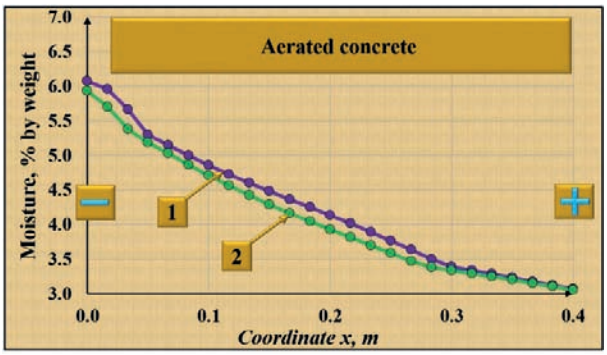

Figure 3. The results of the moisture regime calculations for a single-layer enclosing structure made of aerated concrete by its thickness (1 - solving the non-stationary moisture transfer equation by the finite difference method according to an explicit difference scheme; 2 - solving the non-stationary moisture transfer equation using a discrete-continuous approach according to the formula (7))

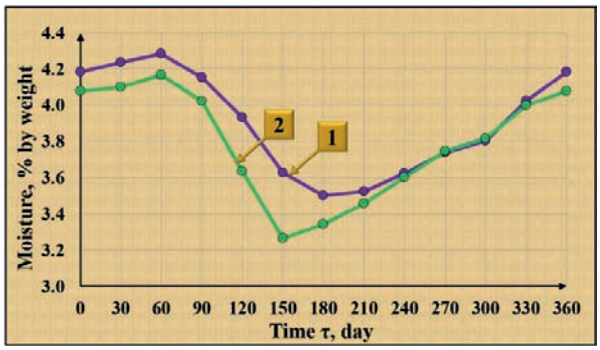

Figure 4. The results of the average moisture content calculations for a single-layer enclosing structure made of aerated concrete throughout a year (1 - solving the non-stationary moisture transfer equation by the finite difference method according to an explicit difference scheme; 2 - solving the non-stationary moisture transfer equation using the discrete-continuous approach according to formula (7))

As can be seen from the graphs, the solution of the moisture transfer equation according to the proposed method both quantitatively and qualitatively coincides with the solution of the moisture transfer equation according to the finite difference method. However, the discrete-continuous approach is carried out

according to the final formula, which simplifies the calculation.

5. CONCLUSIONS

The discrete-continuous approach enables us to propose a new efficient method for assessing the unsteady humidity regime which can be used by engineers in the design of enclosing structures.

6. ACKNOWLEDGMENTS

The author expresses gratitude to V.G. Gagarin, professor, Doctor of Engineering Sciences, V.K. Akhmetov, professor, Doctor of Engineering Sciences and V.V. Kozlov, Candidate of Engineering Sciences, for providing valuable advice during the work.

REFERENCES

1. **Petrov A., Ivantsov A.** Design and calculation of the internal roof drain system structure in terms of thermal protection and moisture condensation. // IOP Conference Series: Materials Science and Engineering, 2020, Vol. 890, № 022141.
2. **Statsenko E.A., Musorina T.A., Ostrovaia A.F., Olshevskiy V., Antuskov A.L.** Moisture transport in the ventilated channel with heating by coil. // Magazine of Civil Engineering, 2017, No. 2(70), pp. 11-17.
3. **Musorina T., Olshevskyi V., Ostrovaia A., Statsenko E.** Experimental assessment of moisture transfer in the vertical ventilated channel. // MATEC Web of Conferences, 2016, No. 02002.
4. **Hoseini A., Bahrami A.** Effects of humidity on thermal performance of aerogel insulation blankets. // Journal of building engineering, Vol. 13, 2017, pp. 107-115.
5. **Petrov A.S., Kupriyanov V.N.** About operational factor influence on vapor permeability of heat-insulating materials. // International Journal of Pharmacy and Technology, 2016, Vol. 8(1), pp. 11248-11256.
6. **Galbraith G.H., Guo G.H., McLean R.C.** The effect of temperature on the moisture permeability of building materials. // Building research and information, Vol. 28 Iss. 4, 2000 – pp. 245-259.
7. **Bespalov V., Kotlyarova E.** Improving the environmental assessment of objects in the system of construction engineering. // E3S Web of Conferences. 2020, Vol. 164, L 01009.
8. **Bespalov V., Kotlyarova E., Adamyan R.** Scientific and methodological principles of forming an assessment of the level of environmental safety of construction projects in urban areas. // E3S Web of Conferences, 2020, Vol. 193, No. 02007.
9. **Qu K., Chen X., Wang Y., Calautit J., Riffat S., Cui X.** Comprehensive energy, economic and thermal comfort assessments for the passive energy retrofit of historical buildings – A case study of a late nineteenth-century Victorian house renovation in the UK. // Energy, 2020, Vol. 220, No. 119646.
10. **Gumerova E., Gamayunova O., Meshcheryakova T.** Energy efficiency upgrading of enclosing structures of mass housing of the Soviet Union. // Advances in Intelligent Systems and Computing, 2017, Vol. 692, pp. 432-439.
11. **Vavrovic, B.** Importance of envelope construction renewal in panel apartment buildings in terms of basic thermal properties. // Advanced Materials Research, Vol. 855, 2014, pp. 97-101.
12. **Arfvidsson, J., Claesson J.** Isothermal moisture flow in building materials: modelling, measurements and calculations based on Kirchhoff's potential. // Building and environment. Vol. 35, Iss. 6, 2000, pp. 519-536.

13. **Gagarin V.G., Akhmetov V.K., Zubarev K.P.** Unsteady-state moisture behavior calculation for multilayer enclosing structure made of capillary-porous materials // IOP Conference Series: Earth and Environmental Science, 2019, Vol. 177(1), pp. 925-932.
14. **Gagarin V.G., Kozlov V.V., Zubarev K.P.** Determination of maximum moisture zone on enclosing structures. // Cold Climate HVAC 2018: Sustainable Buildings in Cold Climates, 2019, pp. 925-932.
15. **Zubarev K.P.** Using discrete-continuous approach for the solution of unsteady-state moisture transfer equation for multilayer building walls. // International Journal for Computational Civil and Structural Engineering, 2021, Vol. 17, No. 2, pp. 50-57.
16. **Akimov P.A., Mozgaleva M.L., Kaytukov T.B.** Numerical Solution of the Problem of Isotropic Plate Analysis with the Use of B-Spline Discrete-Continual Finite Element Method. // International Journal for Computational Civil and Structural Engineering, 2020, Vol. 16, No. 4, pp. 14-28.
17. **Mozgaleva, M. L., Akimov P.A., Kaytukov T.B.** Localization of Solution of the Problem of Isotropic Plate Analysis With the Use of B-Spline Discrete-Continual Finite Element Method // International Journal for Computational Civil and Structural Engineering, 2021, Vol. 17, No 1, pp. 55-74.
18. **Zolotov A.B., Mozgaleva M.L., Akimov P.A., Sidorov V.N.** Ob odnom diskretno-kontinualnom podkhode k resheniyu odnomernoy zadachi teploprovodnosti [About one discrete-continual method of solution of one-dimensional heat conductivity problem]. // Academia. Architecture and Construction (Academia. Arkhitektura i stroitelstvo), Iss. 3, 2010, pp. 287-291.
19. **Zolotov A.B., Mozgaleva M.L., Akimov P.A., Sidorov V.N.** Diskretno-kontinualnyy podkhod k resheniyu zadachi teploprovodnosti [Discrete-continual approach for thermal conductivity problem solution]. // Bulletin of Moscow State University of Civil Engineering (Vestnik MGSU), Iss. 3, 2010. pp. 58-62.
20. **Sidorov V.N. Matskevich S.M.** Discrete-analytical solution of the unsteady-state heat conduction transfer problem based on the finite element method. // IDT 2016 - Proceedings of the International Conference on Information and Digital Technologies 2016. 2016, pp. 241-244.
21. **Sidorov V.N. Matskevich S.M.** Solving unsteady boundary value problems using discrete-analytic method for non-iterative simulation of temperature processes in time. // Key Engineering Materials, Vol. 685, 2016, pp. 211-216.
22. **Sidorov V.N. Matskevich S.M.** Discrete-analytic solution of unsteady-state heat conduction transfer problem based on a theory of matrix function. // Procedia Engineering, Vol. 111, 2015, pp. 726-733.

СПИСОК ЛИТЕРАТУРЫ

1. **Petrov A., Ivantsov A.** Design and calculation of the internal roof drain system structure in terms of thermal protection and moisture condensation. // IOP Conference Series: Materials Science and Engineering, 2020, Vol. 890, № 022141.
2. **Statsenko E.A., Musorina T.A., Ostrovaia A.F., Olshevskiy V., Antuskov A.L.** Moisture transport in the ventilated channel with heating by coil. // Magazine of Civil Engineering, 2017, No. 2(70), pp. 11-17.
3. **Musorina T., Olshevskyi V., Ostrovaia A., Statsenko E.** Experimental assessment of moisture transfer in the vertical ventilated channel. // MATEC Web of Conferences, 2016, No. 02002.

4. **Hoseini A., Bahrami A.** Effects of humidity on thermal performance of aerogel insulation blankets. // Journal of building engineering, Vol. 13, 2017, pp. 107-115.
5. **Petrov A.S., Kupriyanov V.N.** About operational factor influence on vapor permeability of heat-insulating materials. // International Journal of Pharmacy and Technology, 2016, Vol. 8(1), pp. 11248-11256.
6. **Galbraith G.H., Guo G.H., McLean R.C.** The effect of temperature on the moisture permeability of building materials. // Building research and information, Vol. 28 Iss. 4, 2000 – pp. 245-259.
7. **Bespalov V., Kotlyarova E.** Improving the environmental assessment of objects in the system of construction engineering. // E3S Web of Conferences. 2020, Vol. 164, L 01009.
8. **Bespalov V., Kotlyarova E., Adamyan R.** Scientific and methodological principles of forming an assessment of the level of environmental safety of construction projects in urban areas. // E3S Web of Conferences, 2020, Vol. 193, No. 02007.
9. **Qu K., Chen X., Wang Y., Calautit J., Riffat S., Cui X.** Comprehensive energy, economic and thermal comfort assessments for the passive energy retrofit of historical buildings – A case study of a late nineteenth-century Victorian house renovation in the UK. // Energy, 2020, Vol. 220, No. 119646.
10. **Gumerova E., Gamayunova O., Meshcheryakova T.** Energy efficiency upgrading of enclosing structures of mass housing of the Soviet Union. // Advances in Intelligent Systems and Computing, 2017, Vol. 692, pp. 432-439.
11. **Vavrovic, B.** Importance of envelope construction renewal in panel apartment buildings in terms of basic thermal properties. // Advanced Materials Research, Vol. 855, 2014, pp. 97-101.
12. **Arfvidsson, J., Claesson J.** Isothermal moisture flow in building materials: modelling, measurements and calculations based on Kirchhoff's potential. // Building and environment. Vol. 35, Iss. 6, 2000, pp. 519-536.
13. **Gagarin V.G., Akhmetov V.K., Zubarev K.P.** Unsteady-state moisture behavior calculation for multilayer enclosing structure made of capillary-porous materials // IOP Conference Series: Earth and Environmental Science, 2019, Vol. 177(1), pp. 925-932.
14. **Gagarin V.G., Kozlov V.V., Zubarev K.P.** Determination of maximum moisture zone on enclosing structures. // Cold Climate HVAC 2018: Sustainable Buildings in Cold Climates, 2019, pp. 925-932.
15. **Zubarev K.P.** Using discrete-continuous approach for the solution of unsteady-state moisture transfer equation for multilayer building walls. // International Journal for Computational Civil and Structural Engineering, 2021, Vol. 17, No. 2, pp. 50-57.
16. **Akimov P.A., Mozgaleva M.L., Kaytukov T.B.** Numerical Solution of the Problem of Isotropic Plate Analysis with the Use of B-Spline Discrete-Continual Finite Element Method. // International Journal for Computational Civil and Structural Engineering, 2020, Vol. 16, No. 4, pp. 14-28.
17. **Mozgaleva, M. L., Akimov P.A., Kaytukov T.B.** Localization of Solution of the Problem of Isotropic Plate Analysis With the Use of B-Spline Discrete-Continual Finite Element Method // International Journal for Computational Civil and Structural Engineering, 2021, Vol. 17, No 1, pp. 55-74.
18. **Золотов А.Б., Мозгалева М.Л., Акимов П.А., Сидоров В.Н.** Об одном дискретно-континуальном подходе к решению одномерной задачи теплопроводности. // Academia.

Архитектура и строительство, Iss. 3, 2010, pp. 287-291.
19. **Золотов А.Б. Мозгалева М.Л., Акимов П.А., Сидоров В.Н.** Дискретно-континуальный подход к решению задачи теплопроводности. // Вестник МГСУ, Iss. 3, 2010. pp. 58-62.
20. **Sidorov V.N. Matskevich S.M.** Discrete-analytical solution of the unsteady-state heat conduction transfer problem based on the finite element method. // IDT 2016 - Proceedings of the International Conference on Information and Digital Technologies 2016. 2016, – pp. 241-244.
21. **Sidorov V.N. Matskevich S.M.** Solving unsteady boundary value problems using discrete-analytic method for non-iterative simulation of temperature processes in time. // Key Engineering Materials, Vol. 685, 2016, pp. 211-216.
22. **Sidorov V.N. Matskevich S.M.** Discrete-analytic solution of unsteady-state heat conduction transfer problem based on a theory of matrix function. // Procedia Engineering, Vol. 111, 2015, pp. 726-733.

Zubarev Kirill Pavlovich, PhD (Candidate of Engineering Sciences), Senior Lecturer at the Department of Heat and Gas Supply and Ventilation of the Moscow State University of Civil Engineering, 129337, Moscow, Yaroslavskoe shosse, 26; Associate Professor at the Department of General and Applied Physics of the Moscow State University of Civil Engineering, 129337, Moscow, Yaroslavskoe shosse, 26; Senior Researcher at the Laboratory of Building Thermal Physics of the Research Institute of Building Physics of Russian Academy of Architecture and Construction Sciences, 127238, Moscow, Lokomotivny proezd, 21; Associate Professor at the Department of Civil Engineering of the Engineering Academy of the Peoples' Friendship University of Russia 117198, Moscow, st. Miklukho-Maclay, 6; Tel. +7 (905) 706-77-63. e-mail.: zubarevkirill93@mail.ru.

Зубарев Кирилл Павлович, кандидат технических наук, старший преподаватель кафедры теплогазоснабжения и вентиляции Национального исследовательского Московского государственного строительного университета 129337, г. Москва, Ярославское шоссе, 26; доцент кафедры общей и прикладной физики Национального исследовательского Московского государственного строительного университета 129337, г. Москва, Ярославское шоссе, 26; старший научный сотрудник лаборатории строительной теплофизики Научно-исследовательского института строительной физики Российской академии архитектуры и строительных наук 127238, г. Москва, Локомотивный проезд, 21; доцент департамента строительства инженерной академии Российского университета дружбы народов 117198, г. Москва, ул. Миклухо-Маклая, 6; тел. +7 (905) 706-77-63. e-mail.: zubarevkirill93@mail.ru.

DOI:10.22337/2587-9618-2021-17-4-91-105

NUMERICAL STUDY OF THE PUNCHING SHEAR MECHANISM FOR THIN AND THICK REINFORCED CONCRETE SLABS

Oleg V. Kabantsev [1], Sergey B. Krylov [2], Sergey V. Trofimov [1,2]
[1] National Research Moscow State University of Civil Engineering, Moscow, RUSSIA
[2] Research Institute of Concrete and Reinforced Concrete named after A.A. Gvozdev, Moscow, RUSSIA

Abstract: The assessment of the punching shear capacity for reinforced concrete slabs, carried out according to the regulatory documents of a number of countries, leads to significantly various results. At the same time, the results of the calculated forecast may have great differences from the experimental data. A great influence on the accuracy of the results of the calculated forecast is exerted by the thickness of the examined slabs, as well as the value of longitudinal reinforcement. These parameters determine the features of the mechanisms of destruction of slabs in case of the punching shear mechanism, as indicated by individual interpretations of the results of experimental studies. In order to determine the features of the punching shear mechanism of reinforced concrete slabs of various thicknesses, numerical studies of the process of cracking and destruction of slabs of different thicknesses have been performed. Differences in the mechanism of formation and development of cracks in thin and thick slabs are revealed. The paper shows that the behavior of thin and thick slabs has qualitative distinctions at the initial stages of formation and development of the cracks leading to destruction. The authors have also shown the difference between stress-strain state of thick and thin slabs before destruction. In conclusion, it was established that the influence of longitudinal reinforcement on the strength during punching in thick slabs is much less than in thin ones.

Keywords: modeling, numerical methods, design model, stress-strain state, reinforced concrete structures, punching failure.

ЧИСЛЕННЫЕ ИССЛЕДОВАНИЯ ОСОБЕННОСТЕЙ МЕХАНИЗМОВ РАЗРУШЕНИЯ ТОНКИХ И ТОЛСТЫХ ПЛИТ В РЕЖИМЕ ПРОДАВЛИВАНИЯ

О.В. Кабанцев [1], С.Б. Крылов [2], С.В. Трофимов [1,2]
[1] Московский государственный строительный университет, Москва, РОССИЯ
[2] Научно-исследовательский институт бетона и железобетона имени А.А. Гвоздев, Moscow, RUSSIA

Аннотация: Оценка несущей способности на продавливание железобетонных плит, выполненная по нормативным документам разных стран, приводит к существенно отличающимся результатам. При этом результаты расчётного прогноза могут иметь значительные отличия от опытных данных. Большое влияние на точность результатов расчётного прогноза оказывает толщина рассчитываемых плит, а также величина продольного армирования. Указанные параметры определяют особенности механизмов разрушения плит в режиме продавливания, на что указывают отдельные трактовки результатов экспериментальных исследований. В целях определения особенностей работы железобетонных плит различной толщины в режиме продавливания проведены численные исследования процесса трещинообразования и разрушения плит разной толщины. Выявлены различия в механизме образования и развития трещин в тонких и толстых плитах. Показано, что работа тонких и толстых плит имеет качественные отличия на начальных этапах процесса образования и развития трещин, приводящих к разрушению. Показаны различия в напряжённо-деформированном состоянии толстых и тонких плит перед разрушением. Установлено, что влияние продольной арматуры на прочность при продавливании в толстых плитах значительно меньше, чем в тонких.

Ключевые слова: моделирование, численные методы, расчетная модель, напряженно-деформированное состояние, железобетонные конструкции, продавливание.

1. INTRODUCTION

One of the most actual problems in the bearing capacity of reinforced concrete slabs according to the punching shear criterion is the issue of the behavior of slabs with longitudinal reinforcement. The prediction of the punching shear capacity based of reinforced concrete slabs with longitudinal reinforcement and without transverse reinforcement in the support zone is carried out using the basic formulas, which, as a rule, do not take consider the features of the failure of thin and thick slabs. The methods accepted in codes of number of countries have some differences, some one of which is very significant. Thus, the norms of the European Union EN 1992-1-1 Eurocode 2 [1] (hereinafter EC2) and in fib Model Code 2010 [2] (hereinafter MC2010) provide accounting the longitudinal reinforcement of the stretched zone but according to various methods. The building code of the Russian Federation [3] (SP 63.13330.2018) does not take into account the work of longitudinal tensile reinforcement when calculating the punching shear capacity of the slab. Such significant deviations in the standardization of the punching shear design led to significant differences in the forecast of the bearing capacity. Experimental investigations on the behavior of slabs of various thicknesses have also established the differences between the actual level of capacity and the forecast one for various standards. Table 1 shows the analysis of various regulatory approaches based on experimental research data which were previously presented in the work [4].

Table 1

Specimen	B, m	h_0, m	r_g, m	ρ, %	f_c, MPa	f_y, MPa	V_{ex}, kN (100%)	$V_{Rd,c}$ (EC2), kN/%	$V_{Rd,c}$ (MC2010), kN/%	$F_{b,ult}$ (SP 63.1330), kN /%
1	2	3	4	5	6	7	8	9	10	11
PG1 [5]	3	0.21	1.5	1.5	27.6	573	1023	950/7.1	841/17.8	947.5/7.4
PG2 [5]	3	0.21	1.5	0.25	40.5	552	440	594/-35.0	420/4.5	1263.36/-187.1
PG3 [5]	6	0.456	2.85	0.33	32.4	520	2153	2340/-8.7	1730/19.6	4806.6/-123.3
PG4 [5]	3	0.21	1.5	0.25	32.2	541	408	550/-34.8	344/15.7	1066/-161.3
PG5 [5]	3	0.21	1.5	0.33	29.3	555	550	583/-6.0	455/17.3	987/-79.5
PG7 [5]	1.5	0.1	0.75	0.75	34.7	550	241	189/21.6	197/18.3	257.6/-6.9
PG8 [5]	1.5	0.117	0.75	0.28	34.7	525	140	178/-27.1	137/2.1	323.7/-131.2
PG9 [5]	1.5	0.117	0.75	0.22	34.7	525	115	165/-43.5	109/5.2	323.7/-181.5
PG10 [5]	3	0.21	1.5	0.33	28.5	577	540	577/-6.9	454/15.9	987/-82.8
PG11 [5]	3	0.21	1.5	0.75	31.5	570	763	788/-3.3	682/10.6	1066/-39.7
PV1 [6]	3.0	210	1.38	1.5	34.0	709	974	1019/-4.6	792/18.7	1105.4/-13.5
PL4 [6]	3.0	267	1.38	1.58	30.5	531	1625	1538/5.4	1191/26.7	1685.5/-3.7
PL5 [6]	3.0	353	1.38	1.5	31.9	580	2491	2505/-0.6	2255/9.5	3023.2/-21.4
П-4 [7]	1.98	360	0.79	1.06	29.6	385	1670	1804/-8.0	1830/-9.6	1822/-9.1
П-5 [7]	2.34	460	0.97	0.83	27.9	385	2260	2189/3.1	2431/-7.6	2599/-15.0
П-6 [7]	2.68	550	1.14	0.89	23.7	432	2450	2265/7.6	3368/-37.5	3152/-28.7
P300 [8]	1.975	300	0.89	0.76	39.4	468	1381	1392/-0.8	1220/11.7	1860/-34.7
P400 [8]	1.975	400	0.89	0.76	39.4	468	2224	2377/-6.9	2442/-9.8	3472/-56.1
P500 [8]	1.975	500	0.89	0.76	39.4	433	2681	3414/-27.3	3919/-46.2	4960/-85.0
C_{h100} [9]	0.6	0.076	0.25	0.66	15	500	133.3	80/40.0	84/37.0	71.2/46.6
C_{h120} [9]	0.6	0.096	0.25	0.52	15	500	161	110/31.7	121/24.8	101/37.3

Note: the designations in Table 1 are adopted in accordance with EN2 [1] and MC2010 [2]. % were determined by the following formula: $(V_{ex} - V_{Rd,c}) / V_{ex}$

Comparative analysis of the results of the normative forecast of the bearing capacity with the data of experimental studies shows:
- taking into account the longitudinal reinforcement in the normative forecast of the capacity of the slabs according to the punching shear criterion provides a better correlation with the results of experimental studies;
- the value of the increase in the bearing capacity does not have a linear correlation with the increase in the thickness of the slab.

Table 2 presents changes in the value of the slab capacity due to the change in the thickness for slabs of medium and large thickness.

Table 2

No	Investigation	Specimen	h_0, mm	h_0, %	Vex, kN	Vex, %	h_0, %	Vex, %
1	2	3	4	5	6	7	8	9
1	S. Lips [6]	PV1	210	100	974	100	-	-
2		PL4	267	127.1	1625	166.8	100	100
3		PL5	353	168.1	2491	255.7	132.2	153.3
4	S. Guandalini [5]	PG-10	210	100	540	100	-	-
5		PG-3	456	217.1	2153	398.7	-	-
6	N.N. Korovin [7]	П-4	360	100	1670	100	-	-
7		П-5	460	127.8	2260	135.3	100	100
8		П-6	550	152.8	2450	146.7	119.5	108.4
9	Li K. K. L. [8]	P300	300	100	1381	100	-	-
10		P400	400	133.3	2224	161.0	100	100
11		P500	500	166.7	2681	194.1	125	120.5

Analysis of the change in the value of the capacity makes it possible to establish some features of the behavior of slabs of various thicknesses. With an increase in the thickness of the slab, an increase in the capacity according to the punching shear criterion is observed in the entire range of the investigated slab depths. However, the tendency for an increase in capacity for slabs of medium and large depths ($h0 \geq 0.25$ m) changes significantly in relation to slabs of small thickness. In the range of medium and large slab depths, the increase in the capacity (%) decreases in relation to the increase (%) in thickness compared to thin slabs. See data in columns 8 and 9 of Table 2. In the most pronounced form, this phenomenon was observed in specimens of N.N. Korovin [7], Li K. K. L. [8] et al. In scientific publications, this effect was called as "size effect".

The EC2 [1] and MC2010 [2] standards consider the size effect, but accounting methods differ significantly. SP 63.13330 does not take into account the size effect. Fig. 1 shows the influence of the size effect on slab capacity in accordance with experimental data and EC2 norms.

The current situation with the scientific substantiation of the size effect and the corresponding punching mechanisms of slabs of medium and large thickness requires additional scientific research. Therefore, the subject addressed in this article is worthy of investigation.

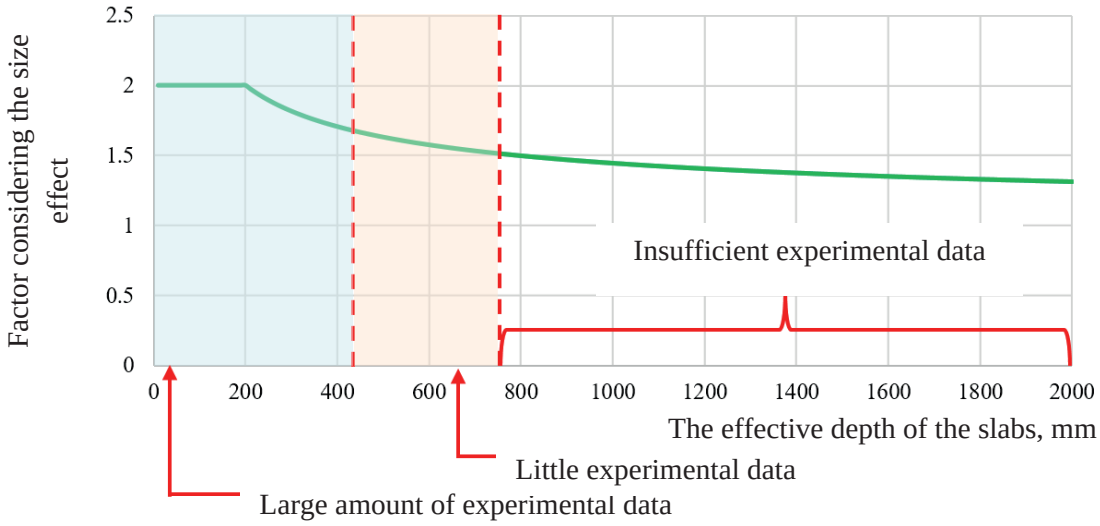

Figure 1. Influence of the size effect in the normative assessment of the punching shear capacity of the slab according to EC2

2. OBJECTIVE AND METHOD OF RESEARCH

Currently, there are two main concepts that explain the size effect when punching reinforced concrete slabs of medium and large thickness with longitudinal reinforcement in the stretched zone. The first concept is based on fracture mechanics [10], the second one on the critical shear crack theory (CSCT) [11].

According to the fracture mechanics [10, 12]: if the destruction of a reinforced concrete slab during compression is caused by the destruction of concrete, and not by the achievement of the yield strength of the reinforcement, then the dimensional effect appears. That is, if geometrically similar specimens are tested, differing only in thickness, then the nominal tensile stresses (σ_n) traditionally determined by formula (1) are higher in smaller specimens when it fracture. However, the traditional technique for determining stresses (1) does not explain the existing size effect.

$$\sigma_N = \frac{F}{u \cdot h_0} \qquad (1)$$

Where F is an ultimate breaking load; u is a perimeter of the design cross-section contour; h_0 is an effective depth of the reduced cross section.

Consequently, if the fracture occurs due to the localization of cracks, which is typical for reinforced concrete structures, the capacity for the action of the transverse force decreases with increasing h0. According to P. Bažant [12], the main reason for the size effect is the nonlinear dependence between the energy released during the formation and development of a crack and the height of the reinforced concrete section. This energy effect corresponds to a situation where the main crack grows steadily until the maximum load is reached, and the size effect is due to the energy release rate growth with an increase in the structure size according to the fracture mechanism.

The fracture model of reinforced concrete slabs based on the critical shear crack theory (CSCT) was developed by A. Muttoni [11, 13]. The method for calculating slabs according to the punching criterion based on CSCT has been included in MS2010, where the punching shear strength of concrete slab without transverse reinforcement (VRd, c) takes into consideration the rotation angle of the slab support zone ψ and it is determined according to formula (2):

$$V_{Rd,c} = k_{\psi} \cdot \frac{\sqrt{f_c}}{\gamma_c} \cdot b_0 \cdot d \qquad (2)$$

Where γ_c is the partial factor for concrete in compression; b_0 is a perimeter of the design cross-sectional contour with rounded corners at a distance of 0.5d from the loading area; d is effective depth of the reduced section; f_c is the compressive strength of concrete; k_ψ is coefficient taking into account the angle of rotation of the slab ψ, which is determined by the formula (3).

$$k_{\psi} = \frac{1}{1.5 + 0.9 \cdot k_{dg} \cdot \psi \cdot d} \qquad (3)$$

Where k_{dg} is the coefficient taking into consideration the grain size of coarse aggregate; ψ is the angle of rotation of the slab. When calculating according to MC2010, the influence of the size effect on the punching shear strength of the slab is considered for the angle of rotation of the slab ψ according to the formula (4):

$$\psi = 1.5 \cdot \frac{r_s}{d} \cdot \frac{f_y}{E_s} \cdot \left(\frac{m_s}{m_R}\right)^{1.5} \qquad (4)$$

Where r_s is the distance to the point where the radial bending moment equals to zero (for experimental specimens, the distance from the center of the specimen to the point of attachment); E_s is the modulus of elasticity of the reinforcement; f_y is the yield strength of the reinforcement; m_s is the bending moment in the slab average through the width b_s caused by the applied load. Here $b_s = 1.5 \cdot r_s$; m_R is an ultimate bending moment.

The concepts presented for considering the size effect make it possible to establish the actual mechanisms of destruction of slabs of various thicknesses under punching and to perform a comparative analysis of such mechanisms. In this paper, we investigate the features of the failure for thin and thick slabs, including the formation and development of cracks, as well as schemes for the slab destruction. The table 1 presents data of such physical experiments. In numerical studies, we considered a model of a thin slab from [9] and thick slab model from [7].

Numerical studies were carried out using the ATENA software [14]. The applicability of this software for the analysis of reinforced concrete slabs under punching was substantiated in the work [4].

The main provisions of the ATENA PC methodology are as follows

Modeling of structures in ATENA software is generally performed taking into account the specific features of materials. Concrete is modeled by volumetric FE, reinforcement elements are modeled, as a rule, by bar elements. However, in some cases, it is quite acceptable to simulate reinforcement by specifying the percentage of reinforcement in the volume of concrete. The bond between concrete and reinforcing bars is modeled by introducing special connector that work according to the law specified by the user. In the studies presented in this work, the model of longitudinal reinforcement is made of discrete bars. The joint work of concrete and reinforcing bars was modeled under the assumption of ideal adhesion according to the verification work [15]. ATENA software includes dedicated models for finite element analysis of concrete and reinforced concrete structures. According to the official reference manual [14], the concrete model combines the equations of the theory of plasticity (in compression) and fracture mechanics (in tension). For concrete, the model uses the criterion of maximum principal stresses to assess the strength, an exponential law of softening. At the same time, the crack can be specified as rotating or stationary. The tensile behavior of concrete is modeled by nonlinear fracture mechanics combined with a smeared crack model. The main parameters of this approach are tensile strength of concrete, the nature and form of cracking, and the energy of destruction. The phenomenon of cracking is described by a model of smeared cracks in the form of a belt model [16]. Fig. 2 shows the crack formation law for the ATENA PC is shown in general.

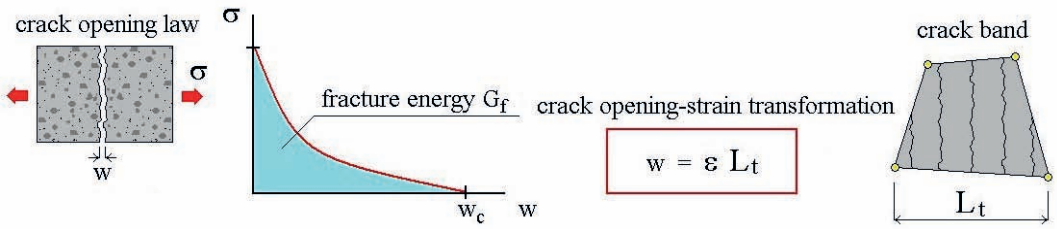

Figure 2. The cracking model adopted in the ATENA software according to [14]

The cracking process can be divided into three stages as shown in fig. 3. The stage without cracks corresponds to the work of the material until it reaches the ultimate tensile strength. Crack formation occurs in the potential crack zone with a decrease in tensile stresses in this area. Then crack opening continues at zero tensile stresses at the crack tip.

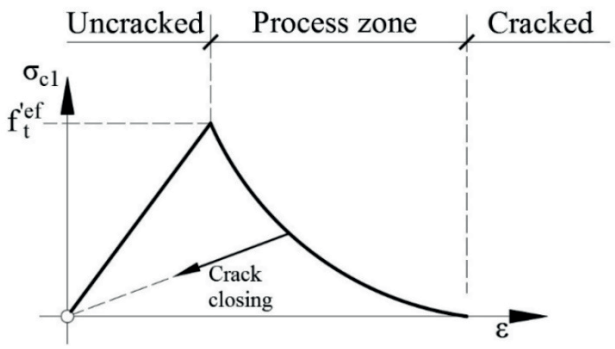

Figure 3. Stages of formation and development of cracks in the ATENA PC according to [14]

For the plastic model concrete in compression, the Menetrey-Willam strength criterion is used. An algorithm has been developed that combines the fracturing model and the plasticity model. An important feature of the ATENA software is that the two above models are formulated independently of each other, but they are used together in the calculation. Another significant characteristic of the concrete model is the use of the so-called limiters of localization of deformations during destruction. This principle is used to designate discrete fracture planes independent of the finite element mesh. In the case of tension, these planes are represented by cracks. In the case of compression, it is shown by areas of crushing. In the computational model, these discrete fracture regions have dimensions that do not depend on the dimensions of the element. For this reason, the planes of destruction are presented in the model as planes that do not depend on the dimensions of the FE mesh. For the case of tensile failure, this approach is known as the fracture belt model. ATENA software uses a similar approach for compression failure detection. Thus, limits of strain localization allow us eliminating two significant drawbacks of the traditional FE model of concrete: the effect of the size and orientation of the FE mesh on the result. Appliance of the smeared cracks' model makes it possible calculates and plots the propagation of discrete cracks quite accurately. Moreover, according to the developers of the software [17], this model does not inferior to models that implement discrete cracks in accuracy.

3. RESEARCH RESULTS

For the purpose of a comparative analysis, the research results are grouped for each of the considered parameters. The design model represents 1/4 of the support zone of the reinforced concrete slab (Fig. 4). The longitudinal reinforcement of the tensioned and compressed zone of the slab was modeled with bar finite elements. The load on the slab was transmitted through the column at the geometric center of the slab. The model of external restrains corresponds to the specimen support on a steel rectangular distribution frame along the contour. The slab, column, and support structure were modeled with 3D finite elements. The dimensions of the volumetric finite elements for the design model of the slab are determined in accordance with the requirements of the ATENA software [14].

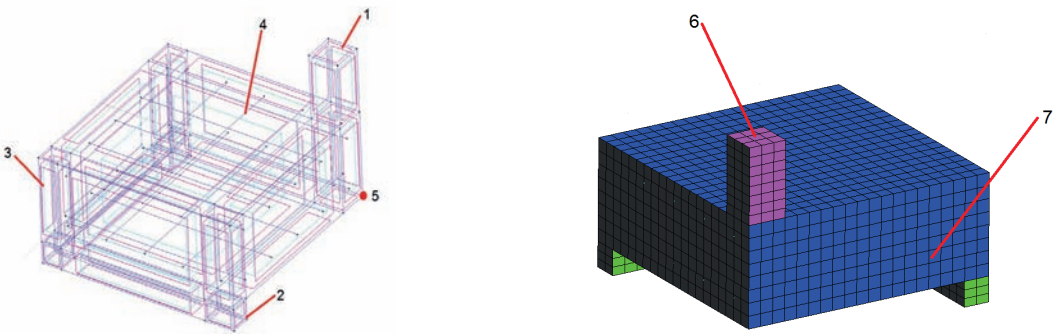

Figure 4. 3D (left) and FE (right) model for numerical studies using ATENA software. 1 - Column; 2 - Supporting structure; 3 - Floor slab; 4 - Reinforcement bars; 5 - Point for monitoring of displacement along the vertical axis; 6 - Place of load application; 7 - Restraints of the specimen along the axis of symmetry

Based on the results of the finite element analysis, it was established that the destructive loads obtained in numerical experiments have an acceptable correlation with the results of physical experiments. Deviations of P_{max} from V_{ex} are: for the design model of the P-6 sample according to [7] 10.45%, for the design model of the Ch120 sample according to [9] 2.28%. The results of numerical studies are presented in Fig. 5, 7 - 9.

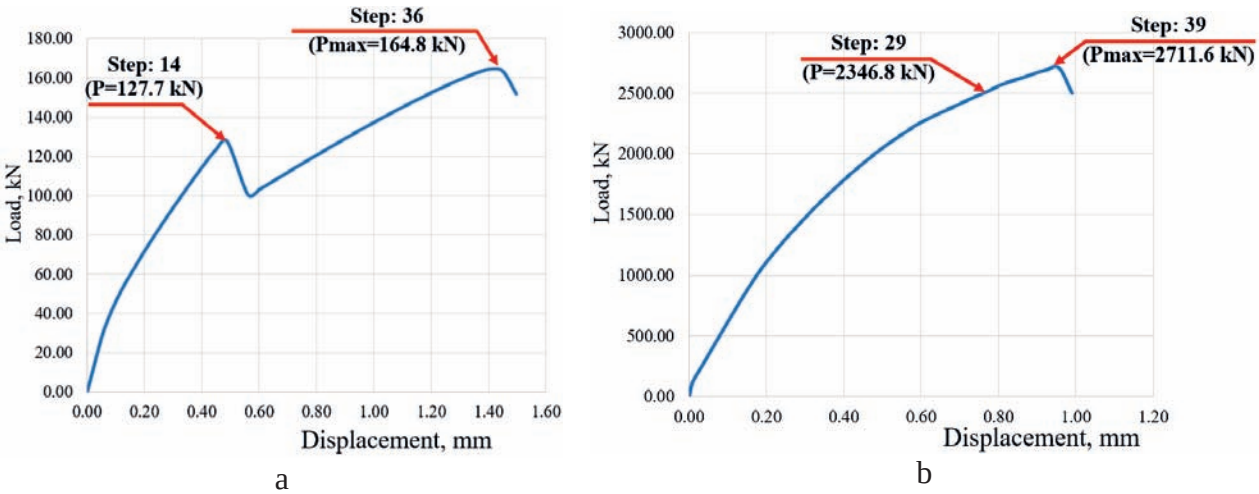

a b

Figure 5. Diagrams of deformation vs. values of ultimate loads (kN) for numerical models; a - model of the C_{h120} sample [9]; b - model of specimen P-6 [7]

Analysis of the deformation diagrams demonstrates significantly different punching mechanisms of slabs of various thicknesses. In a thin slab, a pronounced unloading section is formed (after the 14th step of the calculation). In a thick slab, the unloading phenomenon is not observed. It should be noted that the phenomena of unloading in thin slabs were also established in previous studies [4]. To study the case, refer to fig. 6. Thus, the formation of the unloading section during loading and deformation of thin slabs can be defined as one of the most important features of the operation of such slabs under punching.

Fig. 7 shows the state of the models at the moment of initial fracturing.

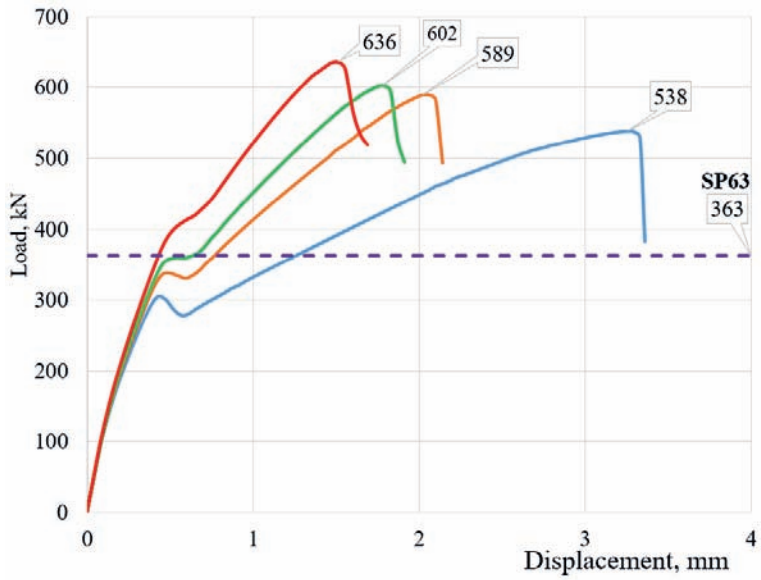

Figure 6. Diagram deformation vs. magnitude of ultimate loads (kN) of thin slabs (thickness of 200 mm) obtained numerically for specimens from the work [4]

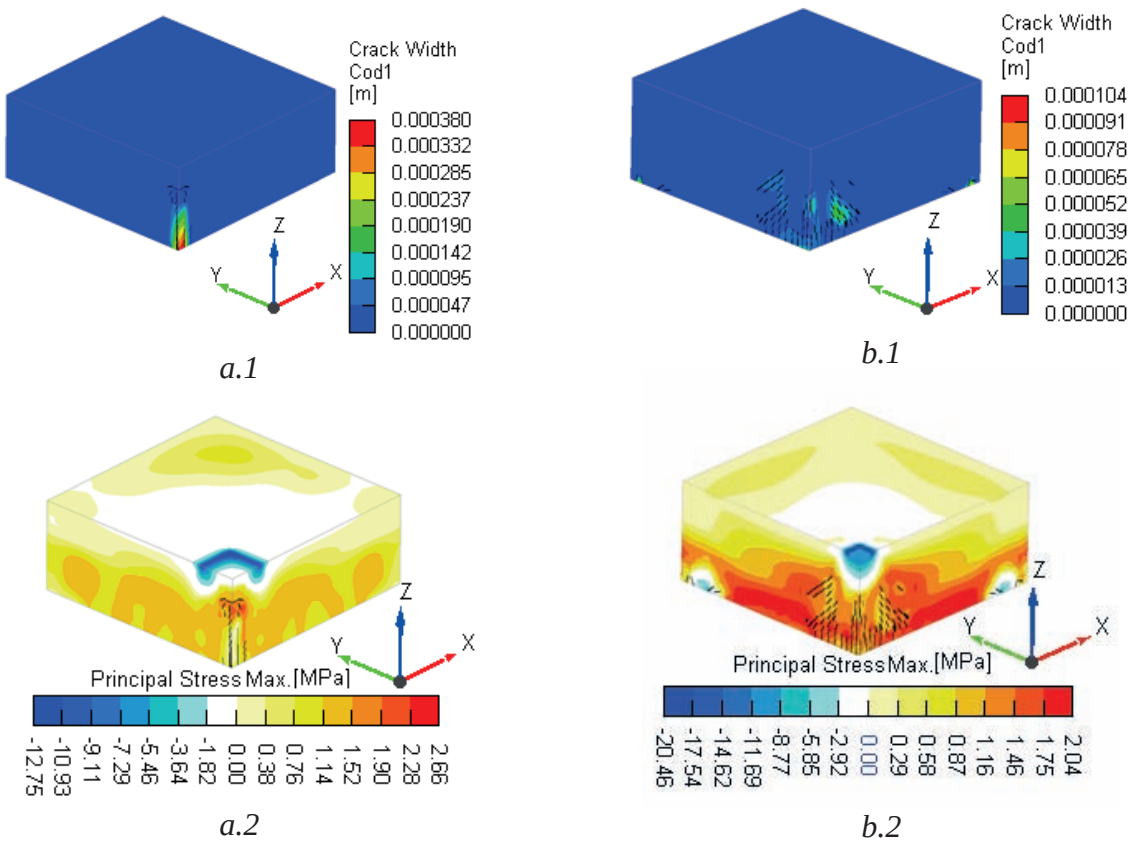

Figure 7. Crack formation diagram in models a.1 and b.1; isofield of principal stresses (max) a.2 and b.2 at the cracking moment; a - 14th stage of calculating the specimen Ch120 [9]; b - 29th stage of calculating specimen P-6 [7]

Analysis of the stress-strain state at the time of initial cracking demonstrates significantly different operating schemes for slabs of various thicknesses. In a thin slab, a crack is formed in the tensile zone of concrete [9], which corresponds to the pattern of cracking of a bent element. A similar picture of cracking in the tensile zone according to the bending element scheme was established for all specimens of thin slabs in studies [4] (Fig. 6), in which the parameters of longitudinal reinforcement were varied (from 0.48% to 1.93%). In accordance with the provisions of the mechanics of reinforced concrete flexure structures, cracking in the tensioned zone forms the unloading mechanism, which is confirmed by the diagram in Fig. 7a. In a thick slab, initial cracks are formed in the middle part of the section (thickness) of the slab [7]. Such a cracking scheme does not form a mechanism for unloading the sample as a whole, and diagram of the deformation does not have an inflection point. An important feature characterizing the process of formation and development of cracks is the diagram of the directions of the main tensile stresses in the studied slab samples (Fig. 8).

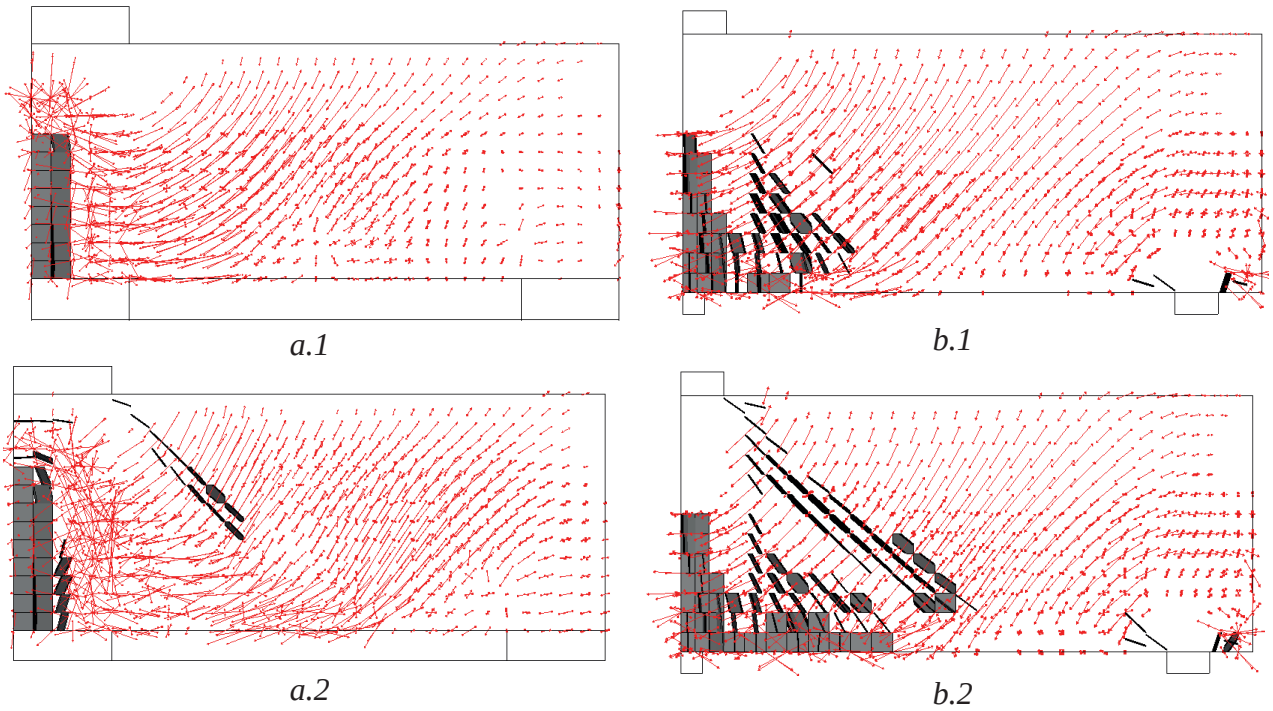

Figure 8. Diagram of the directions of the principle tensile stresses at the moment of cracking (a) and at the moment of failure (b); a.1 - 14th stage of calculating the specimen Ch120 [9], a.2 - 36th stage of calculating the specimen Ch120 [9]; b.1 - 29th stage of calculating specimen P-6 [7], b.2 - 39 stage of calculating specimen P-6 [7].

Analysis of the diagram of the directions of the principle tensile stresses provides the summary of the reasons for the formation and development of cracks up to the destruction of the specimen under an increasing load. In accordance with the laws of mechanics, Figures 8.a.1 and 8.b.1 show that cracks in concrete are formed in the zones of maximum tensile stresses, and the crack axis is perpendicular to the directions of the main tensile stresses. At the stage of calculation, corresponding to the failure (Fig. 8.a.2 and 8.b.2), the directions of the principle tensile stresses in the fracture zone are distributed chaotically.

The analysis of the isofields of the principal stresses (max) at the moment of initial cracking

also demonstrates fundamentally different schemes for the operation of thin and thick slabs. In a thin slab, the tensile stresses in the lower concrete zone are significantly less than those in a thick slab [9]. Such a scheme is formed as a result of stress relaxation in a thin slab during the formation of a crack in the stretched zone with the subsequent inclusion of the stretched reinforcement into operation. In a thick slab, the concrete of the lower zone is in tension with parameters close to the limiting ones [7], but it does not exceed them. The diagram of the distribution of the principal stresses in the thin and thick slabs corresponds to the diagram of the deformation of the specimen under investigation. It seems important to analyze such characteristic of stress-strain state as the value of the loss of concrete strength according to the tensile criterion at the beginning of cracking (Fig. 9).

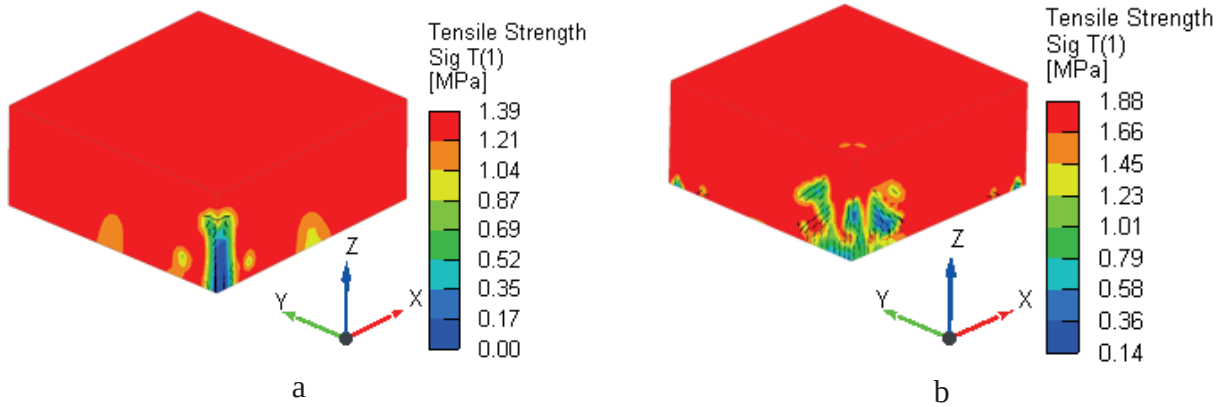

Figure 9. Isofields of concrete strength loss according to the tensile criterion in models a - stage 14 of the model calculation [9]; b - 29 stage of calculation model [7]

The analysis of the isofields of the loss of concrete strength by the tensile criterion demonstrates various schemes of slab operation. In the center of a thin slab specimen, localization of finite elements in a narrow zone with an almost complete loss of tensile strength is observed [9], which corresponds to the formation of a normal crack according to the flexure element scheme. In a thick slab, areas of concrete with a loss of tensile strength are localized in the zones of formation of cracks in the thickness of the slab [7]. This allows us to conclude that in a thick slab, the cause of the formation of inclined cracks at the initial stage is tensile stresses, the maximum values of which in accordance with the basic principles of mechanics are localized in the central zones of the thickness of solid structures under the accepted loading schemes. Fig. 10 shows destruction of the models.

The analysis of the stress-strain state at the destruction of the specimens demonstrates significantly different schemes of slab operation. In a thin slab, destruction occurs according to the normal crack propagation pattern [9], which is typical for bending elements. In this case, in addition to a normal crack, a system of inclined cracks with corresponding stress relaxation zones is formed (Fig. 10 a.2). The scheme of destruction of a thin slab is most clearly shown in Fig. 10 a.3 as isofields of the loss of tensile strength of concrete.

In a thick slab, destruction occurs due to the formation of a system of inclined cracks, forming a punching prism, with single normal cracks in the lower zone. Such normal cracks have a slight development along the depth of the slab. The general scheme of the destruction of a thick slab corresponds to the formation of a punching shear prism, which is clearly seen in the diagram of

isofields for the loss of tensile strength of concrete (Fig. 10 b.3).

Analysis of stresses in the reinforcement of the tensile zone of concrete, thin [9] and thick [7] slabs demonstrate significantly different levels of stresses and, consequently, the growth of the crack opening width in tensioned concrete. In a thin slab, the tensile stresses in the reinforcement are 1.6 - 3.7 times higher than the similar parameter of the reinforcement of a thick slab at various stages. Even without taking into account the more complex factors of the influence of the thickness of the slab on the magnitude of stresses in the reinforcement of the tensile zone of concrete, it can be seen that there are large deviation in the factors of the influence of longitudinal reinforcement on the formation of cracks and the processes of destruction of thin and thick slabs.

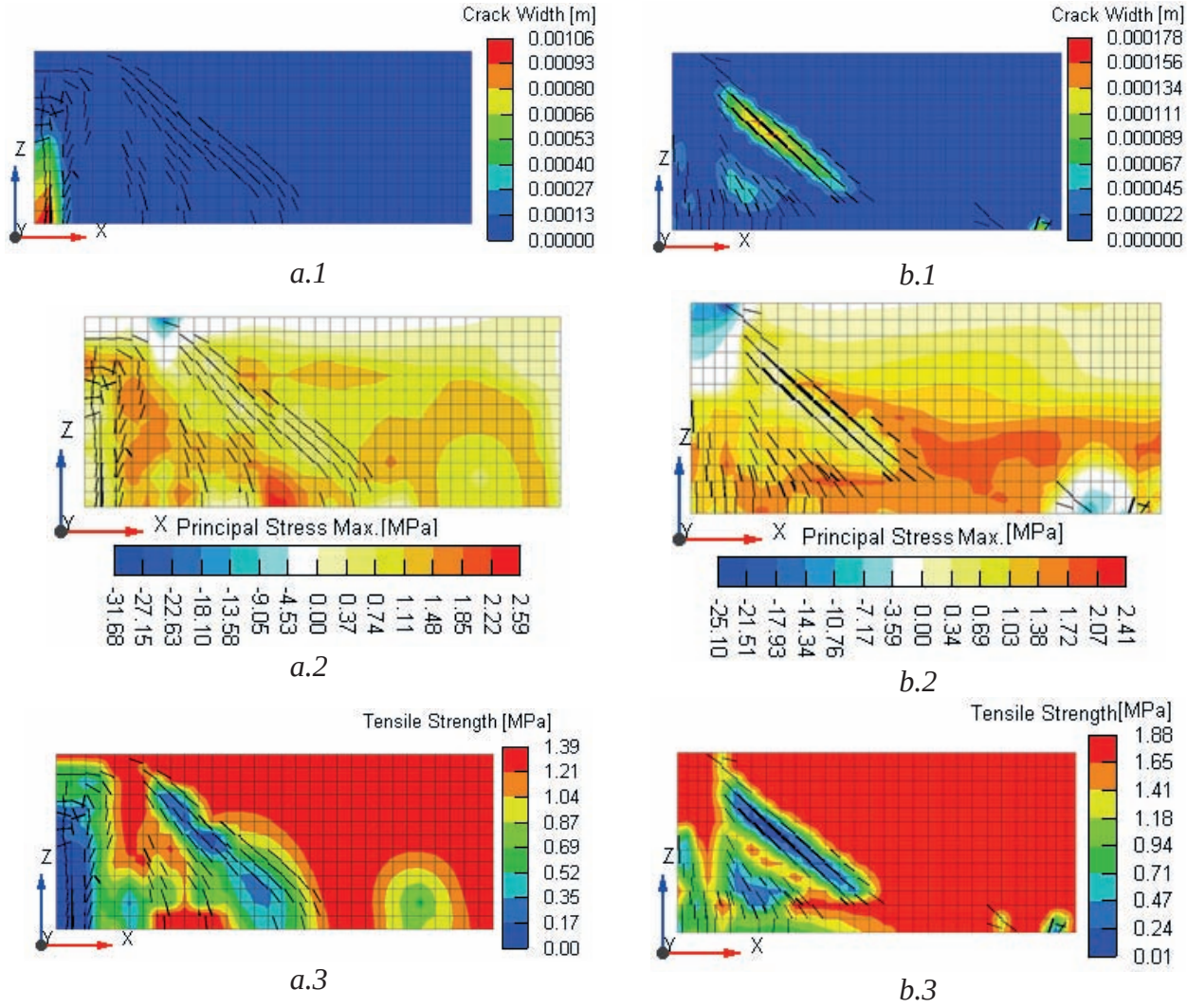

Figure 10. Crack formation diagram a.1 and b.1; isofields of principal stresses (max) a.2 and b.2; isofields of loss of tensile strength of concrete a.3 and b.3 b at the moment of destruction;
a - 36th stage of the model calculation [9]; b - 39th stage of calculation model [7]

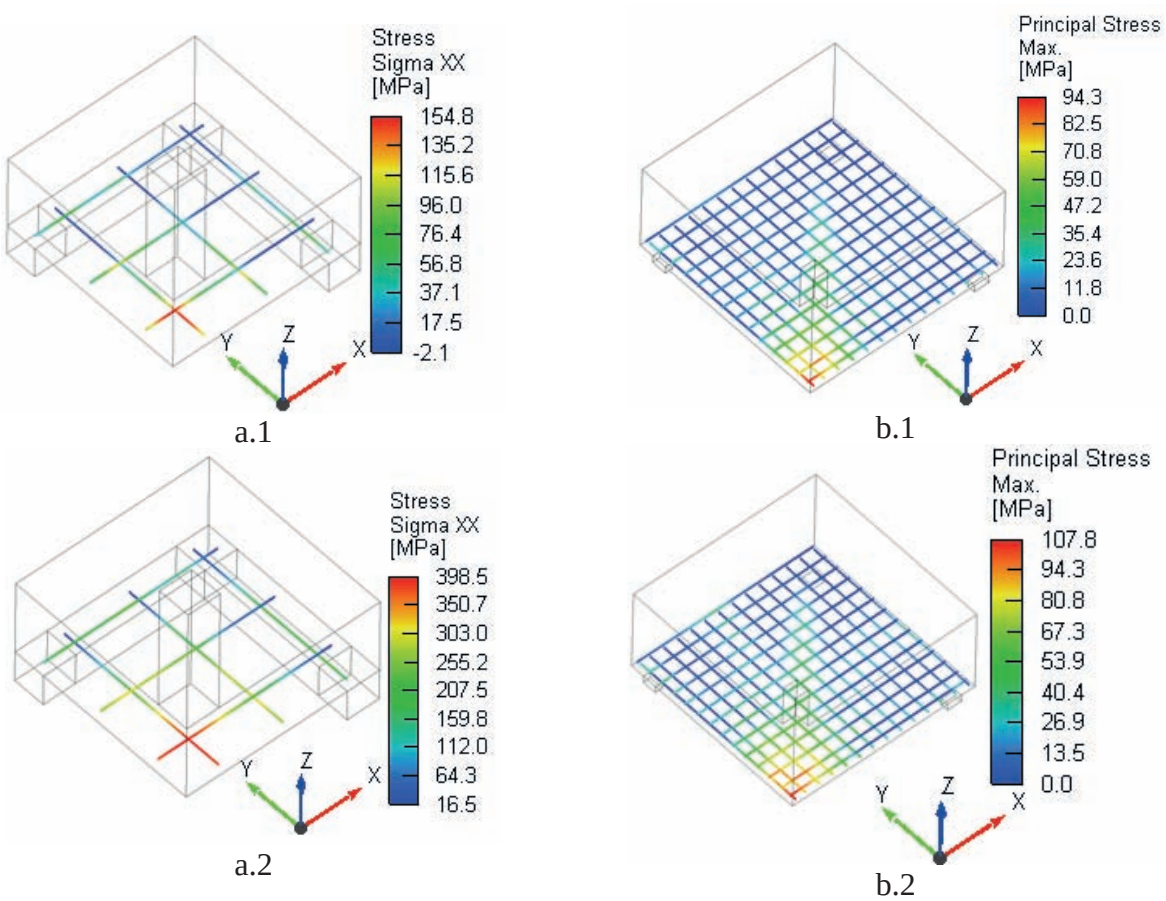

Figure 11. Stresses in reinforcement in tension at the moment of cracking (a) and at the moment of failure (b); a.1 - 14th stage of calculating the specimen Ch120 [9], a.2 - 36th stage of calculating the specimen C_{h120} [9]; b.1 - 29th stage of calculating specimen P-6 [7], b.2 - 39th stage of calculating specimen P-6 [7]

4. CONCLUSION

As a result of numerical studies, it was found that the failure of thin and thick slabs under punching have significant differences.

Thin slabs are destroyed, as a rule, by the mechanism of the formation of an initial normal crack under load. And this leads to the formation of an unloading phenomenon in the deformation pattern of the "column - slab" structural joint. The formation of a normal crack together with the inclusion of longitudinal reinforcement in the work leads to relaxation of stresses in concrete. By the time of failure, concrete in the zone of a normal crack and concrete in the zone of a system of inclined cracks is destroyed according to the tensile strength criterion. Thus, in thin slabs, longitudinal reinforcement plays an important role in the general fracture mechanism according to the punching shear criterion.

Thick slabs are destroyed by a mechanism with the formation of inclined cracks forming a punching prism. At the initial stage, inclined cracks are formed in the middle zone of the slab thickness, where the extrema of the principal tensile stresses exceeding the ultimate tensile strength of concrete are localized. With an increase in the load, the number of inclined cracks increases with the formation of a system of such cracks, the length of which grows from the central zone of the slab to the upper and lower planes. By the moment of destruction, concrete in the zone of the system of inclined cracks is destroyed according to the tensile strength criterion. Thus, in thick slabs, the fracture mechanism corresponds to the formation of a system of inclined

cracks, which are formed due to an increase in the principal tensile stresses with an excess of the tensile strength of concrete. The contribution of the longitudinal reinforcement of the stretched zone to the punching failure resistance of thick slabs is not as significant as for thin slabs.

ACKNOWLEDGMENT

This work was financially supported by the Ministry of Science and Higher Education OF Russian Federation (grant # 075-15-2021-686). All tests were carried out using research equipment of The Head Regional Shared Research Facilities of the Moscow State University of Civil Engineering

REFERENCES

1. EN 1992-1-1: 2004 Eurocode 2: Design of concrete structures - Part 1-1: General rules and rules for buildings, CEN, 2004.
2. Fib Model Code for Concrete Structures 2010, Ernst & Sohn, 2011.
3. Building Code of Russian Federation SP 63.13330.2018 "Concrete and reinforced concrete structures. Basic provisions", Standartinform, 2019.
4. **Kabantsev O.V., Krylov S.B., Trofimov S.V.** "Numerical Analysis of Longitudinal Reinforcement Effect on Rc Slab Punching Shear Resistance by Strength and Crack Propagation Criteria," International Journal for Computational Civil and Structural Engineering, vol. 17, pp. 21-33, 2021.
5. **Guandalini S., Burdet O., Muttoni A.** "Punching tests of slabs with low reinforcement ratios," ACI Struct Journal, vol. 106, pp. 87-95, 2009.
6. **Lips S., Fernández Ruiz M., Muttoni A.** "Experimental Investigation on Punching Strength and Deformation Capacity of Shear-Reinforced Slabs," ACI Structural Journal, vol. 109, pp. 889-900, 2012.
7. **Korovin N.N., Golubev A.Yu.** "Pushing thick reinforced concrete slabs," Concrete and reinforced concrete, vol. 11, pp. 20-23, 1989.
8. **Li K. K. L.** "Influence of Size on Punching Shear Strength of Concrete Slabs," McGill University, 2000, pp. 1-65.
9. **Trekin N.N., Sarkisov D.Yu., Trofimov S.V., Krylov V.V., Evstafieva E.B.** "Experimental and theoretical study of the punching shear strength of slabs," Vestnik MGSU, vol. 16, pp. 1006-1014, 2021.
10. **Bažant Z.P.** "Fracture Mechanics of Concrete Structures," Elsevier Applied Science, pp. 1-140, 1992.
11. **Muttoni A., Fernández Ruiz M., Simões J.T.** "The theoretical principles of the critical shear crack theory for punching shear failures and derivation of consistent closed form design expressions," Structural concrete, pp. 1-17, 2017.
12. **Dönmez A., Bažant Z.P.** "Size Effect on Punching Strength of Reinforced Concrete Slabs with and without Shear Reinforcement," ACI Structural Journal, vol. 114, pp. 875-886, 2017.
13. **Fernández Ruiz M., Muttoni A.** "Size effect in shear and punching shear failures of concrete members without transverse reinforcement: Differences between statically determinate members and redundant structures," Structural concrete, pp. 1-11, 2017.
14. **Cervenka V., Jendele L., Cervenka J.,** "ATENA Program Documentation. Part 1. Theory," Cervenka Consulting, pp. 1-344, 2020.
15. **Rimkus A., Cervenka V., Gribniak V., Cervenka J.** "Uncertainty of the smeared crack model applied to RC beams," Engineering Fracture Mechanics, pp. 1-15, 2020.
16. **Bažant Z.P.** "Crack band theory for fracture of concrete," Materials and Structures, vol. 16, pp. 155-177, 1983.
17. **Cervenka J., Cervenka V.** "the uniqueness of numerical solutions of shear failure of deep concrete beams: comparison of smeared and discrete crack approaches," Computational Modeling of Concrete structures, pp. 281-290, 2010

СПИСОК ЛИТЕРАТУРЫ

1. EN 1992-1-1:2004 Eurocode 2: Design of concrete structures - Part 1-1: General rules and rules for buildings, CEN, 2004.
2. fib Model Code for Concrete Structures 2010, Ernst&Sohn, 2011.
3. СП 63.13330.2018 "Бетонные и железобетонные конструкции. Основные положения", Стандартинформ, 2019.
4. **Kabantsev O.V., Krylov S.B., Trofimov S.V.** "Numerical Analysis of Longitudinal Reinforcement Effect on Rc Slab Punching Shear Resistance by Strength and Crack Propagation Criteria," International Journal for Computational Civil and Structural Engineering, vol. 17, pp. 21-33, 2021.
5. **Guandalini S., Burdet O., Muttoni A.** "Punching tests of slabs with low reinforcement ratios," ACI Struct Journal, vol. 106, pp. 87-95, 2009.
6. **Lips S., Fernández Ruiz M., Muttoni A.** "Experimental Investigation on Punching Strength and Deformation Capacity of Shear-Reinforced Slabs," ACI Structural Journal, vol. 109, pp. 889-900, 2012.
7. **Коровин Н.Н., Голубев А.Ю.** "Продавливание толстых железобетонных плит," Бетон и железобетон, vol. 11, pp. 20-23, 1989.
8. **Li K. K. L.** "Influence of Size on Punching Shear Strength of Concrete Slabs," McGill University, 2000, pp. 1-65.
9. **Трекин Н.Н., Саркисов Д.Ю., Трофимов С.В., Крылов В.В., Евстафьева Е.Б.** "Экспериментально-теоретическое исследование прочности плит на продавливание," Вестник МГСУ, vol. 16, pp. 1006-1014, 2021.
10. **Bažant Z.P.** "Fracture Mechanics of Concrete Structures," Elsevier Applied Science, pp. 1-140, 1992.
11. **Muttoni A., Fernández Ruiz M., Simões J.T.** "The theoretical principles of the critical shear crack theory for punching shear failures and derivation of consistent closed form design expressions," Structural concrete, pp. 1-17, 2017.
12. **Dönmez A., Bažant Z.P.** "Size Effect on Punching Strength of Reinforced Concrete Slabs with and without Shear Reinforcement," ACI Structural Journal, vol. 114, pp. 875-886, 2017.
13. **Fernández Ruiz M., Muttoni A.** "Size effect in shear and punching shear failures of concrete members without transverse reinforcement: Differences between statically determinate members and redundant structures," Structural concrete, pp. 1-11, 2017.
14. **Cervenka V., Jendele L., Cervenka J.** "ATENA Program Documentation. Part 1. Theory," Cervenka Consulting, pp. 1-344, 2020.
15. **Rimkus A., Cervenka V., Gribniak V., Cervenka J.** "Uncertainty of the smeared crack model applied to RC beams," Engineering Fracture Mechanics, pp. 1-15, 2020.
16. **Bažant Z.P.** "Crack band theory for fracture of concrete," Materials and Structures, vol. 16, pp. 155-177, 1983.
17. **Cervenka J., Cervenka V.** "the uniqueness of numerical solutions of shear failure of deep concrete beams: comparison of smeared and discrete crack approaches," Computational Modeling of Concrete structures, pp. 281-290, 2010

Oleg V. Kabantsev, Dr.Sc.; Professor of the Department of Reinforced Concrete and Stone Structures National Research Moscow State University of Civil Engineering; 26, Yaroslavskoe Shosse, Moscow, 129337, Russia; phone: + 7(916)695-77-30; E mail: ovk531@gmail.com.

Кабанцев Олег Васильевич, доктор технических наук; профессор кафедры железобетонных и каменных конструкций Национального исследовательского Московского государственного строительного университета; 129337, Россия, г. Москва, Ярославское шоссе, дом 26; телефон: + 7(916)695-77-30; Email: ovk531@gmail.com.

Sergey B. Krylov, corresponding member of the Russian Academy of Architecture and Construction Sciences, Dr.Sc.; Head of the Laboratory of Reinforced Concrete Mechanics of Research Institute of Concrete and Reinforced Concrete (NIIZHB) named after A.A. Gvozdev, JSC Research Center of Construction; 6, 2nd Institutskaya, Moscow,109428, Russia; phone: +7(499) 174-74-07; Email: niizhb_lab8@mail.ru.

Sergey V. Trofimov, graduate student of National Re-search Moscow State University of Civil Engineering; engineer of Reinforced Concrete Mechanics of Research Institute of Concrete and Reinforced Concrete (NIIZHB) named after A.A. Gvozdev, JSC Research Center of Construction; 26, Yaroslavskoe Shosse, Moscow, 129337, Russia; Email: serkeypro@yandex.ru.

Крылов Сергей Борисович, член-корреспондент РААСН, доктор технических наук; заведующий лаборатории №8 «Механики железобетона» НИИЖБ им. А.А. Гвоздева АО «НИЦ «Строительство»; 109428, Россия, г. Москва, 2-я Институтская улица, дом 6, корпус 5; телефон:+7(499) 174-74-07; Email: niizhb_lab8@mail.ru.

Трофимов Сергей Владиславович, аспирант Национального исследовательского Московского государственного строительного университета; инженер лаборатории №8 «Механики железобетона» НИИЖБ им. А.А. Гвоздева АО «НИЦ «Строительство»; 129337, Россия, г. Москва, Ярославское шоссе, дом 26; Email: serkeypro@yandex.ru.

DOI:10.22337/2587-9618-2021-17-4-106-114

ESTIMATION OF THE DEFECT HAZARD CLASS IN BUILDING STRUCTURES: A DECISION SUPPORT SYSTEM

Vladislav A. Kats, Lyubov A. Adamtsevich
National Research Moscow State University of Civil Engineering, Moscow, RUSSIA

Abstract. Technical condition monitoring of building structures located on hazardous facilities is a necessary requirement for their sustainable functioning. In this regard, the problem of development intellectual monitoring systems that allow to detect and classify operating defects by the hazardous level becomes very urgent. The study presents an approach of building decision support system (DSS) for detecting defects in building structures and estimation of their hazard class. Proposed approach is based on multi-criteria assessment of consecutive measurements acquired by acoustic emission method. A distinctive characteristic of the proposed approach is the ability to take into account the evolution of defects by mapping each AE time-series to diagnostic features matrix and analysing these matrices in sliding windows with overlay. Each matrix is validated by two criteria that form the necessary and sufficient conditions of the existence the evolving defects in building structure. They include the criterion for changing the number of clusters and the criterion for changing the acoustic emission activity. Proposed method was verified on the experimental data acquired from the technical condition monitoring of the vertical oil tanks. The results obtained from the experiment confirm the proposal that this approach can be utilized for effectively solving the problem of conditional monitoring of building structures located on the hazardous facilities allowing to detect and classify defects by their hazardous level.

Keywords: decision support system, acoustic emission, feature extraction, clustering, defect hazard class estimation, image processing, distance transform.

СИСТЕМА ПОДДЕРЖКИ ПРИНЯТИЯ РЕШЕНИЙ ДЛЯ ОЦЕНКИ КЛАССА ОПАСНОСТИ ДЕФЕКТОВ СТРОИТЕЛЬНЫХ КОНСТРУКЦИЙ

В.А. Кац, Л.А. Адамцевич
Национальный исследовательский Московский государственный строительный университет, Москва, РОССИЯ

Аннотация. Осуществление мониторинга технического состояний строительных конструкций, расположенных на опасных производственных объектах, является необходимым требованием для их устойчивой и непрерывной работы. В этой связи актуальной проблемой становится разработка интеллектуальных систем мониторинга, способных осуществлять детектирование и классификацию эксплуатационных дефектов конструкций по классам опасности. В работе представлен метод построения системы поддержки принятия решений (СППР), позволяющий классифицировать дефекты по степени опасности, основанный на многокритериальной оценке последовательных измерений данных, полученных методом акустической эмиссии. Отличительной характеристикой предложенного метода является способность учитывать эволюцию дефектов посредством расчета матриц диагностических признаков от исходных временных рядов акустической эмиссии в скользящем временном окне с перекрытием. Каждая матрица диагностических признаков проверяется двумя критериями, которые формируют необходимые и достаточные условия существования эксплуатационных дефектов в строительных конструкциях, а именно, критерий изменения количества кластеров и критерий изменения активности акустической эмиссии. Валидация указанного подхода произведена на экспериментальных данных, полученных в результате мониторинга технического состояния вертикальных нефтяных резервуаров. Результаты, полученные в ходе эксперимента, подтверждают предположение о том, что предложенный метод может быть использован для эффективного решения проблемы мониторинга технического состояния строительных конструкций, расположенных на опасных объектах, позволяющих обнаруживать и классифицировать дефекты по их степени опасности.

Ключевые слова: система поддержки принятия решений, акустическая эмиссия, методы извлечения диагностических признаков, оценка класса опасности, обработка изображений.

INTRODUCTION

Continuous evaluation of the technical condition of building structures located on hazardous facilities is critically important for providing their smooth and trouble-free operation. One of the perspective method of conducting periodic conditional monitoring is an acoustic emission method (AE) [1]. It is a common knowledge that the acoustic emission signal emits in the material under the process of its deformation or destruction. Meanwhile, the AE signal parameters correlate with evolution dynamics of the defects that are developing during the operation of the facility [2]. In this regard, the problem of developing a decision support system (DSS) based on AE data, which allows identifying the appearance of operating defects in the structure of the construction material in real time and classifying defects by hazard classes, seems urgent. According to the regulatory document [3], the condition of the defect can be described by one of the four hazard classes:

1) The I class source corresponds to non-hazardous defect
2) The II class source is an evolving defect, moderately hazardous.
3) The III class source corresponds to critically hazardous evolving defect
4) The IV class source is catastrophically hazardous defect.

Common systems of AE data processing are primarily based on the analysis of integral parameters of AE flow such as mean or peak amplitude, the oscillation number, signal duration, MARSE (the area under the AE signal envelope higher than the amplitude discrimination threshold) and are suitable in the conditions of threshold data acquisition. Such approaches also include the wavelet-analysis of AE data [4]. These methods have weak noise immunity and which leads to their low efficiency under the signal-to-noise ratio (SNR) < 1.

Authors of paper [5] propose to estimate the hazard class of the defect by utilizing k-means algorithm. One of the main disadvantage of this method is the requirement of determining the number of clusters before the calculation. Furthermore, this approach based on the estimation of the data of current measurement and as a result, it does not consider the evolution of the defect.

The authors of the approach described in the article [6] propose to calculate periodic statistics on a set of integral time and frequency diagnostic parameters, such as amplitude, duration, energy, signal rise time, average frequency, peak power, etc. By the calculated statistics they determine and measure the distances between two classes, one of which is a reference (its characteristics obtained during pilot operation), and the other corresponds to monitoring data [6]. This approach is the most promising of presented, as it allows detecting defect in the controlled facility. Nevertheless, the main drawback of the method proposed in paper is that the comparison between the two classes by calculating distance metrics does not allow to determine the hazard class of the defect.

This study presents an innovative approach of building an effective decision support system that provides reliable detection of evolving defects. Within the framework of the approach, we describe a method that allows detecting the moments of transition of operational defects arising in the construction facility to the stage of a hazardous developing defect and a critically hazardous developing defect.

It is further noted that proposed method is an integral part of a comprehensive methodology for developing a decision support system for detecting operational defects in construction structures and assessing their hazard class. Other aspects of the implementation of the methodology related to algorithms for preprocessing measurement data, methods for extracting diagnostic features and reducing the dimension of the feature space, as well as training DSS, are described in [7, 8].

1. METHODS

The proposed method of the defect's hazard class determination is based on a multi-criteria

assessment of diagnostic features extracted from acoustic emission time series, which are acquired during the non-destructive testing. This assessment is a combination of necessary and sufficient conditions, the simultaneous satisfaction of which allows to detect a defect in the structure and to determine its hazard class. A distinctive characteristic of the proposed method is the ability to take into account the evolution of defects over time by analyzing their diagnostic features, which are calculated in the sliding time-domain windows [8]. Meanwhile, the analysis of multiple consecutive measurements data collected within different intervals of time provides trends identification in diagnostic feature values changes.

In order to improve the accuracy of detecting developing defects in conditions of random non-stationary noise, we also propose an original algorithm based on processing a series of measurements by means of a multi-criteria assessment of the defect hazard class.

Figures/Tables should be centred within the page width and numbered sequentially. Figures/Tables should be numbered separately. Multiple figures should be referred using letters (e.g. Fig. 1a or 1b).

A set of k consecutive measurements of a given length forms a series of measurements. The measurements are grouped in series by applying a sliding window with overlap. Accordingly, the series is formed from k - 1 measurements related to the previous series, and one new measurement. Each series consists of a set of diagnostic feature matrices, which represent statistical parameters of acoustic emission time series obtained during preprocessing [9] and the feature extraction procedure [7]. This approach allows to ensure resistance to possible prolonged non-stationary interference and thereby protecting against false alarms of the DSS.

The proposed method for identifying the evolution of the hazard class of a defect in the object of control is based on two criteria:

1) Necessary - a criterion of clusters number changing that corresponds to defects with different hazard classes.

2) Sufficient - a criterion for the activity of acoustic emission, determined by the results of detecting anomalies in the diagnostic feature space.

Let ξ_i – diagnostic feature matrix of i-th measurement, while k – the number of measurements forming a series. Then $S_j = \{\xi_{i-k} \dots \xi_i\}$ is a diagnostic feature series per time interval $(i-k;i)$. Consider two cases.

1) The defect is initially absent or is not in evolving condition (I-class).

Then the necessary condition of existence of the hazardous evolving defect in the inspecting structure is:

$$\forall\, \xi_i \in S_j\ (Nclust(\xi_i) > 1) \wedge (Nclust(\xi_i) > Nclust(\xi_{i-k}) \dots Nclust(\xi_{i-1})) \quad (1)$$

where $Nclust(\xi_i)$ – the number of clusters calculated from diagnostic feature matrix ξ_i of i-th measurement. This condition should fulfil for any matrices of diagnostic features, collected during measurements $i-k \dots i$. The method of cluster number estimation will be considered further in this paper.

We formulate the sufficient condition as follows:

$$\forall\, \xi_i \in S_j\ A_{min} < A(\xi_i) < A_{max} \quad (2)$$

where $A(\xi_i)$ – activity coefficient of measurement i, A_{min} – the threshold value of activity coefficient for moderately hazardous defect, A_{max} – the threshold of the activity coefficient for the critically hazardous defect.

2) The defect initially exists and corresponds to moderately hazardous evolving defect (II-class).

Then the necessary condition of the defect transition to a critically hazardous class is:

$$\forall\, \xi_i \in S_j\ (Nclust(\xi_i) > 2) \wedge (Nclust(\xi_i) > Nclust(\xi_{i-k}) \dots Nclust(\xi_{i-1})) \quad (3)$$

while the sufficient condition is formulated as follows:

$$\forall\ \xi_i\ \in S_j\ \ A(\xi_i) > A_{max} \qquad (4)$$

Now we consider the methods of criteria values calculation $Nclust(\xi_i)$, $A(\xi_i)$ and in detail.

1.1. The method calculation the cluster number $Nclust(\xi_i)$.

Determining the hazard class of a defect requires studying the data on the evolution of AE diagnostic features. AE events obtained from a defect of the same hazard class form a cluster. Meanwhile, the number of clusters increases when the defect hazard class changes [7]. Based on this statement, in formulas (1), (3), we formualte a criterion of changing the number of clusters by comparing the number of clusters in diagnostic feature matrices of a sequential set of measurements (series). There are several ways to determine the number of clusters $Nclust(\xi_i)$. Most of them are related to the calculation of metrics based on intracluster and intercluster distances in the space of diagnostic features, in particular the criterion of Calinski-Harabasz, Davies-Bouldin and Silhouette [10]. However, these criteria often lead to erroneous results, especially for convex clusters. Recently, there has been a growing interest in approaches based on visual assessment of clusters [11]. By translating the unmarked data into an image of n x n size, where the objects are ordered in such a way as to simplify the identification of a potential cluster structure in the data. Meanwhile, each pixel in the image corresponds to the degree of difference between pairs of objects [11]. This image highlights potential clusters as "dark blocks" along the diagonal axis of the image, corresponding to sets of objects with a low degree of difference.

As part of this paper, we propose a modified algorithm for determining the number of clusters based on the clustering visual representation algorithm (VAT) [11]. The VAT algorithm maps the difference matrix D as a grayscale image, each element of which corresponds to the value of the difference metric d_{ij} between objects o_i and. At the same time, if the object o_i belongs to a certain cluster, then it is a part of a submatrix with small values of the difference metric, i.e. it belongs to one of the "dark blocks" on the diagonal of the corresponding image. We propose to determine the number of "dark blocks" as follows:

1) Segmentation of the matrix image D

Due to the fact that information about the cluster data structure is displayed in the dark blocks of the difference matrix image, an important step of the algorithm is threshold image processing. The histogram of the matrix D has multiple modes, meanwhile the first mode corresponds to the average value of intracluster distances.

In order to identify the binarization threshold we utilize a combination of Otsu algorithms. The Otsu algorithm maximizes the intercluster variance. It is based on the assumption that all pixels on the image belong to two classes. However, the image of the difference matrix D contains blurred boundaries of dark blocks. In such case the algorithm cannot correctly identify the threshold value. To identify and suppress noise objects in the image, we propose to use the multi-threshold Otsu method [12]. After noise objects are suppressed, the standard image binarization method is used, which converts the original image to a binary one, where the pixel value on the image is equal to 1, if it is greater than the threshold in grayscale, otherwise it is equal to 0.

2) Projecting the image onto the main diagonal

In order to obtain a more informative image that allows to clearly distinguish the structure of the "dark blocks", it is necessary to consider the pixel values along the main diagonal of the image. As part of this work, it is proposed to project an image onto the main diagonal by summing the pixel intensity values along the diagonal of the image. However, the original binary image may have residual noise. In order to minimize the effect of residual noise on the result of counting the number of clusters, it is necessary to convert the binary image obtained in the previous step into such a representation that the value of each pixel of the resulting image is the distance from this pixel to the nearest non-zero pixels in the binary image. This representation is called Distance Transform

[13]. The conversion of distances together with the projection on the main diagonal gives a more visual representation of the VAT image and allows to translate it into a one-dimensional signal. Thus, it is possible to define the number of clusters as the number of peaks on a one-dimensional signal.

3) Determination of the number of peaks on a one-dimensional diagonal projection signal

In this paper, we propose to utilize a first-order derivative to detect peaks in the signal. However, this approach should be used in combination with smoothing methods in order to reduce the likelihood of false positives. There are several ways to smooth the original signal. One of the most frequently used is the moving average [13]. Its main disadvantage is that averaging can lead to significant losses in the informative component of the original signal, which in turn will not allow to identify the appearance of a new cluster that corresponds to an evolving defect. In this paper, we propose to utilize a linear interpolation between the local maxima of the original signal. This method allows reaching required level of smoothing without losses in the informative component of original signal.

1.2. The method of calculation the activity coefficient $A(\xi_i)$

The acoustic emission activity coefficient [14] allows to determine the presence of long-term trends in acoustic emission data. Therefore, it can serve as a criterion for detecting defects. The activity coefficient is calculated based on the results of the anomaly detection method proposed in [8], which consists in determining the optimal position of the separating hyperplane between "normal" events and "anomalies". In the context of this work, abnormal events include AE signals emitted by defects of hazard classes II and III during monitoring. Normal events include hazard class I events, as well as various types of interference detected during pilot operation. In current paper, we propose to define the activity coefficient as the ratio of the number of abnormal events to the total number of AE events received per unit of time.

Comparison of the activity coefficient with the reference threshold values allows us to determine the moment of transition of the object to hazard classes II and III (2), (4). The threshold values for defects of class II and III are specific for each construction facility and require clarification at the stage of pilot operation.

2. RESULTS AND DISCUSSION

Fig. 1 demonstrates the fragments of experimental AE time series obtained during the non-destructive testing of oil reservoir located in Norilsk. We can see from the fig. 1 that the amplitude of AE signals increase with the growth of the hazard class. The data acquisition was conducted by the means of non-threshold AE collection method and the AE sensors with the sampling frequency of 2.5MHz. The preliminary processing was carried out by extracting diagnostic features utilizing method proposed in [7]. A set of calculated diagnostic feature matrices applied further for this research and was a source data for the verification of the methods proposed in current paper.

Fig. 2(a, b) contain the comparison of proposed criterion of cluster number determination with the known criterion Davies-Bouldin, based on intracluster distances calculation. Fig. 2b demonstrates computation graphs of optimal cluster number via Davies-Bouldin criterion utilizing three methods of cluster analysis: k-means, hierarchical clustering and Gaussian mixture distribution. The figure shows that the quality of the results of the proposed method does not depend on the type of clustering algorithm, it is based on image analysis of the cluster data structure, while the Davis-Boldin index changes significantly when using various methods of cluster analysis. The effectiveness of the proposed criterion for evaluating cluster changes was confirmed by the presence of peaks on the first-order derivative of the one-dimensional image projection of cluster structure in Fig. 2a. Thus, the proposed criterion has the high sensitivity to detecting the moments of occurrence of evolving defects.

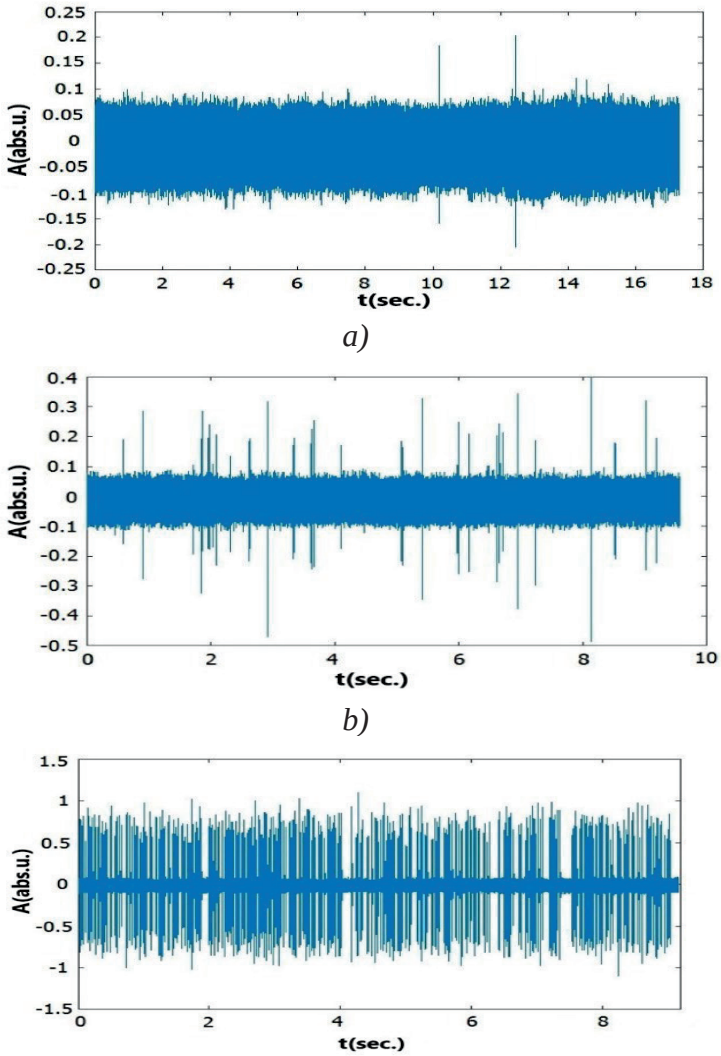

Figure 1. a) the defect of the I hazard class, b) the defect of the II hazard class, c) the defect of the III hazard class

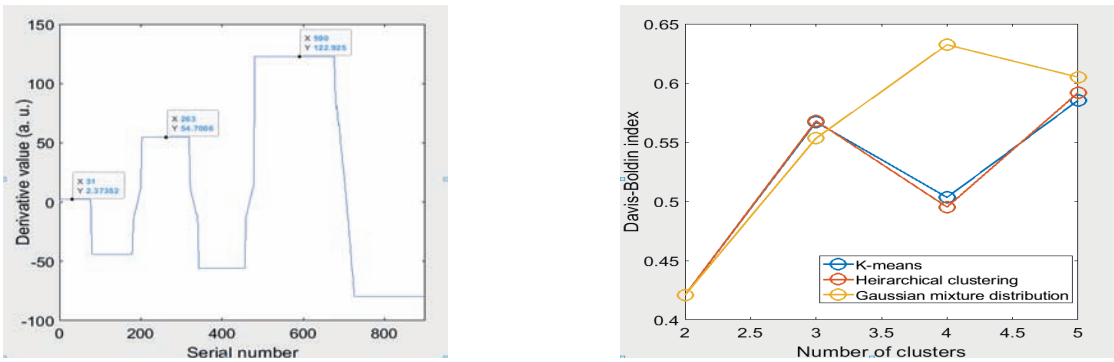

a) b)

Figure 2. Comparison of the proposed modification of VAT method with Davies-Bouldin index. a) First-order derivative of VAT image diagonal projection b) Davis-Bouldin optimization results based on various clustering methodsa) the defect of the I hazard class, b) the defect of the II hazard class, c) the defect of the III hazard class

Fig. 3 shows the results of calculating the proposed criterion for changing the activity coefficient of acoustic emission. It follows from the figure that at the moment of defect state transition to a higher hazard class, the activity of acoustic emission increases significantly. In the intervals between the transition moments, the activity coefficient fluctuates around the average value with a small variance. The level of threshold values was chosen based on the median value of the activity coefficient for defects of the second and third hazard classes identified during pilot operation. For the second hazard class, the threshold value was 0.01, for the third – 0.27

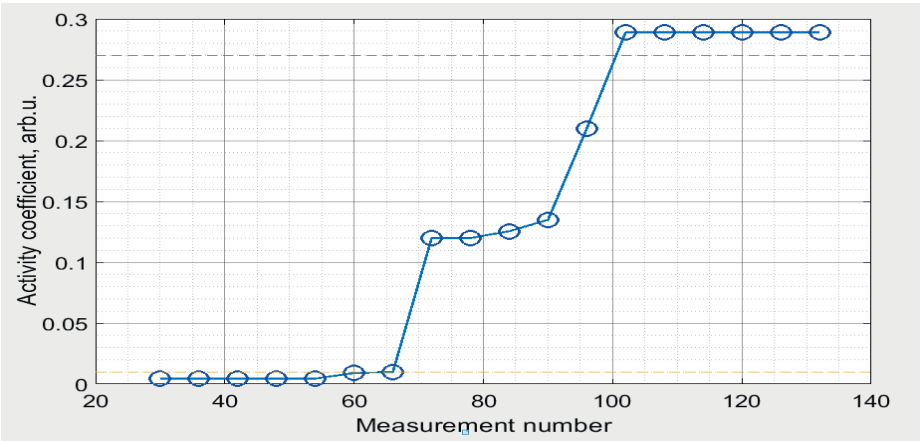

Figure 3. Comparison of the proposed modification of VAT method with Davies-Bouldin index

CONCLUSION

1) The paper presented an approach for developing a DSS that identifies the defect and determines its hazard class based on a multi-criteria assessment of diagnostic features extracted from the acoustic emission time series that are obtained during the diagnostics of construction structures.

2) We propose to utilize a set of two criteria that form the necessary and sufficient conditions under which it is possible to detect moderately hazardous and critically hazardous evolving defects in the construction facilities. They include a criterion for changing the number of clusters and a criterion for changing the acoustic emission activity.

3) We described the original method of applying the proposed criteria, which is based on the process of grouping single consecutive measurements in a series by using a sliding window with overlaps. The proposed approach provides protection against false positives in the presence of stationary long-term noise of various nature occurring during the condition monitoring.

4) The verification of the proposed method was conducted on real construction of oil and gas facilities – vertical steel tank containing a defective weld.

5) Based on a numerical comparison of the results with prior known defects hazard classes it was verified that the proposed method allows to effectively determine the hazard class of evolving defects in construction facilities and detect the processes of their evolution.

ACKNOWLEDGMENTS

The reported study was funded by RFBR according to the research project № 20-37-90089. Authors thank companies Strategia NK Ltd. and Diaform Ltd. for the help in conducting acoustic emission diagnostics on the controlled facility.

REFERENCES

1. **Verstrynge E.** A review on acoustic emission monitoring for damage detection in masonry structures. Construction and Building Materials, 268, 121089 (2021).
2. **Gholizadeh S, Baharudin, B.** A review of the application of acoustic emission technique in engineering. Structural Engineering & Mechanics, 54, 1075-1095 (2015).
3. GOST R 52727-2007. Technical diagnostics. Acoustic-emission diagnostics. General requirements, 16 (2007).
4. **Agletdinov E., Merson D., Vinogradov A.** A new method of low amplitude signal detection and its application in acoustic emission. Applied Sciences, 10, 73 (2020).
5. **Pomponi E.; Vinogradov A.** A real-time approach to acoustic emission clustering. Mech. Syst. Sig. Process. 40, 791–804 (2013).
6. **Kattis S.** Noesis-Advanced Data Analysis, Pattern Recognition & Neural Networks Software for Acoustic Emission Applications. Kolloquium Schallemission, Statusberichte zur Entwicklung und Anwendung der Schallemissionsanalyse, 9-10 (2017).
7. **Kats V., Volkov A.** Features extraction from non-destructive testing data in cyber-physical monitoring system of construction facilities. Journal of Physics: Conference Series, 1425, 012149 (2019)
8. **Kats V.** Structural health monitoring system of construction facilities: enhanced training approach. Journal of Physics: Conference Series, 1694(1) (2020)
9. **Giannakopoulos T., Pikrakis A.** Introduction to Audio Analysis - A MATLAB Approach. Elsevier Ltd., 262 (2014).
10. **Wang Xu, Yusheng Xu.** An improved index for clustering validation based on Silhouette index and Calinski-Harabasz index. IOP Conference Series: Materials Science and Engineering, 569(5) (2019).
11. **Kumar D., James C.** Visual approaches for exploratory data analysis: A survey of the visual assessment of clustering tendency (vat) family of algorithms. IEEE Systems, Man, and Cybernetics Magazine, 6(2), 10-48 (2020).
12. **Merzban, H., Mahmoud Elbayoumi.** Efficient solution of Otsu multilevel image thresholding: A comparative study. Expert Systems with Applications, 116, 299-309, (2019).
13. **Saha, Punam K., Felix W. Wehrli, Bryon R.** Fuzzy distance transform: theory, algorithms, and applications. Computer Vision and Image Understanding 86(3), 171-190, (2002).
14. **Chen H.** Effects of bedding orientation on the failure pattern and acoustic emission activity of shale under uniaxial compression. Geomechanics and Geophysics for Geo-Energy and Geo-Resources 7(1), 1-17 (2021).

СПИСОК ЛИТЕРАТУРЫ

1. **Verstrynge E.** A review on acoustic emission monitoring for damage detection in masonry structures. Construction and Building Materials, 268, 121089 (2021).
2. **Gholizadeh S, Baharudin, B.** A review of the application of acoustic emission technique in engineering. Structural Engineering & Mechanics, 54, 1075-1095 (2015).
3. ГОСТ-Р 52727, Техническая диагностика. Диагностика методом акустической эмиссии. Общие требования. – 2007.
4. **Agletdinov E., Merson D., Vinogradov A.** A new method of low amplitude signal detection and its application in acoustic emission. Applied Sciences, 10, 73 (2020).
5. **Pomponi E.; Vinogradov A.** A real-time approach to acoustic emission clustering. Mech. Syst. Sig. Process. 40, 791–804 (2013).

6. **Kattis S.** Noesis-Advanced Data Analysis, Pattern Recognition & Neural Networks Software for Acoustic Emission Applications. Kolloquium Schallemission, Statusberichte zur Entwicklung und Anwendung der Schallemissionsanalyse, 9-10 (2017).
7. **Kats V., Volkov A.** Features extraction from non-destructive testing data in cyber-physical monitoring system of construction facilities. Journal of Physics: Conference Series, 1425, 012149 (2019)
8. **Kats V.** Structural health monitoring system of construction facilities: enhanced training approach. Journal of Physics: Conference Series, 1694(1) (2020)
9. **Giannakopoulos T., Pikrakis A.** Introduction to Audio Analysis - A MATLAB Approach. Elsevier Ltd., 262 (2014).
10. **Wang Xu, Yusheng Xu.** An improved index for clustering validation based on Silhouette index and Calinski-Harabasz index. IOP Conference Series: Materials Science and Engineering, 569(5) (2019).
11. **Kumar D., James C.** Visual approaches for exploratory data analysis: A survey of the visual assessment of clustering tendency (vat) family of algorithms. IEEE Systems, Man, and Cybernetics Magazine, 6(2), 10-48 (2020).
12. **Merzban, H., Mahmoud Elbayoumi.** Efficient solution of Otsu multilevel image thresholding: A comparative study. Expert Systems with Applications, 116, 299-309, (2019).
13. **Saha, Punam K., Felix W. Wehrli, Bryon R.** Fuzzy distance transform: theory, algorithms, and applications. Computer Vision and Image Understanding 86(3), 171-190, (2002).
14. **Chen H.** Effects of bedding orientation on the failure pattern and acoustic emission activity of shale under uniaxial compression. Geomechanics and Geophysics for Geo-Energy and Geo-Resources 7(1), 1-17 (2021).

Vladislav A. Kats. PhD student of the department of Informational technology, systems and automatization in construction of the National Research Moscow State University of Civil Engineering; 129337, Russia, Moscow, Yaroslavskoe shosse, 26. E-mail: vladislavkats1894@gmail.com

Liubov A. Adamtsevich. Candidate of Technical Sciences, Associate Professor, Associate Professor of the department of Informational technology, systems and automatization in construction of the National Research Moscow State University of Civil Engineering; 129337, Russia, Moscow, Yaroslavskoe shosse, 26. E-mail: AdamtsevichLA@mgsu.ru.

Кац Владислав Анатольевич. Аспирант кафедры Информационных систем, технологий и автоматизации в строительстве Национального исследовательского Московского государственного строительного университета, 129337, Москва, Ярославское ш., д. 26, e-mail: vladislavkats1894@gmail.com

*Адамцевич Любовь Андреевн*а, кандидат технических наук, доцент, доцент кафедры Информационных систем, технологий и автоматизации в строительстве Национального исследовательского Московского государственного строительного университета, 129337, Москва, Ярославское ш. ,д.26; тел. +7495-287-49-14 доб.30-42, e-mail: AdamtsevichLA@mgsu.ru ; ORCID: 0000-0002-5843-0076M

DOI:10.22337/2587-9618-2021-17-4-115-122

THE TECHNOLOGY OF WINTER CONCRETING OF MONOLITHIC FRAME STRUCTURES WITH SUBSTANTIATION OF HEAT TREATMENT MODES BY SOLUTIONS OF THE DIFFERENTIAL EQUATION OF THERMAL CONDUCTIVITY OBTAINED BY THE METHOD OF GROUP ANALYSIS

Alexander A. Lazarev
Novosibirsk State University of Architecture and Civil Engineering (Sibstrin), Novosibirsk, RUSSIA

Abstract. An innovative method for calculating thermal fields inside monolithic structures has been developed, based on the use and analysis of nonlinear differential equations. The innovativeness of the method lies in the approach to the analysis of nonlinear physical processes using nonlinear differential equations. Thanks to the method of group analysis, 13 expressions are obtained from complex mathematical equations, which are easy to use and depend on several empirical coefficients. It is assumed that this calculation method is a priori more accurate than the existing ones, as well as available to people at a construction site without higher mathematical education, which makes it a priority for research. The applicability of this method must be proven by linking empirical coefficients and variables to the conditions of the experiments, while obtaining reliable data that will turn out to be more accurate than the existing calculation methods. This article demonstrates a systematic approach to establishing the suitability of using the method of group analysis of differential equations for problems of winter concreting on the basis of laboratory experiments under stationary conditions. The equations were subject to verification, which, according to the physical description, correspond to the real conditions of the course of thermal processes inside monolithic structures. Based on the obtained processing results, it was decided that it was necessary to further study the innovative method in the conditions of the construction site, but only for some expressions that showed the best results at the stage of laboratory tests.

Keywords: Winter concreting, group analysis method, differential equation, experiment, laboratory tests.

ТЕХНОЛОГИЯ ЗИМНЕГО БЕТОНИРОВАНИЯ КАРКАСНЫХ МОНОЛИТНЫХ КОНСТРУКЦИЙ С ОБОСНОВАНИЕМ РЕЖИМОВ ТЕРМООБРАБОТКИ РЕШЕНИЯМИ ДИФФЕРЕНЦИАЛЬНОГО УРАВНЕНИЯ ТЕПЛОПРОВОДНОСТИ, ПОЛУЧЕННЫМИ МЕТОДОМ ГРУППОВОГО АНАЛИЗА

А.А. Лазарев
Новосибирский Государственный Архитектурно-Строительный Университет (Сибстрин), Новосибирск, РОССИЯ

Аннотация. Разработан инновационный метод расчета тепловых полей внутри монолитных конструкций, основанный на использование и анализе нелинейных дифференциальных уравнений. Инновационность метода заключается в подходе к анализу нелинейных физических процессов с помощью нелинейных дифференциальных уравнений. Благодаря методу группового анализа из сложных математических уравнений получены 13 выражений, которые просты в применении и зависят от нескольких эмпирических коэффициентов. Предполагается, что данный метод расчета является априори более точным существующих, а также доступным для людей на строительной площадке без высшего математического образования, что делает его приоритетным для исследования. Применимость данного метода необходимо доказать путем привязки эмпирических коэффициентов и переменных к условиям протекания экспериментов, получая при этом достоверные

данные, которые окажутся точнее существующих методов расчета. В данной статье продемонстрирован системный подход к установлению пригодности применения метода группового анализа дифференциальных уравнений для задач зимнего бетонирования на основе лабораторных экспериментов при стационарных условиях. Проверки подлежали уравнения, которые по физическому описанию соответствуют реальным условиям протекания тепловых процессов внутри монолитных конструкций. Исходя из полученных результатов обработки было принято решение о необходимости дальнейшего изучения инновационного способа в условиях строительной площадки, однако только для некоторых выражений, которые показали наилучшие результаты на этапе лабораторных испытаний.

Ключевые слова: Зимнее бетонирование, метод группового анализа, дифференциальное уравнение, эксперимент, лабораторные испытания.

1. INTRODUCTION

The issue of strength gain of monolithic structures is fundamental for the construction industry. It has long been established that strength directly depends on the holding temperature of monolithic structures [1]. Many methods have been proposed for calculating thermal fields and strength, but all the proposed methods are either approximate or complex and voluminous for use in a construction site for people without higher mathematical education [2,3,4]. A new look at the problem has appeared thanks to the method of group analysis.

The method of group analysis of differential equations, proposed in the middle of the last century [5,6] for solving applied problems using nonlinear differential equations, made it possible to obtain simple and convincing dependences for modeling temperature conditions during heat treatment of concrete hardening in building structures at negative temperatures.

The key parameters of the submodels obtained from the basic nonlinear differential equation of heat conduction are a parameter characterizing the inhomogeneity of the rod and a parameter characterizing the nonlinearity of the process. These parameters depend on many factors. Finding them and matching them for different conditions, for each submodel, will determine its applicability for solving practical problems.

After analyzing the 13 proposed submodels [7,8], 6 were selected that are most suitable for assessing the thermal processes occurring in the concrete of an extended structure of the "column" type. These are submodels #1,2,3,7,10,11. Parameters were determined experimentally for various ambient temperatures and electric power during heating.

2. RESEARCH AND RESULTS

Based on preliminary experiments [9, 10], which demonstrated the prospects of the study, a decision was made on the need for a system of experiments for a more structured analysis.

Laboratory tests were carried out in a freezer with a constant temperature, the values of which during one experiment did not deviate from the set temperature by more than 0.2 ° C, which confirms the ideal conditions for the experiment.

For the experiment, a column model was prepared, consisting of a formwork structure made of FSF18 laminated plywood, 18 mm thick, reinforcing cage, 6 mm thick rods. As a concrete mixture for the possibility of repeated experiments, a model body was used, the characteristics of which are shown in Table 1. As a heating element, a PNSV 1.8mm heating wire (GOST TU 16.K71-013-88) was used.

Table 1. Materials

Materials	**Consumption of materials for 1 m^3, kg**	
	Standard concrete B 22,5	**Model body**
Diabase crushed stone FR 5-20. GOST 10268-70	1250	1250
Quartz sand of the river (Krivodanovsky quarry) M grain= 1.8. GOST 10268-70	530	530
Portland cement M 400. GOST 10178-68	450	-
Crushed sand (S_{unit} = 2900 cm^2/g)	-	450
Industrial water GOST 2874-54	180	180
Bulk weight of concrete / model body, kg/m^3	2410	2410

In order to establish the regularity of the distribution of the values of the empirical coefficients of the method of group analysis, a series of experiments were carried out under different conditions: at each steady-state temperature: 0 ° C, -5 ° C, -10 ° C, -15 ° C, experiments were carried out with different heating power: 56 W, 108 W, 176 W. The section of the column model and the composition of the model body remained the same.

The heating wire was connected to an electrical network with a voltage of 220 V. The electrical power was changed using a laboratory autotransformer AOSN-20-220-75UHL4 (GOST 15150-69). The power was kept constant throughout the experiment. Power measurements were carried out using periodic monitoring of the current and voltage using a voltammeter. The measurements were made at different loads of the laboratory's electrical network. The limiting power fluctuations did not exceed 2 W, which indicates the reliability of the experiments being carried out.

Experiments, the error of which went beyond the specified limits of the error of power and temperature due to failures, according to the indications of the thermodat and personal control, were excluded from the processing of the results of the experiments.

With a view to generate data for the possibility of further research, 7 chromel-copel thermocouples were installed, located in the center of the structure along its central rod. To process the experiments, we used one thermocouple located in the center of the structure. The rest of the thermocouples were used to assess the likelihood of the main thermocouple, as well as to investigate the second phase - temperature propagation along the structure (See Fig. 1).

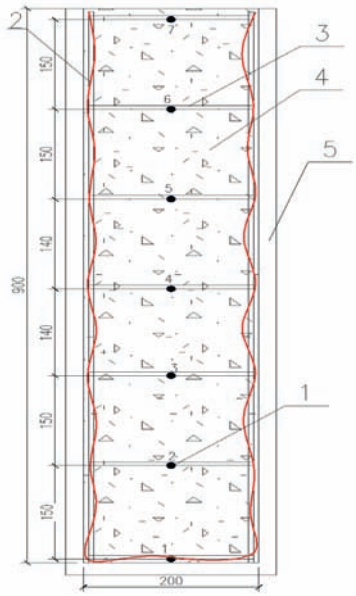

Figure 1. Schematic of the column model. 1 - chromel-copel thermocouples, 2 - heating wire, 3 - reinforcing cage, 4 - model body, 5 - model formwork

When processing these experiments, thermocouples located at the centers of the faces of the column model and in the corners (critical points of a monolithic structure during heating) were

not used to narrow the studied boundaries of applicability of the method of group analysis of differential equations. In the case of a positive verification of the theory in laboratory tests and confirmation by a production experiment, the theory needs to be tested at critical points to create guidelines for the application of the group analysis method.

The results obtained in the laboratory were processed using the Maple software package together with the selection of coefficients, depending on the theoretical equation. The coefficients were selected depending on the best convergence of the theoretical and experimental curves of temperature rise and fall in the column body model.

The results of processing the T_1 submodel according to the experimental data are shown in Table 2.

The results of processing the T_2 submodel according to the experimental data are shown in Table 3.

The results of processing the T_3 submodel according to the experimental data are shown in Table 4.

The results of processing the T_7 submodel according to the experimental data are shown in Table 5.

The results of processing the T_{10} submodel according to the experimental data are shown in Table 6.

The results of processing the T_{11} submodel according to the experimental data are shown in Table 7.

Table 2. Empirical coefficients submodel T_1

Heating the model				**Cooling the model**			
Temperature, °C	Coefficients			Temperature, °C	Coefficients		
	α	β	C_1		α	β	C_1
Low power case 56W							
0	10	3,5	1,53	0	1,6	3	7
-5	7,7	3,3	1,68	-5	1	2	3
-10	3,1	3,3	1,8	-10	-	-	-
-15	-	-	-	-15	1	1,1	4
Medium power case 108W							
0	9	3,24	1,37	0	1,2	2,5	7
-5	6	2,9	2,15	-5	1	2,25	7
-10	2,4	2,37	1,36	-10	1	2	6
-15	1,85	1,66	1,42	-15	-	-	-
High Power Case 176W							
0	6	1,63	1,24	0	0,8	2	8
-5	4,5	3,9	1,45	-5	0,4	2	6
-10	1,75	1,64	1,51	-10	0,4	2,25	16
-15	1,8	1,95	1,58	-15	-	-	-

Table 3. Empirical coefficients submodel T_2

Heating the model			**Cooling the model**		
Temperature, °C	Coefficients		Temperature, °C	Coefficients	
	α	β		α	β
Low power case 56W					
0	1,43	-0,475	0	14	1,5
-5	1,13	-0,745	-5	14,5	1,5
-10	0,83	-1,045	-10	-	-
-15	-	-	-15	15	1,5
Medium power case 108W					
0	1,03	-0,855	0	16,5	1,5
-5	0,5	-1,105	-5	16,45	1,5
-10	0,41	-1,27	-10	15	1,5
-15	0,28	-1,29	-15	-	-
High Power Case 176W					
0	0,5	-1,03	0	18	1,5
-5	0,11	-1,2	-5	16,5	1,5
-10	0,04	-1,29	-10	16,5	1,4
-15	0,01	-1,305	-15	-	-

Table 4. Empirical coefficients submodel T_3

Heating the model				**Cooling the model**			
Temperature, °C	Coefficients			Temperature, °C	Coefficients		
	α	β	C_2		α	β	C_2
Low power case 56W							
0	6	4	4,4	0	3	1	0,33
-5	6	4	3,5	-5	3	1	0,39
-10	6	4	2,3	-10	-	-	-
-15	-	-	-	-15	3	1	0,153
Medium power case 108W							
0	6	4	8,45	0	3	1	0,375
-5	6	4	7,85	-5	3	1	0,4
-10	6	4	5,5	-10	3	1	0,68
-15	6	4	5,5	-15	-	-	-
High Power Case 176W							
0	6	4	12	0	3	1	0,41
-5	6	4	15,5	-5	3	1	0,62
-10	6	4	11	-10	3	1	0,7
-15	6	4	4,95	-15	-	-	-

Table 5. Empirical coefficients submodel T_7

Heating the model				**Cooling the model**			
Temperature, °C	Coefficients			Temperature, °C	Coefficients		
	α	β	C_5		α	β	C_5
Low power case 56W							
0	1,4	1	0,2	0	1,4	1	0,63
-5	1,4	1	0,7	-5	1,4	1	0,645
-10	1,4	1	0,17	-10	-	-	-
-15	-	-	-	-15	1,4	1	0,68
Medium power case 108W							
0	1,4	1	0,64	0	1,4	1	0,86
-5	1,4	1	0,5	-5	1,4	1	0,93
-10	1,4	1	0,52	-10	1,4	1	1,33
-15	1,4	1	0,65	-15	-	-	-
High Power Case 176W							
0	1,4	1	0,8	0	1,4	1	1,34
-5	1,4	1	1,15	-5	1,4	1	2,29
-10	1,4	1	0,85	-10	1,4	1	1,265
-15	1,4	1	5	-15	-	-	-

Table 6. Empirical coefficients submodel T_{10}

Heating the model				**Cooling the model**			
Temperature, °C	Coefficients			Temperature, °C	Coefficients		
	β	C_8	C_9		β	C_8	C_9
Low power case 56W							
0	1,65	5	6	0	1,5	3	2
-5	2	3	4	-5	1,3	3	2
-10	2	1	2	-10	-	-	-
-15	-	-	-	-15	1,25	-1	1
Medium power case 108W							
0	1,45	6	7	0	1,3	4	3
-5	1,5	4	5	-5	1,25	4	3
-10	1,55	2	3	-10	1,15	5	4
-15	1,6	12	12	-15	-	-	-
High Power Case 176W							
0	1,4	7	8	0	1,25	4	3
-5	1,25	5	6	-5	1,05	5	4
-10	1,3	3	4	-10	1,1	5	4
-15	0,8	13	14	-15	-	-	-

Table 7. Empirical coefficients submodel T_{11}

Heating the model				**Cooling the model**			
Temperature, °C	Coefficients			Temperature, °C	Coefficients		
	β	C_{10}	C_{11}		β	C_{10}	C_{11}
Low power case 56W							
0	1,6	2	5	0	1,5	5	8
-5	1,8	2	5	-5	1,3	6	9
-10	2,1	2	5	-10	-	-	-
-15	-	-	-	-15	1,2	2	2
Medium power case 108W							
0	1,32	2	5	0	1,3	5	9
-5	1,36	2	5	-5	1,2	6	9
-10	1,515	2	5	-10	1,1	6	11
-15	1,54	2	5	-15	-	-	-
High Power Case 176W							
0	1,16	2	5	0	1,2	5	7
-5	1,18	2	5	-5	1,05	7	13
-10	1,245	2	5	-10	1	8	9
-15	1,265	2	5	-15	-	-	-

3. CONCLUSION

Drawing a conclusion based on the processing of experimental data according to the criteria: the percentage of discrepancy, the approximate dependence in the values of the coefficients, we can say that only three of the submodels presented have demonstrated a satisfactory result and are recommended for experimental verification by a series of experiments on the construction site in real conditions:

$$T_1 = c_1 x^{\frac{1-\alpha}{\beta+1}} \left(\varepsilon'(t)\right)^{\frac{1}{\beta}}$$

$$T_3 = c_2 x^{-1} \left(\varepsilon'(t)\right)^{\frac{1}{\beta}}$$

$$T_{11} = \left(\varepsilon'(t)\right)^{\frac{1}{\beta}} \left(c_{10} \ln x + c_{11}\right)^{\frac{1}{\beta+1}}$$

This clearly demonstrates their applicability for modeling thermal processes, and hence the acquisition of strength by concrete in structures of the "column" type.

It should be noted that all presented sub-models have several dependences depending on the initial parameters of experiments, such as power and ambient temperature. With a view to streamline the results and precisely identify patterns, it is necessary to conduct a series of reinforcing experiments at the construction site to establish the relationship between heat treatment conditions and empirical coefficients.

REFERENCES

1. Guidelines for the production of concrete work in winter conditions in the regions of the Far East, Siberia and the Far North / TSNIIOMTP Gosstroy of the USSR. - M.: Stroyizdat, 1982 - 213 p.Author, F., Author, S.: Title of a proceedings paper. In: Editor, F., Editor, S. (eds.) CONFERENCE 2016, LNCS, vol. 9999, pp. 1–13. Springer, Heidelberg (2016).
2. **Skramtaev B.G.** About the formula for determining the strength of concrete. Construction industry, 1932, No. 1.

3. **Kondratyev G.M.** Regular thermal regime. M. : GITTL. 1954. – 408 p.
4. **Lykov A.V.** Theory of heat conduction. M. : Higher school. 1967-599 з.
5. **L.V. Ovsyannikov.** Group analysis of differential equations. // M: Nauka, 1978. – 398 p..
6. **Chirkunov Yu.A., Khabirov S.V.** Elements of symmetry analysis of differential equations of continuum mechanics. Novosibirsk. NSTU. 2012.659 p.
7. **Chirkunov Yu.A.** Nonlinear heat propagation in a non-uniform rod under the influence of a non-stationary heat source as applied to the problems of winter concreting. // Izv. universities. Building. 2018. No. 2., 70–76 p.
8. **V.V. Molodin, Yu.A. Chirkunov, S.N. Shpanko, E.V. Garms, K.E. Gorshkova, D.S. Kasyanov, A.A. Lazarev, S.E. Sarafyan.** Nonlinear submodels describing heat propagation during winter concreting of a column in the presence of an external non-stationary heat source. // Izv. universities. Building. 2019. No. 12. – p. 75-86.
9. **V.V. Molodin.** Nonlinear modeling of heat distribution during winter concreting of a column / V.V. Molodin, Yu.A. Chirkunov., N.F. Belmetsev, E.V. Garms, K.E. Gorshkova. A.A. Lazarev // Izvestiya VUZov. Construction. 2020, No. 5, 118-131 p.
10. **V. Molodin, Y. Chirkunov, S. Shpanko, E. Garms, K. Gorshkova, A. Lazarev.** Mathematical modelling of winter concreting//IOP Publishing – 2020, doi:10.1088/1757-899X/953/1/012027

СПИСОК ЛИТЕРАТУРЫ

1. Руководство по производству бетонных работ в зимних условиях в районах Дальнего Востока, Сибири и Крайнего Севера / ЦНИИОМТП Госстроя СССР. – М. : Стройиздат, 1982 – 213 с.
2. **Скрамтаев Б.Г.** О формуле для определения прочности бетона. Строительная промышленность, 1932, №1
3. **Кондратьев Г.М.** Регулярный тепловой режим. М.: ГИТТЛ. 1954. – 408с.
4. **Лыков А.В.** Теория теплопроводности. М.: Высшая школа. 1967– 599 с.
5. **Л.В. Овсянников.** Групповой анализ дифференциальных уравнений. //М. : Наука, 1978. – 398 с.
6. **Чиркунов Ю.А., Хабиров С.В.** Элементы симметрийного анализа дифференциальных уравнений механики сплошной среды. Новосибирск. НГТУ. 2012. 659 с.
7. **Чиркунов Ю.А.** Нелинейное распространение тепла в неоднородном стержне при воздействии нестационарного источника тепла применительно к задачам зимнего бетонирования. // Изв. вузов. Стр-во. 2018. № 2. – С. 70–76.
8. **В.В. Молодин, Ю.А. Чиркунов, С.Н. Шпанко, Е.В. Гармс, К.Е. Горшкова, Д.С. Касьянова, А.А. Лазарев, С.Е. Сарафян**. Нелинейные подмодели, описывающие распространение тепла при зимнем бетонировании колонны при наличии внешнего нестационарного источника тепла. // Изв. вузов. Стр-во. 2019. №12. – С. 75-86
9. **Молодин В.В.** Нелинейное моделирование распределения тепла при зимнем бетонировании колонны / В.В. Молодин, Ю.А Чиркунов., Н.Ф. Бельмецев, Е.В. Гармс, К.Е. Горшкова. А.А. Лазарев // Известия ВУЗов. Строительство.2020, №5 с. 118-131
10. **V. Molodin, Y. Chirkunov, S. Shpanko, E. Garms, K. Gorshkova, A. Lazarev.** Mathematical modelling of winter concreting//IOP Publishing – 2020, doi:10.1088/1757-899X/953/1/012027

Alexander A. Lazarev, Master's student of the Novosibirsk State University of Architecture and Civil Engineering (Sibstrin). E-mail: laz.alexx98@yandex.ru.

Лазарев Александр Андреевич, магистрант Новосибирского Государственного Архитектурно-Строительного Университета (Сибстрин). Эл. почта: laz.alexx98@yandex.ru.

DOI:10.22337/2587-9618-2021-17-4-123-133

NUMERICAL SOLUTION OF THE PROBLEM FOR POISSON'S EQUATION WITH THE USE OF DAUBECHIES WAVELET DISCRETE-CONTINUAL FINITE ELEMENT METHOD

***Marina L. Mozgaleva* [1], *Pavel A. Akimov* [1], *Mojtaba Aslami* [2]**
[1] National Research Moscow State University of Civil Engineering, Moscow, RUSSIA
[2] Fasa University, Fasa, IRAN

Abstract: Numerical solution of the problem for Poisson's equation with the use of Daubechies wavelet discrete-continual finite element method (specific version of wavelet-based discrete-continual finite element method) is under consideration in the distinctive paper. The operational initial continual and discrete-continual formulations of the problem are given, several aspects of finite element approximation are considered. Some information about the numerical implementation and an example of analysis are presented.

Keywords: Daubechies wavelet discrete-continual finite element method, wavelet-based discrete-continual finite element method, discrete-continual finite element method, finite element method, Daubechies wavelet, numerical solution, Poisson's equation.

ЧИСЛЕННОЕ РЕШЕНИЕ КРАЕВОЙ ЗАДАЧИ ДЛЯ УРАВНЕНИЯ ПУАССОНА НА ОСНОВЕ ДИСКРЕТНО-КОНТИНУАЛЬНОГО МЕТОДА КОНЕЧНЫХ ЭЛЕМЕНТОВ С ИСПОЛЬЗОВАНИЕМ МАСШТАБИРУЮЩИХ ФУНКЦИЙ ДОБЕШИ

***М.Л. Мозгалева* [1], *П.А. Акимов* [1], *М. Аслами* [2]**
[1] Национальный исследовательский Московский государственный строительный университет, г. Москва, РОССИЯ
[2] Университет Фаса, г. Фаса, ИРАН

Аннотация: В настоящей статье рассматривается численное решение краевой задачи для уравнения Пуассона на основе дискретно-континуального метода конечных элементов с использованием масштабирующих функций Добеши. Приведены (в операторном виде) исходная континуальная и дискретно-континуальные постановки задачи, рассмотрены некоторые вопросы конечноэлементной аппроксимации. Представлены некоторые сведения о численной реализации и пример расчета.

Ключевые слова: вейвлет-реализация дискретно-континуального метода конечных элементов, дискретно-континуальный метод конечных элементов, метод конечных элементов, функции Добеши, численное решение, уравнение Пуассона.

INTRODUCTION

As is known [1], various problems of continuum mechanics are reduced to the Poisson equation and other similar equations of elliptic type [2-7]. Boundary value problems with the Poisson equation describe, in particular, a stationary temperature field, a stress state during torsion of a rod, membrane deflection, etc. In addition, the operator of the corresponding problem (the Laplace operator) is part of other problems that determine the state of structures under stationary and non-stationary actions.

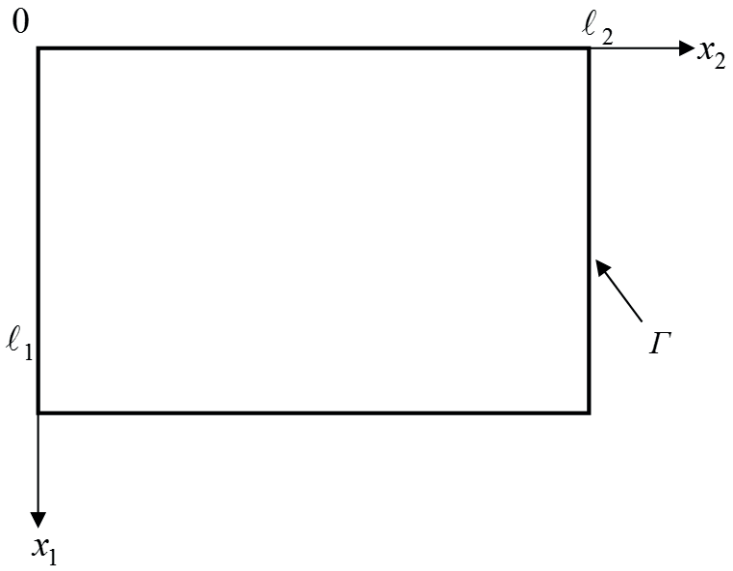

Figure 1.1. About formulation of the problem (initial domain).

From a mathematical point of view, it is the simplest qualitative analogue of other problems and an equivalent operator in iterative processes [8]. In many numerical models, at different time steps, it becomes necessary to solve (numerically) one or several boundary value problems for the Poisson equation, and in some applications the number of time steps during one analysis of the model can be of the order of thousands to millions or more [9]. In this regard, the objective of the distinctive paper is devoted to the semi-analytical method of analysis of corresponding structures with constant physical and geometric parameters in one of the directions (the so-called "basic direction") [8, 10, 11]. This objective seems to be very relevant. The considering method is semi-analytical in the sense that along the basic direction of the structure the problem remains continual and its exact analytical solution is constructed, while in another, non-basic direction, a numerical approximation is performed. In general, this paper continues a series of papers devoted to the research and development of various wavelet-based versions of the discrete-continuous finite element method.

In the theory of boundary value problems for the Poisson and Laplace equations, several classical well-tested solution methods are normally used [2, 12-14], which, in particular, include method of separation of variables or Fourier method, Green's function method and a method of reducing boundary value problems for the Laplace equation to integral equations using potential theory.

Besides, numerical methods (finite element method, boundary element method, finite difference method, variational-difference method, finite volume method, method of point field sources, fast Fourier transform method using parallel computations (with the implementation on the cores of the central processor and on graphic processors (GPU), etc.) for solving the Poisson equation are normally used [9, 15, 16].

1. FORMULATIONS OF THE PROBLEM

Formulation of the problem has the form (Figure 1.1):

$$L\,u = \tilde{F}, \quad 0 \le x_1 \le \ell_1, \quad 0 \le x_2 \le \ell_2\,; \tag{1.1}$$

$$L = -(\partial_1 \theta \partial_1 + \partial_2 \theta \partial_2)\,; \quad \tilde{F} = \theta F + \delta_\Gamma f\,; \tag{1.2}$$

$$F(x_1, x_2) = P\delta(x_1 - 0.5 \cdot \ell_1)\delta(x_2 - 0.5 \cdot \ell_2)\,; \tag{1.3}$$

$$f(x_1, x_2) = 0\,; \tag{1.4}$$

$$\partial_1 = \partial / \partial x_1\,; \quad \partial_2 = \partial / \partial x_2\,; \tag{1.5}$$

$$\theta(x_1, x_2) = \begin{cases} 1, & 0 < x_1 < \ell_1 \wedge 0 < x_2 < \ell_2 \\ 0, & \neg(0 < x_1 < \ell_1 \wedge 0 < x_2 < \ell_2), \end{cases} \tag{1.6}$$

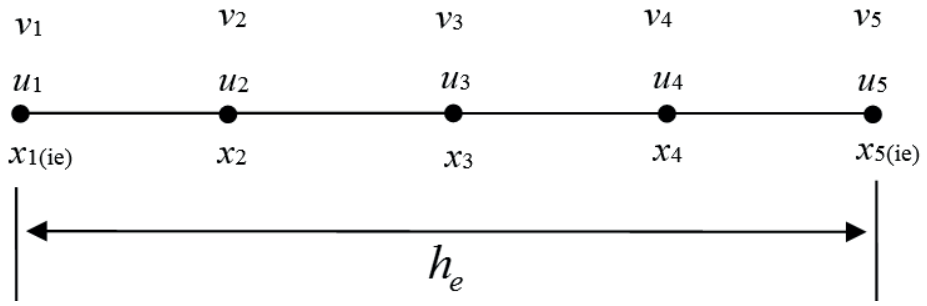

Figure 2.1. Finite element discretication for $N_k = 4$ (sample).

where L is the operator of the problem within the initial domain; $\theta(x_1, x_2)$ is the characteristic function of the domain; $\delta_\Gamma(x_1, x_2)$ is the delta-function of the boundary.

Let x_2 be direction along which parameters of the problem are constant (so-called "main direction"). Let us introduce the following notations

$$L_1 = \theta; \quad L_2 = -\partial_1 \theta \partial_1; \tag{1.7}$$

$$\bar{v} = \partial_2 \bar{u} = \bar{u}'; \quad \bar{v}' = \partial_2 \bar{v}. \tag{1.8}$$

Then we can rewrite (1.1) in the following form:

$$-L_1 v' + L_2 u = F. \tag{1.9}$$

Thus, we have

$$\begin{bmatrix} E & 0 \\ 0 & L_1 \end{bmatrix} \begin{bmatrix} u' \\ v' \end{bmatrix} = \begin{bmatrix} 0 & E \\ L_2 & 0 \end{bmatrix} \begin{bmatrix} u \\ v \end{bmatrix} - \begin{bmatrix} 0 \\ \tilde{F} \end{bmatrix}; \tag{1.10}$$

or

$$\begin{bmatrix} u' \\ v' \end{bmatrix} = \begin{bmatrix} 0 & E \\ L_1^{-1} L_2 & 0 \end{bmatrix} \begin{bmatrix} u \\ v \end{bmatrix} - \begin{bmatrix} 0 \\ L_1^{-1} \tilde{F} \end{bmatrix}, \tag{1.11}$$

where E is identity operator.

Finally we obtain system of differential equations with operational coefficients:

$$\bar{U}' = \tilde{L} \bar{U} + \bar{\tilde{F}}, \tag{1.12}$$

where

$$\tilde{L} = \begin{bmatrix} 0 & E \\ L_1^{-1} L_2 & 0 \end{bmatrix}; \ \bar{\tilde{F}} = \begin{bmatrix} 0 \\ -L_1^{-1} F \end{bmatrix}; \ \bar{U} = \begin{bmatrix} u \\ v \end{bmatrix}; \tag{1.13}$$

$$\bar{U}' = \partial_2 \bar{U} = \begin{bmatrix} \partial_2 u \\ \partial_2 v \end{bmatrix} = \begin{bmatrix} u' \\ v' \end{bmatrix}. \tag{1.14}$$

The system of equations (1.12) is supplemented by boundary conditions, which are set in sections with coordinates $x_2^1 = 0$ and $x_2^2 = \ell_2$.

For instance, for $\bar{U}(x_2)$ from the system of equations (1.12) we have

$$\bar{U}(0) = \bar{U}(\ell_2) = 0. \tag{1.15}$$

2. SOME ASPECTS OF THE FINITE ELEMENT APPROXIMATION

Let us divide the interval $(0, \ell_1)$ segment into N_e parts (elements). Therefore $h_e = \ell_1 / N_e$ is the length of the element. Besides, let us also divide each element into N_k parts (for instance, $N_k = 4$ (Figure 2.1)). Let us use the following notation system: i_e is the element number; $x_1(i_e)$ is the coordinate of the starting point of the i_e-th element; $x_5(i_e)$ is the coordinate of the end point of the i_e-th element. Let $u_i(x_2)$ and $v_i(x_2)$ $(i = 1,2,3,4,5)$ be unknowns per element. Thus, the number of unknowns is equal to $2N$, where $N = 5$. The number of boundary nodes is equal to $N_b = N_e + 1$. The number of inner nodes for all elements is equal to $N_p = N_e(N_k - 1)$. Thus, the total (global) number of unknowns for such approximation is equal to $N_g = 2(N_p + N_b)$.

Let us introduce local coordinates for arbitrary element

$$t = (x - x_{1(ie)}) / h_e, \quad x_{1(ie)} \le x \le x_{5(ie)}, \; 0 \le t \le 1. \tag{2.1}$$

In this case, we have the following relations:

$$\begin{cases} x = x_{1(i_e)} \Rightarrow t = 0 \\ x = x_2 \Rightarrow t = 0.25 \\ x = x_3 \Rightarrow t = 0.5 \\ x = x_4 \Rightarrow t = 0.75 \\ x = x_{5(i_e)} \Rightarrow t = 1; \end{cases} \quad \frac{d}{dx} = \frac{d}{dt} \cdot \frac{dt}{dx} = \frac{1}{h_e} \frac{d}{dt};$$

$$dx = h_e \cdot dt. \tag{2.2}$$

In order to construct the local stiffness matrix corresponding to the operator L_2 (formula (1.7)), we consider the bilinear form taking into account relations (2.2)

$$\begin{aligned} B(y,z) &= < L_2 y, z > = -\int_{x_{1(i_e)}}^{x_{5(i_e)}} \frac{d^2 y}{dx^2} z \, dx = \\ &= \int_{x_{1(i_e)}}^{x_{5(i_e)}} \frac{dy}{dx} \cdot \frac{dz}{dx} dx = \frac{1}{h_e} \int_0^1 \frac{dw}{dt} \cdot \frac{dv}{dt} dt = \\ &= B(w,v), \end{aligned} \tag{2.3}$$

where we consider the following functions

$$y(x) = w(t) = \sum_{k=0}^{N-1} \alpha_k \varphi(t+k); \tag{2.4}$$

$$z(x) = v(t) = \sum_{k=0}^{N-1} \beta_k \varphi(t+k), \tag{2.5}$$

where $x_{1(i_e)} \le x \le x_{5(i_e)}$; $0 \le t \le 1$; $\varphi(s)$ is Daubechies scaling function, $[0, N] \subseteq \operatorname{sup} p \varphi$. Let us substitute (2.4) and (2.5) into (2.3):

$$\begin{aligned} B(w,v) &= \frac{1}{h_e} \int_0^1 \frac{dw}{dt} \cdot \frac{dv}{dt} dt = \\ &= \sum_{i=0}^{N-1} \sum_{j=0}^{N-1} \alpha_i \beta_j \frac{1}{h_e} \int_0^1 \varphi'(t+j) \varphi'(t+j) \, dt = \\ &= (K_{\alpha\beta}^{i_e} \overline{\alpha}, \overline{\beta}) = B_{i_e}(\overline{\alpha}, \overline{\beta}), \end{aligned} \tag{2.6}$$

where

$$K_{\alpha\beta}^{i_e}(i,j) = \frac{1}{h_e} \int_0^1 \varphi'(t+j) \varphi'(t+j) \, dt; \tag{2.7}$$

$$\varphi' = \frac{d\varphi}{dt}. \tag{2.8}$$

Let us define the parameters α_k through the nodal unknowns on the element:

$$\begin{aligned} y_1 &= w(0) = \sum_{k=0}^{N-1} \alpha_k \varphi(k) \\ y_2 &= w(0.25) = \sum_{k=0}^{N-1} \alpha_k \varphi(k+0.25) \\ y_3 &= w(0.5) = \sum_{k=0}^{N-1} \alpha_k \varphi(k+0.5) \\ y_4 &= w(0.75) = \sum_{k=0}^{N-1} \alpha_k \varphi(k+0.75) \\ y_5 &= w(1) = \sum_{k=0}^{N-1} \alpha_k \varphi(k+1). \end{aligned} \tag{2.9}$$

We can rewrite (2.9) in matrix form:

$$\overline{y}^{i_e} = T \overline{\alpha}, \tag{2.10}$$

where we have

$$\overline{y}^{i_e} = [y_1 \;\; y_2 \;\; y_3 \;\; y_4 \;\; y_5]^T; \tag{2.11}$$

$$\overline{\alpha} = [\alpha_0 \;\; \alpha_1 \;\; \alpha_2 \;\; \alpha_3 \;\; \alpha_4]^T; \tag{2.12}$$

$$T = \begin{bmatrix} \varphi(0) & \varphi(1) & \varphi(2) & \varphi(3) & \varphi(4) \\ \varphi(0.25) & \varphi(1.25) & \varphi(2.25) & \varphi(3.25) & \varphi(4.25) \\ \varphi(0.5) & \varphi(1.5) & \varphi(2.5) & \varphi(3.5) & \varphi(4.5) \\ \varphi(0.75) & \varphi(1.75) & \varphi(2.75) & \varphi(3.75) & \varphi(4.75) \\ \varphi(1) & \varphi(2) & \varphi(3) & \varphi(4) & \varphi(5) \end{bmatrix}. \tag{2.13}$$

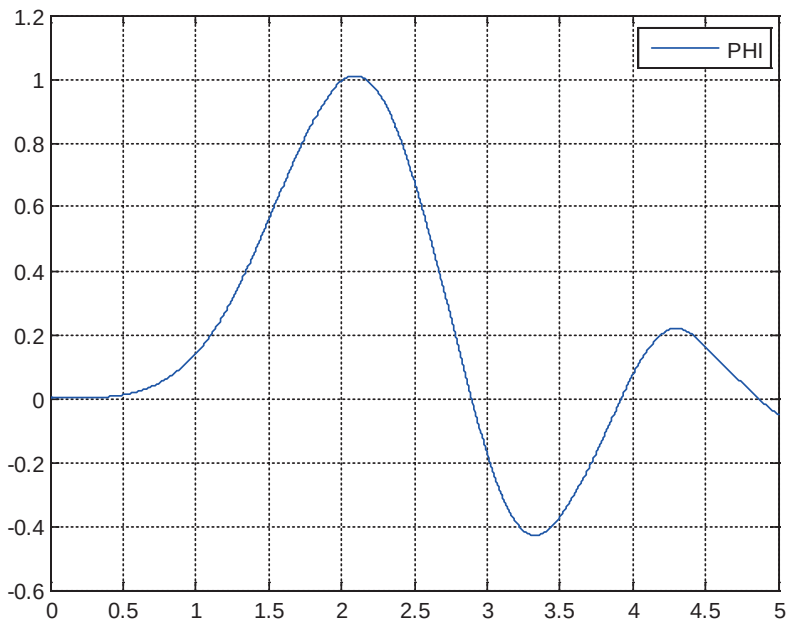

Figure 3.1. Daubechies scaling function.

We can also get

$$\bar{z}^{i_e} = T\bar{\beta}\,. \qquad (2.14)$$

Using (2.10) and (2.14) we can obtain

$$\bar{\alpha} = T^{-1}\bar{y}^{i_e}; \quad \bar{\beta} = T^{-1}\bar{z}^{i_e}. \qquad (2.15)$$

Thus, we can rewrite (2.6) in the following form:

$$\begin{aligned}(K^{i_e}_{\alpha\beta}\bar{\alpha}, \bar{\beta}) &= (K^{i_e}_{\alpha\beta}T^{-1}\bar{y}^{i_e}, T^{-1}\bar{z}^{i_e}) = \\ &= ((T^{-1})^{\mathrm{T}} K^{i_e}_{\alpha\beta}T^{-1}\bar{y}^{i_e}, \bar{z}^{i_e}) = \\ &= (K^{i_e}\bar{y}^{i_e}, \bar{z}^{i_e}),\end{aligned} \qquad (2.16)$$

where

$$K^{i_e} = (T^{-1})^{\mathrm{T}} K^{i_e}_{\alpha\beta} T^{-1} \qquad (2.17)$$

is the local stiffness matrix.

3. NUMERICAL IMPLEMENTATION

The presented algorithm can be implemented using MATLAB software tools. In particular, the call to the standard function

```
wavefun('db8',0)
```

allows to obtain the values of the Daubechies scaling function [17-32] φ (Figure 3.1) on the interval (segment) $[0, 15] = \operatorname{sup}\mathrm{p}\varphi$ with a step $h_t = 1/256 = 2^{-8}$. Let us denote $N_t = 256 = 2^8$. For the value under consideration ($N = 5$) we can use the first $N_l = N_t \cdot N + 1$ values determined on the interval $[0, N] = [0, 5]$. With such a small step, we find it will natural to compute the derivatives (Figure 3.2) in the form of finite differences:

$$\varphi'(t_k) \approx d\varphi_k = \frac{\varphi_{k+1} - \varphi_{k-1}}{2h_t}, \quad k = 1, 2, \ldots, N_l, \qquad (3.1)$$

where we have $\varphi_k = \varphi(t_k)$ and $t_k = k \cdot h_t$. If $t_k \notin [0,19]$ then $\varphi_k = \varphi(t_k) = 0$.

When computing the coefficients of the local stiffness matrix (formula (2.7)), one can use the simplest quadrature formulas for numerical integration, in particular, the formula for "mean" rectangles with a step $2h_t$.

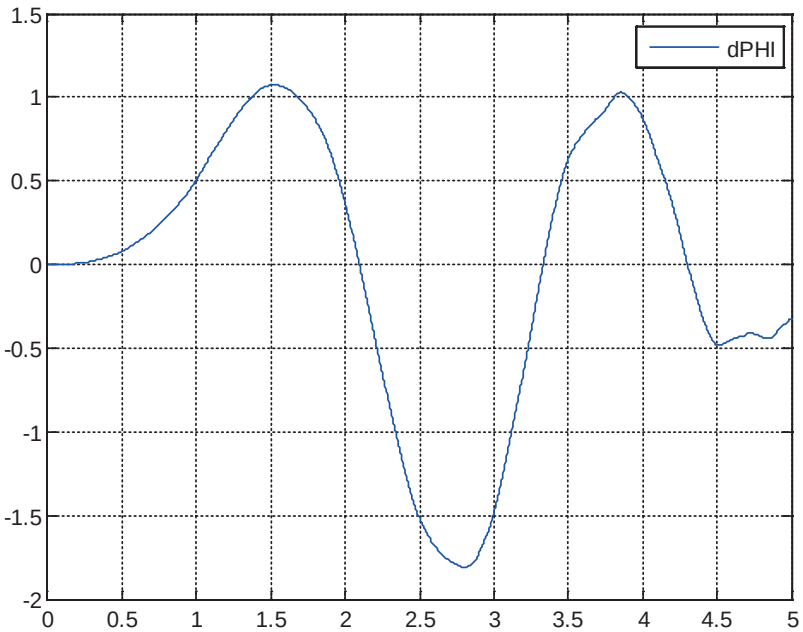

Figure 3.2. The first direvative (finite-difference) of Daubechies scaling function.

4. EXAMPLE OF ANALYSIS

For the numerical implementation, let us set, in particular, the following numerical parameters:

$$P = 100; \quad \ell_1 = 2.0; \quad \ell_2 = 2.6.$$

Let $N_e = 16$ be the number of elements (finite elements). Then the total number of nodal points in the discrete direction is equal to

$$N_1 = N_p + N_b = 3 \cdot 16 + 17 = 65.$$

Then the total number of unknowns is equal to

$$N_g = 2N_1 = 130.$$

The length of the element is equal to

$$h_e = \ell_1 / N_e = 2/16 = 0.125.$$

The distance between the coordinates of the nodes is equal to

$$h_p = h_e / 4 = 0.125/4 = 0.03125.$$

For comparison (verification purpose), we can use the variational-difference discrete-continual method with a step of discretization h_p along the discrete direction x_1.

Graphical comparison of the corresponding results is presented at Figure 4.1, where we use the following notation system: `Udb` is the result obtained using the Daubechies scaling function; `Uvr` is the result obtained on the basis of the variational-difference method; `d1U` is a finite-difference analogue of the derivative with a step; `d2U` is derivative, $\partial_2 u = v$; $h_1 = h_p = 0.03125$ and $h_2 = 0.1$ are steps for visualization of results along directions x_1 and x_2 respectively.

As researcher can see, the results obtained are almost completely identical.

REFERENCES

1. **Mozgaleva M.L., Akimov P.A.** Localization of Solution of the Problem for Poisson's Equation with the Use of B-Spline Discrete-Continual Finite Element Method. // International Journal for Computational Civil and Structural Engineering, 2021, Volume 17, Issue 3, pp. 157-172.

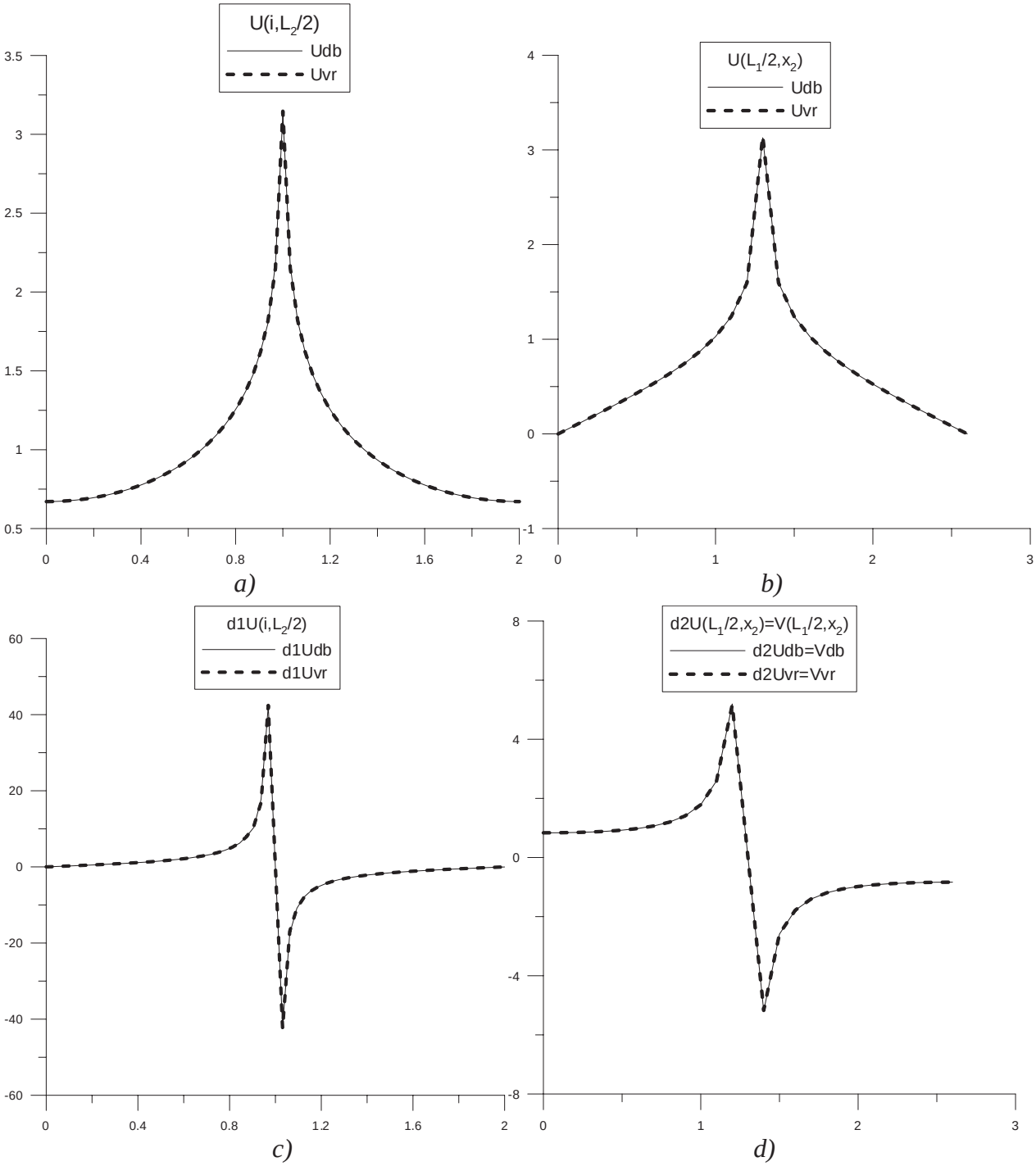

Figure 4.1. Comparison of results.

2. **Tihonov A.N., Samarskij A.A.** Uravnenija matematicheskoj fiziki [Equations of mathematical physics]. Moscow, Nauka, 2004, 798 pages (in Russian).
3. **Ivlev D.D.** Mehanika plasticheskih sred. Tom 1. Teorija ideal'noj plastichnosti. [Mechanics of plastic media. Volume 1. The theory of ideal plasticity]. Moscow, Fizmatlit, 2001, 445 pages (in Russian).
4. **Ivlev D.D.** Mehanika plasticheskih sred. Tom 2. Obshhie voprosy. Zhestkoplasticheskoe i uprugoplasticheskoe sostojanie tel. Uprochnenie. Deformacionnye teorii. Slozhnye sredy. [Mechanics of plastic media. Volume 2. General problems. Rigid-

plastic and elasto-plastic state of bodies. Strengthening. Deformation theories. Complex environments]. Moscow, Fizmatlit, 2002, 448 pages (in Russian).

5. **Ivlev D.D., Ershov L.V.** Metod vozmushhenij v teorii uprugoplasticheskogo tela [Perturbation method in the theory of an elastoplastic body]. Moscow, Nauka, 1978, 208 pages (in Russian).
6. **Lur'e A.I.** Teorija uprugosti [Theory of Elasticity]. Moscow, Nauka, 1970, 939 pages (in Russian).
7. **Aleksandrov V.M.** Zadachi mehaniki sploshnyh sred so smeshannymi granichnymi uslovijami [Problems of Continuum Mechanics with Mixed Boundary Conditions]. Moscow, Nauka, 1986, 329 pages (in Russian).
8. **Zolotov A.B., Akimov P.A., Mozgaleva M.L.** Mnogourovnevye diskretnye i diskretno-kontinual'nye realizacii variacionno-raznostnogo metoda [Multilevel discrete and discrete-continuous realizations of the variational-difference method]. Moscow, ASV, 2013, 416 pages (in Russian).
9. **Mingalev O.V., Mel'nik M.N.** Chislennoe reshenie kraevyh zadach dlja uravnenija Puassona metodom bystrogo preobrazovanija Fur'e s ispol'zovaniem parallel'nyh vychislenij [Numerical solution of boundary value problems for the Poisson equation by the fast Fourier transform method using parallel computations]. // *Trudy Kol'skogo nauchnogo centra RAN*, 2018, Issue 5-4(9), pp. 165-182 (in Russian).
10. **Akimov P.A., Belostotskiy A.M., Mozgaleva M.L., Mojtaba Aslami, Negrozov O.A.** Correct Multilevel Discrete-Continual Finite Element Method of Structural Analysis. // Advanced Materials Research Vol. 1040 (2014), pp. 664-669.
11. **Akimov P.A., Sidorov V.N.** Correct Method of Analytical Solution of Multipoint Boundary Problems of Structural Analysis for Systems of Ordinary Differential Equations with Piecewise Constant Coefficients. // Advanced Materials Research Vols. 250-253, 2011, pp. 3652-3655.
12. **Sharfanec B.P., Sharfanec E.B.** O vybory metodov reshenija uravnenija Puassona v obshhem sluchae raspredelenija objemnoj plotnosti zarjada i o postanovke kraevyh uslovij v jelektrokineticheskih zadachah (obzor) [On the choice of methods for solving the Poisson equation in the general case of the distribution of the volume charge density and on the formulation of boundary conditions in electrokinetic problems (review)]. // *Nauchnoe priborostroenie*, 2015, Volume 25, Issue 1, pp. 65-75 (in Russian).
13. **Vladimirov V.S.** Uravnenija matematicheskoj fiziki [Equations of mathematical physics]. Moscow, Nauka, 1981, 512 pages (in Russian).
14. **Koshljakov N.S., Gliner Je.B., Smirnov M.M.** Uravnenija v chastnyh proizvodnyh matematicheskoj fiziki [Partial differential equations of mathematical physics]. Moscow, Vysshaja shkola, 1970, 712 pages (in Russian).
15. **Vorozhcov E.V., Shapeev V.P.** Chislennoe reshenie uravnenija Puassona v poljarnyh koordinatah metodom kollokacij i naimen'shih nevjazok [Numerical solution of the Poisson equation in polar coordinates by the collocation and least residual method]. // *Modelirovanie i analiz informacionnyh sistem*, 2015, Volume 22, Issue 5, pp. 648-664 (in Russian).
16. **Knjazev S.Ju., Shherbakova E.E., Engibarjan A.A.** Chislennoe reshenie kraevyh zadach dlja uravnenija Puassona metodom tochechnyh istochnikov polja [Numerical solution of boundary value problems for the Poisson equation by the method of point field sources]. // *Vestnik DLGTU*, 2014, Volume 15, Issue 2(77), pp. 15-20 (in Russian).
17. **Dobeshi I.** Desjat' lekcij po vejvletam [Ten lectures on wavelets]. Izhevsk: NIC «Reguljarnaja i haoticheskaja dinamika», 2001, 464 pages (in Russian).
18. **Chui K.** Vvedenie v vejvlety [Introduction to wavelets]. Moscow, Mir, 2001, 412 pages (in Russian).

19. **Chen X.F., Yang S.J., Ma J.X.** The construction of wavelet finite element and its application. // Finite Elem. Anal. Des., 2004, 40, pp. 541-554.
20. **Daubechies I.** Orthonormal bases of compactly supported wavelets. // Commun. Pure Appl. Math., 1988, 41, pp. 909-996.
21. **Jin J.M., Xue P.X., Xu Y.X., Zhu Y.L.** Compactly supported non-tensor product form two-dimension wavelet finite element. // Appl. Math. Mech., 2006, 27, pp. 1673-1686.
22. **Li B., Cao H.R., He Z.J.** The construction of one-dimensional Daubechies wavelet-based finite elements for structural response analysis. // J. Vibroeng., 2011, 13, pp. 729-738.
23. **Li B., Chen X.** Wavelet-based numerical analysis: A review and classification. // Finite Elements in Analysis and Design, 2014, 81, pp. 14-31.
24. **Ma J.X., Xue J.J.** A study of the construction and application of a Daubechies wavelet-based beam element. // Finite Elem. Anal. Des., 2003, 39, pp. 965-975.
25. **Mitra M., Gopalakrishnan S.** Extraction of wave characteristics from wavelet-based spectral finite element formulation. // Mech. Syst. Signal Process, 2006, 20, pp. 2046-2079.
26. **Mitra M., Gopalakrishnan S.** Wave propagation analysis in anisotropic plate using wavelet spectral element approach. // J. Appl. Mech., 2008, 75, pp. 1-6.
27. **Mitra M., Gopalakrishnan S.** Wavelet based spectral finite element modelling and detection of delamination in composite beams, // Proceed. R. Soc. A, 2006. 462, pp. 1721-1740.
28. **Mitra M., Gopalakrishnan S.** Wavelet Spectral element for wave propagation studies in pressure loaded axisymmetric cylinders. // J. Mech. Mater. Struct., 2007, 4, pp. 753-772.
29. **Mozgaleva M.L., Akimov P.A., Kaytukov T.B.** About Wavelet-Based Computational Beam Analysis with the Use of Daubechies Scaling Functions. // International Journal for Computational Civil and Structural Engineering, 2019, Volume 15, Issue 2, pp. 95-110.
30. **Mozgaleva M.L., Akimov P.A., Kaytukov T.B.** Wavelet-based Discrete-Continual Finite Element Plate Analysis with the Use of Daubechies Scaling Functions. // International Journal for Computational Civil and Structural Engineering, 2019, Volume 15, Issue 3, pp. 96-108.
31. **Patton R.D., Marks P.C.** One-dimensional finite elements based on the Daubechies family of wavelets. // AIAAJ, 1996, 34, pp. 1696-1698.
32. **Zhou Y.H., Zhou J.** A modified wavelet approximation of deflections for solving PDEs of beams and square thin plates. // Finite Elem. Anal. Des., 2008, 44, pp. 773-783.

СПИСОК ЛИТЕРАТУРЫ

1. **Mozgaleva M.L., Akimov P.A.** Localization of Solution of the Problem for Poisson's Equation with the Use of B-Spline Discrete-Continual Finite Element Method. // International Journal for Computational Civil and Structural Engineering, 2021, Volume 17, Issue 3, pp. 157-172.
2. **Тихонов А.Н., Самарский А.А.** Уравнения математической физики. – М.: Наука, 2004. – 798 с.
3. **Ивлев Д.Д.** Механика пластических сред. Том 1. Теория идеальной пластичности. – М.: Физматлит, 2001. – 445 с.
4. **Ивлев Д.Д.** Механика пластических сред. Том 2. Общие вопросы. Жесткопластическое и упругопластическое состояние тел. Упрочнение. Деформационные теории. Сложные среды. – М.: Физматлит, 2002. – 448 с.
5. **Ивлев Д.Д., Ершов Л.В.** Метод возмущений в теории упругопластического тела. – М.: Наука, 1978. – 208 с.
6. **Лурье А.И.** Теория упругости. – М.: Наука, 1970. – 939 с.

7. **Александров В.М.** Задачи механики сплошных сред со смешанными граничными условиями. – М.: Наука, 1986. – 329 с.
8. **Золотов А.Б., Акимов П.А., Мозгалева М.Л.** Многоуровневые дискретные и дискретно-континуальные реализации вариационно-разностного метода. – М.: АСВ, 2013. – 416 с.
9. **Мингалев О.В., Мельник М.Н.** Численное решение краевых задач для уравнения Пуассона методом быстрого преобразования Фурье с использованием параллельных вычислений. // Труды Кольского научного центра РАН, 2018, №5-4(9), с. 165-182.
10. **Akimov P.A., Belostotskiy A.M., Mozgaleva M.L., Mojtaba Aslami, Negrozov O.A.** Correct Multilevel Discrete-Continual Finite Element Method of Structural Analysis. // Advanced Materials Research Vol. 1040 (2014), pp. 664-669.
11. **Akimov P.A., Sidorov V.N.** Correct Method of Analytical Solution of Multipoint Boundary Problems of Structural Analysis for Systems of Ordinary Differential Equations with Piecewise Constant Coefficients. // Advanced Materials Research Vols. 250-253, 2011, pp. 3652-3655.
12. **Шарфанец Б.П., Шарфанец Е.Б.** О выборы методов решения уравнения Пуассона в общем случае распределения объемной плотности заряда и о постановке краевых условий в электрокинетических задачах (обзор). // Научное приборостроение, 2015, том 25, №1, с. 65-75.
13. **Владимиров В.С.** Уравнения математической физики. – М.: Наука, 1981. – 512 с.
14. **Кошляков Н.С., Глинер Э.Б., Смирнов М.М.** Уравнения в частных производных математической физики. – М.: Высшая школа, 1970. – 712 с.
15. **Ворожцов Е.В., Шапеев В.П.** Численное решение уравнения Пуассона в полярных координатах методом коллокаций и наименьших невязок. // Моделирование и анализ информационных систем, 2015, том 22, №5, с. 648-664.
16. **Князев С.Ю., Щербакова Е.Е., Енгибарян А.А.** Численное решение краевых задач для уравнения Пуассона методом точечных источников поля. // Вестник ДЛГТУ, 2014, том 15, №2(77), с. 15-20.
17. **Добеши И.** Десять лекций по вейвлетам. – Ижевск: НИЦ «Регулярная и хаотическая динамика», 2001. – 464 с.
18. **Чуи К.** Введение в вейвлеты. – М.: Мир, 2001. – 412 с.
19. **Chen X.F., Yang S.J., Ma J.X.** The construction of wavelet finite element and its application. // Finite Elem. Anal. Des., 2004, 40, pp. 541-554.
20. **Daubechies I.** Orthonormal bases of compactly supported wavelets. // Commun. Pure Appl. Math., 1988, 41, pp. 909-996.
21. **Jin J.M., Xue P.X., Xu Y.X., Zhu Y.L.** Compactly supported non-tensor product form two-dimension wavelet finite element. // Appl. Math. Mech., 2006, 27, pp. 1673-1686.
22. **Li B., Cao H.R., He Z.J.** The construction of one-dimensional Daubechies wavelet-based finite elements for structural response analysis. // J. Vibroeng., 2011, 13, pp. 729-738.
23. **Li B., Chen X.** Wavelet-based numerical analysis: A review and classification. // Finite Elements in Analysis and Design, 2014, 81, pp. 14-31.
24. **Ma J.X., Xue J.J.** A study of the construction and application of a Daubechies wavelet-based beam element. // Finite Elem. Anal. Des., 2003, 39, pp. 965-975.
25. **Mitra M., Gopalakrishnan S.** Extraction of wave characteristics from wavelet-based spectral finite element formulation. // Mech. Syst. Signal Process, 2006, 20, pp. 2046-2079.
26. **Mitra M., Gopalakrishnan S.** Wave propagation analysis in anisotropic plate using wavelet spectral element approach. // J. Appl. Mech., 2008, 75, pp. 1-6.
27. **Mitra M., Gopalakrishnan S.** Wavelet based spectral finite element modelling and

detection of delamination in composite beams, // Proceed. R. Soc. A, 2006. 462, pp. 1721-1740.

28. **Mitra M., Gopalakrishnan S.** Wavelet Spectral element for wave propagation studies in pressure loaded axisymmetric cylinders. // J. Mech. Mater. Struct., 2007, 4, pp. 753-772.
29. **Mozgaleva M.L., Akimov P.A., Kaytukov T.B.** About Wavelet-Based Computational Beam Analysis with the Use of Daubechies Scaling Functions. // International Journal for Computational Civil and Structural Engineering, 2019, Volume 15, Issue 2, pp. 95-110.
30. **Mozgaleva M.L., Akimov P.A., Kaytukov T.B.** Wavelet-based Discrete-Continual Finite Element Plate Analysis with the Use of Daubechies Scaling Functions. // International Journal for Computational Civil and Structural Engineering, 2019, Volume 15, Issue 3, pp. 96-108.
31. **Patton R.D., Marks P.C.** One-dimensional finite elements based on the Daubechies family of wavelets. // AIAAJ, 1996, 34, pp. 1696-1698.
32. **Zhou Y.H., Zhou J.** A modified wavelet approximation of deflections for solving PDEs of beams and square thin plates. // Finite Elem. Anal. Des., 2008, 44, pp. 773-783.

Marina L. Mozgaleva, Senior Scientist Researcher, Dr.Sc.; Professor of Department of Applied Mathematics, National Research Moscow State University of Civil Engineering; 26, Yaroslavskoe Shosse, Moscow, 129337, Russia; phone/fax +7(499) 183-59-94; Fax: +7(499) 183-44-38; Email: marina.mozgaleva@gmail.com.

Pavel A. Akimov, Full Member of the Russian Academy of Architecture and Construction Sciences, Professor, Dr.Sc.; Rector of National Research Moscow State University of Civil Engineering; 26, Yaroslavskoe Shosse, Moscow, 129337, Russia; phone: +7(495) 651-81-85; Fax: +7(499) 183-44-38; E-mail: AkimovPA@mgsu.ru, rector@mgsu.ru, pavel.akimov@gmail.com.

Mojtaba Aslami, Ph.D; Assistant Professor; Fasa University; University, Fasa, Iran; E-mail: aslami.mojtaba@gmail.com

Мозгалева Марина Леонидовна, старший научный сотрудник, доктор технических наук; профессор кафедры прикладной математики Национального исследовательского Московского государственного строительного университета; 129337, Россия, г. Москва, Ярославское шоссе, дом 26; телефон/факс: +7(499) 183-59-94; Email: marina.mozgaleva@gmail.com.

Акимов Павел Алексеевич, академик РААСН, профессор, доктор технических наук; ректор Национального исследовательского Московского государственного строительного университета; 129337, Россия, г. Москва, Ярославское шоссе, дом 26; телефон: +7(495) 651-81-85; факс: +7(499) 183-44-38; Email: AkimovPA@mgsu.ru, rector@mgsu.ru, pavel.akimov@gmail.com.

Моджтаба Аслами, кандидат технических наук; доцент Университета Фесы; Феса, Иран; E-mail: aslami.mojtaba@gmail.com.

DOI:10.22337/2587-9618-2021-17-4-134-145

THE HISTORY OF THE LIMIT STATE DESIGN METHOD

Anatoly V. Perelmuter
SCAD Soft Ltd., Kyiv, UKRAINE

Abstract. This paper analyzes the 70-year history of development of the limit state design method (LSDM) focusing on the fundamentals of the design codes based on this method and considers proposals for improving the LSDM and its justification. It was also noted that the reaction of the system in any of its fixed states is not always sufficient to assess the reliability of the system, and therefore it is necessary to analyze the rate of loss of resistance of load-bearing structures. However, probabilistic considerations were not enough due to the lack of reliable statistical data in the area of extreme sections of the distribution curves and a number of other circumstances (features of control procedures, different behavior of the material in the structure and in the samples, etc.). This paper analyzes some fundamental issues that should be solved when developing the method for the nonlinear analysis.

Keywords: structural design, limit state design method, computing, reliability theory.

О РАЗВИТИИ ОСНОВНЫХ ИДЕЙ МЕТОДА РАСЧЕТНЫХ ПРЕДЕЛЬНЫХ СОСТОЯНИЙ

А.В. Перельмутер
SCAD Soft Ltd., Киев, УКРАИНА

Аннотация. Анализируется 70-тилетняя история развития метода расчетных предельных состояний (МРПС). Основное внимание уделено принципиальным положениям нормативных документов, которые основаны на этом методе. Рассматривалась история развития основных положений МРПС и их представления в нормативных документах, указываются работы, в которых выдвигались предложения по совершенствованию МРПС, и его обоснованию. При этом отмечено, что реакция системы в каких бы то ни было фиксированных ее состояниях не всегда является достаточной для оценки надежности системы и указывается на необходимость анализа темпа потери отпорности несущих конструкций. Рассмотрен отход от использования только вероятностных соображений, который произошел ввиду отсутствия надежных статистических данных в области крайних участков кривых распределения, а также с учетом ряда других обстоятельств (особенности контрольных процедур, различное поведение материала в конструкции и в образцах и др.). Анализируются некоторые принципиальные вопросы, которые следует решить при развитии метода в нелинейном варианте анализа.

Ключевые слова: проектирование конструкций, метод предельных состояний, расчеты, теория надежности.

INTRODUCTION

This year marks 70 years since the release of the fundamental book [1], where the limit state design method was presented to the engineering community, which was soon adopted as the basis for design codes. This method became an ideological basis for the formulation of the structural reliability requirements, and in this capacity it was used in the reliability theory that appeared in the 50s. The issues of the formation and development of the theory of reliability of buildings and structures have been repeatedly considered and analyzed by various authors [2], [3], [4], but the limit state design method itself has not been subjected to such analysis, although the history of its development is no less informative.

The practical implementation of the ideological basis of the method, which was related to a

number of not always explicitly formulated assumptions, required additional research to substantiate them. In some cases, this kind of research has indeed confirmed the accepted approach. However, it often led to the conclusion that adjustments and clarifications were in fact necessary.

That is actually what the development process and the resulting procedures for improving the codes were all about. In this paper, we will consider some fundamental issues related to the refinement or correction of the basic ideas of the limit state design method, both taken into account in the mentioned series of design codes, and those under discussion [5], [6]. We mainly consider the Ukrainian and Russian experience, although it should be noted that many of the issues discussed below have found their solution in Eurocodes [7], often in a different form.

METHODS

This work is based on the analysis of various sources describing an approach to the problem of design justification of reliability and safety of buildings and structures using the limit state design method. It focuses on the fundamentals of the design codes which indicate the goals and determine the approach for solving this problem. The paper considers the history of their development and works with proposals for improving the LSDM and its justification [8, 9, 10], as well as the ways of their implementation in SCAD, LIRA, MicroFE. After all, it is the software implementation that is one of the best ways to identify inconsistencies and contradictions, if there are any in the codes.

One of the important sources of a critical approach to standards and their assessment was a design code I have a developed [11] devoted to the general principles of ensuring the reliability and safety of buildings and structures, as well as to the implementation of standard requirements in SCAD [12].

RESULTS

The issues discussed below are related to certain key aspects of the limit state design method. Not only do they reflect the history of its formation and development, but also highlight the problems that need to be resolved.

The limit state design method is based on the following:

- of all possible technical states of the operated structure, only its limit states are analyzed;
- the general safety factor is represented by a product of partial factors, each one related to a certain physical phenomenon (loading, resistance, simplification of the design model, etc.);
- values of the partial safety factors are substantiated by statistical data on the variability of the corresponding physical parameters.

Let us consider some clarifications, modification and adjustments of the design codes. In total, since 1954 there have been six versions of the fundamental design code [13], [14], [15], [16], [17], [18] and some changes were introduced into their texts.

Analysis of Fixed States of the System

This method is based on the idea of performing a detailed analysis only for the limit states of the structure, while almost completely ignoring all other structural states, which, by the way, correspond to the majority of the operating time. It is at this time that many destructive changes occur (corrosion, fatigue accumulation, erosion, etc.).

Besides the known advantages, this approach has a serious disadvantage. If, for example, we consider the strength condition as one of the limit states and design the structure ensuring that this condition is not violated during the entire service life with a certain degree of confidence, we know almost nothing about the level of actual stresses corresponding to the normal (non-limit) state under the most frequent operating conditions.

The states of the structure most frequently occurring under the operating conditions usually define its durability. However, the following structures can turn out to be almost equivalent according to the limit state analysis:

- a dam with a normal loading not far from the allowable value (for example, 80% of the design value),
- a chimney with a very rare design load and a normal loading equal to, for example, 15% of the design value.

Since most of the structural lifetime corresponds to the normal operating states, during which the destructive changes occur in the material (for example, corrosion processes or the fatigue accumulation), then in order to ensure operational reliability and durability it is important to perform the analysis of a structure that is normally operating and is far from exhausting its strength and stability.

According to [19] there is a certain failure due to the loss of design control over the structure during its transition from a “healthy” (normal, operational) state to the limit one. It would seem that the serviceability limit state checks could eliminate this methodological failure, but the thing is that these are limit states as well, i.e. correspond to rather rare extreme structural and environmental parameters.

It should be noted that the reaction of the system in any of its fixed states is not always sufficient to assess the reliability of the system under variable interaction with the environment. The simplest example of comparing two systems S_1 and S_2, a graphic illustration of which is shown in Fig. 1 in the form of a relationship between the reaction F and the intensity of the action P. Even a slight increase in P in the S_1 system leads to a sharp increase in the reaction, up to its critical value, which is not observed in the S_2 system.

Hence, a proposal appeared to introduce the concept of the limit behavior of the system, which limits the gradient $g = dF/dP$ [20].

It is easy to see that the gradient g characterizes the rigidity of the system, i.e. we are dealing with a new limit state in the form of limiting the rate of possible decrease in the rigidity of the system (loss of its resistance).

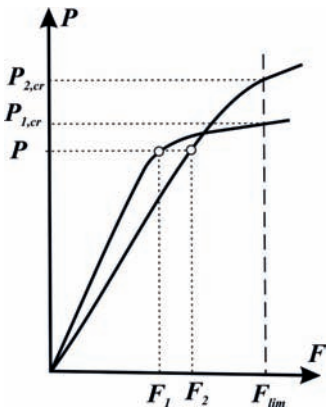

Figure 1

In fact, this approach is almost always used in experimental studies of the operation of a structure, where it is difficult (and sometimes impossible) to accurately capture the limit state and the experiment stops when, for example, deflections start increasing rapidly.

Statistical Justification of the Design Parameters

Since about the mid-60s, when the theory of reliability of building structures was actively developed, the limit state design method has been perceived as a tool for ensuring reliability. This was clearly indicated in GOST 27751-88. In accordance with Sec. 1.5 of this document, the limit state design is performed in order to ensure the reliability of a building or structure throughout the entire service life, as well as during the construction. The design values of loads or forces caused by them, stresses, deformations, displacements, crack opening widths must not exceed the corresponding limit values established by the design codes.

Since it is not possible to determine the reliability of the entire structure due to its extreme complexity, the reliability of the entire structure is determined by the reliability of its individual members. In fact, element-by-element analysis is performed, and the required reliability (probability of failure-free operation) of each individual element is provided. This

element-by-element check according to the weakest-link method assigns the entire structure a topology of series-connected members, which in reality is not always the case. **As a result, it is impossible to determine the actual value of the reliability of the designed structure**.

This fact reflects a logical contradiction in assessing reliability using the limit state design method, since reliability is the ability to fulfill the functional purpose, and it is normalized not by this indicator, but by the absence of failures.

The reliability of building structures is determined using the probabilistic approach [21], [22], [23]. Moreover, it is widely believed that only the probabilistic description of the structural behavior makes it possible to assess the reliability of buildings. And the limit state design method itself was created under the prevailing influence of the problem of random variability of the loading and resistance parameters of the structure. For example, when the method had just been created, the design values of the resistances were treated as statistically justified. However, due to the lack of reliable statistical data in the area of extreme sections of the distribution curves and a number of other circumstances (features of control procedures, different behavior of the material in the structure and in the samples, etc.), in 1971 it was decided that probabilistic considerations were not enough to justify the design resistances [9].

This process turned out to be uncontrollable, and today it is already difficult to say which of the partial safety factors, and to what extent, are not statistically justified, but are based on other considerations.

Reliability Management

The reliability requirements should obviously be formulated based on the actual facility (its importance, etc.). Hence, a reliability management mechanism is required.

In fact, management is implemented by using different design values for the considered actions (the higher the importance the higher the value), and assuming different service life. The differentiation of the approach was used in the limit state design method from the very beginning and was reduced to taking into account the differences between permanent and temporary structures, and to the use of various design combinations of loads (main, additional, special).

The direct mechanism of reliability management was introduced in 1981 and it lied in allowing for the importance of the structure, while all facilities were divided according to this criterion into three classes [24]: increased, normal and reduced levels of importance. The purpose of such a differentiation of reliability is the socio-economic optimization of resources used in construction taking into account the expected consequences of failure and the cost of construction. And the mechanism for allowing for the importance level was implemented in the form of another partial safety factor, which was introduced as a factor to the load effect.

Differentiation by class of importance was also used in relation to other aspects of ensuring the reliability of structures. Importance classes are involved, for example, in the engineering research and even in the applied calculation procedure (the linear spectral analysis or the analysis based on accelerograms), as is customary when checking the seismic response.

In relation to a structure or a structural member, reliability is considered as the ability not to reach a limit state over a certain period of time. Another parameter used in the reliability management is the design service life of the structure. It determines that during this period of time, the structure or its part should be used for its intended purposes with the necessary maintenance, but without large-scale repair work. This parameter is taken into account when developing measures to ensure the durability of structures and their foundations [18] or when assigning design values of climatic actions, as provided, for example, by the codes of Ukraine [11].

Post-critical Behaviour of a Structure

Considering the limit state as a critical and absolutely unacceptable design case, which underlay the classical version of the limit state design method, did not take into account the

possibility that the transition through the boundary outlined by the description of the limit state is not always fatal (Fig. 2.*a*). There are the so-called reversible limit states, which disappear once the actions that have caused them are removed (Fig. 2.*b*). Deflection of an elastic structure is a typical example. For such states, it can be useful to establish not only the defining boundary, but also the time period during which the structure can be outside this boundary.

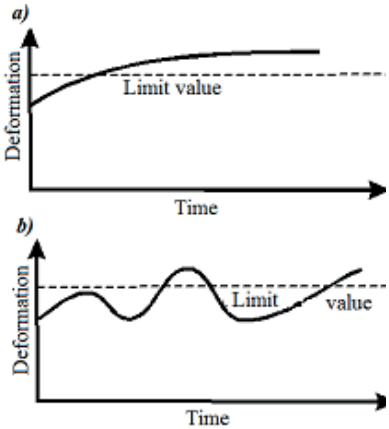

Figure 2

The design of highly directional antennas can serve as a typical example here, where the angular displacement is normalized, and its value directly determines the quality of radio transmission. If you agree to sacrifice this quality, for example, within 1% of the time, the wind load, under the action of which the deflection angle is determined, is reduced by 2-3 times.

However, consideration of a system in its post-critical state can be related not only to the reversible limit states. Thus, in the classical approach the ultimate limit states were assumed to be absolute and their violation was not allowed. This postulate was quickly violated in the theory of seismic protection.

A new definition of the concept of "limit state" was formulated in [25]. It was different from the classical one, where for the ultimate states it was identified with the impossibility of further operation of the facility. Some buildings damaged by an earthquake can still be operated after repair and restoration, so it was proposed to assume that they have not reached their ultimate limit state yet. The transition to multilevel seismic analysis, which implemented this innovation, pointed to the problem of formulating a series of limit states that differ in the degree of conservation and the possibility of using the facility under seismic actions of varying intensity (more precisely, different recurrence [26]).

Nonlinear Analysis Problems

The method was created at a time when all verification calculations were performed in a linear formulation, which significantly affected the technical side of the method. The widespread use of computer technology and the related increasing spread of nonlinear analysis indicated a number of problems that were not taken into account at the time [27].

Thus for all linear systems, the main inequality of the limit state design method is presented in a form that provides for the possibility of a separate description of the parameters of the structural behavior, depending on the load, and the parameters that determine the strength properties of the structure

$$\psi\gamma_n\gamma_f F_n \leq \gamma_c\gamma_m R_n.$$

However, this is not always feasible in nonlinear problems, where the uncertainties of the impact model and the resistance model can be closely related, for example, through the use of the same physical relationship $\sigma = f(\varepsilon)$. This issue occurs in some linear problems as well. Thus, for example, the reactions of the soil and its resistance cannot be considered separately, since the active pressure of the soil and its resistance depend on the action.

Checks of fulfillment of the inequalities usually operate not with the values of the design loads F_d, but with the values of the effects from these loads S_d (forces, stresses, displacements, etc.). One of the classical postulates of the limit state design method was the assumption of a deterministic and linear relationship between the action F and the effect of this action S. On its

basis, the partial safety factor for load was attributed to the effect of the action (stress, displacement, internal force, etc.). It was shown in [28] that this postulate is not always applicable.

Probabilistic characteristics S_d are often identified with the probabilistic characteristics of the load F_d, using the safety factor γ_f for S_d, the value of which is determined by the properties of the load. However, the effect of the action is a function of the action itself and the design model, therefore its variability V_S may differ from the characteristics of the variability of the action itself V_F. Such a coincidence always takes place for a linear relationship between S and F, but it will no longer exist for a nonlinear relationship $S = f(F)$. In this case the relationship between the rate of increase in stresses or other similar factors, which can be higher or lower than the rate of change of the external action, plays an important role (Fig. 3).

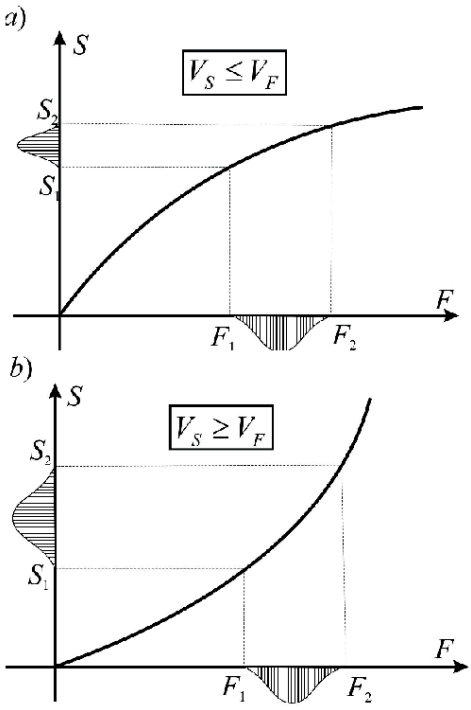

Figure 3

An even more complicated situation arises when the transition from F to S, even with a linear relationship $S=cF$, is such that the influence coefficient c turns out to be a random variable. A fairly typical case illustrating the last statement is the case of crane actions [28], when the design combination of loads (and the characteristics of the spread of their values) or the design combination of internal reactions of the system (forces, stresses, displacements) do not coincide. The transition from F to S takes place under the influence of a number of other random parameters, such as the random positions of the crane bridge on the crane girder and the trolley on the crane bridge. Consequently, the characteristics of the spread of the load values do not coincide with the similar characteristics of the load effects, which should actually lead to the use of different values of the safety factor for load (more precisely, for the load effect) when considering different problems.

Special Limit States

In his work [8] N.S. Streletsky pointed out two postulates that are inherent in the limit state design method: (a) the analysis is related to a failure-free state of structures and (b) an adequate structure immediately becomes inadequate the moment it passes the limit state. Ukrainian and Russian standards did not consider accidental situations for a long time, proclaiming that the considered limit states correspond not to accidental, but to pre-accidental situations. The introduction in 2010 of the third group of special limit states in GOST R 54257 was an attempt against the inviolability of these postulates.

It is usually assumed that special limit states caused by special accidental actions (impacts, explosions, etc.) occur in the form of a local destruction. These special limit states are studied in order to assess the possibility that such local destruction will not lead to a general collapse or an unacceptably large number of collapses.

In fact, we are dealing with the analysis of structural robustness, although this problem reduced to checking the ability of a damaged structure to perform its functions (possibly with some loss of quality) has been replaced by

checking for the absence of progressive (disproportionate) collapse. It should be noted that unlike the usual ultimate limit state analysis, where the local bearing capacity of a design section is analyzed, the concept of "bearing capacity" must be given a broader meaning and we must consider the structure as a whole when it comes to checking special limit states. However, it is much more difficult to formulate the criterion for reaching the limit state of an entire structure than of its individual section, and perhaps this is the reason for the indicated substitution.

The fact that this approach is not always applicable for the problems of robustness can be demonstrated with an example of the structures of gas holders, oil reservoirs etc. If such a structure is damaged, for example, a small crack appears, collapse will not occur, but the loss of integrity will lead to leakage of the stored substance, and therefore to the loss of the structural function. This is a vivid example that the absence of progressive collapse does not yet guarantee robustness.

The current state of the problem of analyzing special limit states does not yet have a clear conceptual justification. Such documents as SP 296.1325800.2017 [29] have only identified the problem and given some prescription recommendations. A common approach that is applicable not only for buildings is yet to be developed.

We, apparently, need a document like the General Safety Rules in the nuclear industry, which uses, for example, a principle of single failure and provides only rules of behavior for the beyond design basis accidents (notification, evacuation etc.), but not a requirement to resist them.

The very concept of special action has to be clarified. The current rule that does not consider the simultaneous action of two or more special loads is based on the fact that such actions have a very short duration and the probability of coincidence of such intervals is negligible. However, even a very short action can lead to long lasting consequences, which might still be present when another special action occurs. Actions arising from the wetting of subsidence soils or their subsidence in areas of mine workings and in karst areas can serve as an example. For example, an earthquake may well occur in the mined territories of Kuzbass.

Vulnerability Assessment

The limit state design method assumes that all loads and actions that may occur during the life cycle of the designed facility are considered and taken into account. However, besides the predictable loads, there is always a possibility of an accidental action not predicted neither by the design codes nor by the designer. American economist Nicolas Nassim Taleb called similar events "black swans"[1]. From the point of view of these surprise events vulnerability of the design object is an important characteristic.

Vulnerability characterizes a possibility of causing damages of any nature to the considered system by some external means or factors. Vulnerability is closely related to a well-known characteristic of "robustness" and to an additional characteristic — "mobilization" recently suggested in [30]. The robustness is considered as in a manner spatial characteristic which shows how a local perturbation spreads throughout the space of the system and whether this local destruction can get a disproportionately large development "in breadth".

Mobilization shows the readiness and ability of the system to react to a local in time (pulse) unexpected perturbation. In both cases, the perturbation can be so strong that we would have to deal with its consequences, and its nature is such that it is not possible to predict the moment and place of its occurrence, as well as other quantitative characteristics. Noticeable absence of the structural mobilization, as well as insufficient robustness, should serve as a reason for the increased attention and use of some protective measures.

[1] Juvenal said: "rara avis in terris nigroque simillima cygno"(lat.) - a "good man is as rare, as a black swan", since there was a hypothesis that all swans were white. It had been correct until a black Australian swan was discovered in 1700.

DISCUSSION

The limit state design method is constantly developing, allowing and undergoing improvements not only in its purely technical aspects, but also in some ideological foundations. At the same time, a number of issues related to such changes remain unresolved. We will consider only some of them.

A) The issue about the relationship between probabilistic and deterministic justification of partial safety factors is one of the fundamental ones. It is generally accepted that safety margins are intended to prevent the five main causes of failure:

(1) Loads are greater than anticipated.

(2) Material has poorer properties than anticipated.

(3) The theory of the considered failure mechanism is imperfect.

(4) Possible unknown and therefore unaccounted for causes of failure.

(5) Potential human errors (e.g. in the design).

The first two options can, generally speaking, be classified as variability in design parameters, so they are available for probabilistic estimation. The last three types of failure causes operate not with probabilities, but with possibilities, they are difficult or even impossible to represent in probabilistic terms, and therefore they belong to the category of non-statistical uncertainty.

And if we assume that the safety margin is intended to compensate for the main sources of failure, then we can assume that in the first two cases it is preferable to rely on probabilistic information. The main advantage of assigning safety factors on a non-statistical basis concerns the other three sources of failure. Therefore, the probabilistic approach should only be one of several tools for assessing reliability, and both approaches have their advantages, so they cannot be considered as mutually exclusive.

B) The group of special limit states introduced quite recently, where many things remain unclear, requires serious improvement. For example, the unusually widely understood tendency to use the method of exclusion of a structural member to test the possibility of progressive collapse, when it turned out that all statically determinate design models were impossible to use, raises many questions. This is a typical example, when they are trying to replace the method of analyzing a dangerous situation with a conditional technique having a limited scope (not explicitly specified).

C) In the design practice, the issues of analysis of load-bearing structures equipped with protection systems (seismic protection, fire protection, overload protection, etc.) are increasingly raised. For a load-bearing structure, these systems change the nature of action, their intensity and statistical properties. Both issues of checking the load-bearing capacity of a protected structure (what is the safety factor for load) and checking the protection system itself, which should have a certain guaranteed operability margin (what are the partial factors for such a check).

There are other problems related to the development of the limit state design method as well. In particular, the limit states arising in the course of long-term degradation (corrosion, wear, minor mechanical damage) remain unknown, which we try to analyze only at the end of the process, when the structure is on the verge of failure. In particular, a problem formulation of limiting the degradation rate is possible and, consequently, the problem of ensuring reliability for this indicator, including checking the limit state for violation of this rate.

CONCLUSIONS

For construction facilities, the issues of ensuring their existence and use for their intended purpose over the past decades have been interpreted as a subject of study of reliability problems. And the issues of practical implementation of the recommendations developed by the theory of reliability, which are the essence of the limit state design method, remained outside the scientific analysis. Consideration of the history of improvement of

the limit state design method shows that the method itself should be a subject of special consideration.

There has to be a clear formulation of the main provisions of the method, taking into account a number of new circumstances that are dictated by modern design practice:

- more frequent use of nonlinear analysis;
- limited and uncertain data on the expected operating conditions of the structure, when probabilistic methods are not applicable;
- using additional information that is available during the analysis of the behavior of existing structures (repair, restoration);
- the ability to use risk analysis when considering non-standard situations.

These and other similar issues should have become a subject of a specially organized scientific discussion, similar to the one that took place in the early seventies on the initiative of N.S. Streletsky at MGSU [31].

REFERENCES

1. **Baldin V.A., Goldenblat I.I., Kochenov V.I., Pildish M.Ya., Tal K.E.** Calculation of Building Structures According to the Limit States, M.: Stroyizdat, 1951 – 371 p.
2. **Randall F.A.** Historical Notes on Structural Safety // Proc. Amer. Concrete Inst., Vol. 70, 1977, pp. 669–679.
3. **Elishakoff I.** Essay on reliability index, probabilistic interpretation of safety factor and convex models of uncertainty // Reliability Problems: General Principles and Applications in Mechanics of Solids and Structures (F. Casciati and J. B. Roberts, eds.), Springer, 1991 – pp. 237–271.
4. **Raizer V.D.** Essay on the Development of the Theory of Reliability and Design Standards for Building Structures // Seismic Design. Safety of Structures, 2014, No. 2, pp. 29–35.
5. **Perelmuter A.V.** Selected Problems of Structural Safety and Reliability. 3-rd edition, revised and updated. – M.: ASV Publishing House, 2007. – 256 p.
6. **Perelmuter A.V., Kabantsev O.V. Pichugin S.F.** Fundamentals of the Limit State Design Method – M.: SCAD Soft, ASV, 2019. – 240 p.
7. **Gulvanesyan Kh., Kalgaro Zh.-A., Golitski M.** Designers' Guide to Eurocode 1990: Basis of Structural Design – M.: MGSU, 2011. – 258 p.
8. **Streletsky N.S.** Priority Issues of the Development of the Limit State Methodology // Development of the Limit State Design Method. – M.: Stroyizdat, 1971. – pp. 5-37.
9. **Baldin V.A., Gvozdev A.A., Streletsky N.N., Bat A.A., Efimov M.G., Lyalin I.B., Mitkheev V.V., Otstavnov V.A., Tal K.E**. To the release of SNiP II-A.10-71 "Structural Components and Foundations. Fundamental Design Principles" // Structural Mechanics and Analysis of Constructions, 1972, No.4. – pp. 56-59.
10. **Otstavnov V.A., Smirnov A.F., Rayzer V.D., Sukhov Yu.D.** Importance of Buildings and Structures in the Design Codes // Structural Mechanics and Analysis of Constructions, 1981, No.1. – P. 11–14.
11. DBN V.1.2-14-2018. General Principles of Reliability and Structural Safety of Buildings, Structures and Foundations – K.: Minregionbud, 2018. – 29 p.
12. **V.S. Karpilovsky, E.Z. Kriksunov, A.A. Malyarenko et.al.** "SCAD Office. Implementation of SNiP in Computer-Aided Design Applications". 4-th edition – M.: SCAD SOFT, 2018. – 567 p.
13. SNiP II-B.1-54. Main Recommendations for the Analysis of Building Structures // Construction Rules and Regulations. Part II. Construction Standards – M.: Gosstryizdat, 1954 – pp. 41–48.
14. SNiP II-A.10-62. Building Structures and Foundations. Basic Design Provisions – M.: Gosstryizdat, 1962 – 44 p.

15. SNiP II-A.10-71 “Structural Components and Foundations. Fundamental Design Principles” – M.: Stroyizdat, 1971 – 7 p.
16. GOST 27751-1988. Reliability for Constructions and Foundations. General Principles – M.: Standardinform, 1088 – 7 p.
17. GOST R 54257-2010. Reliability of Constructions and Foundations. Basic Principles and Requirements. – M.: Standardinform, 2021. – 13 p
18. GOST 27751-2014 Reliability for Constructions and Foundations. General Principles – M.: Standardinform, 2021 – 16 p.
19. **Iosilevsky L.I.** Practical Methods of Managing the Reliability of Reinforced Concrete Bridges – M. : SRC “Engineer”, 1999. – 295 p.
20. **Katyushin, V.V.** Buildings with Steel Frames of Variable Cross-Section (Analysis, Design, Construction) – M.: Stroyizdat, 2005. – 656 p.
21. **Bolotin V.V.** Application of the Methods of the Theory of Probability and the Theory of Reliability to Analysis of Structures. – M.: Stroyizdat, 1982. – 351 p.
22. **Rzhanitsyn A.R.** Theory of Reliability Analysis of Building Structures. – M.: Stroyizdat, 1978. – 239 p.
23. **Raizer V.D.** Probabilistic Methods in the Analysis of Reliability and Robustness of Structures – Moscow: ASV, 2018. – 396 p.
24. **Otstavnov V.A., Smirnov A.F., Rayzer V.D., Sukhov Yu.D.** Importance of Buildings and Structures in the Design Codes // Structural Mechanics and Analysis of Constructions, 1981, No.1. – P. 11–14.
25. **Bykhovsky V.A., Goldenblat I.I.** Designing Reliable and Optimal Earthquake-Resistant Structures // Seismic Resistance of Buildings and Engineering Structures – M.: Stroyizdat, 1967 – pp. 4-9.
26. **Perelmuter A.V., Kabantsev O.V**. On Conceptual Provisions of Design Standards for Earthquake-Resistant Construction // Vestnik MGSU, 2020, V. 15, Issue 12 – pp. 1673–1684. DOI: 10.22227/1997-0935. 2020.12.1673-1684.
27. **Perelmuter A.V., Tur V.V.** Are we ready to move on to nonlinear analysis in design? // International Journal for Computational Civil and Structural Engineering, 2017. Vol. 13, No 3 – pp. 86-102.
28. **Perelmuter A.V.** Statistical Modeling of Crane Loads and Design Combinations of Forces // International Journal for Computational Civil and Structural Engineering, 2017. Vol. 13, No 2. – pp. 136–144.
29. SP 296.1325800.2017. Buildings and Structures. Accidental Actions – M: Ministry of Construction of Russia, 2017 – 23 p.
30. **Perelmuter A.V.** Mobilization as a Characteristic of Reliability of Structures // International Journal for Computational Civil and Structural Engineering, 2017. Vol. 13, No 1. – pp. 86- 93.
31. Development of the Limit State Design Method / Collection of articles edited by Belenia E.I. – M.: Stroyizdat, 1971. – 175 p.

ЛИТЕРАТУРА

1. **Балдин В.А., Гольденблат И.И., Коченов В.М., Пильдыш М.Я., Таль К.Э.** Расчет строительных конструкций по предельным состояниям. – М.-Л.: Госстройиздат, 1951 – 371 с.
2. **Randall F.A.** Historical Notes on Structural Safety // Proc. Amer. Concrete Inst., Vol. 70, 1977, pp. 669–679.
3. **Elishakoff I.** Essay on reliability index, probabilistic interpretation of safety factor and convex models of uncertainty // Reliability Problems: General Principles and Applications in Mechanics of Solids and Structures (F. Casciati and J. B. Roberts, eds.), Springer, 1991, – P. 237–271.
4. **Райзер В.Д.** Очерк развития теории надежности и норм проектирования строительных конструкций // Сейсмостойкое строительство. Безопасность сооружений, 2014, №2 – С. 29–35.

5. **Перельмутер А.В.** Избранные проблемы надежности и безопасности строительных конструкций. 3-е изд, исправленное и дополненное. – М.: Изд-во Ассоциации строительных вузов, 2007. – 256 с
6. **Перельмутер А.В., Кабанцев О.В. Пичугин С.Ф.** Основы метода расчетных предельных состояний – М.: Издательство СКАД Софт, Издательский дом АСВ, 2019 – 240 с.
7. **Гульванесян Х., Калгаро Ж.-А., Голицки М.** Руководство для проектировщиков к Еврокоду 1990: Основы проектирования сооружений – М.: МГСУ, 2011 – 258 с.
8. **Стрелецкий Н.С.** К вопросу развития методики расчета по предельным состояниям // Развитие методики расчета по предельным состояниям. – М.: Стройиздат, 1971 – С. 5–37.
9. **Балдин В.А., Гвоздев А.А., Стрелецкий Н.Н., Бать А.А., Ефремов М.Г., Лялин Н.Б., Михеев В.В., Отставнов В.А., Таль К.Э.** К выходу СНиП II-А.10-71 «Строительные конструкции и основания. Основные положения проектирования» // Строительная механика и расчет сооружений, 1972, №4 – С. 56–59.
10. **Отставнов В.А., Смирнов А.Ф., Райзер В.Д., Сухов Ю.Д.** Учет ответственности зданий и сооружений в нормах проектирования строительных конструкций // Строительная механика и расчет сооружений, 1981, №1 – С. 11-14.
11. ДБН В.1.2-14-2018. Загальні принципи забезпечення надійності та конструктивної безпеки будівель, споруд, будівельних конструкцій та основ — К.: Мінрегіонбуд, 2018 — 29 с.
12. **Карпиловский В.С., Криксунов Э.З., Маляренко А.А., и др**. SCAD Office. Реализация СНиП в проектирующих программах. 4-е изд. – М.: Издательство СКАД СОФТ, 2018. – 567 с.
13. СНиП II-Б.1-54. Основные положения по расчету строительных конструкций // Строительные нормы и правила. Часть II. Нормы строительного проектирования – М.: Госстройиздат, 1954 – С. 41-48.
14. СНиП II-А.10-62. Строительные конструкции и основания. Основные положения проектирования – М.: Госстройиздат, 1962 – 44 с.
15. СНиП II-А.10-71. Строительные конструкции и основания. Основные положения проектирования – М.: Стройиздат, 1971 – 7 с.
16. .ГОСТ 27751-1988. Надежность строительных конструкций и оснований. Основные положения – М.: Издательство стандартов, 1088 – 7 с.
17. ГОСТ Р 54257-2010. Надежность строительных конструкций и оснований. Основные положения – М.: Стандартинформ, 2021 – 13 с.
18. ГОСТ 27751-2014 Надежность строительных конструкций и оснований. Основные положения – М.: Стандартинформ, 2021 – 16 с.
19. **Иосилевский Л.И.** Практические методы управления надежностью железобетонных мостов – М.: НИЦ «Инженер», 1999. – 295 с.
20. **Катюшин В.В.** Здания с каркасами из стальных рам переменного сечения (расчет, проектирование, строительство) – М.: ОАО «Издательство Стройиздат», 2005 – 656 с.
21. **Болотин В.В.** Методы теории вероятностей и теории надежности в расчетах сооружений – М.: Стройиздат, 1982 – 351 с.
22. **Ржаницын А.Р.** Теория расчета строительных конструкций на надежность – М.: Стройиздат, 1978 – 239 с.
23. **Райзер В.Д.** Вероятностные методы в анализе надежности и живучести сооружений – М.: Изд-во АСВ, 2018 – 396 с.
24. **Отставнов В.А., Смирнов А.Ф., Райзер В.Д., Сухов Ю.Д.** Учет ответственности зданий и сооружений в нормах проектирования строительных конструкций

// Строительная механика и расчет сооружений, 1981, №1 – С. 11-14.
25. **Быховский В.А., Гольденблат И.И.** К вопросу о надежности и оптимальности сейсмостойкого строительства // Сейсмостойкость зданий и инженерных сооружений – М.: Стройиздат, 1967 – С. 4-9.
26. **Перельмутер А.В., Кабанцев О.В.** О концептуальных положениях норм проектирования сейсмостойкого строительства // Вестник МГСУ, 2020, Т. 15, Вып. 12 – С. 1673–1684. DOI: 10.22227/1997-0935. 2020.12.1673-1684.
27. **Перельмутер А.В., Тур В.В.** Готовы ли мы перейти к нелинейному анализу при проектировании? // International Journal for Computational Civil and Structural Engineering, 2017. Vol. 13, No 3 – С. 86-102.
28. **Перельмутер А.В.** Статистическое моделирование крановых нагрузок и расчетные сочетания усилий // International Journal for Computational Civil and Structural Engineering, 2017. Vol. 13, No 2. – С. 136-144.
29. СП 296.1325800.2017. Здания и сооружения. Особые воздействия – М: Минстрой России, 2017 – 23 с.
30. **Перельмутер А.В.** Мобилизованность как характеристика надежности строительных конструкций // International Journal for Computational Civil and Structural Engineering, 2017. Vol. 13, No 1. – С. 86- 93.
31. Развитие методики расчета по предельным состояниям / Сборник статей пол ред. Е.И. Беленя – М.: Стройиздат, 1971 – 175 с.

Anatolii V. Perelmuter, Foreign member of Russian Academy of Architecture and Construction Sciences, Doctor of Science, Professor; SCAD Soft, Ltd; Kyiv 03037, Ukraine, 3a Osvity street, office. 1,2; phones: +38 044 249 71 93 (91), +38 050 382 1625, e-mail: AnatolyPerelmuter@sgmail.com. ORCID ID: 0000-0001-9537-2728

Перельмутер Анатолий Викторович, иностранный член РААСН, доктор технических наук, профессор; НПО СКАД Софт, 03037, Украина, г. Киев, ул. Просвящения, 3а, Офис 2; тел. +38 044 249 71 93 (91), +38 050 382 1625, e-mail: AnatolyPerelmuter@sgmail.com, ORCID ID: 0000-0001-9537-2728

DOI:10.22337/2587-9618-2021-17-4-146-152

NONLINEAR STRUCTURAL ANALYSIS BASED ON THE MODIFIED SEQUENTIAL LOAD METHOD

Vladilen V. Petrov

Saratov State Technical University named after Y. Gagarin, Saratov, RUSSIA
Research Institute of Building Physics of the Russian Academy of Architecture and Building Sciences, Moscow, RUSSIA

Abstract: The article discusses ways to improve the accuracy of solving problems of nonlinear structural mechanics. It is shown that the combination of the method of sequential loading and the Newton-Kantorovich method can improve the accuracy of the solution and reduce the complexity of obtaining results. The solution of the given linear equations can be obtained by numerical and approximate methods known in the literature.

Keywords: nonlinear mechanics, practical convergence, construction of an initial approximation, incremental equations, Freshet's derivative, Taylor series, abstract function.

РЕШЕНИЕ НЕЛИНЕЙНЫХ ЗАДАЧ СТРОИТЕЛЬНОЙ МЕХАНИКИ МОДИФИЦИРОВАННЫМ МЕТОДОМ ПОСЛЕДОВАТЕЛЬНЫХ НАГРУЖЕНИЙ

В.В. Петров

Саратовский государственный технический университет имени Гагарина Ю.А., г. Саратов, РОССИЯ
Научно-исследовательский институт строительной физики Российской академии архитектуры и строительных наук, г. Москва, РОССИЯ

Аннотация: В статье обсуждаются способы повышения точности решения задач нелинейной строительной механики. Показано, что сочетание метода последовательных нагружений и метода Ньютона-Канторовича позволяет повысить точность решения и уменьшить трудоемкость получения результатов. Решение приведенных линейных уравнений может быть получено известными в литературе численными и приближенными методами.

Ключевые слова: нелинейная механика, практическая сходимость, построение начального приближения, инкрементальные уравнения, дифференциал Фреше, ряд Тейлора, абстрактная функция.

Analysis of the majority of applied research in nonlinear mechanics shows that the mathematical foundations used in them often fundamentally differ from the classical mathematics logic. For example, when investigating the stress-strain state of a real structure, the proof of the convergence of an infinite process of improving the solution or checking the fulfillment of the conditions of the corresponding theorem on convergence are replaced by the clarification of the approximate convergence of this process. For this purpose, it requires small number of steps to increase the accuracy. And if a clear tendency towards convergence is found, then the solution refining process stops. Thus, we replace the endless process of striving for an exact solution by a finite number of steps to obtain an approximate solution.

When solving nonlinear problems by approximate methods, both of two key problems always arise: the choice or obtaining of an initial approximation to the solution and the choice or creation of a converging iterative process, which allows refining the initial approximation. Since the solution of nonlinear equations is not known in advance and it is not always possible to indi-

cate in advance the diameter of the region where it can be located, the problem of choosing an initial approximation often becomes essential.

It is known if the initial approximation belongs to the region of convergence of the iterative process, then the iterative process will converge to solving a nonlinear problem [1]. However, the radius of the convergence region changes during the process of solving a nonlinear problem with changing coefficients. For a weak nonlinearity, it is large enough. In this case, one can take the solution of a linear equation as an initial approximation, which is obtained by discarding the nonlinear terms in the original equations. For example, one applies this technique in framework of the method of elastic solutions [2] when solving problems based on the deformation theory of plasticity.

With an increase in nonlinearity, the size of the convergence region decreases, and the above method of the initial approximation obtaining can lead to the situation when it will be outside the convergence region. Then the use of an iterative procedure will generate a process converging to the convergence region boundary, and not to solving a nonlinear problem. In this case, it is necessary to organize the search for a suitable initial approximation. It should be borne in mind that in small neighborhoods of limiting points and bifurcation points, the convergence region decreases significantly and practically contracts to a point. In this regard, the problem arises of choosing or obtaining an initial approximation which falls into the region of convergence of the solution.

One of the methods for the approximate solution of nonlinear equations of solid mechanics is the sequential load method published in 1959 [3]. It allows one to obtain the solution of nonlinear problems by sequentially solving linear problems. This method is based on the principle of scientific determinism, which states that the subsequent states of a physical system are completely determined by its previous states. A detailed presentation of this method and its development for solving various problems of nonlinear mechanics of plates and shells can be found in the works [4 - 7].

The main idea of this method is quite simple. It is clear from physics if a load acts on a structure and causes large displacements or deformations, or both together, then the same stress and strain states of the structure can be obtained as follows. Let us imagine the load as a set of thin layers, the impact of each causes small deflections and deformations in the structure. At the first stage of the solution, we apply the first thin layer of the load and use the equations of the linear theory of elasticity to determine the stress-strain state of the structure. At the second stage of loading, we attach the second thin layer to the structure the deformations and internal forces of which is known from the first stage of loading. Then, second load layer causes additional small displacements and deformations, which are also determined from linear equations. Let us summarize the deformations and displacements found at the first and second stages of loading, and proceed to the third stage of loading with a small load layer. This process of sequential loading of the structure is repeated until the sum of the load layers reaches the specified value.

Durring the calculation process at each loading stage, we deal with a new computational linear system that has known deformations, forces and variable coefficients of linear equations from the results of previous loading. The advantage of the method is that in the process of calculations we determine the stress-strain state of the beam, plate or shell at all loads less than a given range, solving the similar recurrent equations. In addition, the procedure for constructing the zero approximation disappears. This approach to solving the problem is called incremental (from the word 'increment' that means an increase or addition, especially one of a series on a fixed scale).

The advantages of the sequential load method include the following. The principle of superposition is valid at each stage of loading. In the process of the problem solving, it is possible to determine the moment of appearance of plastic

deformations or a change in boundary conditions (constructive nonlinearity) and change the design scheme of the structure. The sequental load method makes it possible to select from the set of real solutions of nonlinear equations such a solution that corresponds to a continuous change in the load. As a result, we get a solution taking into account the loading history.

Incremental equations of the sequential load method can be obtained using the concepts and terminology of functional analysis. The set of equations of nonlinear solid mechanics or the resolving equation for a structural member under consideration can be written in the form of an operator equation:

$$A(u) = p \quad or \quad A(u,p) = 0 \qquad (1)$$

Further, we restrict research area by studying the behavior of the solution to this equation when it changes the load parameter.

Let us accept $E_1, E_2 -$ as linear normed Euclidean spaces, *A is a* – nonlinear display from E_1 to E_2. *A* is a nonlinear twice differentiable positive definite operator of Frechet in the Hilbert space *H; u* is the required element of this functional space. Operator A is defined on a certain set of functions with domain of definition $D(A)$. The functions and their first derivatives are absolutely continuous in the region Ω. Here Ω is the finite region of the coordinate space occupied by a beam, plate or shell. On the boundary Γ of the region Ω, the functions must satisfy the specified boundary conditions. The possibilities of using the operator form of equations for geometrically nonlinear problems are considered in the work [8]

Let us consider some fixed state $A(u_0) = p_0$. In an adjacent (perturbed) state caused by a small change in load, this equation takes the form

$$A(u_0 + \Delta u) = p_0 + \Delta p \qquad (2)$$

where Δu is an arbitrary element of Hilbert space *H*. Subtracting the original unperturbed equation from the perturbed equation, we obtain

$$A(u_0 + \Delta u) - A(u_0) = \Delta p \qquad (3)$$

Expanding the left part of this equation in a Taylor series in powers Δu, as a result, we obtain

$$A(u_0 + \Delta u) - A(u_0) = l(u_0)\Delta u + \omega(u_0, \Delta u) \quad (4)$$

The first term of the right part of this equality is a linear function of Δu which approximates the left part side up to values of the order of smallness that higher than the increment rate $\|\Delta u\|$.

$$\text{If} \quad \|\omega(u_0, \Delta u)\| \cdot [\![\Delta u]\!]^{-1} \to 0 \quad \text{for} \quad \|\Delta u\| \to 0$$

then $l(u_0)\Delta u$ is a Frechet derivative of an abstract function at a point u_0 that corresponds to increment of argument Δu, and the final member is the error due to the discarded terms with powers Δu greater than one.

Linear operator $l(u)$ is usually denoted as $A'(u)$ and called Frechet derivative of nonlinear operator A at the point *u*. Linear function $l(u_0)\Delta u$ can be considered as Gateaux derivative which is defined by formula

$$A'(u_0)\Delta u = \frac{d}{d\lambda} A(u_0 + \lambda \Delta u)\Big|_{\lambda=0}$$

where $\lambda -$ is variable small parameter.

Thus, taking into account the accepted designations, Eq. (4) can take the form

$$A(u_0 + \Delta u) - A(u_0) = A'(u_0)\Delta u + O(\|\Delta u\|) \quad (5)$$

Therefore, taking into account Eq. (3), the approximate incremental equation takes the form

$$A'(u)\Delta u = \Delta p \qquad (6)$$

In order to transform this equation in a recurrent form, we introduce the notation for the number of sequential loading *n*, and obtain the incremental equation of the sequential load method

$$A'(u_n)\Delta u_{n+1} = \Delta p_{n+1} \qquad (n = 0,1,2,3,...) \quad (7)$$

If E_1 is an Euclidean space, and E_2 is an abstract space (general linear space), then *A* mapping is called as an abstract function defined in E_1 *with* range E_2. This function can be written in the form $y = f(x)$, which is adopted in mathematics and operator equation (1) takes the form $p = Au$ [9].

Considering operator equation (1) as an abstract function, we can obtain equation (6) by geometric construction.

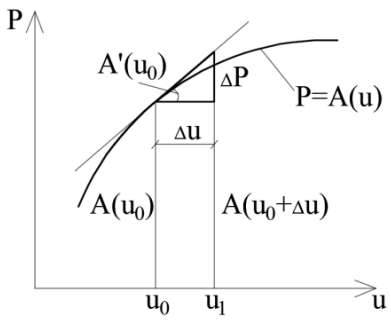

Figure 10

Figure 1 show that a continuous abstract function is replaced by some broken line as a result of the application of the sequential load method and the errors increase with an increase in the value of the load parameter. As follows from (5), the solution error can be regulated by decreasing the value of the loading step.

Let us consider another possibility of refining the solution obtained by the sequential load method. The total approximate solution obtained by the sequential load method at the nth stage of loading is denoted as u_n, where *n* is the number of the load layer. When refining the solution, we take it as the zero approximation $u_n^{(0)}$.

In order to refine the solution at the achieved value of the total load $p_n = \sum_n \Delta p_n$, we consider the adjacent disturbed state $A\left(u_n^{(0)} + \Delta u_n, p_n\right)$. Subtracting the original one from it, we get the differential expression

$$A\left(u_n^{(0)} + \Delta u_n, p_n\right) - A\left(u_n^{(0)}, p_n\right) \qquad (8)$$

Expanding it in a Taylor series in powers Δu_n, we get

$$A\left(u_n^{(0)} + \Delta u_n, p_n\right) - A\left(u_n^{(0)}, p_n\right) = A'\left(u_n^{(0)}\right)\Delta u_n + O\left(\|\Delta u_n\|\right) \qquad (9)$$

where the last term is the error of the order of the increment rate, arising due to the discarded terms with powers Δu_n greater than one. Keeping only the linear term in expansion (9), we obtain the equation

$$A\left(u_n^{(0)} + \Delta u_n, p_n\right) - A\left(u_n^{(0)}, p_n\right) = A'\left(u_n^{(0)}\right)\Delta u_n \quad (10)$$

Let us introduce the designation $\Delta u_n = u_n^* - u_n^{(0)}$, where u_n^* – a solution close to the exact solution of the equation (1). Taking this notation into account, Eq. (10) takes the form

$$A\left(u_n^{(0)} + u_n^* - u_n^{(0)}, p_n\right) - A\left(u_n^{(0)}, p_n\right) = A'\left(u_n^{(0)}\right)\left(u_n^* - u_n^{(0)}\right) \qquad (11)$$

This equation can be written like this

$$A'\left(u_n^{(0)}\right)\left(u_n^* - u_n^{(0)}\right) = A\left(u_n^*, p_n\right) - A\left(u_n^{(0)}, p_n\right) \quad (12)$$

where u_n^* is solution located closer to an exact solution than the initial approximation $u_n^{(0)}$. If the initial approximation $u_n^{(0)}$ is chosen close enough to the exact solution, then we can put $A\left(u_n^*, p_n\right) \approx 0$. Taking this into account, we obtain the equation

$$A'\left(u_n^{(0)}\right)\left(u_n^* - u_n^{(0)}\right) = -A\left(u_n^{(0)}, p_n\right) \quad (13)$$

the structure of which allows you to organize an iterative process of approximation to the exact solution. For this purpose, it is necessary to enter the iteration number *k* into this equation. We assume in equation (13) $u_n^{(0)} = u_n^{(k)}, \quad u_n^* = u_n^{(k+1)}$, and as a result, at each iteration, taking into account (1), we will have the linear equation

$$A'\left(u_n^{(k)}\right)\left(u_n^{(k+1)} - u_n^{(k)}\right) = p_n - A\left(u_n^{(k)}\right), \quad \left(k = 0, 1, 2, \ldots\right) \quad (14)$$

Equation (14) is written in full functions. If we introduce the notation $u_n^{(k+1)} - u_n^{(k)} = \Delta u_n^{(k+1)}$, where $\Delta u_n^{(k+1)} -$ is the change in the solution at the $k+1$ iteration, and the solution in full functions at this iteration is determined by the formula $u_n^{(k+1)} = u_n^{(k)} + \Delta u_n^{(k+1)}$, then, taking into account Eq. (1), we get the equation in increments.

$$A'\left(u_n^{(k)}\right)\Delta u_n^{(k+1)} = p_n - A\left(u_n^{(k)}\right), \quad \left(k = 0, 1, 2, \ldots\right) \quad (15)$$

where *k* is an iteration number, and *n* is a number of sequential load for which the initial approximation was chosen and the solution is refined. Equation (14) in full functions and equation (15) in incremental form have the form of equations of the Newton-Kantorovich method [3].

Operator equation (15) has the disadvantage that the Gateaux derivative $A'\left(u_n^{(k)}\right)$ depends on the iteration number *k*. Therefore, in order to obtain each of the kth approximations, it is necessary to re-solve equation (15). If the initial approximation $u_n^{(0)}$ is chosen close enough to the desired solution, then, due to the continuity of the operator A', the elements $A'\left(u_n^{(k)}\right)$ and $A'\left(u_n^{(0)}\right)$ will differ little. On this basis, L.V. Kantorovich proposed a modified method in which the sequence of approximations is determined from the solutions of the equations

$$A'\left(u_n^{(0)}\right)\Delta u_n^{(k+1)} = p_n - A\left(u_n^{(k)}\right), \qquad \left(k = 0,\ 1, 2, \ldots\right) \quad (16)$$

where for all *k*, when we find all approximations, the same Gateaux derivative $A'\left(u_n^{(0)}\right)$ is applied. Of course, the convergence rate of the modified method is lower, but L.V. Kantorovich proved theorems on the uniqueness of the solution and the convergence of the modified method to this solution.

The combination of two solution methods: the sequential load method and the Newton-Kantorovich method will be called the modified sequential load method, in which the initial approximation is constructed by the sequential load method, and the refinement is performed by the Newton-Kantorovich method. It should be noted that in this case the procedure for choosing the initial approximation disappears, since the initial approximation $u_n^{(0)}$ is the result of solving the problem at the end of the nth stage of loading.

Thus, the implementation of the modified sequential load method for solving problems of nonlinear structural mechanics is carried out as follows. The lateral load acting on the structure is presented in the form of a set of rather thin layers, which sequentially load the structure under consideration.

At the first stage of loading, we solve the usual problem of linear structural mechanics. At the subsequent stages of loading, we solve the following equations

$$A'\left(u_{n-1}\right)\Delta u_n = \Delta p_n, \qquad \left(n = 1, 2, \ldots\right) \quad (17)$$

Figure 2 shows that increasing in the number of loading stages n leads to accumulation of the solution error due to linearization of the original equation (1). This can be reduced by decreasing the value of the load increment (curves 1, 2). However, this increases the number of loading stages and the complexity of the solution. In addition, it is necessary to separately decide on the choice of the value of the load increment.

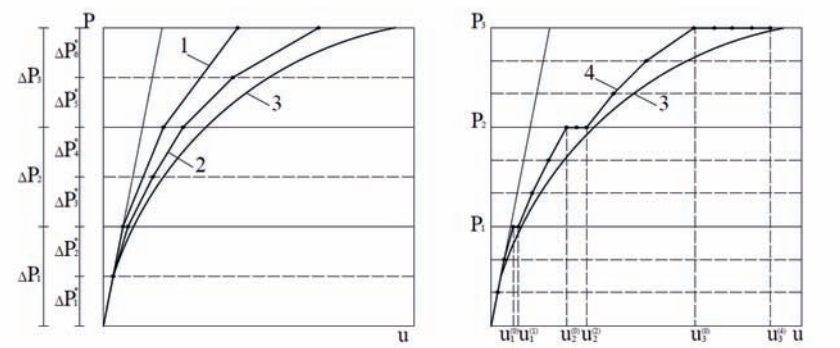

Figure 2

At the end of each nth loading stage or after several loading stages, the linearization error is reduced by the Newton-Kantorovich method (15) or its modification (16), in which the value $u_n^{(0)} = \sum_n \Delta u_n$ obtained at the end of the nth loading stage is taken as the initial approximation. Note, when we refine the solution, the iteration number k increases, while the number of the loading step n remains constant.

The solution refined by the Newton-Kantorovich method at the nth stage of loading is taken as an initial approximation for further solution by the sequential load method. Note, when we refine the solution, only the number of the loading step n increases, while the iteration number k remains constant. After the implementation of several or each of the sequential loads, the solution is refined by the Newton-Kantorovich method (see Fig. 2, curve 4). The value of sequentially applied load layers can be significantly increased and it can be changed in the process of solving depending on the features of the problem being solved. This reduces the complexity of obtaining a solution. Boundary value problems are realized by well-known methods for solving linear equations.

REFERENCES

1. **Vlasova L.A., Zarubin V.S., Kuvyrkin G.N.** Priblizhennyye metody matematicheskoy fiziki [Approximate methods of

mathematical physics]. Moscow: Publishing of MGTU named after N.E. Bauman, 2001. – 700 p.
2. **Il'yushin A.A.** Plastichnost' [Plasticity]. Moscow – Leningrad: OGIZ. 1948, ch. 1.
3. **Petrov V.V.** K raschetu pologikh obolochek pri konechnykh progibakh [Calculation of shallow shells with finite deflections]. – Nauchnyye doklady vysshey shkoly. Stroitel'stvo [Scientific reports of higher education. Construction], 1959, No 1.
4. **Petrov V.V.** Metod posledovatel'nykh nagruzheniy v nelineynoy teorii plastinok i obolochek [The sequential load method in the nonlinear theory of plates and shells]. Publishing of Saratov State University, 1975.
5. **Petrov V.V., Ovchinnikov I.G., Yaroslavskiy V.I.** Raschet plastinok i obolochek iz nelineyno-uprugogo materiala [Calculation of plates and shells made of nonlinear elastic material]. Publishing of Saratov State University, 1976.
6. **Petrov V.V.** Nelineynaya inkremental'naya stroitel'naya mekhanika [Non-linear incremental building mechanics]. – Moscow: Infra-Inzheneriya, 2014. – 480 p.
7. **Petrov V.V.** Nelineynaya stroitel'naya mekhanika [Non-linear construction mechanics]. Moscow: Publishing ASV, 2019. – 432 p.
8. **Srubshchik L.S.** Vypuchivaniye i poslekriticheskoye povedeniye obolochek [Buckling and post-critical behavior of shells]. Publishing of Rostov State University. 1981.
9. **Lyusternik L.A., Sobolev V.I.** Elementy funktsional'nogo analiza [Elements of functional analysis]. Publishing “Nauka”. Moscow 1965.
10. **Kantorovich L.V., Akilov G.P.** Funktsional'nyy analiz [Functional analysis]. Moscow, Nauka, 1977.

СПИСОК ЛИТЕРАТУРЫ

1. **Власова Л.А., Зарубин В.С., Кувыркин Г.Н.** Приближенные методы математической физики. М.: Изд-во МГТУ им. Н.Э. Баумана, 2001. – 700.
2. **Ильюшин А.А.** Пластичность. М. – Л. ОГИЗ. 1948, ч. 1.
3. **Петров В.В.** К расчету пологих оболочек при конечных прогибах. – Научные доклады высшей школы. Строительство, 1959, №1.
4. **Петров В.В.** Метод последовательных нагружений в нелинейной теории пластинок и оболочек. Изд-во Саратовского ун-та, 1975.
5. **Петров В.В., Овчинников И.Г., Ярославский В.И.** Расчет пластинок и оболочек из нелинейно-упругого материала. Изд-во Саратовского ун-та, 1976.
6. **Петров В.В.** Нелинейная инкрементальная строительная механика. – М.: Инфра-Инженерия, 2014. – 480 с.
7. **Петров В.В.** Нелинейная строительная механика. Изд-во АСВ. М. 2019. – 432 с.
8. **Срубщик Л.С.** Выпучивание и послекритическое поведение оболочек. Изд-во Ростовского ун-та. 1981.
9. **Люстерник Л.А., Соболев В.И.** Элементы функционального анализа. Изд-во «Наука». М. 1965.
10. **Канторович Л.В., Акилов Г.П.** Функциональный анализ. М. Наука, 1977.

Vladilen V. Petrov, full member of the Russian Academy of Architecture and Construction Sciences (RAASN), Doctor of Technical Sciences, Professor of the Department of Theory of Structures and Building Structures, Saratov State Technical University named after Y. Gagarin; 410054, Russia, Saratov, st. Polytechnic, 77; Tel. +7 (909) 388-41-20; e-mail: vvp@sstu.ru, vladilen307@gmail.com

Петров Владилен Васильевич, академик Российской академии архитектуры и строительных наук (РААСН), доктор технических наук, профессор кафедры «Теория сооружений и строительных конструкций» Саратовского государственного технического университета имени Гагарина Ю.А.; 410054, Россия, г. Саратов, ул. Политехническая, 77; тел. +7(909)388-41-20; e-mail: vvp@sstu.ru, vladilen307@gmail.com

DOI:10.22337/2587-9618-2021-17-4-153-160

ANSYS CFX STUDY OF AERODYNAMIC CHARACTERISTICS DURING BLADE PROFILE ROTATION

Andrey Yu. Proskurin, Yulia G. Zheglova

Moscow State University of Civil Engineering, Moscow, RUSSIA

Abstract. Currently, wind energy is one of the most developing areas, which is primarily due to the absence of emissions of harmful substances into the atmosphere. Wind power allows providing electricity to remote areas, where fuel delivery, as well as the construction of thermal power plants is laborious and expensive. The effective development of wind turbines should solve the following tasks: the creation of the necessary driving force and the possibility of using a high coefficient of wind energy, which does not contradict the maintenance of the ecological balance of the territory. An electric generator for a household wind turbine must provide electricity in a wide range of rotation speeds and be able to work independently without automation and external energy sources. The study of the numerical implementation of the method of aerodynamic analysis of the wind turbine blade in rotational motion in the ANSYS CFD software package is by far the most promising and dynamically developing direction in the field of aerodynamics calculations. The results of approbation of the mixed calculation method using a dynamically variable and stationary finite-volume mesh are presented. The use of a mixed design scheme allows for calculations of wind turbines inside the building, while it becomes possible to minimize the required power for the study.

Keywords: numerical simulation, aerodynamic processes, Ansys CFD, energy efficiency, alternative energy sources in construction, wind turbine, wind turbine blade, navier-stokes equations.

ИССЛЕДОВАНИЕ АЭРОДИНАМИЧЕСКИХ ХАРАКТЕРИСТИК ПРИ ВРАЩЕНИИ ПРОФИЛЯ ЛОПАСТИ В ANSYS CFX

А.Ю. Проскурин, Ю.Г. Жеглова

Московский Государственный Строительный Университет, Москва, РОССИЯ

Аннотация. В настоящее время ветроэнергетика является одним из наиболее развивающихся направлений, что обусловлено, прежде всего, отсутствием выбросов вредных веществ в атмосферу. Ветроэнергетика позволяет обеспечить электроэнергией отдаленные районы, где доставка топлива, а также строительство тепловых электростанций трудоемки и затратны. Эффективное развитие ветроэнергетики должно решать следующие задачи: создание необходимой движущей силы и возможность использования высокого коэффициента использования энергии ветра, что не противоречит поддержанию экологического баланса территории. Электрогенератор для бытовой ветроустановки должен обеспечивать электроэнергию в широком диапазоне скоростей вращения и иметь возможность автономной работы без автоматики и внешних источников энергии. Исследование численной реализации метода аэродинамического анализа лопасти ветрогенератора во вращательном движении в программном комплексе ANSYS CFD на сегодняшний день является наиболее перспективным и динамично развивающимся направлением в области расчетов аэродинамики. Предварительно представлены результаты апробации смешанного метода расчета с использованием динамически изменяемой и стационарной конечно-объемной сетки. Использование смешанной расчетной схемы позволяет проводить расчеты ветровых турбин внутри здания, при этом появляется возможность минимизировать необходимую для исследования мощность.

Ключевые слова: численное моделирование, аэродинамические процессы, Ansys CFD, энергоэффективность, альтернативные источники энергии в строительстве, ветротурбина, лопасть ветротурбины, уравнения Навье-Стокса.

INTRODUCTION

The task of creating energy-independent buildings in the modern world is very important for the whole world. The resources of the earth are inexorably running out and mankind needs to place great emphasis on the development of new alternative energy sources. Modern architectural solutions in the construction of metropolitan areas seek to use high-tech photovoltaic facades and flexible solar membranes to obtain the solar energy needed for the construction of capital construction projects. Through the combined use of wind and solar energy, we have the opportunity to design a building that integrates different methods of generating clean energy, which, in turn, will bring the building to its intended full self-sufficiency in electricity.

1 Materials and methods

1.1 Problem definition

To solve the problem of assessing the aerodynamic characteristics, a single-blade orthogonal high-efficiency turbine was adopted. (US patent Victor Lyatkher, US 8007235 B1, August 30, 2011, RF patent 2426911 C1). Since the profile of the investigated blade corresponds in cross-section with the aviation profile NACA-0021, it was decided to accept the geometric characteristics according to the reference materials. [3] Fig. 1 shows a cross-section of the blade profile under investigation.

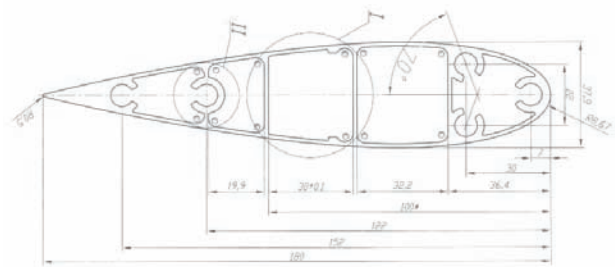

Figure 1. The cross-section of the blade profile under investigation

The aim of this work is to test the technique of numerical simulation of a rotating blade under the influence of an aerodynamic load in an unsteady turbulent flow in a two-dimensional setting. The problem of this installation is the occurrence of vibrations during the rotation of the blade at the points of attachment to the pedestal. At the moment, the study consists in determining the aerodynamic characteristics and an average assessment of the energy efficiency of the installation. As a research method, we used computer simulation of air flow around a wind turbine blade in the ANSYS software package [13].

In this work, this method takes into account the position of the blade in time, analyzing the equations of the translational and rotational motion of a rigid body. The solution of the unsteady Navier-Stokes equation is carried out at each calculated time, taking into account the previous results obtained at the previous step. This technique is very time consuming and resource consuming, but it allows you to analyze the behavior of the flow when flowing around a rotating body[11].

1.2 Stages of the Grid Convergence Study

Since there is no data on which it appears possible to determine the parameters of the calculated grid, it was concluded that it is necessary to conduct a series of verification calculations. The geometrical parameters of the grids can be seen in Table 1.

Using the built-in Ansys Workbench Meshing module, a tetraidal mesh was created. In all cases, the mesh size in the cylinder area and in the tail area the mesh has the same dimension of 0.06 m; in the outer area, the dimension was taken equal to 0.75 m. The problem was solved for four variants of the computational grid in order to find the optimal parameters of the computational grid. For the results to be accurate, it is necessary to create a boundary layer area all along the blade profile. The dimension of the boundary layer was determined based on the profile geometry, Reynolds number and turbulence model [4].

Table 1. Characteristics of computational grids

Model	Hydraulic diameter	Reynolds number	Estimated Y +	Estimated distance from the wall	Thickening of the mesh in the longitudinal direction
1	0.38	5.0e+4	1	1.3e-4	1.0e-2
2	0.38	5.0e+4	8	1.0e-3	1.0e-3
3	0.38	5.0e+4	40	5.0e-3	5.0e-2
4	0.38	5.0e+4	50	6.3e-3	1.0e-2
5	0.38	5.0e+4	80	1.0e-2	1.0e-2

Table 2-3 show the results of the verification tasks. The tables show the aerodynamic characteristics at different geometric characteristics and different Y+ coefficients.

Table 2. Comparison of aerodynamic coefficients with experimental data (Cd, Cl, Cm) for all calculation options (Y + = 1, Y + = 40, Y + = 50, Y + = 80).

Y +	Cd (experiment)	Cd (payment)	Cd Error	Cl (experiment)	Cl (payment)	Cl Error	Cm (experiment)	Cm (payment)	Cm Error
1	0.042	0.029	-30.9 %	0.79	0.469	-40.6%	-0.045	-0.018	-60%
40	0.042	0.024	-42.85%	0.79	0.7	-11.39%	-0.045	-0.028	-37.7%
50	0.042	0.039	-19.04%	0.79	0.72	-8.86%	-0.045	-0.039	13.6%
80	0.042	0.0323	-23.09%	0.79	0.749	-5.189%	-0.045	-0.03	-33.3%

Table 3. Comparison of aerodynamic coefficients (Cd, Cl, Cm) for all calculation options (Y + = 1, Y + = 40, Y + = 50, Y + = 80).

Y +	50 (Reference)	1	Error	50 (Reference)	40	Error	50 (Reference)	80	Error
Cd	0.034	0.029	20.8%	0.024	0.024	0%	0.034	0.0223	-7.1%
Cl	0.72	0.469	-34.9%	0.72	0.7	-2.7%	0.72	0.749	4.1%
Cm	-0.039	-0.02	-37.8%	-0.039	-0.03	-3.4%	-0.039	-0.03	7.1%
Cd	0.034	0.029	20.8%	0.024	0.024	0%	0.034	0.0223	-7.1%

After analyzing and comparing the results of the calculated parameters of CFD calculations with the results presented in the source [3], the Y + 50 model is the most accurate for the performed non-stationary calculation based on the previous experience, which showed the smallest error in determining the aerodynamic coefficients in aggregate. In the case of estimating the drag coefficient, the largest error is -46.9%, the lift coefficient is -40.6%, and the lift coefficient is -60%. As a result of verification studies, the smallest discrepancy in criterion parameters with exper-

imental data was obtained for the design case with Y + = 50, therefore, it was decided to use this mesh as a design mesh for modeling a rotating blade under the influence of an aerodynamic load.

1.3 Boundary and initial conditions.Calculation parameters

The calculated geometry is presented in the form of a circle, which makes it possible to investigate the problem at different angles of air flow incursion. The flow velocity was assumed to be 15 m/s with a percentage of turbulence up to 7%. On both sides of the model, the conditions were built so as to take into account the curvature of the circle and simulate the flowing perpendicular to the blade of the wind turbine. On the lower part of the model, "slip walls" conditions were adopted (FreeSlipWall, U = V = W = 0 m/s). Open boundary conditions were set on the upper part. The RigidBody Solution was used to solve the blade rotation problem with the possibility of rotation with respect to the Z-axis. The cylindrical domain was created as a subdomain with adjustment of the finite element mesh recalculation due to blade rotation. The subdomain, domain interfaces, and vane must share the same air characteristics. This is necessary because the inner cylinder and solid must move and rotate at the same speed to properly isolate the motion. All relative motion between the inner cylinder and vane will be eliminated, resulting in a null grid deformation inside the inner cylinder. [10].

The interface for one domain has been changed to limit the rotational movement of the mesh surrounding the subdomain. The mesh located on the inner cylindrical interface of the domain will have the same physical properties as in the solid form. Since the rotation cannot start without outside help, the initial angular velocity was initialized, no other external accelerations were initialized.

The interface of the second domain was configured in such a way that the air flow freely and without loss of properties passed from one computational domain to another. Both areas of a larger radius and a smaller one are stationary and do not require special settings for a finite-volume mesh. A visualization of the calculation model can be seen in Fig. 2.

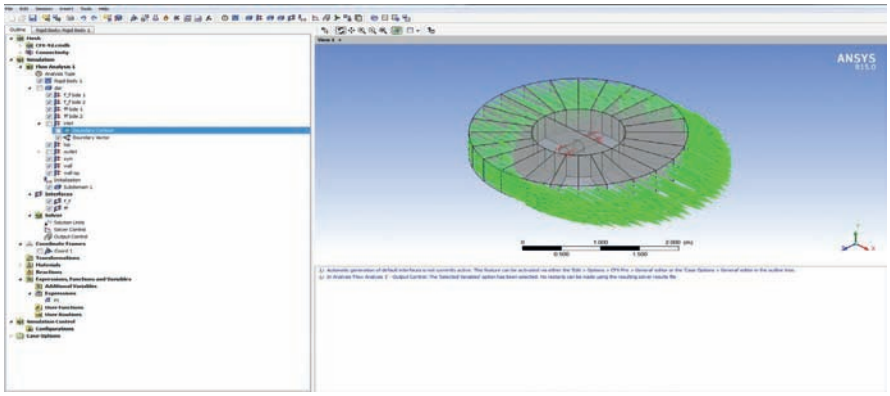

Figure 2. Calculation in the CFX software package (boundary conditions)

2 Results of the study

2.1 Results of computer simulations in ANSYS CFD

The calculations were carried out in a three-dimensional non-stationary setting. The following basic physical characteristics of the flow are given for aerodynamic calculations Re = 50,000. Fig. 3-7 show the main results of computational studies performed in the rotation of the blade of the wind turbine at different moments of time, the analysis of aerodynamic characteristics.

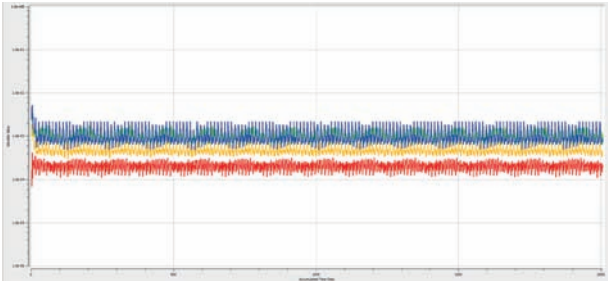

Figure 3. Calculation in the CFX software package (Masses and Moments)

Fig. 4-5 show the distribution of pressure values at different points in time. The figures show the change in blade position over time, leading to different pressure patterns on the profile itself. It can be seen that the pressure reaches its maximum value at the points where the profile experiences the maximum airflow resistance.

Fig. 8 shows graphs of frequencies of aerodynamic forces as the blade rotates

The graphs of the investigated forces show the non-stationarity of the modeled process, each wave corresponds to 1 rotation of the blade.

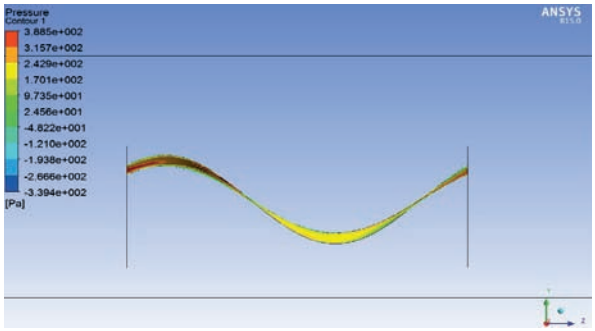

Figure 4. Isofield of pressures on the blade (frontal part) at time moment 0.5 sec

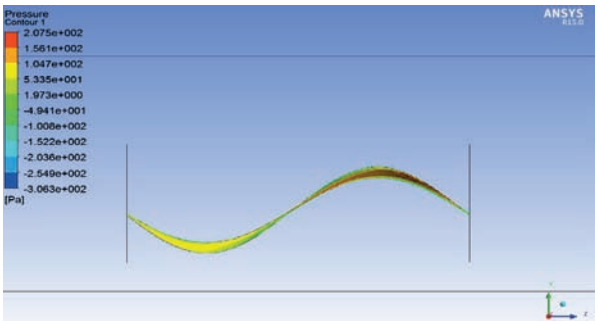

Figure 5. Isofield of pressures on the blade (frontal part) at time moment 5.5 sec

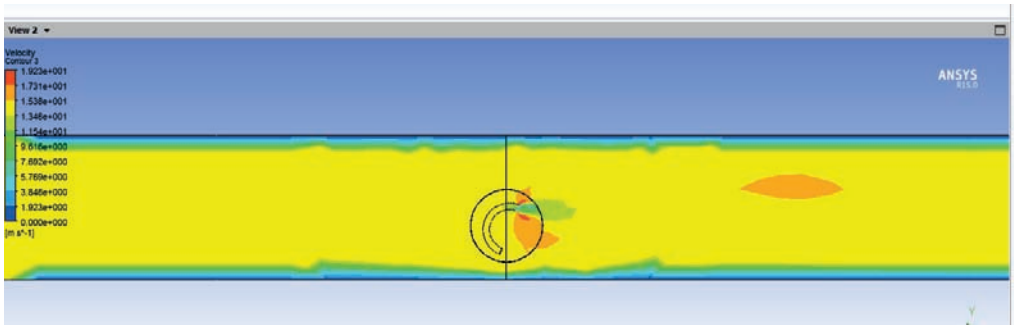

Figure 6. Isofields of pressures in the common domain at the time of 2.5 sec

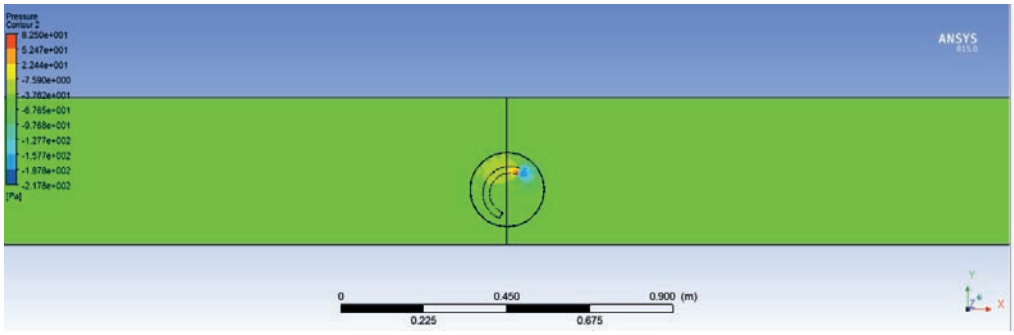

Figure 7. Isofields of velocities in the common domain at the time of 2.5 sec

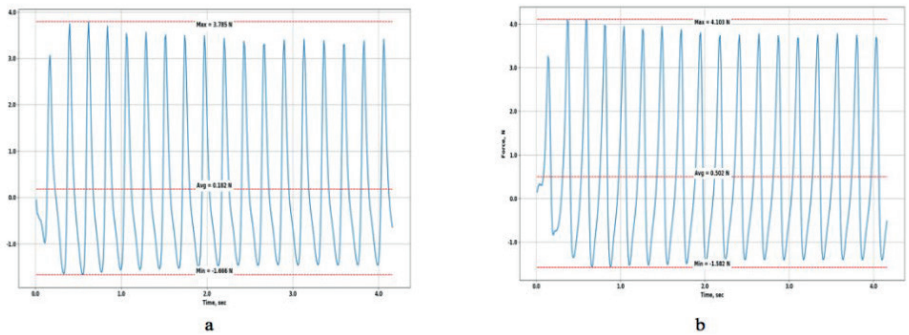

a b

Figure 8. Graphs of the investigated aerodynamic characteristics during the rotation of the blade a) Lift force in time b) The force of frontal resistance in time

2.2 Energy efficiency calculation

Unfortunately, the initial data is not enough for a complete analysis of energy efficiency data, however, the known dimensions make it possible to determine the amount of energy generated based on the throwing area.

Table 4 shows the values of generated energy at different air flow velocities. These values are calculated based on the size of the swept area.

Table 4. Power Generated Summary Table

Flow rate,m/s	Air density, kg/m3	The amount of generated energy, kW.
2	1.185	0.09
5	1.185	1.475
10	1.185	11.8
15	1.185	39.8
20	1.185	94.4
25	1.185	184.3

DISCUSSION

The analysis of frequencies, see Fig. 8, shows the coincidence with the rotational speed of the blade, while the rotational speed remains constant, the time of 1 revolution of the blade is 1.7 seconds. What can be said about the fact that the wind turbine rotates normally. The study shows the consistency of the method for calculating the blade, taking into account the take-off of the blade from the effect of the air flow.

As can be seen from Table 4, at a flow rate of 25 m / s, the blade almost completely allows a small house to be supplied with energy. This allows us to conclude that a large number of such generators will be able to replace the current "harmful" power plants with more environmentally friendly ones. At the current stage, it was possible to fully implement the dynamic calculation, with the implementation of the rotation of the wind turbine blade under the action of the air flow. The use of a mixed calculation will allow further research into the integration of a wind turbine blade into the structure of a building. With the creation of geometric design features that will increase the oncoming flow velocity.

CONCLUSIONS

The solution of the current problems showed the consistency of the project and its relevance, in the future it is necessary to carry out a numerical

solution of a coherent problem, which will consist of calculating the bearing capacity of the building, taking into account the aerodynamic component and parallel calculation of the wind turbine for energy efficiency and aerodynamic characteristics and transmission of vibrations from the rotation of the wind generator.

REFERENCES

1. **Garbaruk A.V., Strelets M.Kh., Shur M.L.**: Turbulence Modelling in Combined Flow Calculations. Tutorial, St. Petersburg (2012).
2. **Lutsky A.E., Severin A.V.** The simplest implementation of the method of wall functions. Preprints of the Keldysh Institute M.V. Keldysh,38 (2013).
3. Handbook of Aviation Profiles.
4. **Schlichting, G.** Boundary Layer Theory. Nauka,Moscow (1974).
5. **Gorlin S.M.** Experimental Aerodynamics. Vysshaya Shkola, Moscow (1970).
6. ANSYS, Inc., "ANSYS 15 Help", 2014.
7. **Tominaga, Y., Mochida, A.** AIJ guidelines for practical applications of CFD to pedestrian wind environment around buildings. Journal of Wind Engineering and Industrial Aerodynamics 96, 1749-1761 (2008).
8. **Kozhukhov Yu.V., Reshetnikova L.V., Zhalmurzieva G.I.** Numerical experiment in software package ansys cfx for impeller and bladeless diffuser model of medium frequency centrifugal compressor stage. Polytechnic University Press, St. Petersburg (2012).
9. **Kozhukhov Yu.V., Tribunskaya K.S.** Numerical experiment and data analysis of axial turbocharger compressor stage calculation in ansys cfx software package. Polytechnic University Press, St. Petersburg (2012).ANSYS CFX 14.5: Руководство пользователя / ANSYS Inc., 2014.
10. **Roach, P**. Computational Fluid Dynamics. Mir, Moscow (1980).
11. **Federova. N., ValgerS., Danilov M., Zakharova Y.** Fundamentals of Ansace 17. DMK Publishing House (2017).
12. **Kozhukhov, Yu.V., Lebedev A.A., Danilishin A.M., Davletgareev E.V.** Auditing Characteristics of Wind Turbine Generators Using CFD Modeling on Supercomputer. Polytechnic University Press (2016).
13. **Afanasieva N. I., Lantsova I. Yu.** Numerical modelling of elastic structure behaviour under transient fluid flow excitation. Proceedings of the AIP 1800 Conference, 1-10 (2017).
14. **Simiu E., Scanlan R.** Influence of Wind on Buildings and Structures. Stroyizdat,Moscow (1984).
15. **Savitsky G.A.** Wind loads on structures. Publishing House of Literature on Construction, Moscow (1972).
16. **S. Andreev. V., Bondarev A.E., Bondarenko A.V., Vizilter Y., Galaktionov V.A., Gudkov A.V., Zheltov S.Yu., Zhukov V.T., Ilovajskaya E.B., Kniaz V.A., Manukovsky K.V., Novikova N.D., Ososkov M.V., Silaev N.Yu., Feodoritova O.B., Bondareva N.A.:** Simulation and Visualization of the Complex Shape Blade Assembly in Power Plant. Journal of Scientific Visualization 4(7), 1-12 (2015).
17. **Kholshchevnikov K.V.** Theory and Calculation of Aircraft Blades. Mashinostroenie, Moscow (1970).

СПИСОК ЛИТЕРАТУРЫ

1. **Гарбарук А.В., Стрелец М.Х., Шур М.Л.** Моделирование турбулентности в расчетах сложных течений. Учебное пособие. // СПб., 2012.
2. **А. Е. Луцкий, А. В. Северин,** “Простейшая реализация метода пристеночных функций”, Препринты ИПМ им. М. В. Келдыша, 2013, 038, 22 с.
3. Справочник Авиационных Профилей.
4. Strojniški vestnik - Journal of Mechanical Engineering 60(2014)12 Received for review: 2014-02-03 © 2014.
5. **Шлихтинг Г.** Теория пограничного слоя 36 с.

6. **Берг О.И.** Принципы построения и элементы систем управления автономных комплексов электроснабжения на возобновляемых источниках энергии, 2015, 88 с.
7. **Горлин С.М.** Экспериментальная аэродинамика. // М.: «Высшая школа», 1970. – 423 с.
8. ANSYS, Inc., “ANSYS 15 Help”, 2014.
9. MInternational Journal for Computational Civil and Structural Engineering
10. **Tominaga, Y., Mochida, A.** AIJ guidelines for practical applications of CFD to pedestrian wind environment around buildings // Journalof Wind Engineering and Industrial Aerodynamics, Volume 96, Issues 10-11,October-November 2008, p. 1749-1761.
11. **Кожухов Ю.В., Решетникова Л.В., Жалмурзиева Г.И.** Численный эксперимент в программном комплексе ansyscfx для рабочего колеса и безлопаточного диффузора модельной центробежной компрессорной ступени средней быстроходности. [XLI Неделя науки СПбГПУ.: материалы международной научно-практической конференции. Ч. III.] -СПб.: (Изд-во Политехн. ун-та, 2012. 104 с)
12. **Кожухов Ю.В., Трибунская К.С.** «Проведение численного эксперимента и анализ данных расчёта ступени осевого компрессора турбонаддува в программном комплексе ansyscfx.» // [XLI Неделя науки СПбГПУ.: материалы международной научно-практической конференции. Ч. III.] - СПб.: (Изд-во Политехн. ун-та, 2012. 102 с.)
13. **Горлин С.М.** Экспериментальная аэродинамика. // М.: «Высшая школа», 1970. – 423 с.
14. ANSYS CFX 14.5: User's Manual [Электронныйресурс] / ANSYS Inc., 2014. http://www.ansys.com
15. **Руденко В.А.** Разработка и исследование системы метрологического обеспечения измерений и учёта попутного нефтяного газа.
16. **Роуч П.** Вычислительная гидродинамика. // М.: Мир, 1980. – 616 с.

Zheglova Julia Germanovna, PhD in Technical Sciences, Associate Professor of Information Systems, Technologies and Construction Auto-mation Department, Moscow State University of Civil Engineering. Russian Federation, Moscow, Yaroslavskoe shosse 26k1. +7(495)287-49-19 (ext. 30-41) email: uliagermanov-na@yandex.ru ORCID - 0000-0001-8121-8535, ScopusID - 57202228987

Proskurin Yu. Andrei, Lecturer of Department of Informatics and Applied Mathematics, Mos-cow State Construction University. Russian Federation, Moscow, Yaroslavskoe shosse 26k1. 8-495-183-59-94 email: proskurina-yu@mgsu.ru

Жеглова Юлия Германовна, кандидат технических наук, доцент кафедры информационных систем, технологий и автоматизации в строительстве Московского Государственного строительного университета. Российская Федерация, г Москва Ярославское шоссе 26к1. +7(495)287-49-19 (доб. 30-41) email : uliagermanovna@yandex.ru ORCID - 0000-0001-8121-8535, ScopusID – 57202228987

Проскурин Андрей Юрьевич, преподаватель кафедра информатики и прикладной математики Московского Государственного строительного университета. Российская Федерация, г Москва, Ярославское шоссе 26к1 . 8-495-183-59-94 email : proskurina-yu@mgsu.ru

DOI:10.22337/2587-9618-2021-17-4-161-180

FORCE DRIVEN VIBRATIONS OF NONLINEAR PLATES ON A VISCOELASTIC WINKLER FOUNDATION UNDER THE HARMONIC MOVING LOAD

Marina V. Shitikova, Anastasiya I. Krusser

Voronezh State Technical University, Voronezh, RUSSIA

Abstract: In the present paper, the forced driven nonlinear vibrations of an elastic plate in a viscoelastic medium and resting on a viscoelastic Winkler-type foundation are studied. The damping features of the surrounding medium and foundation are described by the Kelvin-Voigt model and standard linear solid model with fractional derivatives, respectively. The dynamic response of the plate is described by the set of nonlinear differential equations with due account for the fact that the plate is being under the conditions of the internal resonance accompanied by the external resonance. The expressions for the stress function and nonlinear coefficients for different types of boundary conditions are presented.

Keywords: nonlinear vibrations of thin plates, viscoelastic Winkler-type foundation, fractional derivative model, boundary conditions, combination of internal and external resonances

АНАЛИЗ ВЫНУЖДЕННЫХ НЕЛИНЕЙНЫХ КОЛЕБАНИЙ ПЛАСТИНКИ НА ВЯЗКОУПРУГОМ ОСНОВАНИИ ВИНКЛЕРА ОТ ДЕЙСТВИЯ ПОДВИЖНОЙ НАГРУЗКИ

М.В. Шитикова, А.И. Круссер

Воронежский государственный технический университет, г. Воронеж, РОССИЯ

Аннотация: Исследованы нелинейные вынужденные колебания упругой пластины в вязкоупругой среде и на вязкоупругом основании Винклера. Демпфирующие свойства окружающей среды и основания описываются при помощи моделей Кельвина-Фойгта и стандартного линейного твердого тела с дробной производной соответственно. Колебания пластинки описываются системой нелинейных дифференциальных уравнений, с учетом того, что пластинка находится в условиях сочетания внутреннего и внешнего резонансов. Получены выражения для функции напряжений и коэффициентов при нелинейных членах для различных типов граничных условий.

Ключевые слова: нелинейные колебания пластинок, вязкоупругое основание типа Винклера, модель с дробной производной, граничные условия, сочетание внутреннего и внешнего резонансов

1. INTRODUCTION

Nonlinear dynamic response of elastic plates on the viscoelastic foundation is of great interest among researchers in the recent years. The analysis of free and force driven vibrations of nonlinear systems is of great importance for defining the dynamic parameters dependent on the amplitude-phase relationships and modes of vibration [1-3]. Moreover, nonlinear vibrations could be accompanied by such a phenomenon as the internal resonance, resulting in strong coupling between the modes of vibrations involved, and hence in the energy exchange between the interacting modes. The described type of resonance can be characterized as a structural resonance, since external resonance, for example, could be eliminated by the simplest change in the frequency of the harmonic force. Both types of resonances

separately are extremely unfavorable phenomena, and their combination can lead to the distraction of not only one element, but the entire structure as a whole. The process of the nonlinear vibrations of the plates under conditions of internal resonances has been widely studied in [4-7].

Depending on the applications of the considered foundation, several models have been proposed to describe their properties [8]. The viscoelastic Winkler-type or Pasternak-type foundations, damping features of which are described by the fractional derivative approach, are becoming increasingly widespread nowadays due to the important role of fractional calculus in solving problems of structural mechanics [9].

In the literature there are mainly reports on the analysis of vibrations of plates on a viscoelastic foundation in the linear formulation of the problem [10-17]. Nevertheless, there are papers in which nonlinear vibrations of plates on the foundation are considered. Thus, large deflection dynamic response of isotropic thin rectangular plates resting on Winkler, Pasternak and nonlinear Winkler elastic foundations was investigated in [18]. The dynamic response of a rectangular nonlinear plate resting on a viscoelastic Winkler-type foundation, the damping features of which are described by the fractional derivative Kelvin-Voigt model, for the first time was studied in [19]. The standard linear solid model with fractional derivatives for defining the viscoelastic properties of the Winkler-type foundation was applied in [20] for the analysis of free vibrations of the plate.

The problems of dynamic response of the rectangular plate supported by viscoelastic foundations and subjected to moving loads are studied in [16, 21-23]. This problem could find many engineering applications, such as aircraft–runway interaction or vehicle-road interaction, pavement-foundation system, dynamics of the helipad system, ship deck (especially aircraft carriers), soil-foundation system of offshore structures, railway track system, reinforced warehouse floor, etc [1].

However, the dynamic problems considering time-dependent properties of the material of the plate or foundation are usually restricted to simply supported plates. But in the literature there are solutions for rectangular plates with different combinations of simple boundary conditions (i.e., either clamped (C), simply supported (SS), or free (F)) [24]. Thus, nonlinear frequencies of vibrations of rectangular plates for three different types of boundary conditions (B.Cs) have been calculated in [1]. The linear dynamic response of thin plates resting on a fractional derivative Kelvin-Voigt viscoelastic foundation subjected to a moving point load is investigated in [16] for four types of boundary conditions. Semi-analytical solutions and comparative analysis of natural frequencies and midpoint displacements for vibration of the viscoelastic Kirchhoff–Love plate on the Kelvin-Voigt viscoelastic foundation with various B.Cs are presented in [25].

In the present paper, the nonlinear vibrations of the “elastic plate – viscoelastic foundation” system is studied for the case of combination of one-to-one internal and external resonances. The properties of the foundation and of the surrounding medium are described by the fractional derivative standard linear solid model and Kelvin–Voigt model, respectively. The nonlinear force driven vibrations of the plate on the viscoelastic foundation are studied under the harmonic moving load for different types of boundary conditions.

2. PROBLEM FORMULATION

Let us consider nonlinear vibrations of a simply supported elastic plate rested on a viscoelastic Winkler-type foundation (Fig.1), the dynamic response of which is described by the von Karman equation in terms of plate’s lateral deflection $w = w(x, y, t)$ and Airy’s stress function ϕ:

$$D\nabla^4 w + \rho h \frac{\partial^2 w}{\partial t^2} - \frac{\partial^2 w}{\partial x^2}\frac{\partial^2 \phi}{\partial y^2} - \frac{\partial^2 w}{\partial y^2}\frac{\partial^2 \phi}{\partial x^2} + \\ +2\frac{\partial^2 w}{\partial x \partial y}\frac{\partial^2 \phi}{\partial x \partial y} = q - F_1 - F_2, \quad (1)$$

$$\nabla^4 \phi = Eh\left[\left(\frac{\partial w}{\partial x \partial y}\right)^2 - \frac{\partial^2 w}{\partial x^2}\frac{\partial^2 w}{\partial y^2}\right], \quad (2)$$

where $D = Eh^3/12(1-\nu^2)$ is the plate's cylindrical rigidity, E and ν are the elastic modulus and Poisson's ratio of the plate's material, respectively, h and ρ are its thickness and density, t is the time, $q = P\delta(x-g(t))\delta(y-b/2)\sin\Omega_F t$ is external load, P and Ω_F are the magnitude and the frequency of the applied force, respectively, δ is the Dirac delta function, and $g(t)$ is the function defining the position of moving load, $g(t) = Vt$ for a load moving with a constant velocity. Besides, $g(t)$ must satisfy $0 \le g(t) \le a$.

In equation (1), F_2 is the reaction force of the viscoelastic Winkler-type foundation, $F_1 = æ_1 \tau_1^{\gamma_1} D_{0+}^{\gamma_1} w$ is the damping force of the viscoelastic medium possessing the retardation time τ_1 and damping coefficient $æ_1$, which is modeled by the viscoelastic Kelvin-Voigt model with the Riemann-Liouville derivative $D_{0+}^{\gamma_1}$ of the fractional order γ_1 $(0 < \gamma_1 \le 1)$ [9,26]

$$D_{0+}^{\gamma} x(t) = \frac{d}{dt}\int_0^t \frac{x(t-t')dt'}{\Gamma(1-\gamma)t'^{\gamma}} \quad (0 < \gamma = \gamma_1 \le 1), \quad (3)$$

and $\Gamma(1-\gamma)$ is the Gamma function.

Let us assume, following [27], that the compliance operator of a viscoelastic foundation is described by the standard linear solid model with the Riemann-Liouville fractional derivative D_{0+}^{γ} (3) at $\gamma = \gamma_2$:

$$\tilde{\lambda} = \lambda_\infty \left[1 - \nu_\varepsilon \frac{1}{1+\tau_2^{\gamma} D_{0+}^{\gamma_2}}\right], \quad (4)$$

where λ_∞ is the coefficient of instantaneous compliance of the foundation, $\nu_\varepsilon = \Delta\lambda\lambda_\infty^{-1}$, $\Delta\lambda = \lambda_\infty - \lambda_0$ is the defect of the compliance, i.e., the value characterizing the decrease in the compliance operator from its non-relaxed value to its relaxed value.

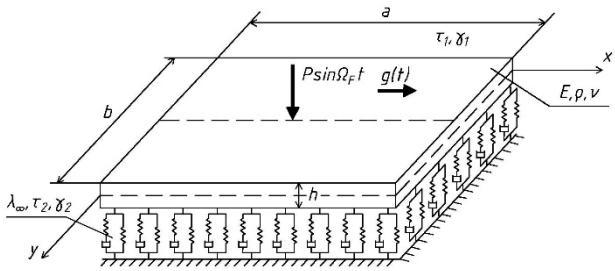

Figure 1. Plate on a viscoelastic foundation subjected to a moving harmonic load

The following boundary conditions could be added to the set of equations (1) and (2) at each edge:

1) Simply supported edges (S)

$$\text{at} \quad x = 0 \text{ and } a, \quad w = \frac{\partial^2 w}{\partial x^2} = 0, \\ \text{at } y = 0 \text{ and } b, \quad w = \frac{\partial^2 w}{\partial y^2} = 0; \quad (5)$$

2) Clamped edges (C)

$$\text{at} \quad x = 0 \text{ and } a, \quad w = \frac{\partial w}{\partial x} = 0, \\ \text{at } y = 0 \text{ and } b, \quad w = \frac{\partial w}{\partial y} = 0. \quad (6)$$

Therefore, the following four types of boundary conditions (B.Cs) for the plate will be considered: all edges are simply-supported (SSSS), all edges are clamped (CCCC), two opposite edges are clamped and other two edges are simply supported (CSCS), and one edge is simply supported and others are clamped (CCSC). In the abbreviation of B.Cs the letter symbols are used, for example, CSCS means a plate with edges $x=0$ and $x=a$ clamped (C), $y=0$ and $y=b$ simply supported (S).

In order to identify the possibility of the occurrence of the internal resonance during nonlinear vibrations of a plate rested on a viscoelastic foundation and to carry out its subsequent analysis, suppose that only two natural modes of vibrations with numbers m_1n_1 и m_2n_2 are excited. Then the deflection of the plate could be represented in the following form:

$$w(x,y,t)=x_1(t)W_{m_1n_1}\left(x,y\right)+x_2(t)W_{m_2n_2}\left(x,y\right), \quad (7)$$

where $x_i(t)$ $(i=1,2)$ are generalized displacements, and $W_{m_in_i}\left(x,y\right)$ are the eigen functions. The mode shape functions for various B.Cs are presented in Table1 [25].

Table 1. Plate mode shapes and natural frequencies for different B.Cs.

B.Cs.	$W_{m_in_j}\left(x,y\right)$	Ω_i^2
SSSS	$\sin\frac{\pi m_i x}{a}\sin\frac{\pi n_i y}{b}$	$\Omega_i^2=\frac{E\pi^4h^2}{12\rho(1-\nu^2)b^4}\left(\xi^2m_i^2+n_i^2\right)^2$
CCCC	$(1-\cos\frac{2\pi m_i x}{a})(1-\cos\frac{2\pi n_i y}{b})$	$\Omega_i^2=\frac{4E\pi^4h^2}{27\rho(1-\nu^2)b^4}\left(3\xi^4m_i^4+2\xi^2m_i^2n_i^2+3n_i^4\right)$
CSCS	$(1-\cos\frac{2\pi m_i x}{a})\sin\frac{\pi n_i y}{b}$	$\Omega_i^2=\frac{E\pi^4h^2}{9\rho(1-\nu^2)b^4}\left(4\xi^4m_i^4+2\xi^2m_i^2n_i^2+0.75n_i^4\right)$
CCSC	$(\cos\frac{3\pi m_i x}{2a}-\cos\frac{\pi m_i x}{2a})(1-\cos\frac{2\pi n_i y}{b})$	$\Omega_i^2=\frac{E\pi^4h^2}{18\rho(1-\nu^2)b^4}\left(3.85\xi^4m_i^4+5\xi^2m_i^2n_i^2+8n_i^4\right)$

Substituting the proposed solution (7) in (2), taking into account the boundary conditions to be considered for each specific case and integrating with account for the orthogonality conditions of sines, we obtain the expressions for the stress function for different types of boundary conditions, which are presented in Appendix A.

Substituting the assumed two-term expansion for the deflection function of the plate (7) and the corresponding stress function in the equation of motion of the plate (1) resting on the viscoelastic Winkler-type foundation yields the following set of nonlinear differential equations with respect to the generalized displacements:

$$\ddot{x}_1+\omega_1^2x_1+\alpha_1x_1^3+\alpha_2x_1x_2^2+\varepsilon^2\mu_1D_{0+}^{\gamma_1}x_1-\\-\varepsilon^2\mu_2\,\text{Э}_\gamma^*(\tau_2^{\gamma_2})x_1=P_1\left(t\right), \quad (8)$$

$$\ddot{x}_2+\omega_2^2x_2+\alpha_3x_2^3+\alpha_4x_2x_1^2+\varepsilon^2\mu_1D_{0+}^{\gamma_1}x_2-\\-\varepsilon^2\mu_2\,\text{Э}_\gamma^*(\tau_2^{\gamma_2})x_2=P_2\left(t\right), \quad (9)$$

where

$$P_i(t) = \left(\int_0^a \int_0^b P \sin \Omega_F t \; \delta(x - g(t)) \delta(y - 0.5b) \times \right. \\ \left. \times W_{m_i n_i}(x, y) \, dxdy \right) / \rho h \int_0^a \int_0^b \left[W_{m_i n_i}(x, y) \right]^2 dxdy, \quad (10)$$

α_i are the coefficients depending on numbers of the vibration modes which are given in Appendix B, ε is a small dimensionless parameter, μ_i are finite values, $\varepsilon^2 \mu_1 = \dfrac{E_0 \tau_1^{\gamma_1}}{\rho h}$, $\varepsilon^2 \mu_2 = \dfrac{\lambda_\infty \nu_\varepsilon}{\rho h}$, ω_1^2 and ω_2^2 are vibration frequencies of the mechanical system "plate + viscoelastic foundation"

$$\omega_i^2 = \Omega_i^2 + \frac{\lambda_\infty}{\rho h}, \quad (11)$$

and Ω_i^2 are the natural frequencies of the linear vibration of the plate presented in Table 1, and $\text{э}_\gamma^* (\tau_2^{\gamma_2})$ is the Rabotnov dimensionless fractional operator defined as follows [28]

$$\text{э}_\gamma^* (\tau_2^{\gamma_2}) = \frac{1}{1 + \tau_2^{\gamma_2} D_{0+}^{\gamma_2}}. \quad (12)$$

When deriving relations (8) and (9), the filtering property of the delta function should be taken into account:

$$\iint \delta(x - x_0) \delta(y - y_0) f(x, y) \, dxdy = f(x_0, y_0). \quad (13)$$

Considering (13), equation (10) for the case of a simply supported plate is reduced as

$$P_i(t) = P \sin \Omega_F t \iint \delta(x - Vt) \delta(y - b/2) \times \\ \times \sin\left(\frac{\pi m_i x}{a} \right) \sin\left(\frac{\pi n_i y}{b} \right) dxdy = \\ = P \sin\left(\frac{\pi m_i V t}{a} \right) \sin\left(\frac{\pi n_i}{2} \right) \sin \Omega_F t. \quad (14)$$

Then with due account for (14) the governing equations (8) and (9) could be written as

$$\ddot{x}_1 + \omega_1^2 x_1 + \alpha_1 x_1^3 + \alpha_2 x_1 x_2^2 + \varepsilon^2 \mu_1 D_{0+}^{\gamma_1} x_1 - \\ - \varepsilon^2 \mu_2 \, \text{э}_\gamma^* (\tau_2^{\gamma_2}) x_{11} - 4\varepsilon^3 f_1 \sin \omega_{f_1} t \sin \Omega_F t = 0, \quad (15)$$

$$\ddot{x}_2 + \omega_2^2 x_2 + \alpha_3 x_2^3 + \alpha_4 x_2 x_1^2 + \varepsilon^2 \mu_1 D_{0+}^{\gamma_1} x_2 - \\ - \varepsilon^2 \mu_2 \, \text{э}_\gamma^* (\tau_2^{\gamma_2}) x_2 - 4\varepsilon^3 f_2 \sin \omega_{f_2} t \sin \Omega_F t = 0, \quad (16)$$

where $\omega_{f_i} = \dfrac{\pi m_i V}{a}$ are frequencies, and $\varepsilon^3 f_i = \dfrac{P}{ab\rho h} \sin\left(\dfrac{\pi n_i}{2} \right)$.

3. METHOD OF SOLUTION

In order to solve the set of Eqs. (15)-(16), the method of multiple time scales [29,30] could be utilized, according to which the generalized displacements $x_i(t)$ could be represented via the following expansion in two time scales T_0 and T_2:

$$x_i(t) = \varepsilon X_{i1}(T_0, T_2) + \varepsilon^2 X_{i2}(T_0, T_2) + \\ + \varepsilon^3 X_{i3}(T_0, T_2) + \ldots, \quad (17)$$

where $T_n = \varepsilon^n t$ are new independent variables, among them: $T_0 = t$ is a fast scale characterizing motions with the natural frequencies, and $T_2 = \varepsilon t^2$ is a slow scale characterizing the modulation of the amplitudes and phases of the modes with nonlinearity.

Recall that the first and the second time derivatives, as well as fractional derivative could be expanded in terms of the new time scales, respectively, as follows [29]:

$$\frac{d}{dt} = D_0 + \varepsilon^2 D_2 + ..., \qquad \frac{d^2}{dt^2} = D_0^2 + 2\varepsilon^2 D_0 D_2 + ... \tag{18}$$

$$D_+^\gamma = \left(\frac{d}{dt}\right)^\gamma = \left(D_0 + \varepsilon^2 D_2 + ...\right)^\gamma = = D_0^\gamma + \varepsilon^2 \gamma D_0^{\gamma-1} D_2 + ..., \tag{19}$$

where $D_0 = \partial / \partial T_0$, and $D_2 = \partial / \partial T_2$.

Expansion of the Rabotnov dimensionless fractional operator in a Taylor series in terms of a small parameter has the form [20]:

$$э_\gamma^* (\tau^\gamma) = \frac{1}{1+\tau^\gamma D_{0+}^\gamma} = (1+\tau^\gamma D_0{}^\gamma)^{-1} - -\varepsilon^2 (1+\tau^\gamma D_0{}^\gamma)^{-2} \tau^\gamma \gamma D_0{}^{\gamma-1} D_2 + ... \tag{20}$$

Substituting expansion (17) with account for relationships (18)-(19), after equating the coefficients at like powers of ε to zero, we are led for the case of forced vibrations to the following set of recurrence equations to various orders:

to order ε

$$D_0^2 X_{11} + \omega_1^2 X_{11} = 0, \tag{21}$$

$$D_0^2 X_{21} + \omega_2^2 X_{21} = 0, \tag{22}$$

to order ε^3

$$D_0^2 X_{13} + \omega_1^2 X_{13} = -2D_0 D_2 X_{11} - X_{11}\left(\bar{\mu}_1 D_0^{\gamma_1} - -\bar{\mu}_2 (1+\tau_2^{\gamma_2} D_0^{\gamma_2})^{-1}\right) - \alpha_1 X_{11}^3 - \alpha_2 X_{11} X_{21}^2 + +2 f_1 \cos\left((\omega_{f_1} - \Omega_F) T_0\right) + 2 f_1 \cos\left((\omega_{f_1} + \Omega_F) T_0\right), \tag{23}$$

$$D_0^2 X_{23} + \omega_2^2 X_{23} = -2D_0 D_2 X_{21} - X_{21}\left(\bar{\mu}_1 D_0^{\gamma_1} - -\bar{\mu}_2 (1+\tau_2^{\gamma_2} D_0^{\gamma_2})^{-1}\right) - \alpha_3 X_{21}^3 - \alpha_4 X_{21} X_{11}^2 + +2 f_2 \cos\left((\omega_{f_2} - \Omega_F) T_0\right) + 2 f_2 \cos\left((\omega_{f_2} + \Omega_F) T_0\right), \tag{24}$$

where $\bar{\mu}_i = \dfrac{\mu_i}{\rho h}$ $(i = 1, 2)$.

The solution of linear equations (21) and (22) has the form

$$X_{j1} = A_j(T_2) \exp\left(i\omega_j T_0\right) + +\bar{A}_j(T_2) \exp\left(-i\omega_j T_0\right), \tag{25}$$

where $A_j(T_2)(j = 1, 2)$ are yet unknown functions, and $\bar{A}_j(T_2)$ are conjugate functions with $A_j(T_2)$.

Substituting relationships (25) in equations (23) and (24) yields

$$\begin{aligned} D_0^2 X_{13} + \omega_1^2 X_{13} &= -2i\omega_1 D_2 A_1 \exp\left(i\omega_1 T_0\right) - \\ &-\left[\bar{\mu}_1 (i\omega_1)^{\gamma_1} - \bar{\mu}_2 (1+\tau_2^{\gamma_2} (i\omega_1)^{\gamma_2})^{-1}\right] A_1 \exp\left(i\omega_1 T_0\right) - \\ &-\alpha_1 \left[A_1 \exp\left(3i\omega_1 T_0\right) + 3\bar{A}_1 \exp\left(i\omega_1 T_0\right)\right] A_1^2 - \\ &-\alpha_2 \left\{A_2^2 \exp\left[(\omega_1 + 2\omega_2) T_0\right] + 2A_2 \bar{A}_2 \exp\left(i\omega_1 T_0\right) + \right. \\ &\left. +\bar{A}_2^2 \exp\left[i(\omega_1 - 2\omega_2) T_0\right]\right\} A_1 + f_1 \exp\left(i(\omega_{f_1} - \Omega_F) T_0\right) + \\ &+ f_1 \exp\left(i(\omega_{f_1} + \Omega_F) T_0\right) + cc, \end{aligned} \tag{26}$$

$$\begin{aligned} D_0^2 X_{23} + \omega_2^2 X_{23} &= -2i\omega_2 D_2 A_2 \exp\left(i\omega_2 T_0\right) - \\ &-\left[\bar{\mu}_1 (i\omega_2)^{\gamma_1} - \bar{\mu}_2 (1+\tau_2^{\gamma_2} (i\omega_2)^{\gamma_2})^{-1}\right] A_2 \exp\left(i\omega_2 T_0\right) - \\ &-\alpha_3 \left[A_2 \exp\left(3i\omega_2 T_0\right) + 3\bar{A}_2 \exp\left(i\omega_2 T_0\right)\right] A_2^2 - \\ &-\alpha_4 \left\{A_1^2 \exp\left[(2\omega_1 + \omega_2) T_0\right] + 2A_1 \bar{A}_1 \exp\left(i\omega_2 T_0\right) + \right. \\ &\left. +\bar{A}_1^2 \exp\left[i(\omega_2 - 2\omega_1) T_0\right]\right\} A_2 + f_2 \exp\left(i(\omega_{f_2} - \Omega_F) T_0\right) + \\ &+ f_2 \exp\left(i(\omega_{f_2} + \Omega_F) T_0\right) + cc. \end{aligned} \tag{27}$$

The analysis of relations (26)-(27) shows that the case of the occurrence of the one-to-one internal resonance is possible, when any two vibration frequencies of the mechanical system "plate+viscoelastic foundation" are close to each other, namely:

$$\omega_1 = \omega_2, \quad \text{and therefore,} \quad \Omega_1 = \Omega_2. \tag{28}$$

From equations (26) and (27) it follows that the internal resonance could be accompanied by the external resonance when one of the following conditions is fulfilled:

$$(1)\ \omega_i = \omega_{fi} - \Omega_F,$$

$$(2)\ \omega_i = \omega_{fi} + \Omega_F. \tag{29}$$

The condition for eliminating secular terms in equations (26) and (27) with account for relationships (28)-(29) leads to a set of two governing equations:

$$2i\omega_1 D_2 A_1 + \left[\bar{\mu}_1 (i\omega_1)^{\gamma_1} - \bar{\mu}_2 (1+\tau_2^{\gamma_2}(i\omega_1)^{\gamma_2})^{-1}\right] A_1 + \\ +3\alpha_1 A_1^2 \bar{A}_1 + \alpha_2 \bar{A}_1 A_2^2 + 2\alpha_2 A_1 A_2 \bar{A}_2 - f_1 = 0, \tag{30}$$

$$2i\omega_2 D_2 A_2 + \left[\bar{\mu}_1 (i\omega_2)^{\gamma_1} - \bar{\mu}_2 (1+\tau_2^{\gamma_2}(i\omega_2)^{\gamma_2})^{-1}\right] A_2 + \\ +3\alpha_3 A_2^2 \bar{A}_2 + \alpha_4 \bar{A}_2 A_1^2 + 2\alpha_4 A_2 A_1 \bar{A}_1 - f_2 = 0. \tag{31}$$

Multiplying (30) by $\bar{A}_1$ and (31) by $\bar{A}_2$, adding and subtracting the equations conjugate to them, and representing functions A_i in the polar form

$$A_i = a_i e^{i\varphi_i} \quad (i = 1, 2), \tag{32}$$

where $a_i = a_i(T_2)$ and $\varphi_i = \varphi_i(T_2)$ are the functions of amplitudes and phases of vibrations, yield the following set of equations:

$$\left(a_1^2\right)^{\square} + s_1 a_1^2 + \omega_1^{-1}\alpha_2 a_1^2 a_2^2 \sin\delta + \\ + f_1 \omega_1^{-1} a_1 \sin\varphi_1 = 0, \tag{33}$$

$$\left(a_2^2\right)^{\square} + s_2 a_2^2 - \omega_2^{-1}\alpha_4 a_1^2 a_2^2 \sin\delta + \\ + f_2 \omega_2^{-1} a_2 \sin\varphi_2 = 0, \tag{34}$$

$$\dot{\varphi}_1 - \frac{1}{2}\lambda_1 - \frac{3}{2}\alpha_1 \omega_1^{-1} a_1^2 - \alpha_2 \omega_1^{-1} a_2^2 - \\ -\frac{1}{2}\alpha_2 \omega_1^{-1} a_2^2 \cos\delta + \frac{1}{2} f_1 \left(\omega_1 a_1\right)^{-1} \cos\varphi_1 = 0, \tag{35}$$

$$\dot{\varphi}_2 - \frac{1}{2}\lambda_2 - \frac{3}{2}\alpha_3 \omega_2^{-1} a_2^2 - \alpha_4 \omega_2^{-1} a_1^2 - \\ -\frac{1}{2}\alpha_4 \omega_2^{-1} a_1^2 \cos\delta + \frac{1}{2} f_2 \left(\omega_2 a_2\right)^{-1} \cos\varphi_2 = 0, \tag{36}$$

(31)

where $\delta = 2(\varphi_2 - \varphi_1)$ is the phase difference,

$$s_i = \bar{\mu}_1 \omega_i^{\gamma_1 - 1} \sin\psi_1 + \bar{\mu}_2 \omega_i^{-1} R_i \sin\Phi_i + \\ + \bar{\mu}_3 \omega_i^{\gamma_2 - 1} \sin\psi_2, \\ \lambda_i = \bar{\mu}_1 \omega_i^{\gamma_1 - 1} \cos\psi_1 - \bar{\mu}_2 \omega_i^{-1} R_i \cos\Phi_i + \\ + \bar{\mu}_3 \omega_i^{\gamma_2 - 1} \cos\psi_2, \tag{37}$$

$$\psi_i = \frac{1}{2}\pi\gamma_i \quad (i = 1, 2),$$

$$R_i = \sqrt{1 + 2(\tau_2 \omega_i)^{\gamma_2} \cos\psi_2 + (\tau_2 \omega_i)^{2\gamma_2}},$$

$$\tan\Phi_i = \frac{(\tau_2 \omega_i)^{\gamma_2} \sin\psi_2}{1 + (\tau_2 \omega_i)^{\gamma_2} \cos\psi_2}.$$

The set of equations (33)-(36) is the governing one for the amplitudes and phases of nonlinear force driven vibrations of the elastic simply supported plate on a nonlinear viscoelastic Winkler-type foundation, damping features of which are defined by the fractional derivative standard linear solid model (4), when vibrations occur in a viscoelastic surrounding medium, properties of which are described by the fractional derivative Kelvin-Voigt model.

For other types of boundary conditions, the governing set of equations could be obtained in a similar way by changing the vibration

frequencies (see Table 1) and coefficients $\alpha_1 - \alpha_4$ (presented in Appendix B) in the expressions (33)-(36), as well as the terms depending on the external load.

4. NUMERICAL EXAMPLE

Equations (33)-(36) were solved numerically in the «Mathcad 15» system by using the method suggested in [31] for the cases of free and forced driven vibrations of the SSSS plate. A quadratic plate was considered as an example with the following geometric parameters: $a = b = 10m$, $h = 0,3m$, $m_1 = n_2 = 1$, $m_2 = n_1 = 3$ and material parameters $E = 3,25 \cdot 10^7 kPa$, $\rho = 2400 kg/m^3$, and $\nu = 0.3$. The harmonic load is moving with the constant velocity $V = 30 m/s$ and frequency $\Omega_F = 95 s^{-1}$ along the *x*-axis. The vibrations of the plate are studied for three cases of external load: $P = 2140N$ (Fig. 2b), $P = 5000N$ (Fig. 2c), and $P = 7140N$ (Fig. 2d).

The plate is subjected to the conditions of the internal resonance 1:1 at $\omega_1 = \omega_2 = 104,42 s^{-1}$, accompanied by the external resonance:

$$\omega_1 = \omega_{f_1} + \Omega_F = \frac{3,14 \cdot 1 \cdot 30}{10} + 95 = 104,42 s^{-1}.$$

Figure 2 clearly shows the energy exchange between interacting modes of nonlinear free vibrations and force driven vibrations of the simply supported plate on the elastic ($\gamma_2 = 0$) and viscoelastic ($\gamma_2 \neq 0$) foundation via the fractional calculus standard linear solid for different values of external load. It is seen that an increase in the magnitude of the external force results in the increase in dimensionless amplitudes of vibrations of the plate. The dependence of the amplitudes of nonlinear vibrations on the values of fractional parameters γ_1 and γ_2 is shown in Figure 3. With the appearance of the damping properties of the viscoelastic medium, the damping of vibrations increases.

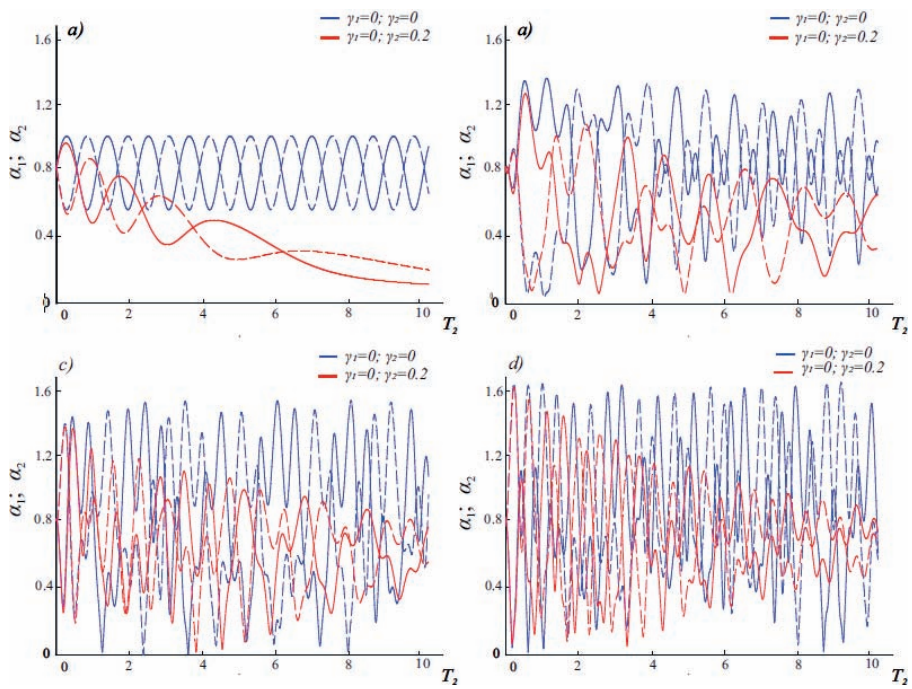

Figure 2. The dimensionless T_2-dependence of the dimensionless amplitudes of nonlinear vibrations for SSSS-plate for $m_1 = n_2 = 1$, $m_2 = n_1 = 3$: a) free vibrations, and force driven vibrations at b) $f_1 = -3$, $f_2 = 3$; c) $f_1 = -7$, $f_2 = 7$; d) $f_1 = -10$, $f_2 = 10$; solid line – a_2, dashed line – a_1

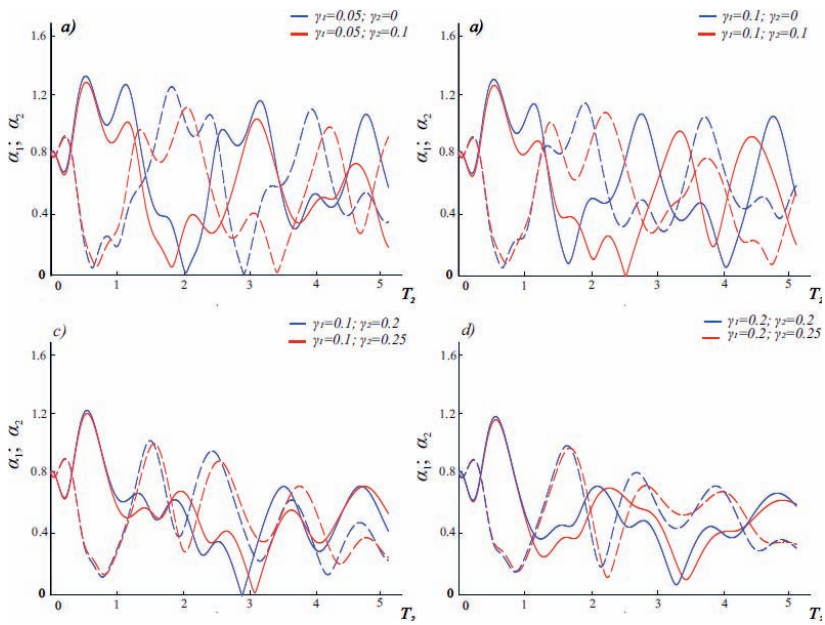

Figure 3. The dimensionless T_2-dependence of the dimensionless amplitudes of nonlinear vibrations of SSSS-plate for different values of fractional parameters at $f_1 = -3,\ f_2 = 3;\ m_1 = n_2 = 1,$ $m_2 = n_1 = 3;$ *solid line – a_2, dashed line – a_1*

5. CONCLUSION

In the present paper, the problem of nonlinear vibrations of a von Karman elastic plate based on a viscoelastic Winkler-type foundation and subjected to moving load is solved. The damping features of the viscoelastic foundation are described by the fractional derivative standard linear solid model, while the damping properties of the environment in which the vibrations occur are described by the Kelvin-Voigt model with the Riemann-Liouville fractional derivative. The expressions for the stress function and nonlinear coefficients for SSSS, CCCC and CSCS types of boundary conditions are presented. The governing equations are obtained for determining nonlinear amplitudes and phases in the case of forced driven vibrations, when the natural frequencies of the two dominant vibration modes are close to each other and to the frequency of the external load. The resulting set of equations allows one to control the damping properties of the external environment and the foundation by changing the fractional parameters from zero, what corresponds to an elastic medium and/or elastic foundation, to unit, what conforms to the traditional standard linear solid model, resulting in the expansion of the range of applicability of the solution obtained.

The derived set of equations has been solved numerically for the SSSS case of boundary conditions using the approach described in [31].

ACKNOWLEDGMENTS

This research was supported by the Russian Foundation for Basic Research under the Grant No. 20-01-00443. The studies have been carried out using the facilities of the Collective Research Center named after Professor Yu. M. Borisov, Voronezh State Technical University, which is partly supported by the Ministry of Science and Education of the Russian Federation, Contract No 075-15-2021-662.

REFERENCES

1. **Amabili M.** Nonlinear vibrations of rectangular plates with different boundary conditions: theory and experiments // Computers & Structures, 2004, 82, pp. 2587-2605.
2. **Amabili M.** Nonlinear vibrations of viscoelastic rectangular plates // Journal of Sound and Vibration, 2016, 362, pp. 142–156.
3. **Breslavsky I.D.**, **Amabili M.**, **Legrand M.** Physically and geometrically non-linear vibrations of thin rectangular plates // International Journal of Non-Linear Mechanics, 2014, 58, pp. 30-40.
4. **Rossikhin Yu.A.**, **Shitikova M.V.** Analysis of free non-linear vibrations of a viscoelastic plate under the conditions of different internal resonances // International Journal of Non-Linear Mechanics, 2006, 2, pp. 313-325.
5. **Ribeiro P.**, **Petyt M.** Nonlinear free vibration of isotropic plates with internal resonance // International Journal of Non-Linear Mechanics, 2000, 35, pp. 263-278.
6. **Chang S.I.**, **Bajaj A.K.**, **Krousgrill C.M.** Non-linear vibrations and chaos in harmonically excited rectangular plates with one-to-one internal resonance // Nonlinear Dynamics, 1993, Vol. 4(5), pp 433–460.
7. **Anlas G.**, **Elbeyli O.** Nonlinear vibrations of a simply supported rectangular metallic plate subjected to transverse harmonic excitation in the presence of a one-to-one internal resonance // Nonlinear Dynamics, 2002, 30(1), pp.1-28.
8. **Younesian D., Hosseinkhani A., Askari H., Esmailzadeh E.** Elastic and viscoelastic foundations: a review on linear and nonlinear vibration modeling and applications // Nonlinear Dynamics, 2019, 97, pp. 853–895.
9. **Rossikhin Yu.A., Shitikova M.V.** Application of fractional calculus for dynamic problems of solid mechanics: Novel trends and recent results // Applied Mechanics Reviews, 2010, 63(1), Article ID 010801.
10. **Zhu H., Liu L., Ye X**. Response of a loaded rectangular plate on fractional derivative viscoelastic foundation // Journal of Basic Science and Engineering, 2011, 19(2), pp. 271-278.
11. **Kou L.** Response of rectangular plate on fractional derivative two-parameter viscoelastic foundation // Chinese Quarterly of Mechanics, 2013, 34(1), pp. 154-160.
12. **Kou L., Bai Y.** Dynamic response of rectangular plates on two-parameter viscoelastic foundation with fractional derivatives // Journal of Vibration and Shock, 2014, 33(8), pp. 141-147.
13. **Zhang C., Zhu H., Shi B., Liu L.** Theoretical investigation of interaction between a rectangular plate and fractional viscoelastic foundation // Journal of Rock Mechanics and Geotechnical Engineering, 2014, 6 (4), 373-379.
14. **Cai W., Chen W., Xu W.** Fractional modeling of Pasternak-type viscoelastic foundation // Mechanics of Time-Dependent Materials, 2017, 21(1), pp. 119-131.
15. **Praharaj R., Datta N.** On the transient response of plates on fractionally damped viscoelastic foundation // Computational & Applied Mathematics, 2020, 39(4), DOI: 10.1007/s40314-020-01285-6.
16. **Praharaj R., Datta N.** Dynamic response of plates resting on a fractional viscoelastic foundation and subjected to a moving load // Mechanics Based Design of Structures and Machines, 2020, DOI: 10.1080/15397734.2020.1776621.
17. **Hosseinkhani A., Younesian D., Farhangdoust S.** Dynamic analysis of a plate on the generalized foundation with fractional damping subjected to random excitation // Mathematical Problems in Engineering, 2018, 2018(2), pp. 1-10.
18. **Dumir P.C.** Nonlinear dynamic response of isotropic thin rectangular plates on elastic

foundations // Acta Mechanica, 1988, 71, pp. 233-244.

19. **Shitikova M.V., Kandu V.V.** Analysis of the nonlinear vibrations of an elastic plate on a viscoelastic foundation in the presence of the one-to-one internal resonance (in Russian) // News of Higher Educational Institutions. Construction, 2020, 3, pp. 5-22.
20. **Shitikova M.V., Krusser A.I**. Nonlinear vibrations of an elastic plate on a viscoelastic foundation modeled by the fractional derivative standard linear solid model // EASD Procedia EURODYN, 2020, pp. 355-368.
21. **Luong V., Cao T., Lieu Q. et al**. Moving element method for dynamic analyses of functionally graded plates resting on Pasternak foundation subjected to moving harmonic load // International Journal of Structural Stability and Dynamics, 2020, 20(01), 2050003, DOI: 10.1142/S0219455420500030.
22. **Wu J., Lee M., Lai T.** The dynamic analysis of a flat plate under a moving load by the finite element method // The International Journal for Numerical Methods in Engineering, 1987, 24, pp. 743–762, DOI: 10.1002/nme.1620240407.
23. **Li M., Qian T., Zhong Y. et al.** Dynamic response of the rectangular plate subjected to moving loads with variable velocity // Journal of Engineering Mechanics, 2014, 140 (4), 06014001, DOI: 10.1061/(ASCE)EM.1943-7889.0000687.
24. **Leissa A.** Vibration of Plates. Scientific and Washington D.C: Technical Information Division, Office of Technology Utilization, NASA, 1969.
25. **Kiasat M., Zamani H., Aghdam M**. On the transient response of viscoelastic beams and plates on viscoelastic medium // International Journal of Mechanical Sciences, 2014, 83, pp. 133-145.
26. **Samko S., Kilbas A., Marichev O.** Fractional Integrals and Derivatives. Theory and Applications. Switzerland: Gordon and Breach Science Publishers, 1993.
27. **Rossikhin Yu.A., Shitikova M.V.** A new method for solving dynamic problems of fractional derivative viscoelasticity // International Journal of Engineering Science, 2001, 39, pp. 149-176.
28. **Rossikhin Yu.A., Shitikova M.V.** Centennial jubilee of Academician Rabotnov and contemporary handling of his fractional operator // Fractional Calculus and Applied Analysis, 2014, 17, pp. 674-683.
29. **Rossikhin Yu.A., Shitikova M.V.** Application of fractional calculus for analysis of nonlinear damped vibrations of suspension bridges // Journal of Engineering Mechanics, 1998, 124, pp. 1029–1036.
30. **Shitikova M.V.** The fractional derivative expansion method in nonlinear dynamic analysis of structures // Nonlinear Dynamics, 2020, 99, pp. 109-122.
31. **Shitikova M.V., Kandu V.V.** Force driven vibrations of fractionally damped plates subjected to primary and internal resonances // The European Physical Journal Plus, 2019, 134(9), 423, DOI: 10.1140/epjp/i2019-12812-x.

СПИСОК ЛИТЕРАТУРЫ

1. **Amabili M.** Nonlinear vibrations of rectangular plates with different boundary conditions: theory and experiments // Computers & Structures, 2004, 82, pp. 2587-2605.
2. **Amabili M.** Nonlinear vibrations of viscoelastic rectangular plates // Journal of Sound and Vibration, 2016, 362, pp. 142–156.
3. **Breslavsky I.D.**, **Amabili M.**, **Legrand M.** Physically and geometrically non-linear vibrations of thin rectangular plates // International Journal of Non-Linear Mechanics, 2014, 58, pp. 30-40.

4. **Rossikhin Yu.A.**, **Shitikova M.V.** Analysis of free non-linear vibrations of a viscoelastic plate under the conditions of different internal resonances // International Journal of Non-Linear Mechanics, 2006, 2, pp. 313-325.
5. **Ribeiro P.**, **Petyt M.** Nonlinear free vibration of isotropic plates with internal resonance // International Journal of Non-Linear Mechanics, 2000, 35, pp. 263-278.
6. **Chang S.I.**, **Bajaj A.K.**, **Krousgrill C.M.** Non-linear vibrations and chaos in harmonically excited rectangular plates with one-to-one internal resonance // Nonlinear Dynamics, 1993, Vol. 4(5), pp 433–460.
7. **Anlas G.**, **Elbeyli O.** Nonlinear vibrations of a simply supported rectangular metallic plate subjected to transverse harmonic excitation in the presence of a one-to-one internal resonance // Nonlinear Dynamics, 2002, 30(1), pp.1-28.
8. **Younesian D., Hosseinkhani A., Askari H., Esmailzadeh E.** Elastic and viscoelastic foundations: a review on linear and nonlinear vibration modeling and applications // Nonlinear Dynamics, 2019, 97, pp. 853–895.
9. **Rossikhin Yu.A., Shitikova M.V.** Application of fractional calculus for dynamic problems of solid mechanics: Novel trends and recent results // Applied Mechanics Reviews, 2010, 63(1), Article ID 010801.
10. **Zhu H., Liu L., Ye X**. Response of a loaded rectangular plate on fractional derivative viscoelastic foundation // Journal of Basic Science and Engineering, 2011, 19(2), pp. 271-278.
11. **Kou L.** Response of rectangular plate on fractional derivative two-parameter viscoelastic foundation // Chinese Quarterly of Mechanics, 2013, 34(1), pp. 154-160.
12. **Kou L., Bai Y.** Dynamic response of rectangular plates on two-parameter viscoelastic foundation with fractional derivatives // Journal of Vibration and Shock, 2014, 33(8), pp. 141-147.
13. **Zhang C., Zhu H., Shi B., Liu L.** Theoretical investigation of interaction between a rectangular plate and fractional viscoelastic foundation // Journal of Rock Mechanics and Geotechnical Engineering, 2014, 6 (4), 373-379.
14. **Cai W., Chen W., Xu W.** Fractional modeling of Pasternak-type viscoelastic foundation // Mechanics of Time-Dependent Materials, 2017, 21(1), pp. 119-131.
15. **Praharaj R., Datta N.** On the transient response of plates on fractionally damped viscoelastic foundation // Computational & Applied Mathematics, 2020, 39(4), DOI: 10.1007/s40314-020-01285-6.
16. **Praharaj R., Datta N.** Dynamic response of plates resting on a fractional viscoelastic foundation and subjected to a moving load // Mechanics Based Design of Structures and Machines, 2020, DOI: 10.1080/15397734.2020.1776621.
17. **Hosseinkhani A., Younesian D., Farhangdoust S.** Dynamic analysis of a plate on the generalized foundation with fractional damping subjected to random excitation // Mathematical Problems in Engineering, 2018, 2018(2), pp. 1-10.
18. **Dumir P.C.** Nonlinear dynamic Response of isotropic thin rectangular plates on elastic foundations // Acta Mechanica, 1988, 71, pp. 233-244.
19. **Шитикова М.В., Канду В.В.** Анализ нелинейных колебаний упругой пластинки на вязкоупругом основании при наличии внутреннего резонанса один-к-одному // Известия вузов. Строительство, 2020, №. 3, С. 5-22.
20. **Shitikova M.V., Krusser A.I**. Nonlinear vibrations of an elastic plate on a viscoelastic foundation modeled by the fractional derivative standard linear solid model // EASD Procedia EURODYN, 2020, pp. 355-368.

21. **Luong V., Cao T., Lieu Q. et al**. Moving element method for dynamic analyses of functionally graded plates resting on Pasternak foundation subjected to moving harmonic load // International Journal of Structural Stability and Dynamics, 2020, 20(01), 2050003, DOI:10.1142/S0219455420500030.
22. **Wu J., Lee M., Lai T.** The dynamic analysis of a flat plate under a moving load by the finite element method // The International Journal for Numerical Methods in Engineering, 1987, 24, pp. 743–762, DOI: 10.1002/nme.1620240407.
23. **Li M., Qian T., Zhong Y. et al.** Dynamic response of the rectangular plate subjected to moving loads with variable velocity // Journal of Engineering Mechanics, 2014, 140 (4), 06014001, DOI: 10.1061/(ASCE)EM.1943-7889.0000687.
24. **Leissa A.** Vibration of Plates. Scientific and Washington D.C: Technical Information Division, Office of Technology Utilization, NASA, 1969.
25. **Kiasat M., Zamani H., Aghdam M**. On the transient response of viscoelastic beams and plates on viscoelastic medium // International Journal of Mechanical Sciences, 2014, 83, pp. 133-145.
26. **Самко С.Г.**, **Килбас А.А.**, **Маричев О.И.** Дробные интегралы и производные: Теория и приложения. Минск: Наука и техника, 1987, 688 с.
27. **Rossikhin Yu.A., Shitikova M.V.** A new method for solving dynamic problems of fractional derivative viscoelasticity // International Journal of Engineering Science, 2001, 39, pp. 149-176.
28. **Rossikhin Yu.A., Shitikova M.V.** Centennial jubilee of Academician Rabotnov and contemporary handling of his fractional operator // Fractional Calculus and Applied Analysis, 2014, 17, pp. 674-683.
29. **Rossikhin Yu.A., Shitikova M.V.** Application of fractional calculus for analysis of nonlinear damped vibrations of suspension bridges // Journal of Engineering Mechanics, 1998, 124, pp. 1029–1036.
30. **Shitikova M.V.** The fractional derivative expansion method in nonlinear dynamic analysis of structures // Nonlinear Dynamics, 2020, 99, pp. 109-122.
31. **Shitikova M.V., Kandu V.V.** Force driven vibrations of fractionally damped plates subjected to primary and internal resonances // The European Physical Journal Plus, 2019, 134(9), 423, DOI: 10.1140/epjp/i2019-12812-x.

APPENDIX A

1) SSSS-plate

$$\phi(x,y,t) = Eh\Bigg[\sum_i\sum_p\sum_q \phi_{ipq} X_{ip} Y_{iq}\, x_i(t)^2 + \\ + \frac{1}{4}\left(B_1^2 M_{11} N_{21} + C_1^2 M_{21} N_{11} - A_1^2 M_{11} N_{11} - D_1^2 M_{21} N_{21}\right) x_1(t) x_2(t)\Bigg], \tag{A.1}$$

where $\xi = \dfrac{b}{a}$, $\eta_i = \dfrac{m_i}{n_i}, i = 1,2$, $X_{ip} = \cos\dfrac{\pi p m_i x}{a}$, $Y_{iq} = \cos\dfrac{\pi q n_i y}{b}$,

$$M_{1p} = \cos\frac{\pi p(m_1+m_2)x}{a}, \quad M_{2p} = \cos\frac{\pi p(m_1-m_2)x}{a}, \ \phi_{i02} = \frac{\xi^2\eta_i^{\,2}}{32}, \quad \phi_{i20} = \frac{1}{32\xi^2\eta_i^{\,2}}$$

$$N_{1q} = \cos\frac{\pi q(n_1+n_2)y}{b}, \quad N_{2q} = \cos\frac{\pi q(n_1-n_2)y}{b},$$

$$A_1 = \frac{\xi\left(m_1n_2-m_2n_1\right)}{\left(m_1+m_2\right)^2\xi^2+\left(n_1+n_2\right)^2}, \qquad B_1 = \frac{\xi\left(m_1n_2+m_2n_1\right)}{\left(m_1+m_2\right)^2\xi^2+\left(n_1-n_2\right)^2},$$

$$C_1 = \frac{\xi\left(m_1n_2+m_2n_1\right)}{\left(m_1-m_2\right)^2\xi^2+\left(n_1+n_2\right)^2}, \qquad D_1 = \frac{\xi\left(m_1n_2-m_2n_1\right)}{\left(m_1-m_2\right)^2\xi^2+\left(n_1-n_2\right)^2}.$$

2) CCCC-plate

$$\begin{aligned}\phi(x,y,t) = Eh\Bigg\{&\sum_i\sum_p\sum_q \phi_{ipq}X_{ip}Y_{iq}\,x_i(t)^2 + \Bigg[\frac{1}{64}\Big(A_1^{\,2}M_{12}N_{12}+D_1^{\,2}M_{22}N_{22}-\\ &-B_1^{\,2}M_{12}N_{22}-C_1^{\,2}M_{22}N_{12}\Big)-\frac{m_1^2n_2^2}{32}\Big(B_2^{\,2}M_{12}Y_{21}+C_2^{\,2}M_{22}Y_{21}-\\ &-A_2^{\,2}X_{11}N_{12}-D_2^{\,2}X_{11}N_{22}-E_2^{\,2}X_{11}Y_{21}\Big)-\frac{m_2^2n_1^2}{32}\Big(B_3^{\,2}M_{12}Y_{11}+C_3^{\,2}M_{22}Y_{11}-\\ &-A_3^{\,2}X_{21}N_{12}-D_3^{\,2}X_{21}N_{22}-E_3^{\,2}X_{21}Y_{11}\Big)\Bigg]x_1(t)x_2(t)\Bigg\},\end{aligned} \tag{A.2}$$

where $\phi_{i04} = -\dfrac{\xi^2\eta_i^{\,2}}{512}, \quad \phi_{i40} = -\dfrac{1}{512\xi^2\eta_i^{\,2}},$

$$\phi_{i42} = \frac{\xi^2\eta_i^2}{32\left[4\eta_i^2\xi^2+1\right]^2}, \quad \phi_{i22} = -\frac{\xi^2\eta_i^2}{32\left[\eta_i^2\xi^2+1\right]^2}, \quad \phi_{i24} = \frac{\xi^2\eta_i^2}{32\left[\eta_i^2\xi^2+4\right]^2},$$

$$A_2 = \frac{\xi}{m_1^{\,2}\xi^2+\left(n_1+n_2\right)^2}, \ B_2 = \frac{\xi}{\left(m_1+m_2\right)^2\xi^2+n_2^{\,2}},$$

$$C_2 = \frac{\xi}{\left(m_1-m_2\right)^2\xi^2+n_2^{\,2}}, \ D_2 = \frac{\xi}{m_1^{\,2}\xi^2+\left(n_1-n_2\right)^2}, \ E_2 = \frac{\xi}{m_1^{\,2}\xi^2+n_2^{\,2}},$$

$$A_3 = \frac{\xi}{m_2^{\,2}\xi^2+\left(n_1+n_2\right)^2}, \ B_3 = \frac{\xi}{\left(m_1+m_2\right)^2\xi^2+n_1^{\,2}},$$

$$C_3 = \frac{\xi}{\left(m_1-m_2\right)^2\xi^2+n_1^{\,2}}, \ D_3 = \frac{\xi}{m_2^{\,2}\xi^2+\left(n_1-n_2\right)^2}, \ E_3 = \frac{\xi}{m_2^{\,2}\xi^2+n_1^{\,2}}$$

3) CSCS-plate

$$\phi(x,y,t)=Eh\left\{\sum_i\sum_p\sum_q\phi_{ipq}X_{ip}Y_{iq}\,x_i(t)^2+\left[\frac{1}{4}\left(A_4{}^2M_{12}N_{11}-D_4{}^2M_{22}N_{21}-B_4{}^2M_{12}N_{21}+C_4{}^2M_{22}N_{11}\right)+\right.\right.$$
$$\left.\left.+\frac{m_1^2n_2^2}{2}\left(A_5{}^2X_{11}N_{21}-B_5{}^2X_{11}N_{11}\right)+\frac{m_2^2n_1^2}{2}\left(C_5{}^2X_{21}N_{21}-D_5{}^2X_{21}N_{11}\right)\right]x_1(t)x_2(t)\right\}, \tag{11}$$

where $A_4=\dfrac{\xi\left(m_1n_2-m_2n_1\right)}{4\left(m_1+m_2\right)^2\xi^2+\left(n_1+n_2\right)^2}$, $B_4=\dfrac{\xi\left(m_1n_2+m_2n_1\right)}{4\left(m_1+m_2\right)^2\xi^2+\left(n_1-n_2\right)^2}$,

$C_4=\dfrac{\xi\left(m_1n_2+m_2n_1\right)}{4\left(m_1-m_2\right)^2\xi^2+\left(n_1+n_2\right)^2}$, $D_4=\dfrac{\xi\left(m_1n_2-m_2n_1\right)}{4\left(m_1-m_2\right)^2\xi^2+\left(n_1-n_2\right)^2}$,

$A_5=\dfrac{\xi}{4m_1{}^2\xi^2+\left(n_1-n_2\right)^2}$, $B_5=\dfrac{\xi}{4m_1{}^2\xi^2+\left(n_1+n_2\right)^2}$,

$C_5=\dfrac{\xi}{4m_2{}^2\xi^2+\left(n_1-n_2\right)^2}$, $D_5=\dfrac{\xi}{4m_2{}^2\xi^2+\left(n_1+n_2\right)^2}$.

APPENDIX B

1) SSSS-plate

$$\alpha_1=-\frac{E}{2\rho ab}\pi^4\int_0^a\int_0^b K_{11}{}^2L_{11}{}^2\left[\frac{m_1^4}{a^4}Y_{12}+\frac{n_1^4}{b^4}X_{12}\right]dxdy, \tag{B.1}$$

$$\alpha_3=-\frac{E}{2\rho ab}\pi^4\int_0^a\int_0^b K_{21}{}^2L_{21}{}^2\left[\frac{m_2^4}{a^4}Y_{22}+\frac{n_2^4}{b^4}X_{22}\right]dxdy \tag{B.2}$$

$$\alpha_2=-\frac{E}{2\rho ab}\pi^4\int_0^a\int_0^b\left\{K_{11}L_{11}\left[\frac{m_1^2m_2^2}{a^4}Y_{22}+\frac{n_1^2n_2^2}{b^4}X_{22}\right]+\frac{2m_2^2}{a^2b^2}K_{21}L_{21}M_{11}\left[-A_1^2\left(n_1+n_2\right)^2N_{11}+B_1^2\left(n_1-n_2\right)^2N_{21}\right]+\right.$$
$$+\frac{2m_2^2}{a^2b^2}K_{21}L_{21}M_{21}\left[-D_1^2\left(n_1-n_2\right)^2N_{21}+C_1^2\left(n_1+n_2\right)^2N_{11}\right]+\frac{2n_2^2}{a^2b^2}K_{21}L_{21}N_{11}\left[B_1^2\left(m_1-m_2\right)^2M_{21}-\right.$$
$$\left.-A_1^2\left(m_1+m_2\right)^2M_{11}\right]+\frac{2n_2^2}{a^2b^2}K_{21}L_{21}N_{21}\left[-D_1^2\left(m_1-m_2\right)^2\cos M_{11}+C_1^2\left(m_1+m_2\right)^2M_{21}\right]-$$
$$-\frac{4m_2n_2}{a^2b^2}X_{21}Y_{21}\left(m_1+m_2\right)S_{11}\left[-A_1^2\left(n_1+n_2\right)T_{11}+B_1^2\left(n_1-n_2\right)T_{21}\right]-$$
$$\left.-\frac{4m_2n_2}{a^2b^2}X_{21}Y_{21}\left(m_1-m_2\right)S_{21}\left[-D_1^2\left(n_1-n_2\right)T_{21}+C_1^2\left(n_1+n_2\right)T_{11}\right]\right\}K_{11}L_{11}dxdy, \tag{B.3}$$

$$\alpha_4 = -\frac{E}{2\rho ab}\pi^4 \int_0^a\int_0^b \Bigg\{ K_{21}L_{21}\left[\frac{m_1^2 m_2^2}{a^4}Y_{12} + \frac{n_1^2 n_2^2}{b^4}X_{12}\right] + \frac{2m_1^2}{a^2b^2}K_{11}L_{11}M_{11}\left[-A_1^2\left(n_1+n_2\right)^2 N_{11} + B_1^2\left(n_1-n_2\right)^2 N_{21}\right] +$$

$$+\frac{2m_1^2}{a^2b^2}K_{11}L_{11}M_{21}\left[-D_1^2\left(n_1-n_2\right)^2 N_{21} + C_1^2\left(n_1+n_2\right)^2 N_{11}\right] + \frac{2n_1^2}{a^2b^2}K_{11}L_{11}N_{11}\left[B_1^2\left(m_1-m_2\right)^2 M_{21} -\right.$$

$$\left.-A_1^2\left(m_1+m_2\right)^2 M_{11}\right] + \frac{2n_1^2}{a^2b^2}K_{11}L_{11}N_{21}\left[-D_1^2\left(m_1-m_2\right)^2 M_{21} + C_1^2\left(m_1+m_2\right)^2 M_{11}\right] -$$

$$-\frac{4m_1 n_1}{a^2b^2}X_{11}Y_{11}\left(m_1+m_2\right)S_{11}\left[-A_1^2\left(n_1+n_2\right)T_{11} + B_1^2\left(n_1-n_2\right)T_{21}\right] -$$

$$-\frac{4m_1 n_1}{a^2b^2}X_{11}Y_{11}\left(m_1-m_2\right)S_{21}\left[-D_1^2\left(n_1-n_2\right)T_{21} + C_1^2\left(n_1+n_2\right)T_{11}\right]\Bigg\} K_{21}L_{21}dxdy, \tag{B.4}$$

where $K_{ip} = \sin\frac{\pi p m_i x}{a}$, $L_{iq} = \sin\frac{\pi q n_i y}{b}$, $S_{1p} = \sin\frac{\pi p(m_1+m_2)x}{a}$, $S_{2p} = \sin\frac{\pi p(m_1-m_2)x}{a}$,

$T_{1q} = \sin\frac{\pi q(n_1+n_2)y}{b}$, $T_{2q} = \sin\frac{\pi q(n_1-n_2)y}{b}$.

2) CCCC-plate

$$\alpha_1 = \frac{16E}{9\rho ab}\pi^4 \int_0^a\int_0^b \Bigg\{ \frac{1}{8}\left[\frac{m_1^4}{a^4}X_{12}(1-Y_{12})(Y_{12}-\frac{Y_{14}}{4}) + \frac{n_1^4}{b^4}Y_{12}\left(1-X_{12}\right)(X_{12}-\frac{X_{14}}{4})\right] -$$

$$+\frac{m_1^4 n_1^4}{8a^2b^2}\Big[A^2 X_{14}Y_{12}(X_{12}+4Y_{12}-5X_{12}Y_{12}+4K_{12}L_{12}) - B^2 X_{12}Y_{12}(X_{12}+Y_{12}-2X_{12}Y_{12}+2K_{12}L_{12}) + \tag{B.5}$$

$$+C^2 X_{12}Y_{14}(4X_{12}+Y_{12}-5X_{12}Y_{12}+4K_{12}L_{12})\Big]\Bigg\}(1-X_{12})(1-Y_{12})dxdy,$$

$$\alpha_3 = \frac{16E}{9\rho ab}\pi^4 \int_0^a\int_0^b \Bigg\{ \frac{1}{8}\left[\frac{m_2^4}{a^4}X_{22}(1-Y_{22})(Y_{22}-\frac{Y_{24}}{4}) + \frac{n_2^4}{b^4}Y_{22}\left(1-X_{22}\right)(X_{22}-\frac{X_{24}}{4})\right] -$$

$$+\frac{m_2^4 n_2^4}{8a^2b^2}\Big[D^2 X_{24}Y_{22}(X_{22}+4Y_{22}-5X_{22}Y_{22}+4K_{22}L_{22}) - E^2 X_{22}Y_{22}(X_{22}+Y_{22}-2X_{22}Y_{22}+2K_{22}L_{22}) + \tag{B.6}$$

$$+F^2 X_{22}Y_{24}(4X_{22}+Y_{22}-5X_{22}Y_{22}+4K_{22}L_{22})\Big]\Bigg\}(1-X_{22})(1-Y_{22})dxdy,$$

$$
\begin{aligned}
\alpha_2 = {} & \frac{16E}{9\rho ab}\pi^4 \int_0^a\int_0^b \left\{ \frac{1}{8}\left[\frac{m_1^2 m_2^2}{a^4} X_{12}(1-Y_{12})\left(Y_{22}-\frac{Y_{24}}{4}\right) + \frac{n_1^2 n_2^2}{b^4} Y_{12}(1-X_{12})\left(X_{22}-\frac{X_{24}}{4}\right)\right] + \right. \\
& + \frac{m_1^2 m_2^2 n_2^4}{8a^2b^2} X_{12}(1-Y_{12})\left[D^2 X_{24}Y_{22} - E^2 X_{22}Y_{22} + 4F^2 X_{22}Y_{24}\right] + \\
& + \frac{n_1^2 n_2^2 m_2^4}{8a^2b^2} Y_{12}(1-X_{12})\left[4D^2 X_{24}Y_{22} - E^2 X_{22}Y_{22} + F^2 X_{22}Y_{24}\right] + \\
& + \frac{m_1 n_1 m_2^3 n_2^3}{4a^2b^2} K_{12}L_{12}\left[2D^2 K_{24}L_{22} - E^2 K_{22}L_{22} + 2F^2 K_{22}L_{24}\right] - \\
& - \frac{m_2^2}{16a^2b^2} X_{22}(1-Y_{22})\left[A_1^2\left(n_1+n_2\right)^2 M_{12}N_{12} + B_1^2\left(n_1-n_2\right)^2 M_{12}N_{22} + \right. \\
& + C_1^2\left(n_1+n_2\right)^2 M_{22}N_{12} + D_1^2\left(n_1-n_2\right)^2 M_{22}N_{22} - 2B_2^2 m_1^2 n_2^4 M_{12}Y_{22} - \\
& - 2C_2^2 m_1^2 n_2^4 M_{22}Y_{22} + 2A_2^2 m_1^2 n_2^2\left(n_1+n_2\right)^2 N_{12}X_{12} + 2D_2^2 m_1^2 n_2^2\left(n_1-n_2\right)^2 N_{22}X_{12} + \\
& + 2E_2^2 m_1^2 n_2^4 X_{12}Y_{22} - 2B_3^2 m_2^2 n_1^4 M_{12}Y_{12} - 2C_3^2 m_2^2 n_1^4 M_{22}Y_{12} + 2A_3^2 m_2^2 n_1^2\left(n_1+n_2\right)^2 N_{12}X_{22} + \\
& \left. + 2D_3^2 m_2^2 n_1^2\left(n_1-n_2\right)^2 N_{22}X_{22} + 2E_3^2 m_2^2 n_1^4 X_{22}Y_{12}\right] - \frac{n_2^2}{16a^2b^2} Y_{22}(1-X_{22}) \times \\
& \times\left[A_1^2\left(m_1+m_2\right)^2 M_{12}N_{12} + B_1^2\left(m_1+m_2\right)^2 M_{12}N_{22} + C_1^2\left(m_1-m_2\right)^2 M_{22}N_{12} + D_1^2\left(m_1-m_2\right)^2 M_{22}N_{22} - \right. \\
& - 2B_2^2 m_1^2 n_2^2\left(m_1+m_2\right)^2 M_{12}Y_{22} - 2C_2^2 m_1^2 n_2^2\left(m_1-m_2\right)^2 M_{22}Y_{22} + 2A_2^2 m_1^4 n_2^2 N_{12}X_{12} + 2D_2^2 m_1^4 n_2^2 N_{22}X_{12} + \\
& + 2E_2^2 m_1^4 n_2^2 X_{12}Y_{22} - 2B_3^2 m_2^2 n_1^2\left(m_1+m_2\right)^2 M_{12}Y_{12} - 2C_3^2 m_2^2 n_1^2\left(m_1-m_2\right)^2 M_{22}Y_{12} + 2A_3^2 m_2^4 n_1^2 N_{12}X_{22} + \\
& \left. + 2D_3^2 m_2^4 n_1^2 N_{22}X_{22} + 2E_3^2 m_2^4 n_1^2 X_{22}Y_{12}\right] - \frac{m_2 n_2}{16a^2b^2} K_{22}L_{22}\left[B_1^2\left(m_1+m_2\right)\left(n_1-n_2\right)S_{12}T_{22} + \right. \\
& + A_1^2\left(m_1+m_2\right)\left(n_1+n_2\right)S_{12}T_{12} + C_1^2\left(m_1-m_2\right)\left(n_1+n_2\right)S_{22}T_{12} + D_1^2\left(m_1-m_2\right)\left(n_1-n_2\right)S_{22}T_{22} - \\
& - 2B_2^2 m_1^2 n_2^3\left(m_1+m_2\right)S_{12}L_{22} - 2C_2^2 m_1^2 n_2^3\left(m_1-m_2\right)S_{22}L_{22} + 2A_2^2 m_1^3 n_2^2\left(n_1+n_2\right)T_{12}K_{12} + \\
& + 2D_2^2 m_1^3 n_2^2\left(n_1-n_2\right)T_{22}K_{12} + 2E_2^2 m_1^3 n_2^3 K_{12}L_{22} - 2B_3^2 m_2^2 n_1^3\left(m_1+m_2\right)S_{12}L_{12} - 2C_3^2 m_2^2 n_1^3\left(m_1-m_2\right) \times \\
& \left.\left. \times S_{22}L_{12} + 2A_3^2 m_2^3 n_1^2\left(n_1+n_2\right)T_{12}K_{22} + 2D_3^2 m_2^3 n_1^2\left(n_1-n_2\right)T_{22}K_{22} + 2E_3^2 m_2^3 n_1^3 K_{22}L_{12}\right]\right\}(1-X_{12})(1-Y_{12})\,dxdy.
\end{aligned}
\tag{B.7}
$$

$$\alpha_4 = \frac{16E}{9\rho ab}\pi^4 \int_0^a\int_0^b \left\{ \frac{1}{8}\left[\frac{m_1^2 m_2^2}{a^4} X_{22}(1-Y_{22})\left(Y_{12}-\frac{Y_{14}}{4}\right) + \frac{n_1^2 n_2^2}{b^4} Y_{22}(1-X_{22})\left(X_{12}-\frac{X_{14}}{4}\right)\right] + \right.$$

$$+\frac{m_1^2 m_2^2 n_1^4}{8a^2b^2} X_{22}(1-Y_{22})\left[A^2 X_{14}Y_{12} - B^2 X_{12}Y_{12} + 4C^2 X_{12}Y_{14}\right] +$$

$$+\frac{n_1^2 n_2^2 m_1^4}{8a^2b^2} Y_{22}(1-X_{22})\left[4A^2 X_{14}Y_{12} - B^2 X_{12}Y_{12} + C^2 X_{12}Y_{14}\right] +$$

$$+\frac{m_2 n_2 m_1^3 n_1^3}{4a^2b^2} K_{22}L_{22}\left[2A^2 K_{14}L_{12} - B^2 K_{12}L_{12} + 2C^2 K_{12}L_{14}\right] -$$

$$-\frac{m_1^2}{16a^2b^2} X_{12}(1-Y_{12})\left[A_1^2\left(n_1+n_2\right)^2 M_{12}N_{12} + B_1^2\left(n_1-n_2\right)^2 M_{12}N_{22} + \right.$$

$$+C_1^2\left(n_1+n_2\right)^2 M_{22}N_{12} + D_1^2\left(n_1-n_2\right)^2 M_{22}N_{22} - 2B_2^2 m_1^2 n_2^4 M_{12}Y_{22} -$$

$$-2C_2^2 m_1^2 n_2^4 M_{22}Y_{22} + 2A_2^2 m_1^2 n_2^2\left(n_1+n_2\right)^2 N_{12}X_{12} + 2D_2^2 m_1^2 n_2^2\left(n_1-n_2\right)^2 N_{22}X_{12} +$$

$$+2E_2^2 m_1^2 n_2^4 X_{12}Y_{22} - 2B_3^2 m_2^2 n_1^4 M_{12}Y_{12} - 2C_3^2 m_2^2 n_1^4 M_{22}Y_{12} + 2A_3^2 m_2^2 n_1^2\left(n_1+n_2\right)^2 N_{12}X_{22} +$$

$$\left.+2D_3^2 m_2^2 n_1^2\left(n_1-n_2\right)^2 N_{22}X_{22} + 2E_3^2 m_2^2 n_1^4 X_{22}Y_{12}\right] - \frac{n_1^2}{16a^2b^2} Y_{12}(1-X_{12})\times$$

$$\times\left[A_1^2\left(m_1+m_2\right)^2 M_{12}N_{12} + B_1^2\left(m_1+m_2\right)^2 M_{12}N_{22} + C_1^2\left(m_1-m_2\right)^2 M_{22}N_{12} + D_1^2\left(m_1-m_2\right)^2 M_{22}N_{22} - \right.$$

$$-2B_2^2 m_1^2 n_2^2\left(m_1+m_2\right)^2 M_{12}Y_{22} - 2C_2^2 m_1^2 n_2^2\left(m_1-m_2\right)^2 M_{22}Y_{22} + 2A_2^2 m_1^4 n_2^2 N_{12}X_{12} + 2D_2^2 m_1^4 n_2^2 N_{22}X_{12} +$$

$$+2E_2^2 m_1^4 n_2^2 X_{12}Y_{22} - 2B_3^2 m_2^2 n_1^2\left(m_1+m_2\right)^2 M_{12}Y_{12} - 2C_3^2 m_2^2 n_1^2\left(m_1-m_2\right)^2 M_{22}Y_{12} + 2A_3^2 m_2^4 n_1^2 N_{12}X_{22} +$$

$$\left.+2D_3^2 m_2^4 n_1^2 N_{22}X_{22} + 2E_3^2 m_2^4 n_1^2 X_{22}Y_{12}\right] - \frac{m_1 n_1}{16a^2b^2} K_{12}L_{12}\left[B_1^2\left(m_1+m_2\right)\left(n_1-n_2\right)S_{12}T_{22} + \right.$$

$$+A_1^2\left(m_1+m_2\right)\left(n_1+n_2\right)S_{12}T_{12} + C_1^2\left(m_1-m_2\right)\left(n_1+n_2\right)S_{22}T_{12} + D_1^2\left(m_1-m_2\right)\left(n_1-n_2\right)S_{22}T_{22} -$$

$$-2B_2^2 m_1^2 n_2^3\left(m_1+m_2\right)S_{12}L_{22} - 2C_2^2 m_1^2 n_2^3\left(m_1-m_2\right)S_{22}L_{22} + 2A_2^2 m_1^3 n_2^2\left(n_1+n_2\right)T_{12}K_{12} +$$

$$+2D_2^2 m_1^3 n_2^2\left(n_1-n_2\right)T_{22}K_{12} + 2E_2^2 m_1^3 n_2^3 K_{12}L_{22} - 2B_3^2 m_2^2 n_1^3\left(m_1+m_2\right)S_{12}L_{12} - 2C_3^2 m_2^2 n_1^3\left(m_1-m_2\right)\times$$

$$\left.\left.\times S_{22}L_{12} + 2A_3^2 m_2^3 n_1^2\left(n_1+n_2\right)T_{12}K_{22} + 2D_3^2 m_2^3 n_1^2\left(n_1-n_2\right)T_{22}K_{22} + 2E_3^2 m_2^3 n_1^3 K_{22}L_{12}\right]\right\}(1-X_{22})(1-Y_{22})dxdy, \tag{B.8}$$

where $A^2 = \frac{32\varphi_{142}}{m_1^2 n_1^2}$, $B^2 = \frac{32\varphi_{122}}{m_1^2 n_1^2}$, $C^2 = \frac{32\varphi_{124}}{m_1^2 n_1^2}$, $D^2 = \frac{32\varphi_{242}}{m_2^2 n_2^2}$, $E^2 = \frac{32\varphi_{222}}{m_2^2 n_2^2}$, $F^2 = \frac{32\varphi_{224}}{m_2^2 n_2^2}$.

3) CSCS-plate

$$\alpha_1 = \frac{8E}{3\rho ab}\pi^4 \int_0^a\int_0^b \left\{ \frac{1}{4} X_{12}L_{11}\left[\frac{m_1^4}{a^4}Y_{12} + \frac{n_1^4}{4b^4}\left(X_{12}-1\right)\right] - \frac{n_1^4}{64b^4} X_{14}L_{11}\left(X_{12}-1\right) - \right.$$

$$\left. -\frac{m_1^4 n_1^4}{16a^2b^2} G^2 L_{11}X_{12}Y_{12}\left(5X_{12}-1\right) - \frac{m_1^4 n_1^4}{4a^2b^2} G^2 K_{12}^2 L_{12}Y_{11}\right\}(1-X_{12})L_{11}dxdy, \tag{B.9}$$

$$\alpha_3 = \frac{8E}{3\rho ab}\pi^4 \int_0^a\int_0^b \left\{ \frac{1}{4} X_{22} L_{21} \left[\frac{m_2^4}{a^4} Y_{22} + \frac{n_2^4}{4b^4}\left(X_{22} - 1 \right) \right] - \frac{n_2^4}{64b^4} X_{24} L_{21} \left(X_{22} - 1 \right) - \right.$$
$$\left. - \frac{m_2^4 n_2^4}{16a^2b^2} H^2 L_{21} X_{22} Y_{22} \left(5X_{22} - 1 \right) - \frac{m_2^4 n_2^4}{4a^2b^2} H^2 K_{22}{}^2 L_{22} Y_{21} \right\} (1 - X_{22}) L_{21} dxdy, \tag{B.10}$$

$$\alpha_2 = \frac{8E}{3\rho ab}\pi^4 \int_0^a\int_0^b \left\{ \frac{1}{4} \left[\frac{m_1^2 m_2^2}{a^4} X_{12} L_{11} Y_{22} + \frac{n_1^2 n_2^2}{4b^4} L_{11} (1 - X_{12})(X_{22} - \frac{X_{24}}{4}) \right] - \right.$$
$$- \frac{m_2^2 n_2^2}{16a^2b^2} H^2 L_{11} X_{22} Y_{22} \left(4m_1^2 n_2^2 X_{12} - n_1^2 m_2^2 (1 - X_{12}) \right) - \frac{m_1 n_1 m_2^3 n_2^3}{4a^2b^2} H^2 K_{12} Y_{11} K_{22} L_{22} -$$
$$- \frac{m_2^2}{2a^2b^2} X_{22} L_{21} \left[-A_4{}^2 \left(n_1 + n_2 \right)^2 M_{12} N_{11} + B_4{}^2 \left(n_1 - n_2 \right)^2 M_{12} N_{21} - \right.$$
$$-C_4{}^2 \left(n_1 + n_2 \right)^2 M_{22} N_{11} + D_4{}^2 \left(n_1 - n_2 \right)^2 M_{21} N_{22} + 2B_5{}^2 m_1^2 n_2^2 \left(n_1 + n_2 \right)^2 X_{12} N_{11} -$$
$$\left. -2C_5{}^2 m_2^2 n_1^2 \left(n_1 - n_2 \right)^2 X_{22} N_{21} - 2A_5{}^2 m_1^2 n_2^2 \left(n_1 - n_2 \right)^2 N_{21} X_{12} + 2D_5{}^2 m_2^2 n_1^2 \left(n_1 + n_2 \right)^2 N_{11} X_{22} \right] -$$
$$+ \frac{n_2^2}{2a^2b^2} (1 - X_{22}) L_{21} \left[-A_4{}^2 \left(m_1 + m_2 \right)^2 M_{12} N_{11} + B_4{}^2 \left(m_1 + m_2 \right)^2 M_{12} N_{21} - \right.$$
$$-C_4{}^2 \left(m_1 - m_2 \right)^2 M_{22} N_{11} + \frac{1}{4} D_4{}^2 \left(m_1 - m_2 \right)^2 M_{21} N_{22} + 2B_5{}^2 m_1^4 n_2^2 X_{12} N_{11} -$$
$$\left. -2C_5{}^2 m_2^4 n_1^2 X_{22} N_{21} - 2A_5{}^2 m_1^4 n_2^2 N_{21} X_{12} + 2D_5{}^2 m_2^4 n_1^2 N_{11} X_{22} \right] +$$
$$+ \frac{m_2 n_2}{a^2b^2} K_{22} Y_{21} \left[-B_4{}^2 \left(m_1 + m_2 \right)\left(n_1 - n_2 \right) S_{12} T_{21} + \right.$$
$$+ A_4{}^2 \left(m_1 + m_2 \right)\left(n_1 + n_2 \right) S_{12} T_{11} + C_4{}^2 \left(m_1 - m_2 \right)\left(n_1 + n_2 \right) S_{22} T_{11} - D_4{}^2 \left(m_1 - m_2 \right)\left(n_1 - n_2 \right) S_{12} T_{22} -$$
$$-2B_5{}^2 m_1^3 n_2^2 \left(n_1 + n_2 \right) T_{11} K_{12} + 2C_5{}^2 m_2^3 n_1^2 \left(n_1 - n_2 \right) T_{21} K_{22} + 2A_5{}^2 m_1^3 n_2^2 \left(n_1 - n_2 \right) T_{21} K_{12} -$$
$$\left. \left. -2D_5{}^2 m_2^3 n_1^2 \left(n_1 + n_2 \right) T_{11} K_{22} \right] \right\} (1 - X_{12}) L_{11} dxdy, \tag{B.11}$$

$$
\begin{aligned}
\alpha_4 = {} & \frac{8E}{3\rho ab}\pi^4 \int_0^a\int_0^b \left\{ \frac{1}{4}\left[\frac{m_1^2 m_2^2}{a^4} X_{22} L_{21} Y_{12} + \frac{n_1^2 n_2^2}{4b^4} L_{21}(1-X_{22})(X_{12} - \frac{X_{14}}{4}) \right] - \right. \\
& - \frac{m_1^2 n_1^2}{16a^2b^2} G^2 L_{21} X_{12} Y_{12} \left(4m_2^2 n_1^2 X_{22} - n_2^2 m_1^2 (1-X_{22})\right) - \frac{m_1^3 n_1^3 m_2 n_2}{4a^2b^2} G^2 K_{22} Y_{21} K_{12} L_{12} \\
& - \frac{m_1^2}{2a^2b^2} X_{12} L_{11} \left[-A_4^{\,2}\left(n_1+n_2\right)^2 M_{12} N_{11} + B_4^{\,2}\left(n_1-n_2\right)^2 M_{12} N_{21} - \right. \\
& - C_4^{\,2}\left(n_1+n_2\right)^2 M_{22} N_{11} + D_4^{\,2}\left(n_1-n_2\right)^2 M_{21} N_{22} + 2B_5^{\,2} m_1^2 n_2^2 \left(n_1+n_2\right)^2 X_{12} N_{11} - \\
& \left. -2C_5^{\,2} m_2^2 n_1^2 \left(n_1-n_2\right)^2 X_{22} N_{21} - 2A_5^{\,2} m_1^2 n_2^2 \left(n_1-n_2\right)^2 N_{21} X_{12} + 2D_5^{\,2} m_2^2 n_1^2 \left(n_1+n_2\right)^2 N_{11} X_{22} \right] - \\
& + \frac{n_1^2}{2a^2b^2}(1-X_{12}) L_{11} \left[-A_4^{\,2}\left(m_1+m_2\right)^2 M_{12} N_{11} + B_4^{\,2}\left(m_1+m_2\right)^2 M_{12} N_{21} - \right. \\
& - C_4^{\,2}\left(m_1-m_2\right)^2 M_{22} N_{11} + \frac{1}{4} D_4^{\,2}\left(m_1-m_2\right)^2 M_{21} N_{22} + 2B_5^{\,2} m_1^4 n_2^2 X_{12} N_{11} - \\
& \left. -2C_5^{\,2} m_2^4 n_1^2 X_{22} N_{21} - 2A_5^{\,2} m_1^4 n_2^2 N_{21} X_{12} + 2D_5^{\,2} m_2^4 n_1^2 N_{11} X_{22} \right] + \\
& + \frac{m_1 n_1}{a^2b^2} K_{12} Y_{11} \left[-B_4^{\,2}\left(m_1+m_2\right)\left(n_1-n_2\right) S_{12} T_{21} + \right. \\
& + A_4^{\,2}\left(m_1+m_2\right)\left(n_1+n_2\right) S_{12} T_{11} + C_4^{\,2}\left(m_1-m_2\right)\left(n_1+n_2\right) S_{22} T_{11} - D_4^{\,2}\left(m_1-m_2\right)\left(n_1-n_2\right) S_{12} T_{22} - \\
& - 2B_5^{\,2} m_1^3 n_2^2 \left(n_1+n_2\right) T_{11} K_{12} + 2C_5^{\,2} m_2^3 n_1^2 \left(n_1-n_2\right) T_{21} K_{22} + 2A_5^{\,2} m_1^3 n_2^2 \left(n_1-n_2\right) T_{21} K_{12} \\
& \left. \left. -2D_5^{\,2} m_2^3 n_1^2 \left(n_1+n_2\right) T_{11} K_{22} \right] \right\} (1-X_{22}) L_{21} dxdy,
\end{aligned}
\tag{B.12}
$$

where $G^2 = -\dfrac{32\varphi_{122}}{m_1^2 n_1^2}$, $H^2 = -\dfrac{32\varphi_{222}}{m_2^2 n_2^2}$.

Marina V. Shitikova, Prof., Dr.Sc., Research Center on Dynamics of Solids and Structures; Voronezh State Technical University; 20-letiya Oktyabrya 84, Voronezh, 394006, Russia; Department of Structural and Theoretical Mechanics, Moscow State University of Civil Engineering, Moscow. Phone +7 (473) 271-42-20; fax +7 (473) 277-39-92; E-mail: mvs@vgasu.vrn.ru; ORCID: 0000-0003-2186-1881.

Anastasiya I. Krusser, Ph.D. student; Junior Researcher; Research Center on Dynamics of Solids and Structures, Voronezh State Tchnical University; E-mail: an.krusser@yandex.ru; ORCID: 0000-0001-6203-2495.

Шитикова Марина Вячеславовна, профессор, доктор физико-математических наук; руководитель международного научного центра по фундаментальным исследованиям в области естественных и строительных наук имени Заслуженного деятеля науки РФ, профессора Россихина Ю.А.; Воронежский государственный технический университет; 394006, Россия, г. Воронеж, ул. 20 лет Октября, д. 84, E-mail: mvs@vgasu.vrn.ru; ORCID: 0000-0003-2186-1881.

Анастасия И. Круссер, аспирант, младший научный сотрудник международного научного центра по фундаментальным исследованиям в области естественных и строительных наук имени Заслуженного деятеля науки РФ, профессора Россихина Ю.А., Воронежский государственный технический университет; E-mail: an.krusser@yandex.ru; ORCID: 0000-0001-6203-2495.

DOI:10.22337/2587-9618-2021-17-4-181-187

AIMED CONTROL OF THE FREQUENCY SPECTRUM OF EIGENVIBRATIONS OF ELASTIC PLATES WITH A FINITE NUMBER OF DEGREES OF MASS FREEDOM BY INTRODUCING ADDITIONAL GENERALIZED KINEMATIC DEVICES

***Pavel A. Akimov* [1, 2], *Leonid S. Lyakhovich* [2]**

[1] National Research Moscow State University of Civil Engineering, Moscow, RUSSIA

[2] Tomsk State University of Architecture and Building, Tomsk, RUSSIA

Abstract: As is known, targeted regulation of the frequency spectrum of natural vibrations of elastic systems with a finite number of degrees of mass freedom can be performed by introducing additional generalized constraints and generalized kinematic devices. Each targeted generalized constraint increases, and each generalized kinematic device reduces the value of only one selected natural frequency to a predetermined value, without changing the remaining natural frequencies and all forms of natural vibrations (natural modes). To date, for some elastic systems with a finite number of degrees of freedom of masses, in which the directions of mass movement are parallel and lie in the same plane, special methods have been already developed for creating additional constraints and generalized kinematic devices that change the frequency spectrum of natural vibrations in a targeted manner. In particular, a theory and an algorithm for the creation of targeted generalized constraints and generalized kinematic devices have been developed for rods. It was previously proved that the method of forming a matrix of additional stiffness coefficients, specifying targeted generalized constraint, in the problem of natural vibrations of rods can also be applied to solving a similar problem for elastic systems with a finite number of degrees of freedom, in which the directions of mass movement are parallel, but do not lie in the same plane. In particular, such systems include plates. The distinctive paper shows that the method of forming a matrix for taking into account the action of additional inertial forces, specifying targeted kinematic devices in the problem of natural vibrations of rods can also be applied to solving a similar problem for elastic systems with a finite number of degrees of freedom, in which the directions of mass movement are parallel, but do not lie in the same plane. However, the algorithms for the creation of targeted generalized kinematic devices developed for rods based on the properties of rope polygons cannot be used without significant changes in a similar problem for plates. The method of creation of computational schemes of kinematic devices that precisely change the frequency spectrum of natural vibrations of elastic plates with a finite number of degrees of mass freedom is a separate problem and will be considered in a subsequent paper

Keywords: natural frequency, natural mode, targeted generalized constraint, targeted generalized kinematic device, stiffness coefficients, inertial forces

ПРИЦЕЛЬНОЕ РЕГУЛИРОВАНИЕ СПЕКТРА ЧАСТОТ СОБСТВЕННЫХ КОЛЕБАНИЙ УПРУГИХ ПЛАСТИН С КОНЕЧНЫМ ЧИСЛОМ СТЕПЕНЕЙ СВОБОДЫ МАСС ПУТЁМ ВВЕДЕНИЯ ДОПОЛНИТЕЛЬНЫХ ОБОБЩЕННЫХ КИНЕМАТИЧЕСКИХ УСТРОЙСТВ

***П.А. Акимов* [1, 2], *Л.С. Ляхович* [2]**

[1] Национальный исследовательский Московский государственный строительный университет, г. Москва, РОССИЯ

[2] Томский государственный архитектурно-строительный университет, г. Томск, РОССИЯ

Аннотация: Известно, что прицельное регулирование спектра частот собственных колебаний упругих систем с конечным числом степеней свободы масс может выполняться введением дополнительных

обобщённых связей и обобщённых кинематических устройств. Каждая обобщённая прицельная связь увеличивает, а каждое обобщённое кинематическое устройство уменьшает величину лишь одной выбранной собственной частоты до наперёд заданного значения, не изменяя при этом остальные собственные частоты и все формы собственных колебаний. К настоящему времени для некоторых упругих систем с конечным числом степеней свободы масс, у которых направления движения масс параллельны и лежат в одной плоскости, разработаны методы создания дополнительных связей и обобщённых кинематических устройств, прицельно изменяющих спектр частот собственных колебаний. В частности, для стержней разработаны теория и алгоритмы формирования прицельных дополнительных связей и обобщённых кинематических устройств. Ранее было доказано, что метод формирования матрицы дополнительных коэффициентов жесткости, характеризующих прицельную связь, в задаче о собственных колебаниях стержней, может быть применен и при решении аналогичной задачи для упругих систем с конечным числом степеней свободы, у которых направления движения масс параллельны, но не лежат в одной плоскости. В частности, к таким системам относятся пластины. В данной статье показано, что метод формирования матрицы учета действия дополнительных инерционных сил, характеризующих прицельное кинематическое устройство, в задаче о собственных колебаниях стержней, может быть применен и при решении аналогичной задачи для упругих систем с конечным числом степеней свободы, у которых направления движения масс параллельны, но не лежат в одной плоскости. Однако, алгоритмы формирования прицельных обобщённых кинематических устройств, разработанные для стержней на основе свойств верёвочных многоугольников, не могут быть без существенных изменений использованы в аналогичной задаче для пластин. Метод формирования расчётных схем кинематических устройств, прицельно изменяющих спектр частот собственных колебаний упругих пластин с конечным числом степеней свободы масс, представляет собой отдельную задачу и будет в рассмотрен в последующей работе

Ключевые слова: частота собственных колебаний, форма собственных колебаний, обобщенная прицельная дополнительная связь, обобщенное прицельное кинематическое устройство, коэффициенты жесткости, инерционные силы

INTRODUCTION

When designing structures, in some cases it becomes necessary to deduce one or several natural frequencies from a certain frequency interval. As is known [1-4] one of the methods for solving such a problem is the creation of targeted generalized constraints and generalized kinematic devices. Special methods and algorithms of creation of generalized constraints and generalized kinematic devices for elastic rods carrying a finite amount of concentrated masses were developed and presented in the above-mentioned papers. It was shown in [5] that the method of forming a matrix of additional stiffness coefficients, specifying the targeted constraints in the problem of natural vibrations of rods can also be applied to solving a similar problem for elastic systems with a finite number of degrees of freedom, in which the directions of motion of the masses are parallel, but do not lie in the same plane. Let us show in the distinctive paper that a similar approach can be applied to solving the problem of creating targeting generalized kinematic devices for elastic systems with a finite number of degrees of freedom, in which the directions of motion of the masses are parallel, but do not lie in the same plane. In particular, such systems include plates. By analogy with the approach, described in [5], let us firstly present a method of creation of targeted kinematic devices for elastic rods [6] carrying a finite amount of concentrated masses. We can use system shown in Figure 1 [3, 4].

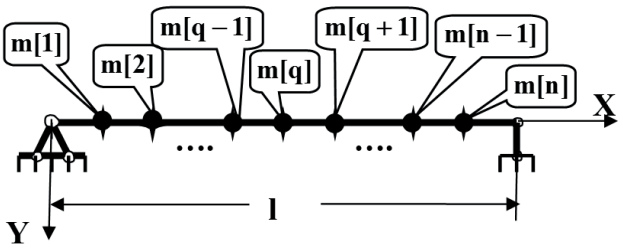

Figure 1. Sample system.

As in [5], the main system of the displacement method was chosen (Figure 1*b*). The equations of the displacement method were written in the form conventional for systems with a finite number of degrees of freedom

$$
\begin{aligned}
&(r[1,1]+m[1]\omega^2)v[1,j]+r[1,2]v[2,j]+...+r[1,q]v[q,j]+...+r[1,n]v[n,j]=0\\
&r[2,1]v[1,j]+(r[2,2]+m[2]\omega^2)v[2,j]+...+r[2,q]v[q,j]+...+r[2,n]v[n,j]=0\\
&.....\\
&.....\\
&r[n,1]v[1,j]+r[n,2]v[2,j]+...+r[n,q]v[q,j]+...+(r[n,n]+m[n]\omega^2)v[n,j]=0
\end{aligned}
\tag{1}
$$

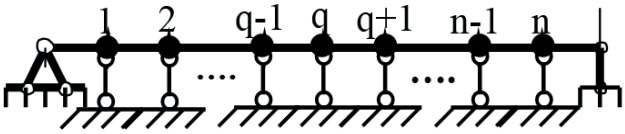

Figure 2. Main system of the displacement method (sample).

Values $r[i,k]$ in (1) form matrix of stiffness coefficients $A=\|r[i,k]\|$; $m[i]$ are the values of the masses, which form a diagonal matrix $M=\|m[i]\|$; ω is the frequency of natural vibrations of the system; $v[k,j]$ are displacements in the direction of motion of the masses in the j-th form of natural vibrations (natural modes).
Roots of the equation

$$\left|A-\omega^2 M\right|=0 \tag{2}$$

determine the spectrum of frequencies of natural vibrations of the system

$$\omega[1],\omega[2],...,\omega[q-1],\omega[q],\omega[q+1],...\omega[n]. \tag{3}$$

For example, in [3, 4] for rods it is shown that a kinematic device with one degree of activity transfers to the structure a generalized targeted inertial force, which reduces the value of only one natural vibration frequency to a given value, leaving the rest of the spectrum frequencies unchanged. The device is formed on the basis of a matrix for taking into account the action of additional inertial forces

$$M_0=M_{m0}M_m, \tag{4}$$

where we have

$$M_m=\|m_0[i,k]\|_{i,k=1}^n. \tag{5}$$

The matrix M_0 must have special properties. If the introduced kinematic device is targeted at the q-th natural frequency, then the coefficients of the matrix M_m ($\|m_0[i,k]\|_{i,k=1}^n$) should be orthogonal to the coordinates of the modes of natural vibrations of the remaining frequencies of the spectrum. That is we have

$$\sum_{k=1}^n m_0[i,k]v_\omega[k,j]=0, \quad (i=1,2,..,n,\ j=1,2,..,q-1,q+1,..,n). \tag{6}$$

With respect to the q-th natural frequency, which is “targeted” by the kinematic device we have

$$\sum_{k=1}^n m_0[i,k]v[k,q]\neq 0, \quad (i=1,2,..,n). \tag{7}$$

It was shown in [3, 4] that conditions (6) and (7) will be satisfied by the coefficients

$$m_0[i,k]=m[i]m[k]v_\omega[i,q]v_\omega[k,q]. \tag{8}$$

The value of the factor M_{m0} is found as the root of the equation

$$\left|(A-\omega_S^2 M)-M_{m0}(\omega_S^2 M_m)\right|=0. \tag{9}$$

Considering that the (q)-th form of natural vibrations remains its form of natural vibrations even at frequency ω_S, the factor M_{mO} can be found as

$$M_{m0} = \\ = \frac{\sum_{i=1}^{n}\sum_{k=1}^{n}(a[i,k]-\omega_S^2 m[i,k])v_\omega[i,(q)]v_\omega[k,(q)]}{\sum_{i=1}^{n}\sum_{k=1}^{n}\omega_S^2 m_0[i,k]v_\omega[i,(q)]v_\omega[k,(q)]}. \quad (10)$$

The result of solving the equation

$$\left|A-\omega^2(M+M_{m0}M_m)\right|=0. \quad (11)$$

must confirm that the modes of natural vibrations have not changed, and the "targeted" frequency has decreased to ω_S.

The kinematic device, which will correspond to the matrix of coefficients for taking into account the action of additional inertial forces

$$M_0 = M_{m0}M_m,$$

where $M_m = \|m_0[i,k]\|_{i,k=1}^{n}$,

should provide the ratio between the nodal displacements the same as between the coordinates of the q-th form of natural vibrations of the original system. In [3, 4] it is also shown that such a relation will be realized if the kinematic device transfers inertial forces to the nodes, the ratios between which will be proportional to the ratios between the forces

$$R_0[i] = m[i]v_\omega[i,q]. \quad (12)$$

An example of such a generalized targeted kinematic system for a rod is a sprengel, the outline of which is determined by a rope polygon built in the plane of motion of masses by forces (see, for example, [3, 4]).

The derivation of the expressions for the coefficients of the matrix for taking into account the action of additional inertial forces (4) for the rods is based on the use of the displacement method in the conventional form and the properties of the modes of natural vibrations (natural modes).

Since the modes of natural vibrations of the plates, as well as for rods, are orthogonal, the problem for elastic plates carrying a finite number of concentrated masses, as well as for rods, will be based on the formation of a matrix for taking into account the action of additional inertial forces. The coefficients $\|m_0[i,k]\|_{i,k=1}^{n}$ must also satisfy conditions (6) and (7) and be determined by dependencies (8).

Let us give an example that confirms that the matrix of additional stiffness coefficients (4) serves as the basis for creating targeted kinematic devices and for elastic plates carrying a finite number of concentrated masses.

Let us consider a plate from [5], carrying 25 concentrated masses (Figure 3).

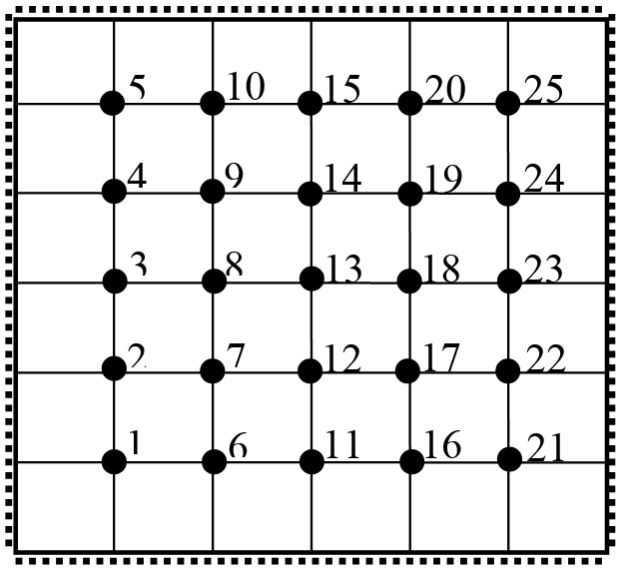

Figure 3. Considering plate (sample).

In node number 9 the mass is equal to 600 kg, in node number 18 the mass is equal to 1000 kg, and in other nodes the mass is equal to 800 kg each. The dimensions of the plate in the plan are 6 m by 6 m, the thickness is equal to 0.12 m. The modulus of elasticity of the plate material is E = 24,000,000,000 n / m2 Poisson's ratio is equal to v_0 = 0.2. With the main system of the displacement method (Figure 4) and one-dimensional numbering of values $v[k, j]$ in accordance with Figure 3, the spectrum of natural vibration frequencies is determined as the roots of equation (2).

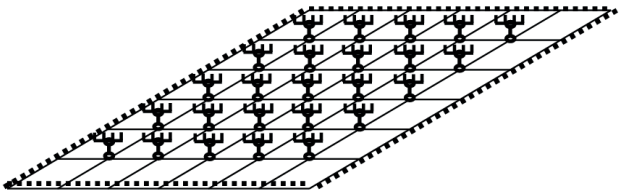

Figure 4. Main system of the displacement method (sample).

The values of the first five frequencies of natural vibrations of the plate and the coordinates of the corresponding eigenmodes are given in Table 1 (columns are initial frequencies and shapes).

Suppose that it is required to expand the interval between the fourth and fifth natural frequencies by reducing the value of the fourth frequency from 146.834 sec^{-1} to 110 sec^{-1}. For this, in accordance with (6), (7) and (8), we can form a matrix of the matrix for taking into account the action of additional inertial forces. The data required for using dependencies (6), (7) and (8) are given in the description of the plate and in Table 1 (columns are initial frequencies and shapes).

After the formation of the matrix of the action of additional inertial forces, taking into account their influence, we determine from equation (11) the modified spectrum of natural frequencies and the corresponding vibration modes.

The first five natural frequencies and their corresponding shapes are shown in Table 1 (columns are modified frequencies and shapes).

It can be seen from Table 1 that taking into account additional stiffness coefficients did not change any of the modes of natural vibrations of the plate, but only reduced the value of one of the frequencies from 146.834 s^{-1} to a given value of 110 s^{-1}. This result clearly illustrates the possibility of using dependencies (6), (7) and (8) for solving the problem of a generalized kinematic device of constraints for elastic plates with a finite number of degrees of freedom of masses.

The generalized kinematic device for the plate, as well as for the rod, must create an additional generalized inertial force that ensures the target of the action.

As noted above, the properties of the kinematic devices for the rods are based on the properties of the natural vibration modes. The same properties apply to elastic plates. This circumstance serves as a justification for using the results of formulating the properties of kinematic devices for rods and in a similar problem for plates.

Thus, for an elastic plate with a finite number of degrees of freedom of masses, the generalized kinematic device must correspond to the matrix for taking into account additional inertial forces (4). If the computational scheme of the constraint is represented by a variant of the hinge-rod system, then it should be with one degree of activity, in the nodes of the plate where the masses are located, racks are installed in the direction of movement of the masses, and during oscillations in the racks of the system, forces should arise, the ratios between which are proportional to the ratios between efforts $R_0[i]$ (12). In this case, in the structure of the constraint there should not be any connections with the plate, except for the racks installed in the nodes of the plate, where the masses are located.

So, in this paper it is shown that the method of forming the account of additional inertial forces that determine the targeted kinematic device in the problem of natural vibrations of rods can also be applied to solving similar problems for elastic systems with a finite number of degrees of freedom of masses, for which the directions of motion of masses parallel, but not in the same plane.

The paper substantiates and formulates the properties and requirements to which the design schemes of targeted kinematic devices in the problem under consideration must correspond.

Design schemes of generalized kinematic devices that meet the above requirements are multivariate and depend on the shape of the plate, the locations of the masses and some other features of the original object. Taking these circumstances into account, the approaches and algorithms for the formation of the corresponding design schemes that purposefully change the spectrum of natural vibration frequencies of elastic plates with a finite number of degrees of freedom of masses represent a separate problem and will be considered in a subsequent work.

Table 1. Results of analysis.

	Initial frequencies and modes					Modified frequencies and modes				
ω	36.6583	91.0084	92.7466	146.834	178.911	36.6583	91.0084	92.7466	110.0000	178.911
1	0.0830	0.1995	0.0499	-0.2495	0.1547	0.0830	-0.1995	-0.0499	0.2495	0.1547
2	0.1434	0.2935	-0.0043	-0.2433	-0.0063	0.1434	-0.2935	0.0043	0.2433	-0.0063
3	0.1649	0.2568	-0.1468	0.0129	-0.1657	0.1649	-0.2568	0.1468	-0.0129	-0.1657
4	0.1420	0.1514	-0.2494	0.2641	-0.0063	0.1420	-0.1514	0.2494	-0.2641	-0.0063
5	0.0818	0.0579	-0.1971	0.2624	0.1548	0.0818	-0.0579	0.1971	-0.2624	0.1548
6	0.1441	0.2533	0.1398	-0.2517	0.2788	0.1441	-0.2533	-0.1398	0.2517	0.2788
7	0.2492	0.3484	0.0840	-0.2447	0.0003	0.2492	-0.3484	-0.0840	0.2447	0.0003
8	0.2867	0.2601	-0.1502	0.0123	-0.2788	0.2867	-0.2601	0.1502	-0.0123	-0.2788
9	0.2468	0.1025	-0.3415	0.2593	0.0003	0.2468	-0.1025	0.3415	-0.2593	0.0003
10	0.1423	0.0090	-0.2912	0.2642	0.2789	0.1423	-0.0090	0.2912	-0.2642	0.2789
11	0.1672	0.1467	0.2455	-0.0058	0.3359	0.1672	-0.1467	-0.2455	0.0058	0.3359
12	0.2895	0.1491	0.2411	-0.0017	0.0088	0.2895	-0.1491	-0.2411	0.0017	0.0088
13	0.3336	0.0082	-0.0119	0.0070	-0.3237	0.3336	-0.0082	0.0119	-0.0070	-0.3237
14	0.2877	-0.1313	-0.2630	0.0124	0.0088	0.2877	0.1313	0.2630	-0.0124	0.0088
15	0.1657	-0.1331	-0.2605	0.0131	0.3359	0.1657	0.1331	0.2605	-0.0131	0.3359
16	0.1454	0.0007	0.2856	0.2417	0.3025	0.1454	-0.0007	-0.2856	-0.2417	0.3025
17	0.2522	-0.0908	0.3339	0.2415	0.0119	0.2522	0.0908	-0.3339	-0.2415	0.0119
18	0.2915	-0.2485	0.1317	-0.0018	-0.2941	0.2915	0.2485	-0.1317	0.0018	-0.2941
19	0.2513	-0.3314	-0.1103	-0.2446	0.0118	0.2513	0.3314	0.1103	0.2446	0.0118
20	0.1446	-0.2398	-0.1592	-0.2432	0.3025	0.1446	0.2398	0.1592	0.2432	0.3025
21	0.0842	-0.0528	0.1956	0.2437	0.1811	0.0842	0.0528	-0.1956	-0.2437	0.1811
22	0.1461	-0.1445	0.2454	0.2416	0.0151	0.1461	0.1445	-0.2454	-0.2416	0.0151
23	0.1688	-0.2486	0.1349	-0.0059	-0.1580	0.1688	0.2486	-0.1349	0.0059	-0.1580
24	0.1457	-0.2827	-0.0135	-0.2517	0.0151	0.1457	0.2827	0.0135	0.2517	0.0151
25	0.0838	-0.1910	-0.0633	-0.2494	0.1811	0.0838	0.1910	0.0633	0.2494	0.1811

REFERENCES

1. **Nudelman Ya.L., Lyakhovich L.S., Giterman D.M.** O naibolee Podatlivyh Svjazjah Naibol'shej Zhestkosti [About the Most Yielding Constraints of the Greatest Rigidity]. // Problems of Applied Mechanics and Mathematics, Tomsk, TSU Publishing House, 1981, pp. 113-126 (in Russian).
2. **Giterman D.M., Lyakhovich L.S., Nudelman Ya.L.** Algoritm Sozdanija Rezonansno-bezopasnyh Zon Pri Pomoshhi Nalozhenija Dopolnitel'nyh Svjazej [Algorithm for Creating Resonance-Safe Zones by Imposing Additional Constraints]. // Dynamics and Strength of Machines, Vol. 39, Kharkov, “Vishcha Schkola”, 1984, pp. 63-69 (in Russian).
3. **Lyakhovich L.S., Maletkin O.Yu.** O Pricel'nom Regulirovanii Sobstvennyh Chastot Uprugih Sistem [About Aimed Control of Natural Frequencies of Elastic Systems]. // Izvestia Vuzov. Construction and Architecture, 1990, No. 1, pp. 113-117 (in Russian).
4. **Lyakhovich L.S.** Osobye Svojstva Optimal'nyh Sistem i Osnovnye Napravlenija ih Realizacii v Metodah Rascheta Sooruzhenij [Special Properties of Optimal Systems and the Main Directions of Their Implementation in the Methods of Calculation of Structures]. Tomsk, Tomsk State University of Architecture and Construction, 2009, 372 pages (in Russian).
5. **Lyakhovich L.S., Akimov P.A.** Aimed control of the frequency spectrum of eigenvibrations of elastic plates with a finite number of degrees of freedom of masses by superimposing additional constraints. // International Journal for Computational Civil and Structural Engineering, 2021, Volume 17, Issue 2, pp. 76-82.

6. **Lyakhovich L.S., Akimov P.A., Tukhfatullin B.A.** Assessment of the proximity of design to minimum material capacity solution of problem of optimization of the flange width of I-shaped cross-section rods with allowance for stability constraints or constraints for the value of the first natural frequency and strength requirements. // International Journal for Computational Civil and Structural Engineering, 2021, Volume 16, Issue 2, pp. 71-82.

СПИСОК ЛИТЕРАТУРЫ

1. **Нудельман Я.Л., Ляхович Л.С., Гитерман Д.М.** О наиболее податливых связях наибольшей жесткости. // Вопросы прикладной механики и математики, Томск, Издательство ТГУ, 1981, с. 113-126.
2. **Гитерман Д.М., Ляхович Л.С., Нудельман Я.Л.** Алгоритм создания резонансно-безопасных зон при помощи наложения дополнительных связей. // Динамика и прочность машин, Вып. 39, Харьков, «Вища школа», 1984, с. 63-69.
3. **Ляхович Л.С., Малеткин О.Ю.** О прицельном регулировании собственных частот упругих систем. // Известия вузов. Строительство и архитектура, 1990, №1, с. 113-117.
4. **Ляхович Л.С.** Особые свойства оптимальных систем и основные направления их реализации в методах расчета сооружений. Томск: Издательство Томского государственного архитектурно-строительного университета, 2009. – 372 с.
5. **Lyakhovich L.S., Akimov P.A.** Aimed control of the frequency spectrum of eigenvibrations of elastic plates with a finite number of degrees of freedom of masses by superimposing additional constraints. // International Journal for Computational Civil and Structural Engineering, 2021, Volume 17, Issue 2, pp. 76-82.
6. **Lyakhovich L.S., Akimov P.A., Tukhfatullin B.A.** Assessment of the proximity of design to minimum material capacity solution of problem of optimization of the flange width of I-shaped cross-section rods with allowance for stability constraints or constraints for the value of the first natural frequency and strength requirements. // International Journal for Computational Civil and Structural Engineering, 2021, Volume 16, Issue 2, pp. 71-82.

Pavel A. Akimov, Full Member of the Russian Academy of Architecture and Construction Sciences, Professor, Dr.Sc.; Rector of National Research Moscow State University of Civil Engineering; Professor of Department of Structural Mechanics, Tomsk State University of Architecture and Building; 24, Ul. Bolshaya Dmitrovka, 107031, Moscow, Russia; phone +7(495) 625-71-63; Fax: +7 (495) 650-27-31; E-mail: akimov@raasn.ru, pavel.akimov@gmail.com.

Leonid S. Lyakhovich, Full Member of the Russian Academy of Architecture and Construction Sciences, Professor, DSc, Head of Department of Structural Mechanics, Tomsk State University of Architecture and Building; 634003, Russia, Tomsk, Solyanaya St., 2; E-mail: lls@tsuab.ru

Акимов Павел Алексеевич, академик РААСН, профессор, доктор технических наук; ректор Национального исследовательского Московского государственного строительного университета; профессор кафедры строительной механики Томского государственного архитектурно-строительного университета; 107031, г. Москва, ул. Большая Дмитровка, д. 24, стр. 1; тел. +7(495) 625-71-63; факс +7 (495) 650-27-31; Email: akimov@raasn.ru, pavel.akimov@gmail.com.

Ляхович Леонид Семенович, академик РААСН, профессор, доктор технических наук, профессор кафедры строительной механики, Томский государственный архитектурно-строительный университет; 634003, Россия, г. Томск, Соляная пл. 2; E-mail: lls@tsuab.ru